Analysis of the composition of latent fingermarks by spectroscopic imaging techniques.

FERGUSON, Leesa Susanne.

REFERENCE

Analysis of the Composition of Latent Fingermarks by Spectroscopic Imaging Techniques

Leesa Susanne Ferguson

A thesis submitted in partial fulfilment of the requirements of Sheffield Hallam University for the degree of Doctor of Philosophy

August 2013

To my beloved daughter,

Sienna

Abstract

Despite the success of DNA fingerprinting, fingermarks remain an efficient means of ascertaining the identity of an individual at many crime scenes. There are numerous enhancement techniques used to develop fingermarks on a range of deposition surfaces. Despite this, there is a need for further intelligence to be gained in situations where fingermarks retrieved at crime scenes do not yield identification.

The majority of the work presented in this thesis utilises MALDI mass spectrometry in profiling and imaging mode to investigate latent fingermarks, with SERS and ATR-FTIR used as complementary techniques.

One of the major issues of using analytical techniques to investigate latent fingermarks is their inadequate application to real crime scene scenarios. Presented within this thesis is a new method of matrix application that makes MALDI-MSI forensically applicable and enables the distribution of various endogenous lipids and exogenous compounds within fingermarks to be visualised.

The work is extended to include detection of various antimicrobial peptides and small proteins in the fingermarks of a cohort of 80 donors using MALDI mass spectrometry profiling followed by multivariate statistical analysis in an attempt to differentiate donors based on their sex.

Chemical imaging of latent fingermarks by SERS and ATR-FTIR is also demonstrated, which could potentially lead to a three step multi-informative analytical approach for chemical characterisation of fingermark residue.

Declaration

I declare that no part of this thesis has been submitted in support of any other degree or qualification at this university or any other institute of learning.

All the work presented in this thesis was undertaken by myself, Leesa Susanne Ferguson, with the exception of the statistical analysis presented in chapter 3, which was carried out by Dr Florian Wulfert and the scanning electron microscopy work presented in chapter 2, which was done by Dr Stuart Creasey, Materials and Engineering Research Institute (MERI), Sheffield Hallam University.

The ATR-FTIR work presented in chapter 4 was done in collaboration with Dr Kerstin Mader, MERI, Sheffield Hallam University.

Contents

List of Figures

List of Tables

Abbreviations

ACN	Acetonitrile
AD	Atopic dermatitis
ATR	Attenuated total reflectance
ATR-FTIR	Attenuated total reflectance Fourier transform infrared
CCD	Charge coupled device
CE	Cholesterol ester
a-CHCA	a-cyano-4-hydroxycinnamic acid
CI	Chemical ionisation
CID	Collision induced dissociation
DAN	1 ,5-Diaminonapthalene
DART	Direct analysis in real time
DC	Direct current
DCD	Dermcidin
DESI	Desorption electrospray ionisation
DESI-MS	Desorption electrospray ionisation mass spectrometry
DFO	1, 8-Diazafluoren-9-one
DG	Diacylglycerides
DHB	2, 5-dihydroxybenzoic acid
dp	Penetration depth
ECA	Ethyl cyanoacrylate
EI	Electron ionisation
ESI	Electrospray ionisation
FET	Fingermark enhancement technique

FETs	Fingermark enhancement techniques
FT-ICR	Fourier transform ion cyclotron resonance
FT	Fourier transform
FTIR	Fourier transform infrared
FWHM	Full width at half maximum
GC-MS	Gas chromatography mass spectrometry
HDMS	High definition mass spectrometry
HV	Accelerating voltage
IgG	Immunoglobulin G
IL	Ionic liquid
InGaAs	Indium gallium arsenide
IMS	Ion mobility spectrometry
IR	Infrared
KBr	Potassium bromide
KNO_3	Potassium nitrate
K_2SO_4	Potassium sulfate
LAESI	Laser ablation electrospray ionisation
LDI	Laser desorption/ionisation
LDI-TOF-MS	Laser desorption/ionisation time of flight mass spectrometry
LOD	Limit of detection
MALDI	Matrix assisted laser desorption/ionisation
MALDI-MS	Matrix assisted laser desorption/ionisation mass spectrometry

MALDI-MSI	Matrix assisted laser desorption/ionisation mass spectrometry imaging
MALDI MSP	Matrix assisted laser desorption/ionisation mass spectrometry profiling
$MgSO_4$	Magnesium sulfate
MS	Mass spectrometry
MALDI-TOF	Matrix assisted laser desorption/ionisation – time of flight
MALDI-TOF-MS	Matrix assisted laser desorption/ionisation - time of flight - mass spectrometry imaging
MoS_2	Molybdenium disulphide
MSI	Mass spectrometry imaging
MS/MS	Tandem mass spectrometry
MSP	Mass spectrometry profiling
m/z	Mass to charge
N_2 laser	Nitrogen laser
NaCl	Sodium chloride
Na_2SO_4	Sodium sulphate
Nd:YAG	Neodymium-doped yttrium aluminium garnet
NIR	Near infrared
oaTOF	Orthogonal acceleration time of flight
PAFFT	Peak alignment by fast Fourier transform
PAGE	Polyacrylamide gel electrophoresis
PDMS	Polydimethylsiloxane
PEG	Polyethylene glycol
PLSDA	Partial least squares discriminant analysis

ppm	parts per million
PVDF	Polyvinylidene fluoride
Q	Quadrupole
QQQ	Triple quadrupole
QTOF	Quadrupole time of flight
QTrap	Quadrupole ion trap
RF	Radio frequency
RI	Refractive index
RP-HPLC	Reverse phase high performance liquid chromatography
SA	Sinapinic acid
SALDI-TOF-MS	Surface assisted laser desorption time of flight mass spectrometry
SELDI-MS	Surface enhanced laser desorption/ionisation-mass spectrometry
SEM	Scanning electron microscopy
SERS	Surface enhanced Raman spectroscopy
SIM	Selected ion monitoring
SIMS	Secondary ion mass spectrometry
SiO_2	Silicon dioxide
SMALDI-MS	Scanning microprobe matrix assisted laser desorption/ionisation mass spectrometry
SOCOs	Scene of Crime Officers
SPR	Small particle reagent
SRIG	Stacked ring ion guide
TFA	Trifluoroacetic acid

TG	Triglyycerides
TLC	Thin layer chromatography
TOF	Time of Flight
TOF-MS	Time of flight-mass spectrometry
TWIMS	Travelling wave ion mobility spectrometry
UK	United Kingdom
UV	Ultra violet
VIP	Variable importance in projection
VMD	Vacuum metal deposition
VP	Variable pressure
ZnSe	Zinc selenide

Lipid Species Tentatively Identified in Ungroomed Fingermarks by High Mass Accuracy

Calculated monoisotopic *m/z*	Experimental *m/z*	*m/z* error ppm (2dp)	Possible lipid species	Ion species
255.2315	255.2319	1.57	FA (16:1) - palmitoleic acid	[M+H]+
283.2632	283.2632	0	FA (18:1) - oleic acid	[M+H]+
285.2788	285.2791	1.05	FA (18:0) - stearic acid	[M+H]+
295.2632	295.2637	1.69	FA (19:2) - nonadecadienoic acid	[M+H]+
297.2792	297.2788	1.35	FA (19:1) - nonadecenoic acid	[M+Hf
307.2632	307.2636	1.30	FA (20:3) - eicosatrienoic acid	[M+Hf
309.2788	309.2790	0.65	FA (20:2) - eicosadienoic acid	[M+H]+
311.3945	311.3943	0.64	FA (20:1)-eicosenoic acid	[M+Hf
523.4722	523.4723	0.19	DG(0-16:0/0:0/12:0)	[M+Hf
535.4697	535.4705	1.49	DG(0-16:0/0:0/13:0)	[M+Naf
549.4860	549.4853	1.27	DG(0-18:0/0:0/12:0)	[M+Naf
640.6026	640.6032	0.94	CE(16:0(NH2))	[M+Hf
668.6339	668.6343	0.60	CE(16:0(NH2))	[M+Hf
757.6316	757.6317	0.13	TG(43:1)21:0/2:0/20:1	[M+Naf
759.6473	759.6470	0.39	TG(43:0)21:0/2:0/20:0	[M+Naf
771.6467	771.6473	0.78	TG(44:1)14:0/14:0/16:0	[M+Naf
773.6629	773.6632	0.39	TG(44:0)14:0/14:0/16:0	[M+Naf
785.6629	785.6630	0.13	TG(45:1)14:0/15:0/16:1	[M+Naf
797.6629	797.6628	0.13	TG(46:2)22:0/22:2/2:0	[M+Naf
815.7099	815.7093	0.74	TG(47:0)15:0/16:0/2:0	[M+Naf

The tentatively identified lipid species detected within ungroomed fingermarks by high mass accuracy measurements. All lipid species are identified with a mass error less than 1.69 ppm and are discussed in chapters 2 and 4 of this thesis.

Other Tentatively Identified Species Detected Within Ungroomed Fingermarks

Experimental *m/z*	Possible species	Ion species
201.2	Dodecanoic acid	$[M+H]^+$
229.2	Tetradecanoic acid	$[M+H]^+$
230.2	13-aminotridecanoic acid	$[M+H]^+$
237.2	Dehydrated palmitoleic acid	$[M-H_2O+H]^+$
243.2	Pentadecanoic acid	$[M+H]^+$
257.2	Palmitic acid	$[M+H]^+$
299.2	Nonadecanoic acid	$[M+H]^+$
304.2	Alkyl (C_{12})-Dimethylbenzylammonium	$[M+H]^+$
369.4	Dehydrated cholesterol	$[M-H_2O+H]^+$
431.2	Vitamin E	$[M+H]^+$
550.6	Dimethyldioctadecylammonium	$[M+H]^+$
583.6	DG	$[M+Na]^+$

Other tentatively identified species within ungroomed fingermarks that are discussed in chapters 2 and 4 of this thesis.

Peptide and Protein Species Tentatively Identified in Fingermarks

Peptide/Protein	***Protonated Theoretical Mass***	**Amino Acid Positions**
DCD-1L	4819.5	63-110
DCD-1	4706.3	63-109
SSL-46	4607.2	63-108
SSL-45	4520.1	63-107
SSL-29	2870.3	63-91
SSL-25	2413.8	63-87
LEK-45	4532.2	66-110
YDP-42 and YPD-42 (dimer)	4303.6/8606.2	20-61
Psoriasin	11,377.2	2-120, serine acylated, 1 disulphide bridge

The protonated theoretical mass and the amino acid sequence of the tentatively identified dermcidin derived peptides and the protein psoriasin that are discussed in chapter 3 of this thesis.

Acknowledgements

First and foremost, I would like to express my sincere thanks and gratitude to my supervisors, Dr Simona Francese and Dr Rosalind Wolstenholme for the help, support and encouragement they've provided during the course of my PhD.

I would also like express my gratitude to Dr Florian Wulfert, Dr Stuart Creasey, Dr Kerstin Mader, Dr Chris Sammon, Professor Malcolm Clench and Dr Vikki Carolan for their input, expertise and advice over the last 4 years.

I would like to thank all of my colleagues at Sheffield Plallam University, for their support and friendship throughout my PhD. I especially want to thank Dr Kate Phillips, for all of her help formatting this thesis and for her friendship. I also wish to offer a very special thank you to Dr Laura Cole, Robert Bradshaw, Eva, Illes-Toth, Dr Philippa Hart, Dr Jillian Newton, Patrick Harrison, Bryn Flinders, Chris Mitchell and Richard Battle for their friendship and support.

To my dear friends, Denise, Rachel, Barbara, Dawn and Neil, thank you for your patience, encouragement and belief.

A very special thank you to my parents, Ian and Susan and my beloved sister Julie, for all the help, support and encouragement they've provided throughout my life. Thanks for walking the dogs, dad.

To my dogs, Mocha, Morph and Jasper, thank you for your loyalty, friendship, love and making me laugh.

Last, but definitely not least, I wish to thank my beloved daughter Sienna. I really couldn't have done it without you. Thank you for being everything I could wish for in a daughter. Love you more than anything.

1 General Introduction

1.1 Fingermarks

Fingermarks result from the transfer of material from the surface of the skin to a surface following contact. They differ from fingerprints, which are control prints where the donor is known and an imprint is obtained using either ink or a direct scan. The friction ridge pattern of fingermarks is unique to every individual and remains unchanged throughout life unless scarred, thereby enabling a means of personal identification (Lambourne, 1977; Reed, 1981).

Fingermarks can be divided into three distinct groups: patent fingermarks, plastic fingermarks and latent fingermarks. Patent fingermarks are visible to the naked eye as they contrast well with the substrate onto which they are deposited. They are formed by the transfer of opaque materials such as blood, make-up or paint onto a surface. Plastic fingermarks are formed when a negative ridge impression is created in a soft substrate such as putty or candle wax. Latent fingermarks are invisible to the naked eye and are the most frequent type of fingermark found at crime scenes. They are predominantly composed of transparent endogenous species and require enhancement by one of the established fingermark enhancement techniques (FETs) to enable visualisation (Bowman, 2005).

In the United Kingdom (UK), fingermarks recovered from crime scenes can be submitted and compared to fingerprints stored on the National Fingerprint Database "Ident1". As of April 2010, the database held 1.9 million unidentified marks on record and 8.3 million individuals' ten-prints. Historically, in the UK, 16 ridge characteristics (*minutiae*) were required for a full identification. Since 2001 however, there is no minimum quantitative standard and the responsibility of ascertaining identification lies with the fingerprint expert, whose opinion must be validated by two other fingerprint professionals (Fraser and Williams, 2009).

1.1.1 History of Fingermarks

The use of fingermarks as a means of identification for criminal purposes dates back to the mid nineteenth century when Sir William Herschel began to acquire the imprint of the right hand of Indian citizens as a way of preventing the forgery of signatures. Indeed, Herschel was the first person to document that an individual's ridge pattern on their hands and feet did not change from birth (Lambourne, 1977; Reed, 1981).

Sir Francis Galton published the first comprehensive work specifically about fingerprints in 1892. The book discussed a classification system based on three distinct ridge patterns (arches, loops and whorls) stating, for the first time, that no two individuals possessed the same ridge pattern, thus offering a possible means of identification (Lambourne, 1977; Saferstein, 2011).

In 1897, Edward R. Henry, Inspector General for the lower India provinces, formulated a workable classification system, based on that of Galton, which came into general use throughout India. Subsequently, in the UK, a committee was established under the chairmanship of Lord Belper to decide whether the system of identification based on body measurements and fingerprints that was in place at the time should be superseded by the Henry classification system. The committee subsequently concluded that immediate steps should be taken to introduce the Henry system of identification in the UK. The system was implemented by Scotland Yard in 1901 and is still employed today in the majority of English speaking countries (Lambourne, 1977; Reed, 1981; Saferstein, 2011).

The first criminal case in the UK, leading to a conviction based on fingermark evidence occurred in 1902. Henry Jackson was convicted after his thumb print was left at the scene of a burglary. The first murder conviction in the UK based

on fingermark evidence occurred three years later; a thumb print was found at the murder scene of a married couple, leading to the death penalty for two brothers Alfred and Albert Stratton (Lambourne, 1977; Reed, 1981).

These early successes led to fingermark evidence becoming established as the dominant means employed to link a suspect to a crime scene, and today it still remains one of the primary methods of ascertaining an individual's identity.

1.1.2 Fingermark Types

The complex pattern of ridges that make up fingermarks can be divided into three main classes dictated by the general ridge flow; loops, whorls and arches. These patterns are formed by the combination of ridge systems that are interconnected around key focal points called *core(s)* and *delta(s)* (Fraser and Williams, 2009). Approximately 60% of the population have loops, 35% whorls and 5% arches. Loops can be subdivided into radial or ulna loops, depending on whether the loop flows and opens towards the radial or ulna bone in the forearm. Whorls can be classified as plain whorl, central pocket loop, double pocket loop or accidental, arches can be either plain or tented (Saferstein, 2011). The general ridge flow of fingermarks is also known as Galton level 1 details. Figure 1.1 shows the three main classes of fingermark ridge patterns and subgroups.

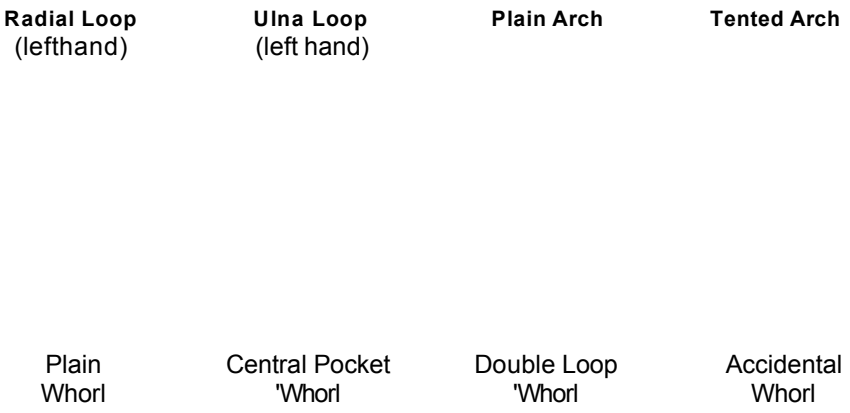

Figure 1-1: The 3 main classification groups of fingermarks; loops*, *whorls and arches and their subgroups.

Approximately 60% of the population have loops, 35% whorls and 5% arches. Image adapted from Federal Bureau of Investigation (1957).

In addition, fingermark patterns can be distinguished further by local characteristics of the ridge pattern called ***minutiae*** (ridge endings, short independent ridges, bifurcations, lakes, islands and spurs), also known as Galton level 2 details (Fraser and Williams, 2009). Figure 1.2 shows a fingerprint containing some of the possible ***minutiae.***

Addition characteristics of fingermarks known as Galton level 3 details include features of the fingermark ridges such as the width of the ridge, the shape of the edge of the ridge and the number and location of pores present within the ridge (Gupta ***et al.,*** 2008).

Figure 1-2: A fingermark showing some of the possible local ridge characteristics (minutiae) that enable fingermarks to be distinguished from one another.

Image obtained from Jackson and Jackson (2011).

1.1.3 Latent Fingermark Composition

Latent fingermarks are the most common type found at crime scenes. They are composed of a mixture of species originating from three sources: (1) the epidermis, (2) the sweat glands within the dermis and (3) semi-exogenous and exogenous contaminants (Girod *et al.*, 2012). The epidermis is responsible for the presence of some proteins in fingermark residue resulting from the desquamation process required for skin renewal (Drapel *et al.*, 2009; Girod *et al.*, 2012), as well as the presence of innate antimicrobial proteins such as psoriasin (Schroder and Harder, 2006). Within the dermis are the three major sweat glands, the eccrine, sebaceous and apocrine glands that are responsible for the secretion of sweat through epidermal pores to the skin's surface.

Between two and four million eccrine sweat glands are distributed throughout the body, with the highest density on the palms of the hands, palmar surfaces, and the soles of the feet, plantar surfaces. Sebaceous glands are absent on the palmar and plantar surfaces, but are present on all other skin surfaces (highest density on the face and scalp). Apocrine glands are located predominantly in the genital and axillary regions. Fingermark residue consists primarily of secretions from the eccrine and sebaceous glands. Even though only eccrine glands are present on the palms of the hands, the fingers become contaminated with sebaceous secretions due to regular contact with other parts of the body such as the hair and face, (Ramotowski, 2001). Eccrine sweat is predominantly composed of water, but also contains numerous organic and inorganic constituents, such as amino acids, proteins and salts (Ramotowski, 2001). Sebaceous sweat consists of mainly organic compounds such as fatty acids, triglycerides, wax esters and sterols (Knowles, 1978). Figure 1.3 shows the three major sweat glands and table 1.1 shows the chemical constituents originating from each of the three glands.

In addition to the endogenous species originating from the epidermis and sweat glands, latent fingermarks may also comprise semi-exogenous compounds such as caffeine, which have been ingested and are subsequently secreted intact or together with their metabolites in sweat. Exogenous contaminants such as toiletries, cleaning products, make-up and even illegal substances such as explosives or drugs of abuse may also be present in latent fingermarks, which could potentially provide additional information relating to the donor's lifestyle.

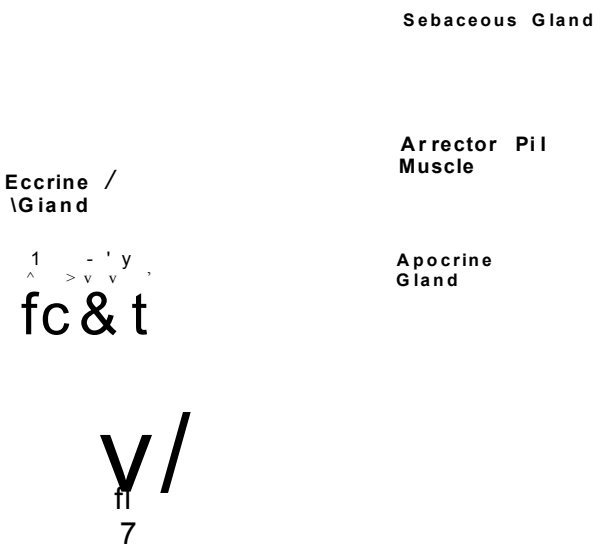

Figure 1-3: The eccrine, sebaceous and apocrine glands.

Eccrine, sebaceous and apocrine glands are responsible for the secretion of sweat through the epidermal pores onto the skin surface. Image obtained from Ramotowski *(2001).*

A summary of the chemical composition of sweat originating from the eccrine, sebaceous and apocrine glands is presented in table 1.1.

	CONSTITUENTS	
SOURCE	**INORGANIC**	**ORGANIC**
Eccrine glands	Chorides Metal Ions Sulfates Phosphates Bicarbonate Ammonia Water (>98%)	Amino acids Proteins Urea Uric acid Lactic acid Sugars Creatinine Choline
Sebaceous glands		Glycerides (30-40%) Wax Esters (20-25%) Fatty Acids (15-25%) Squalene (10-12%) Sterol Esters (2-3%) Sterols (1-3%)
Apocrine glands	Iron Water	Proteins Carbohydrates Sterols

Table 1-1: A summary of the chemical constituents present in the sweat originating from the three major sweat glands.

Table adapted from Ramotowski (2001) and Knowles (1978).

At present, there are numerous FET that are recommended by the Home Office to visualise latent fingermarks at crime scenes. The Home Office collates the information in the "Manual of Fingerprint Development Techniques" (Bowman, 2005). The manual provides guidance and informs Scene of Crime Officers of the appropriate fingermark enhancement techniques to use in any situation and the sequential workflows that should be adhered to, in order to obtain optimum results. An example of a suggested workflow is shown in figure 1.4 for fingermarks present on an untreated metal surface.

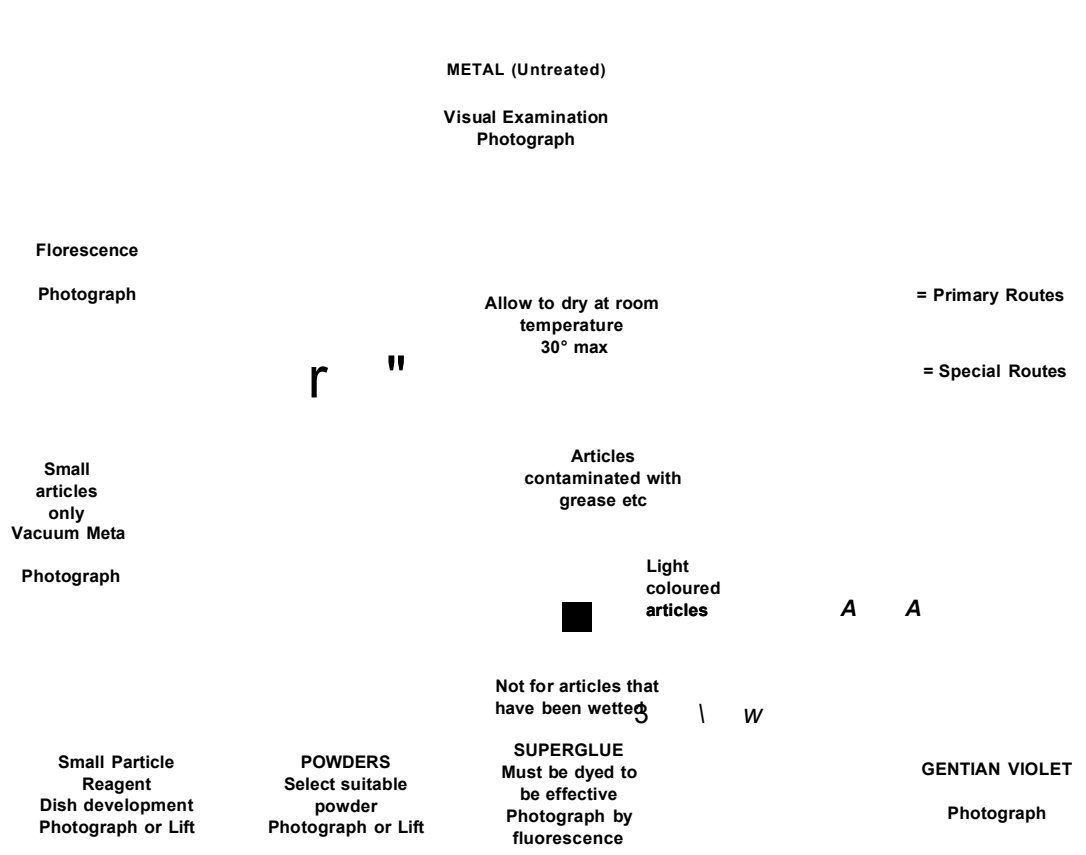

Figure 1-4: A fingermark enhancement technique workflow for fingermarks deposited on an untreated metal surface.

Image adapted from Bowman (2005).

1.1.4 Conventional Fingermark Enhancement Techniques

The main objective of fingermark enhancement is simply to obtain the best optical contrast possible between the fingermark ridge pattern and the underlying deposition surface without destroying any of the available ridge detail (Becue ***et al.,*** 2010). The choice of enhancement method employed to visualise latent fingermarks is primarily dependent on the nature of the deposition surface and the chemical composition of the mark. The majority of fingermark enhancing methods currently employed involve either a physical interaction or a chemical reaction between the selected development reagent and an endogenous constituent of the latent mark.

The techniques employed for the visualisation of latent fingermarks can be divided into four main categories; (1) optical methods, (2) physical methods, (3) physical-chemical methods, and (4) chemical methods (Zhang *et al.,* 2007; Choi *et al.*, 2008). A general limitation of these techniques is that, as fingermarks age, their composition changes. Environmental factors such as temperature, humidity and light greatly contribute to the degradation of endogenous species thus affecting the enhancement and recovery of the fingermark, as many of the constituents to which the development reagent interacts are no longer present (Bowman, 2005).

1.1.4.1 Optical Examination Methods

Optical examination using lasers, high intensity light sources and appropriate viewing filters is often the first enhancement technique implemented at a crime scene as it is non-destructive. When exposed to optical examination, endogenous constituents such as lipids and exogenous contaminants present in latent fingermarks exhibit fluorescence (Menzel and Duff, 1979). Fluorescence occurs when the electrons of molecules in the ground state absorb light of an appropriate wavelength and are promoted to one of the higher energy vibrational levels of the 1st excited electronic state. The excess vibrational energy is lost until the molecules are in the lowest energy vibrational state. The electrons finally return to the ground state, with the emission of a photon of light at a lower energy (longer wavelength) than the absorbed radiation (figure 1.5.).

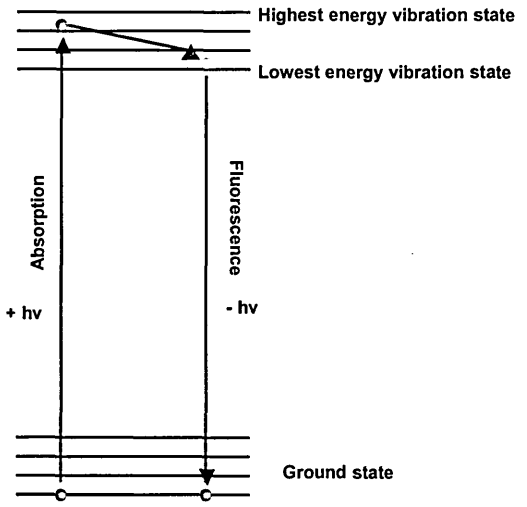

Figure 1-5: Jablonski diagram showing the promotion of an electron in a fluorescent molecule from the ground state to a higher energy vibrational state. *Electrons in fluorescent molecules are promoted from the ground state to a higher energy vibrational state by absorbing energy of an appropriate wavelength. The electrons subsequently drop to a lower energy level and emit a photon of light at a longer wavelength than that of the photon originally absorbed by the molecule. Image adapted from Bleay et al. (2012).*

In addition to the fluorescence displayed by some endogenous compounds and exogenous contaminants of latent fingermarks, some of the chemical treatments applied to fingermarks such as 1, 8 - Diazafluoren-9-one (DFO) also exhibit fluorescence when exposed to appropriate light sources and viewing filters (Bowman, 2005).

1.1.4.2 Physical Enhancement

Physical methods of enhancement do not require chemical reactions and involve the application of fine particles that have a physical affinity for the fingermark residue, enabling their visualisation by creating a contrast against the surface of deposition (James and Nordby, 2009). Physical methods of

enhancement include powdering, vacuum metal deposition (VMD) and small particle reagent (SPR).

1.1.4.2.1 Powdering

Powdering is by far the most commonly employed method for developing latent fingermarks because of its ease of use, speed and low cost, especially *in situ* at a crime scene. If successful, powdering yields instantly visible fingermarks, which can subsequently be recovered with an appropriate lifting tape, mounted on a suitable surface to be photographed and then taken back to the laboratory for further processing where required (Bowman, 2005). The procedure relies on the mechanical adherence of the dusted powder to the aqueous and fatty components deposited by the skin ridges. Therefore, extreme care is necessary when dusting, as contact between the brush and the mark has an unavoidable destructive effect (Lee and Gaensslen, 2001).

There are numerous powder formulations available that are deposition surface specific (Sodhi and Kaur 2001; Liu *et al.,* 2009), and include conventional (black, white or coloured), aluminium, magnetic and fluorescent powders (Bowman, 2005). Recently proposed advances include the use of gold and silver nanoparticles to enhance fingermarks on non-porous surfaces, with improved development and contrast over conventional black powders (Choi *et al.*, 2007; Choi *et al.*, 2008) and silica nanoparticles with hydrophobic coatings incorporating a variety of fluorescent dyes for fresh and aged fingermarks (Theaker *et al.*, 2008). Figure 1.6 shows photographs of latent fingermarks developed on glass slides with rhodamine 6G incorporated nanoparticles, in (a) white light and (b) UV illumination.

Figure 1-6: Latent fingermarks developed on a glass slide by dusting with rhodamine 6G incorporated nanoparticles in (a) white light illumination and (b) UV illumination.

Image obtained from Theaker et al., (2008).

Despite the availability of some recent methodologies, powdering is often not suitable to develop older fingermarks. The endogenous constituents present within fingermark residues degrade over time, therefore, the constituents to which the powders adhere may be no longer present. Furthermore if powdering is used first, it may inhibit the effectiveness of subsequent development techniques (Bowman, 2005).

1.1.4.2.2 Vacuum Metal Deposition

Vacuum metal deposition (VMD) was first described in 1968 for the development of latent fingermarks on paper surfaces (Theys ***et al.,*** 1968). The technique was subsequently used for visualising latent marks on low density polyethylene (polythene) (Kent ***et al.,*** 1976). VMD is particularly effective for old fingermarks, as well as ones that have been exposed to water. The disadvantages associated with the technique are the high initial cost of buying

the necessary equipment, and the experience required to obtain fingermarks of sufficient quality (Jones *et al.*, 2001; Bowman, 2005).

VMD employs vacuum coating technology; a fine invisible coating of gold is deposited onto the items being examined, which is followed by sufficient zinc to enable a visible grey deposit to appear (Jones *et al.,* 2001; Jones *et al.,* 2012). Zinc will only deposit on a non-metallic substrate providing the surface is maintained at a low temperature, or on a nucleating layer of another metal that has been deposited first. Although initially used for detecting latent marks on smooth non-porous surfaces such as glass and plastics, VMD has recently been employed to visualise fingermarks and grab impressions on fabrics as demonstrated in figure 1.7 (Fraser *et al.*, 2011).

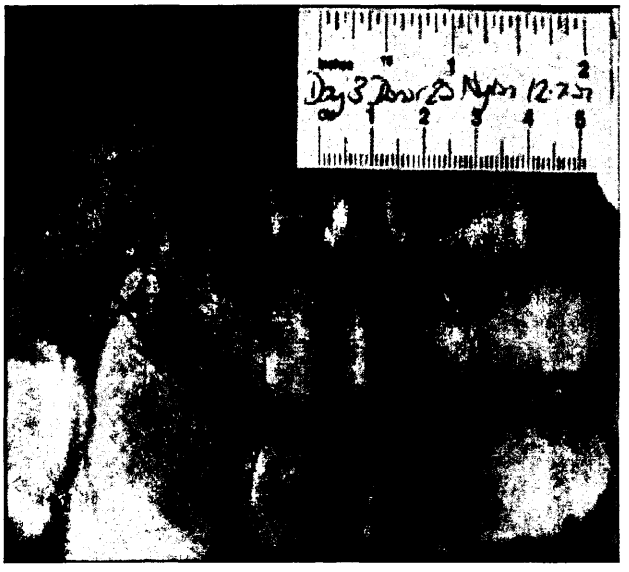

Figure 1-7: A 3 day old grab impression developed on nylon by Vacuum Metal Deposition (VMD).

Image obtained from Fraser et al., (2011).

1.1.4.2.3 Small Particle Reagent

Small particle reagent (SPR) consists of fine molybdenum disulphide (MoS_2) particles suspended in a detergent solution. The MoS_2 particles adhere to the

fatty constituents of latent fingermarks, resulting in a grey deposit. SPR can be applied to fingermarks on non-porous surfaces as either a spray or via dish development (Polimeni ***et al.,*** 2004; Cuce ***et al.,*** 2004; Bowman, 2005). One of the main advantages of SPR is its suitability to be applied to wetted surfaces, although developed marks are easily damaged and should be lifted or photographed immediately (Bowman, 2005). Recent advancements include the development of white SPR and black SPR (Cuce ***et al.,*** 2004), as well as fluorescent variants, which further extend the applicability of the technique (Jasuja ***et al.,*** 2008). Figure 1.8 shows a fingermark developed on a glass slide by cyano blue SPR after immersion in water for 96 hours.

Figure 1-8: A latent fingermark deposited on a glass slide and immersed in water for 96 hours before development by cyano blue Small Particle Reagent (SPR).

Image obtained from Jasuja et al. (2008).

1.1.4.3 Physical-chemical Methods

Physical-chemical methods of enhancement involve the initial physical adherence of a development reagent to the fingermark residue, which

subsequently induces a chemical reaction. Some of the physical-chemical methods employed today include cyanoacrylate fuming and iodine fuming.

1.1.4.3.1 Cyanoacrylate Fuming

Cyanoacrylate (superglue) fuming involves exposing fingermarks to ethylcyanoacrylate (ECA) vapours in an enclosed heated chamber. It is ideally suited to fingermarks deposited on a variety of non-porous surfaces such as metals, plastics, vinyl and rubber (Bowman, 2005; Wargacki *et al.*, 2007). The cyanoacrylate monomer present in the ECA vapour polymerises to give the white polycyanoacrylate deposits on the fingermark ridges, with limited polymer depositing on the substrate (Lewis *et al.*, 2001; Wargacki *et al.*, 2007). The polymerisation mechanism for ECA is shown in figure 1.9, although the exact mechanism by which the polymer develops on fingermark residue remains unclear (Bleay *et al.*, 2012). Even though there are various chemical constituents present in latent marks that are capable of initiating polymerisation, it has been suggested that the primary initiator may be water (Paine *et al.*, 2011). Recent publications have concluded that a relative humidity of 80% provides optimum results, when combined with rapid heating of cyanoacrylate (Kent *et al.*, 1990; Paine *et al.*, 2011). Furthermore, staining with a fluorescent dye such as Basic Yellow 40, followed by fluorescent examination maximises the number of fingermarks visualised (Bowman, 2005).

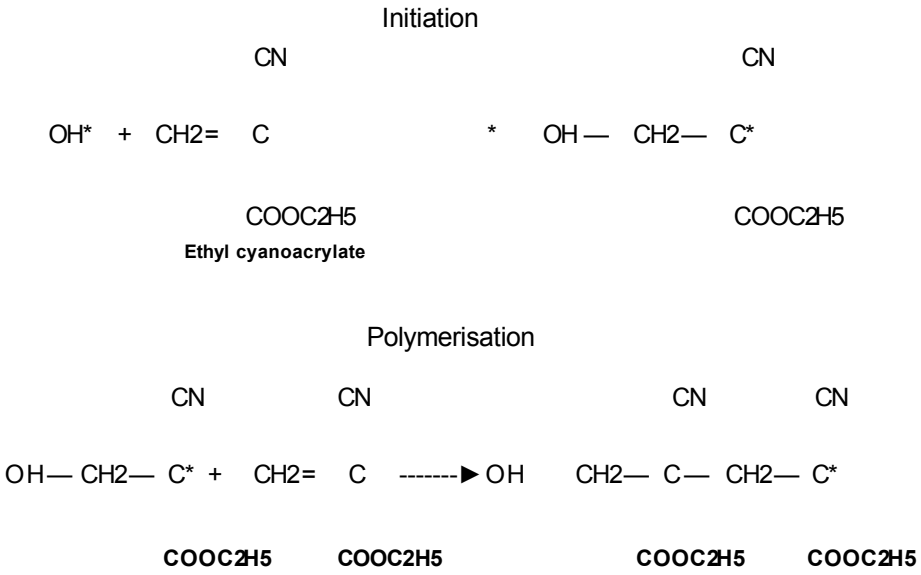

Figure 1-9: The polymerisation mechanism for ethyl cyanoacrylate (ECA).

Figure obtained from Bleay et al. (2012).

1.1.4.3.2 Iodine Fuming

Although iodine fuming is one of the oldest fingermark development techniques, it is rarely used today. Enhancement occurs when iodine crystals undergo sublimation and iodine vapour is absorbed by the unsaturated lipid constituents of latent fingermarks resulting in a yellow/brown image (Bowman, 2005). Iodine fuming can be applied to fingermarks deposited on both porous and non-porous substrates and the technique does not preclude the use of subsequent visualisation techniques. On the majority of surfaces, fingermarks developed by iodine fuming must be photographed immediately as they fade quickly unless fixed with a-naphthoflavone, giving a dark blue image (Bowman, 2005). Recently, iodine fuming was used to permanently develop both fresh and aged eccrine and sebaceous fingermarks without background colouration, on some types of thermal papers without any pre- or post-treatment of the substrate (Jasuja and Singh, 2009). Figure 1.10 shows the fingermarks of two donors developed on glossy paper by iodine fuming.

Figure 1-10: Fingermarks from two donors deposited on glossy paper and developed using iodine fuming.

Image adapted from Bleay et al., (2012).

1.1.4.4 Chemical Enhancement

The last 25 years have seen great progress being made in fingermark detection and development, particularly in the area of chemical enhancement for fingermarks on a variety of substrates.

Chemical enhancement methods such as ninhydrin, DFO and 1, 2 indanedione are primarily used on porous surfaces such as paper. These methods depend upon the detection of amino acids present in fingermark residue. This is due to the fact that amino acids have a strong affinity for paper fibres and therefore do not readily migrate through such matrices (Jelly ***et al.,*** 2009; Becue ***et al.,*** 2010). The usual protocol involves either dipping or spraying the item with a solution of the amino acid reagent followed by heating. The resulting fingermark can then be photographed to enable subsequent examination (Jelly ***et al.,*** 2009).

1.1.4.4.1 Ninhydrin

Ninhydrin (2, 2-dihydroxy-1, 3-indanedione) was the first chemical enhancer to be utilised to visualise the presence of amino acids within latent fingermarks,

(Oden and Von Hofsten, 1954). Siegfried Ruhemann initially synthesised ninhydrin and determined its ability to react with amino acids in 1910, after he observed a colour change when the reagent got on his skin. The subsequent purple colour change is now commonly known as “Ruhemann’s purple”, (Almog ***et al.,*** 2000; Jelly ***et al.,*** 2009; Becue ***et al.,*** 2010). Figure 1.11 shows the generally accepted reaction mechanism between ninhydrin and amino acids to form Ruhemann’s purple. Ninhydrin is still widely used as a fingermark enhancer on porous surfaces, but one limitation is the poor contrast when visualising marks developed on dark substrates. This problem has been overcome by employing post-ninhydrin treatments incorporating metal salts. A fluorescent coordination complex is formed in the reaction between Ruhemann’s purple and the metal salts, and the colour observed depends on the metal salt employed in the reaction (Becue ***et al.,*** 2010).

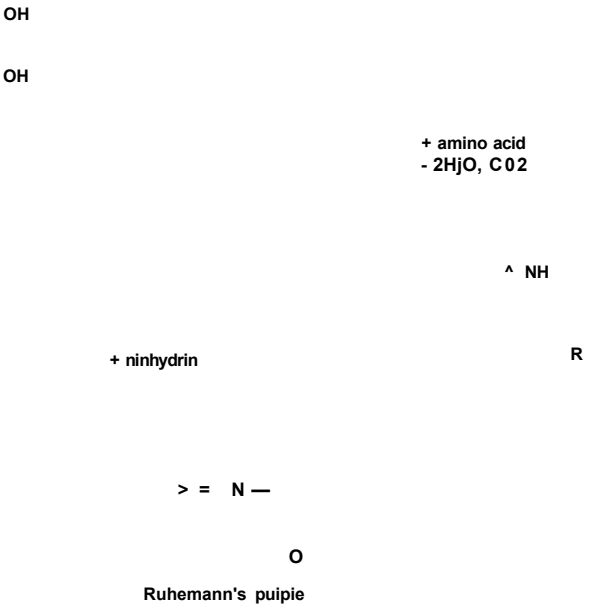

Figure 1-11: The generally accepted reaction mechanism between ninhydrin and amino acids to form Ruhemann’s purple.

Figure obtained from Bleay et al. (2012).

1.1.4.4.2 1, 8-Diazafluoren-9-one

1, 8-Diazafluoren-9-one (DFO), is a ninhydrin analogue which is another amino acid reagent that has been utilised for visualising fingermarks on porous surfaces, (Wilkinson, 2000; Jelly ***et al.,*** 2009; Becue ***et al.,*** 2010). The use of DFO as a fingermark enhancing reagent was first reported in 1990 by Grigg and Mongkolaussavaratana. The paper discussed the reaction of DFO with a-amino acids, resulting in a red-coloured product that was highly fluorescent (Grigg and Mongkolaussavaratana, 1990), which offers an advantage over ninhydrin, as fluorescent results are achievable in one step rather than two. Figure 1.12 shows the proposed reaction mechanism between DFO and amino acids.

Figure 1-12: The proposed reaction mechanism between 1, 8, - Diazafluoren-9-one (DFO) and amino acids.

Figure obtained from Bleay et al. (2012).

1.1.4.4.3 1, 2-Indanedione

1, 2-Indanedione is another fingermark reagent that effectively enhances fingermarks on porous substrates, resulting in pink fingermarks that are strongly luminescent at room temperature. Furthermore, luminescence can be substantially improved by the addition of zinc chloride to the working solution prior to treating the substrate (Wallace-Kunkel ***et al.,*** 2007). For this reason, together with the faster enhancement time, 1, 2-Indanedione is replacing DFO as the method of choice for fingermarks recovered from porous surfaces by many forensic laboratories (Becue ***et al.,*** 2010). Figure 1.13 shows fingermarks developed on paper by 1, 2 - Indanedione and visualised in reflected and fluorescent light.

Figure 1-13: Fingermarks developed on paper by 1, 2- Indanedione and imaged under (a) reflected light, and (b) fluorescent light

Image obtained from Bleay et al. (2012).

1.1.5 Analytical Techniques for the Analysis of Latent Fingermarks

Although there are numerous enhancement methods available, the need for more efficient methods for the detection of latent fingermarks remains. A number of analytical techniques have been used to aid fingermark ridge pattern detection, whilst simultaneously providing information regarding the chemical constituents present, which can be either endogenous or exogenous. These

techniques are potentially useful in three ways: (1) to provide a more detailed understanding of what constituents are present within aged fingermarks and hence which method of enhancement would achieve the best result; (2) to provide useful information such as the presence of exogenous compounds or biomarkers, which may give some indications of the donor's lifestyle or health conditions respectively; (3) to provide an image of the fingermark for suspect identification. These analytical techniques include: Raman spectroscopy (Day *et al.,* 2004a and 2004b; Went and West, 2008 and 2009), Attenuated Total Reflectance - Fourier Transform Infrared (ATR-FTIR) Spectroscopy (Ricci *et al.,* 2007a and 2007b), antibody-magnetic particle conjugates (Hazarika *et al.,* 2009; Boddis and Russell 2011), Gas Chromatography - Mass Spectrometry (GC-MS) (Archer *et al.,* 2005; Croxton *et al.,* 2006; Croxton *et al.*, 2010), Laser Desorption/Ionisation Time-of-Flight Mass Spectrometry (LDI-TOF-MS) (Emerson *et al.*, 2011), Surface Assisted Laser Desorption Ionisation - Time-of-Flight - Mass Spectrometry (SALDI-TOF-MS) (Rowell *et al.,* 2009; Benton *et al.,* 2010), Desorption Electrospray Ionisation - Mass Spectrometry Imaging (DESI-MSI) (Ifa *et al.,* 2008), Secondary Ion - Mass Spectrometry (SIMS) (Bright *et al.*, 2012) and Matrix Assisted Laser Desorption Ionisation – Mass Spectrometry Imaging (MALDI-MSI) (Wolstenholme *et al.,* 2009).

1.1.5.1 Exogenous Compounds Present in Fingermarks

The majority of investigations into the presence of exogenous species have focussed on drugs and their metabolites. Raman spectroscopy for example has been used by various research groups to analyse the presence of drugs of abuse within latent fingermarks. Day *et al.* (2004a) reported its use to detect five drugs of abuse and five compounds, known to be common cutting agents, within "spiked" (artificially loaded with the exogenous compound) ungroomed

(non-sebum enriched) and groomed (sebum loaded) fingermarks. The spectra obtained from the "spiked" ungroomed fingermarks matched the corresponding reference spectra, with no interferences from endogenous components, therefore, enabling each of the ten compounds to be easily identified. The Raman spectra of the "spiked" groomed (sebum-rich) fingermarks were of a poorer quality, with higher background fluorescence due to the presence of sebum. The same authors also reported the possibility of using Raman to detect the same exogenous compounds within sweat rich fingermarks after development by cyanoacrylate fuming (Day *et al.,* 2004b). The authors stated that although all ten compounds could be distinguished by their Raman spectra, the background fluorescence was greater than in the reference spectra due to the presence of the cyanoacrylate polymer and the intensities of the Raman bands were poorer. Raman spectroscopy incorporating a confocal microscope has also been employed to detect drugs of abuse and over the counter analgesics in fingermarks, after dusting with powders and lifting with adhesive tape or hinge lifters. Further analysis of the lifted fingermarks was carried out without removing them from their evidence bags, with all the dopants identified from their Raman spectra (West and Went 2008; West and Went 2009). More recently, Surface Enhanced Raman Spectroscopy (SERS) has been used to image the distribution of acetaminophen in a "spiked groomed fingermark after deposition on a highly reflective slide (Connatser *et al.*, 2010).

SALDI-TOF-MS has also been used to detect illicit drugs and their metabolites in fingermarks after dusting with a silica powder and lifting. The technique enabled mass spectra to be acquired showing the presence of codeine, cocaine, diacetylmorphine, morphine, papaverine and noscapine within fingermarks, the identity of which was confirmed by tandem mass spectrometry (MS-MS) (Rowell

et al., 2009). SALDI-TOF-MS also enables images of analyte distribution to be obtained within fingermarks. However, at present, due to the very low spatial resolution of the technology, the images of the ridge pattern are of insufficient quality for identification purposes (Rowell *et al.,* 2009; Benton *et al.,* 2010).

One technique that is capable of producing high resolution images showing clear ridge detail, as well as the distribution of drugs and drug metabolites within latent fingermarks incorporates fluorescently tagged antibody-magnetic particle conjugates (Hazarika *et al.,* 2009; Boddis and Russell 2011; Boddis and Russell 2012). One of the benefits of the technique is the possibility to simultaneously detect the presence of the drug as well as enabling the identity of an individual to be ascertained, simply by application of the conjugated magnetic powder. The antibody bound to the magnetic particles can be altered in order to detect different illicit substances or their metabolites, based on the antigens present. Thus the main disadvantage of the technique is that it is only feasible if prior knowledge of the drugs involved is known.

Despite the advances made by the analytical techniques described above, the analytes of interest were exogenous species, in particular drugs of abuse rather than endogenous compounds. Although some of the techniques enable fingermark images to be reconstructed, as well as providing potential forensic evidence, valuable information will only be gained in the minority of cases where these contaminants are actually present.

1.1.5.2 Endogenous Compounds Present in Fingermarks

Besides the detection of exogenous compounds, the endogenous chemical composition of latent fingermarks can also be investigated by a range of

analytical methods, some of them allowing images of endogenous constituents to be obtained.

GC-MS has previously been employed to detect fatty acids and amino acids within latent fingermarks (Archer *et al.*, 2005; Croxton *et al.,* 2006; Croxton *et al.*, 2010). Changes in the lipid composition have also been demonstrated by Archer and colleagues (Archer *et al.,* 2005) using GC-MS, who reported substantial differences in the quantities of various fatty acids present in the fingermarks obtained from five male donors, as well as differences over time, thus supporting previous findings achieved by thin layer chromatography (TLC) (Dikshitulu *et al.,* 1986). Although both GC-MS and TLC are not imaging techniques, the authors have stated the potential of the methodologies to determine the age of a fingermark located at a crime scene from its chemical composition, providing corresponding fingermarks can be obtained from a suspect for comparison. However, as both GC-MS and TLC are destructive techniques, they are unlikely to ever be applied on real crime scene samples.

A further analytical development has been the use of ATR-FTIR spectroscopic imaging to obtain both chemical information and distribution images of endogenous lipids and amino acids within latent fingermarks from various donors (Ricci *et al.,* 2007a). ATR-FTIR offers several advantages as it is a non-destructive technique, which requires no sample preparation. Fingermark ageing was also investigated and a general decline in the absorbance of key lipid spectral bands was observed as the ageing temperature increased, which was hypothesised to be the result of the degradation of higher molecular weight constituents to lower ones, which is in agreement with previous studies concerning the changes in lipid composition as fingermarks age (Archer *et al.*, 2005). A major limitation of the methodology applied by Ricci and collaborators

(Ricci *et al.,* 2007a) was that the technique required deposition of fingermarks onto a zinc selenide (ZnSe) crystal, which is not realistic in terms of real crime scene scenarios. This limitation was addressed in a subsequent investigation (Ricci *et al.,* 2007b), in which a gelatine tape was employed to recover latent fingermarks from various non-porous surfaces, before analysis by ATR-FTIR.

Although the use of ATR-FTIR spectroscopy enables images to be generated showing the distribution of specific functional groups and chemical bonds present within fingermarks, the technique is unable to provide unequivocal identification of a species within a fingermark due to poor chemical specificity. This problem is overcome using mass spectrometry techniques such as DESI-MSI, SIMS and MALDI-MSI, as they allow the distribution map of the specific compounds present within the fingermark to be obtained, as determined by their mass-to-charge ratio *(m/z).*

DESI-MSI has recently emerged as a novel approach to image both endogenous lipids and exogenous compounds such as drugs of abuse and explosives within "spiked" fingermarks (Ifa *et al.,* 2008). The technique was able to generate images of fingermarks lifted from plastic and metal substrates, without affecting the spatial resolution of the components present. The nature of DESI-MSI allows an only partially-destructive analysis that requires no sample preparation and allows analysis of samples at atmospheric pressure. Furthermore, DESI can be coupled with a portable mass spectrometer, thus allowing *in situ* crime scene analysis. Although DESI-MSI has greater chemical specificity than vibrational spectroscopic techniques, it still presents low sensitivity and image resolution.

The limitations in sensitivity and the inadequate imaging capabilities of many analytical techniques have led to the need to seek other approaches that are, robust, sensitive and multi-informative. Amongst the techniques recently emerging, MALDI-MSI can be considered a cutting edge technology. In a recent study, Francese's group applied MALDI-MSI, for the first time, to the analysis and imaging of latent fingermarks (Wolstenholme *et al.*, 2009). MALDI- MSI was employed to generate distribution images of a number of endogenous lipids within ungroomed fingermarks thus suggesting a superior sensitivity to DESI-MSI and of course a superior specificity to spectroscopic techniques such as Raman and ATR-FTIR Imaging. Compared to DESI, the wider mass range exploitable also suggests the potential versatility of MALDI-MSI to detect and image a large range of endogenous biocompounds in fingermarks from amino acids to proteins. The possibility of detecting hundreds of ions in a single analysis allows several images of the same fingermark to be generated and, if necessary, overlaid. The possibility to detect and map both endogenous and exogenous substances could potentially be used to obtain information on the lifestyle of the donor (Benton *et al.*, 2010; Boddis *et al.*, 2011). Furthermore, the spatial resolution (150 µm x 150 µm) at which the images were acquired is sufficient to enable the *minutiae* to be observed, making the technology suitable for suspect identification at a comparable level to the conventional methods currently employed. In the study, Wolstenholme and co-workers also demonstrated the potential of MALDI-MSI to successfully retrieve images of aged groomed fingermarks after subjecting fingermarks to three temperatures (4°C, 37°C and 60°C) for seven days. Finally, as the applied matrix could be removed and the fingermark subsequently enhanced by the more conventional method of powdering, MALDI-MSI was proven to be only partially-destructive.

1.2 Mass Spectrometry Instrumentation

Mass spectrometry (MS) is a powerful analytical technique that measures the mass to charge ***(m/z)*** ratio of gas-phase ions and their relative abundance, resulting in a mass spectrum. It can be used to identify and characterise a wide range of compounds from biomolecules to drugs and their metabolites.

There are three fundamental components to a mass spectrometer (figure 1.14):

- The ionization source
- The mass analyser
- The detector

Ionisation sources and mass analysers will be discussed in more detail in sections 1.2.1 and 1.2.2 respectively.

Figure 1-14: Simplified schematic showing the layout of a typical mass spectrometer.

A sample introduced into the mass spectrometer undergoes ionisation in the ion source, producing gas-phase ions that are subsequently separated according to their m/z ratio in a mass analyser before detection, generating a mass spectrum.

1.2.1 Ionisation Sources

A range of different ionisation sources are employed in mass spectrometry depending on the required application. These include, but are not restricted to:

electron ionisation (EI), chemical ionisation (CI), Electrospray Ionisation (ESI), Desorption Electrospray Ionisation (DESI), Direct Analysis in Real Time (DART), Secondary Ion Mass Spectrometry (SIMS), Laser Ablation Electrospray Ionisation (LAESI) and Matrix Assisted Laser Desorption Ionisation (MALDI). Each ionisation source has different attributes including the exploitable mass range and the energies involved in the ionisation process. DART, ESI, DESI and MALDI are considered "soft" ionisation techniques as they produce little (or no) fragmentation, making them ideally suited for the analysis of higher molecular weight species such as proteins and other biopolymers. MALDI is the ionisation source employed in the present study as it is ideally suited for the analysis of latent fingermarks due to its tolerance to contaminants such as salts, its versatility, its low-femtomole detection limits and its ability to work in imaging mode.

1.2.1.1 Matrix Assisted Laser Desorption Ionisation Mass Spectrometry (MALDI-MS)

The principle of MALDI-MS was initially described in 1985 by Karas and co-workers (Karas *et al.*, 1985) and subsequently applied as an ionisation technique by two different research groups in the late 1980s, which led to some controversy over who developed the methodology first (Karas and Hillenkamp, 1988; Tanaka *et al.*, 1988). MALDI is a soft ionisation technique, resulting in no (or little) fragmentation, which produces predominantly singly charged gaseous ions from non-volatile, thermally labile compounds such as proteins (Gasilova *et al.*, 2012; Bechara *et al.*, 2012), polymers (Jagtap and Ambre, 2005), oligosaccharides (Park *et al.*, 2012), lipids (Pannkuk *et al.*, 2012), microorganisms (Xiao *et al.*, 2012) and pharmaceuticals (Kafka *et al.*, 2011). A typical MALDI experiment involves the application of an organic matrix to the

sample, which co-crystallises with the analytes present. Upon irradiation with a laser, the matrix initially absorbs the emitted laser energy, resulting in desorption and ionisation of the matrix-analyte co-crystals (figure 1.15). Commonly used ultra-violet (UV) lasers include nitrogen (N_2) and neodymium-doped yttrium aluminium garnet (Nd:YAG), which emit energy at 355 nm and 337 nm respectively.

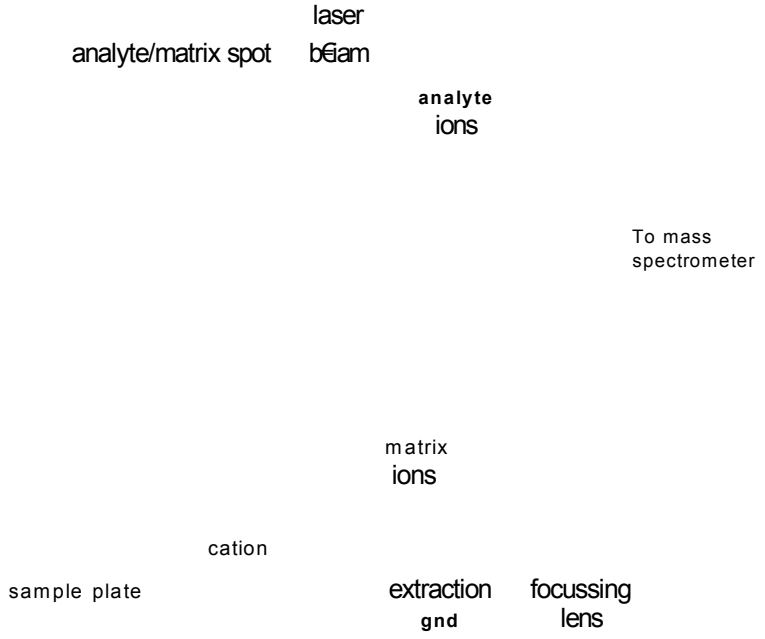

Figure 1-15: A schematic diagram of the process of matrix assisted laser desorption ionisation mass spectrometry (MALDI-MS).

The laser irradiates the solid matrix/analyte co-crystals, resulting in desorption and ionisation of the gas-phase ions, followed by mass analysis in the mass spectrometer. Image obtained from www.chm.bris.ac.uk.

Desorption occurs after the sample under investigation is irradiated by the laser. It is hypothesised that this initially induces fast heating of the matrix-analyte co-crystals in the solid phase through vibrational excitation of the matrix molecules. This incites localised sublimation of the matrix crystals and ablation of the crystals surface, resulting in an expansion of the matrix into the gas phase,

within the clusters formed with the analytes (Dreisewerd, 2003). As laser irradiation results in removal of bulk volumes of matrix and sample, ablation has recently been deemed a more appropriate term than desorption for the subsurface nucleation and subsequent phase explosion that occurs (Knockenmuss, 2006).

The ionisation mechanism in UV-MALDI is an extremely complex phenomenon. The current consensus is that a two-step procedure incorporating primary ionisation mechanisms followed by secondary ion/molecule reactions occurs (Knochenmuss, 2006).

The photoexcitation/pooling model and the cluster model are the two prominent theories currently proposed for primary ionisation in MALDI. The former proposes that the excited matrix is fundamentally involved in the ionisation process, whereas the latter argues the matrix only behaves as a desorption vehicle and the ions are pre-formed in clusters (Karas *et al.*, 2000; Karas and Kruger, 2003; Knochenmuss, 2006). Besides the two principal models, other primary ionisation mechanisms have been proposed including: excited state proton transfer, the polar fluid model and direct multi-photon ionisation of the matrix or matrix/analyte complexes (Knochenmuss, 2006).

The secondary reactions that occur in MALDI after primary ionisation result in secondary ions which are subsequently detected. The secondary reactions that can potentially occur include; proton transfer, cationization and electron transfer (Knockenmuss and Zenobi 2003; Knochenmuss, 2006).

At present for MALDI analysis in positive mode, the most widely accepted theory is that of proton transfer from the photo-ionised matrix molecules to the analytes, either in the solid phase prior to desorption (co-crystals matrix/analyte),

or in the gas phase in the ensuing desorption plume (Hoffmann and Stroobant, 2009).

1.2.2 Mass Analysers

The separation of ions according to their different mass to charge *(m/z)* ratios can be achieved by different physical principles. There are currently seven mass analysers available on the market: magnetic sector, quadrupole, time of flight (TOF), ion trap, orbitrap, ion mobility and Fourier Transform ion cyclotron resonance (FT-ICR) and each has its benefits and limitations (Pol *et al.*, 2010). Different mass analysers are often combined in sequence to enhance versatility and enable multiple experiments to be performed (Hoffman and Stroobant, 2009). Examples are the triple quadrupole (QQQ), or hybrid instruments such as the quadrupole-TOF (Q-TOF) or the quadrupole-ion trap (QTrap) (Hoffmann and Stroobant, 2009). TOFs and Q-TOFs are the commonest mass analysers employed in MALDI instruments and these were used in the present study.

1.2.2.1 Quadrupole

Originally developed by Paul and co-workers, the quadrupole mass analyser separates ions according to their *m/z* ratio, based on the stability of their trajectories in an oscillating electric field (Paul and Steinwedel, 1960). Quadrupoles are composed of four parallel hyperbolic rods, with opposing rods connected electrically. A radio frequency (RF) voltage is applied to each of the opposing pairs together with a direct current (DC) voltage. Ions entering the quadrupole from the ion source travel between the four rods and are repelled by the changing potentials of the rod pairs, resulting in the oscillating flight path depicted in figure 1.16. Quadrupole mass analysers can be operated in either full scan or selected ion monitoring (SIM) modes. In SIM mode, changing the RF ensures only ions of a certain *m/z* ratio have stable trajectories and traverse

the quadrupole, ions with unstable trajectories collide with the rods and do not reach the detector (Hoffmann and Stroobant, 2009). Quadrupole mass analysers are low resolution instruments, typically 2,000 at full width at half mass (FWHM) (*m/z* 1000) and have a limited mass range (up to *m/z* 4,000), although they show excellent selectivity.

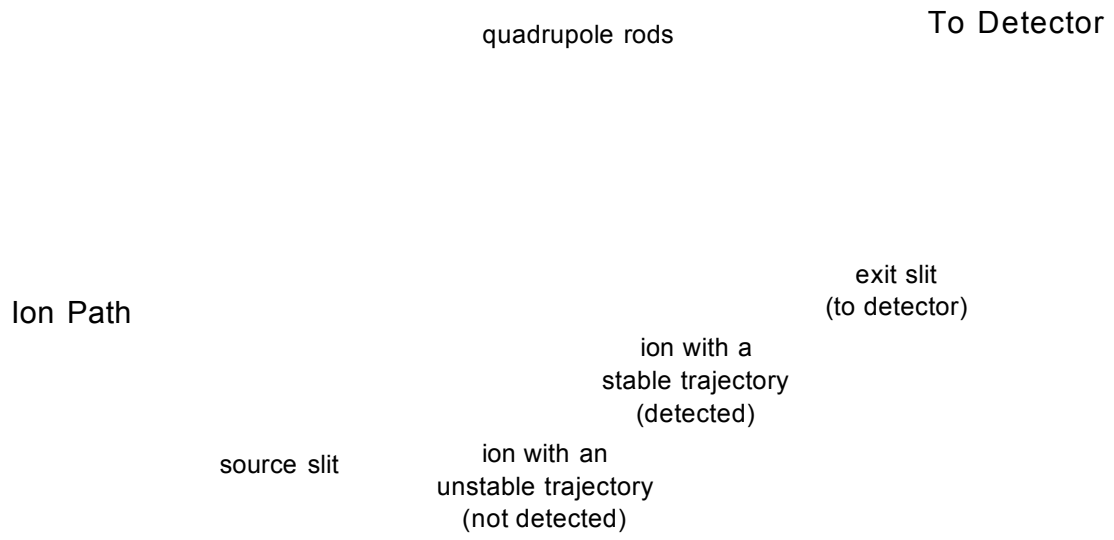

Figure 1-16: Schematic depicting the flight of an ion through a quadrupole mass analyser.

Image adapted from www.chm.bris.ac.uk

1.2.2.2 Time of Flight

Time of Flight (TOF) analysers are ideally suited to pulsed ionisation sources such as MALDI and provide good mass resolution, with a mass resolving power of 40,000 (FWHM) achievable with modern instruments. In TOF mass spectrometers, ions are separated in time, based on their velocity, after being subjected to an applied electric field and accelerated in a field-free region between the source and the detector. As each ion has the same initial kinetic energy, smaller ions travel faster than larger ions and hence reach the detector

first (Chernushevich *et al.*, 2001; Hoffmann and Stroobant, 2009). The benefits of TOF mass analysers include the wide mass range available and their high sensitivity, resulting from the sequential detection of all the ions of differing *m/z* and the high transmission efficiency.

TOF instruments can be operated in linear or reflectron mode. In linear mode, ions are accelerated into the TOF mass analyser at a specific electric field and travel the length of the TOF drift tube to the detector. The relationship between the *m/z* of a given ion and the time (t) required to drift a fixed distance (d) before reaching the detector is shown in equation 1.1, where *t* is the time required to cover the distance *L* before reaching the detector, *m* is the mass of the ion and *z* its charge, and *Vs* is the acceleration potential.

$$t^2 = \frac{m}{z}\left(\frac{L^2}{2eVs}\right)$$

Equation 1-1: The relationship between the m/z of a given ion and the time required to drift the length of a TOF mass analyser.

In TOF analysers, mass resolution is proportional to the flight path and the flight time. One of the most significant limitations of early linear TOF instruments was the inadequate mass resolution. Various factors contributed to the distribution in drift times of ions with the same *m/z*, which resulted in poor mass resolution and hence mass accuracy including; differences in the initial kinetic energy spread of the ions produced in the ion source, the duration of the ion formation pulse and the magnitude of the volume where the ions were created (Hoffmann and Stroobant, 2009).

Delayed extraction provides one means of improving mass resolution and hence mass accuracy by correcting the kinetic energy distribution of ions of identical *m/z* ratios after their ejection from the source. Continuous extraction involves immediate extraction of the ions by a continuously applied voltage. This often results in ions with the same *m/z* ratio reaching the detector at different times, due to differences in their initial kinetic energies. Conversely, delayed extraction involves a time delay between ion formation and extraction, in order to compensate for the initial differences in kinetic energy of ions leaving the source. For ions of the same *m/z*, those with more kinetic energy travel nearer to the detector than those with less energy initially. The extraction pulse applied after the pre-determined time delay delivers additional energy to the ions which remained in the source for a longer duration. These ions are thereby provided with more kinetic energy, so that ions with the same *m/z* reach the detector simultaneously, thereby improving mass resolution (Lennon, 1997; Bahr, 1997; Hoffmann and Stroobant, 2009).

For lower molecular weight species (less than 2000 Da), mass resolution can be improved further by utilising an electrostatic reflector, otherwise known as a reflectron. Reflectron TOF instruments compensate for the kinetic energy spread of ions leaving the source with the same *m/z* ratio. The reflectron provides a charged field that effectively behaves as an ion mirror by deflecting ions back along the drift tube prior to detection, thereby doubling the length the ions travel. Ions with greater kinetic energy penetrate further into the reflectron than those with lower energy and hence travel a slightly longer flight path. This compensates for differences in velocity at which ions with the same *m/z* ratio are travelling, resulting in their simultaneous detection (Cotter *et al.*, 2004;

Hoffmann and Stroobant, 2009). Figure 1.17 displays schematic diagrams of a TOF instrument in both linear and reflectron modes.

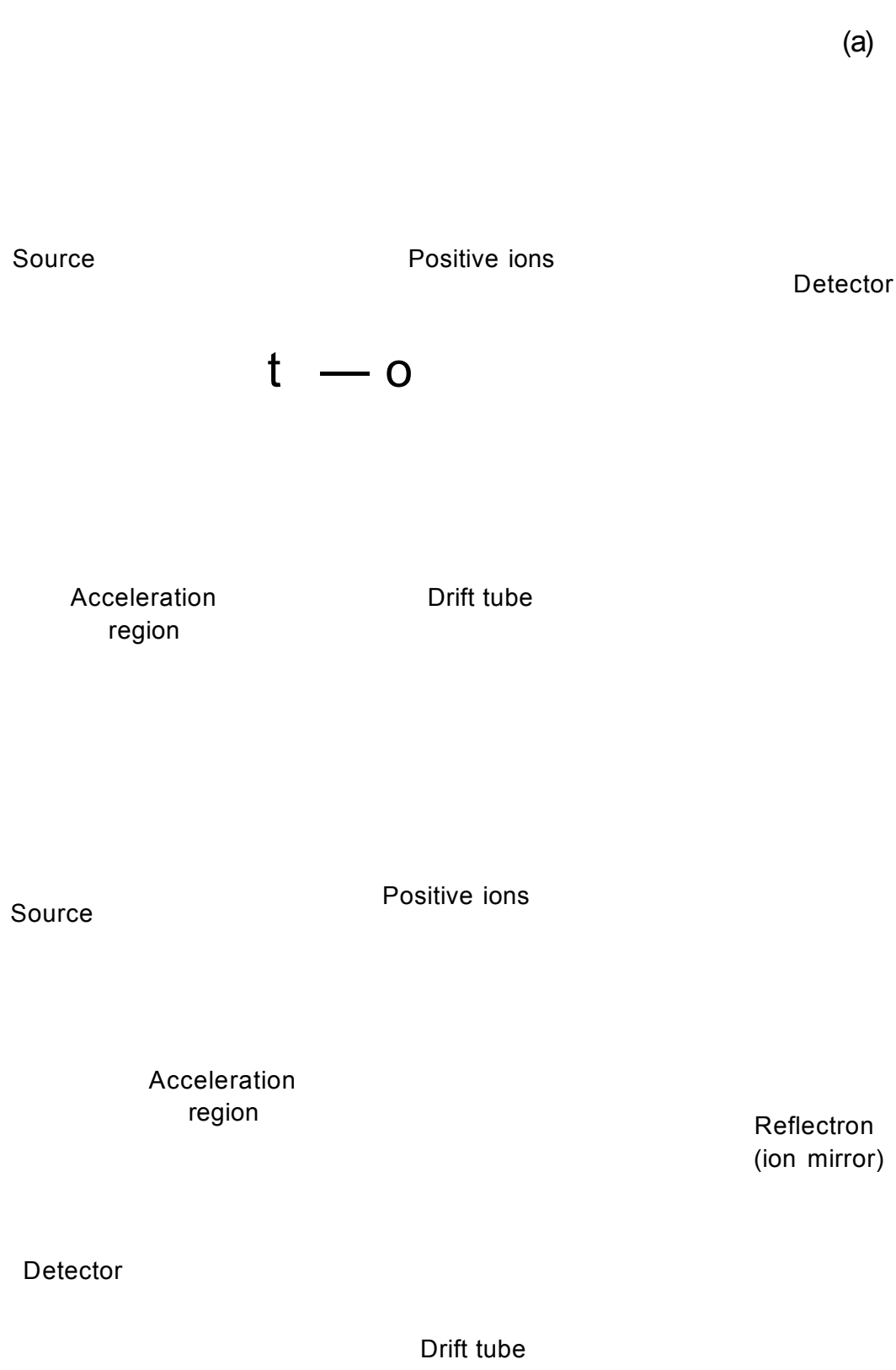

Figure 1-17: A schematic of a time of flight mass spectrometer operating in (a) linear mode, and (b) reflectron mode, showing the flight path of the ions through the field-free drift tube.

Image adapted from Hoffmann and Stroobant (2009) and Lennon (1997).

The peptide/protein work presented in chapter 3 of this thesis was acquired on a Voyager De-STR TOF mass spectrometer operating in linear mode, as the species being investigated had molecular weights ranging between 2000 and 17000 Da. Delayed extraction was employed to correct for variations in the kinetic energies of ions with the same *m/z*.

1.2.2.3 Tandem Instruments

Quadrupoles and TOF mass analysers can be combined resulting in the hybrid QqTOF instrument, where q refers to an RF- only collision cell (Baldwin *et al.*, 2001; Chernushevich *et al.*, 2001). QqTOF instruments such as the Q-Star Pulsar-*i* (Applied Biosystems, Foster City, CA, USA), which was employed in the present study, comprise three quadrupoles (Q0, Q1 and Q2), followed by an orthogonal acceleration TOF (oaTOF) mass analyser. In oaTOF, the ions are accelerated into the drift tube at approximately 90° to their initial direction of travel, which eliminates any experimental discrepancies in the original starting point of the ions as the performance of the mass analyser is independent of the ionisation step (McDonnell and Heeren, 2007).

QqTOFs such as the Q-Star Pulsar-I (Applied Biosystems, Foster City, CA, USA) provide high mass resolution (20,000 FWHM), high sensitivity (femtomole) and high mass accuracy (<10 ppm) in both precursor (MS) and product ion (MS/MS) modes. When used in MS mode, the three quadrupoles act as RF-only ion guides and mass resolution is achieved in the TOF analyser. When used in MS/MS mode, the precursor ion selected in Q1 undergoes collision-induced dissociation (CID) in Q2. The resulting product ions subsequently undergo mass analysis in the oaTOF mass analyser (Baldwin *et al.*, 2001; Chernushevich *et al.*, 2001). MALDI QqTOF mass analysers have been utilised in a wide range of applications including: proteomics (Baldwin *et*

al., 2001; Darie *et al.*, 2005), lipidomics (Trim *et al.*, 2008a; Hart *et al.*, 2011), metabolomics (Burrell *et al.*, 2007), forensic science, (Wolstenholme *et al.*, 2009; Bradshaw *et al.*, 2011; Ferguson *et al.*, 2011; Ferguson *et al.*, 2012) and pharmaceuticals (Bunch *et al.*, 2004; Trim *et al.*, 2008b). Figure 1.18 shows a schematic of the Applied Biosystems/MDS Q-Star Pulsar-*i* mass spectrometer, depicting the QqTOF mass analyser and MALDI ionisation source.

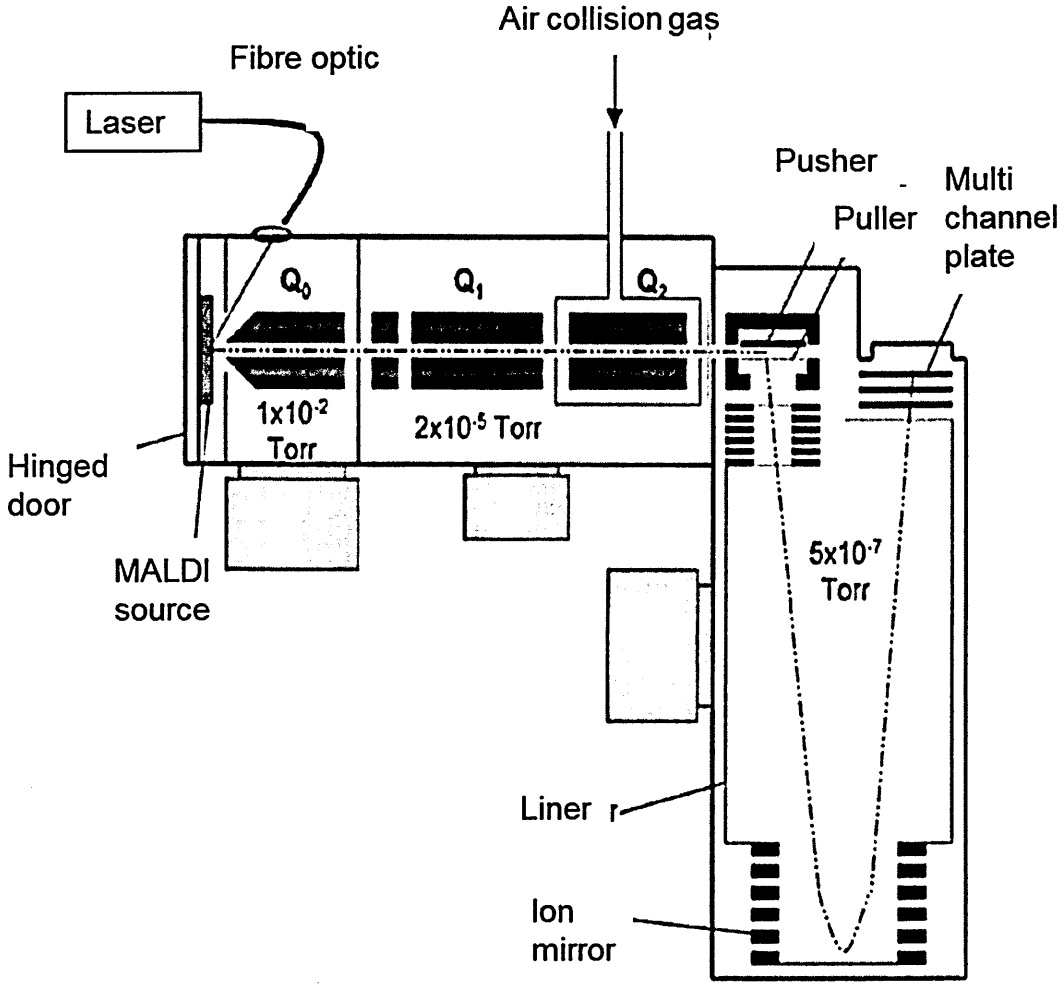

Figure 1-18: Schematic of the Applied Biosystems/MDS Q-Star Pulsar-i mass spectrometer, showing the layout of the QqTOF mass analyser together with the MALDI ionisation source.

Image adapted from Baldwin et al. (2001).

1.2.3 Ion Mobility Separation

Ion mobility separation (IMS) has been employed in a variety of research areas. Its forensic applications include: the detection of explosives (Ewing *et al.*, 2001; Eiceman *et al.*, 2004; Oxley *et al.*, 2008; Cook *et al.*, 2010), drugs of abuse (Verkouteren *et al.*, 2011; Hall *et al.*, 2012), ignitable liquids from fire debris (Lu and Harrington, 2007) and even chemical warfare agents (Kolakowski *et al.*, 2007; Makinen *et al.*, 2010).

Ion mobility spectrometers can be stand-alone instruments or used in conjunction with other analytical techniques such as gas chromatography (Kanu *et al.*, 2008a), liquid chromatography (Kaur-Atwal *et al.*, 2011) and mass spectrometry (Djidja *et al.*, 2009). When used in conjunction with mass spectrometry, ion mobility not only separates gas phase ions according to their *m/z*, but also their shape (collisional cross section), enabling the separation of isobaric species with a reduction in chemical noise. In conventional IMS, ions are separated in drift tubes based on their mobility differences as they migrate through an inert buffer gas in the presence of a constant electric field. The mobility of an ion can be calculated from its observed drift time, which in turn can be used to derive gas-phase collisional cross-sections (Ω) using the following equation:

$$\Omega = \frac{3_{ze}}{16N}\left[\frac{2_{\pi}}{\mu k_{b\mathrm{T}}}\right]^{0.5}\frac{1}{K_0}$$

Equation 1-2: Calculation of gas phase collisional cross-sections in ion mobility

Where N is the background gas number density, Ze the ionic charge, μ the reduced mass of the ion neutral pair, K_b is Boltzmann's constant, T is the gas

temperature and *K*o is the reduced mobility (measured mobility corrected to 273.2 Kelvin and 760 Torr).

Whereas previously, IMS was only possible with gas-phase samples, the development of MALDI (Gillig *et al.*, 2000) and electrospray (Shumate and Hill, 1989) as ion sources for IMS, has extended its applicability to solid-phase and aqueous samples (Kanu *et al.*, 2008a).

Four types of ion mobility spectrometers can be employed with mass spectrometers: they are drift time (Cohen and Karasek, 1970), differential (Buryakov *et al.*, 1993), aspiration (Sacristan and Solis, 1998) and travelling wave (Giles *et al.*, 2004), and each can be interfaced to various mass spectrometers such as magnetic sector, quadrupoles, TOF or tandem instruments (Kanu *et al.*, 2008b).

Recently various advances have been implemented to overcome the inadequate sensitivity issues associated with linear IMS in drift tube devices when coupled to mass spectrometers. These advances include the development of Travelling Wave IMS (TWIMS), which incorporates a travelling voltage wave in a RF ion guide (Giles *et al.*, 2004). TWIMS is discussed in more detail below in section 1.2.3.1.

1.2.3.1 Travelling Wave Ion Mobility Separation (TWIMS)

Travelling Wave Ion Mobility Separation (TWIMS) involves propelling ions through a RF-only stacked ring ion guide (SRIG) by superimposing a repeating pattern of a DC voltage on the confining RF of an electrode, and then transferring the DC pulse onto the next electrode in the series (figure 1.19). This causes the ions to "surf" through the ion mobility cell on the resulting travelling wave in the presence of a buffer gas, where they are separated according to

their average collisional cross sectional area and *m/z* (Giles *et al.,* 2004). The use of elevated pressures within the SRIG ensures ions with lower mobility are overtaken by the travelling waves more frequently than ions with a higher mobility, resulting in these ions being periodically "trapped" behind the waves, increasing their overall drift times within the IMS cell (Smith *et al.,* 2009).

Figure 1-19: A stacked ring ion guide.

A stacked ring ion guide (SRIG), where the opposing phases of an RF voltage are applied to adjacent electrodes in the SRIG, prior to the application of a transient dc voltage, thereby providing an incessant succession of "travelling waves" to propel the ions through the IMS cell. Image obtained from Pringle et al. (2007).

TWIMS technology has subsequently been employed in a novel hybrid quadrupole /T-Wave-IMS/oa-TOF instrument developed by Waters Corporation (Manchester, UK) and named the Synapt HDMS system, with improved separating power and transmission of ions (Pringle *et al.,* 2007).

The Synapt G2 is a second generation quadrupole-IMS-oaTOF instrument. The region responsible for ion mobility separation within the instrument is termed the

Tri-Wave. The Tri-Wave comprises two ion guides, the “Trap” and the “Transfer” and the travelling wave ion mobility cell (Pringle *et al.,* 2007). Ions enter the Tri-Wave region, through a helium gate. In the “Trap” region, the ions are guided into the ion mobility cell, where they are separated as described above. Once separated, the ions enter the “Transfer” region, where they are guided into a TOF mass analyser, which can be operated in either single (“V”) or dual (“W”) reflectron modes. Besides guiding ions into and out of the ion mobility cell, the “Trap” and “Transfer” can also act as collision cells for MS/MS. If collision induced dissociation occurs in the “Trap” prior to ion mobility separation, the product ions have different drift times to the precursor ions. If fragmentation is induced after ion mobility, the precursor and product ions have the same drift time. Figure 1.20 shows a schematic of the Synapt HDMS system, which has been used for high mass accuracy measurements and high resolution imaging as part of work presented in chapter 2 of this thesis.

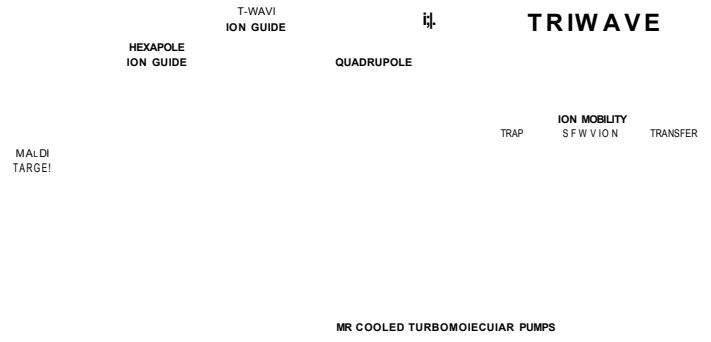

Figure 1-20: A Schematic of the Synapt HDMS system, fitted with a MALDI source.

In the tri-wave region, the "Trap" and "Transfer" act as ion guides, into and out of the ion mobility cell, where gas-phase ions are separated according to their conformation, as well as their m/z. Image obtained from Oppenheimer et al. (2009).

1.3 MALDI Mass Spectrometry Imaging (MALDI-MSI)

Over the last few decades, some mass spectrometry techniques have evolved to include imaging capabilities. Ionisation techniques such as laser ablation electrospray ionisation (LAESI), secondary ion mass spectrometry (SIMS), desorption electrospray ionisation (DESI) and MALDI allow the spatial distribution of the chemical constituents present in a wide variety of samples to be visualised.

LAESI enables depth profiling, which when used with lateral imaging enables three dimensional (3D) images to be acquired, although the lateral resolution is only 100 µm at present. Although LAESI has not been used for imaging latent fingermarks, SIMS (Bright *et al.*, 2012), DESI (Ifa *et al.*, 2008) and MALDI (Wolstenholme *et al.*, 2009) have all been employed in imaging mode to investigate the chemical composition of latent fingermarks. SIMS imaging offers unrivalled spatial resolution, but it has limitations with respect to the mass range that can be exploited, due to in-source fragmentation of larger biomolecules (Amstalden van Hove *et al.*, 2010). Although DESI-MSI requires no sample preparation and is relatively fast, it has limited spatial resolution (approx 200 µm) and low sensitivity (Vickermann, 2011). MALDI-MSI has, therefore, been selected as the primary imaging technique for the work presented in this thesis due to the wider mass range exploitable over SIMS imaging and the enhanced sensitivity and spatial resolution over DESI-MS.

Since Caprioli and collaborators published their first MALDI-MSI paper in 1997, many research areas have benefited from the technology including biomedicine,

pharmaceuticals, biotechnology and recently microbiology (Francese and Clench, 2010). In forensic research, besides fingermarks MALDI-MSI has been employed in the analysis of; drugs of abuse (Mika *et al.*, 2011; Porta *et al.*, 2011), condom lubricants (Bradshaw *et al.*, 2011), dyes (Lovejoy *et al.*, 2012) and blood groups (Gassner *et al.*, 2013). The wide mass range detectable allows images of diverse biomolecules to be acquired including, drugs, lipids, peptides and proteins, without resorting to molecular probes or antibodies. The presence of any compounds of interest can be confirmed using MS-MS.

Whereas MALDI profiling experiments provide molecular profiles of discrete regions on the sample, MALDI imaging experiments enable the spatial distribution of specific ions within a sample to be visualised as shown in figure 1.21. Sample preparation is integral to the success of any MALDI-MSI experiment, with tissue preparation and the choice of matrix (its composition and application), the two most critical parameters.

Initial MALDI-MSI experiments were performed on biological tissues (Caprioli *et al.*, 1997) and tissue preparation prior to matrix application has always been pivotal to the success of MALDI-MSI experiments involving tissues. For biological tissues, the usual protocol involves initially sectioning the tissue of interest using a cryostat. Schwartz and collaborators recommended a tissue thickness of between 10 and 20 μm, due to the ease of handling and robustness of the tissue sections (Schwartz *et al.*, 2003). Other research groups have recommended thinner sections as these dry more quickly, limiting the risk of sample degradation, plus the charging effects are not as prominent (Goodwin *et al.*, 2012). After sectioning, the tissue is typically thaw-mounted onto a MALDI target plate or glass microscope slide, ensuring the tissue retains its shape with minimal degradation or imperfections such as rips.

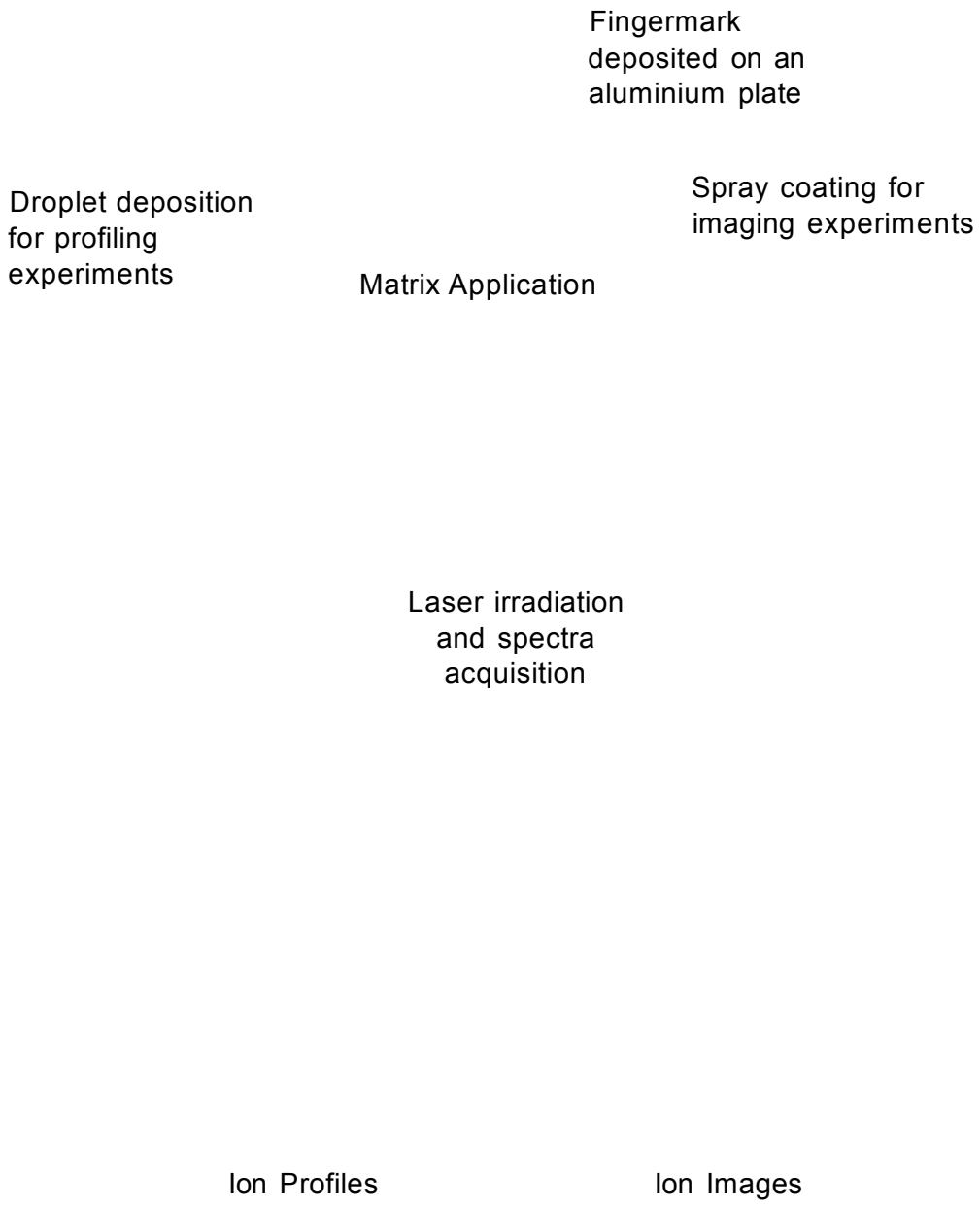

Figure 1-21: Schematic showing the steps involved in MALDI-MS profiling and imaging experiments.

Profiling experiments provide molecular profiles of discrete regions on the sample. Imaging experiments enable the spatial distribution of numerous ions within the sample to be visualised simultaneously.

MALDI-MSI experiments often incorporate a washing step prior to matrix application, in order to remove salts and other impurities that may affect the intensity of the ion signals observed and promote adduct formation (Kaletas *et al.*, 2009). Various washing protocols have been implemented by different research groups. For proteomic studies, the most commonly used protocol involves washing tissues with 70% - 100% ethanol, to remove salts and lipids. Lipids have higher ionisation efficiencies than peptides and proteins, resulting in ion suppression of any proteomic species that may be present in the unwashed tissue (Schwartz *et al.*, 2003; Chaurand *et al.*, 2006). For lipidomics, a recent development has been to wash with either ammonium acetate or ammonium formate at a pH of 6.7 and 6.4 respectively. The washing steps were found to increase the abundance of lipid signals and their intensity significantly, when analysing adult mouse brain sections in negative ion mode, as the electrolytes formed complexes with the ammonium ions, thereby reducing their ion suppression capabilities (Angel *et al.*, 2012).

1.3.1 Matrices for MALDI-MSI

The matrices employed in MALDI-MS are typically weak organic acids, with a strong absorbance at the wavelength of the laser. The matrix chosen essentially absorbs most of the laser energy, minimising fragmentation of the analytes within the sample. The three most common are; α-cyano-4-hydroxycinnamic acid (α-CHCA), 2, 5-dihydroxybenzoic acid (DHB) and 3, 5- dimethoxy-4-hydroxycinnamic acid (sinapinic acid (SA)). DHB and α-CHCA are used primarily for low molecular weight peptides and lipids, whereas SA is mainly used for the analysis of proteins (Goodwin *et al.*, 2012). Other less utilised matrices include; ferulic acid, dithranol, and 9-aminoacridine. Analysis with some of the conventional organic matrices can be problematic, as the matrices

are also ionised, creating strong background peaks particularly in the lower mass range. This can cause ion suppression of the anaytes of interest, or interference due to overlapping peak signals, although this can be partly overcome using various strategies such as ion mobility, high mass resolution analysis or MS/MS (Francese *et al.*, 2009).

Various research groups have advocated combining two matrices. Recently, a binary matrix consisting of DHB and α-CHCA has been reported for the analysis of phospholipids in rat brain tissue. The authors stated that the combined matrix resulted in enhanced signal intensity and signal reproducibility over the conventional matrices alone. Furthermore, the binary matrix enabled MALDI imaging experiments to be performed in both positive and negative modes, which therefore maximises the number of ion signals observed. A major limitation of the matrix system though results from the extensive number of peaks originating from the binary matrix below *m/z* 500, which, therefore, limits its potential for the analysis of lower molecular weight species, as the analyte signal intensity may be suppressed (Shanta *et al.*, 2011).

A relatively recent development is the use of ionic liquid (IL) matrices, which are reported to improve sensitivity and reproducibility and reduce the existence of "sweet spots" in the sample under investigation, as the matrix is reported to crystallise more homogenously, thereby reducing fluctuations in the ion signal intensity. Recently, aniline was combined with α-CHCA for the MALDI-MSI analysis of a variety of biomolecules (Hart *et al.*, 2010; Cole *et al.*, 2010). Similarly, for the analysis of proteins and tryptic peptides, the addition of aniline to SA was shown to improve the signal intensity, resolution and sensitivity compared to using SA alone (Franck *et al.*, 2009). The addition of aniline results in an acid-base reaction between the organic base and the weak organic acid,

which enhances the solubilisation of the solid matrix, aiding crystallisation of the matrix/analyte, thereby improving the results achieved.

Besides the choice of matrix, the method of matrix application is another critical parameter in any MALDI-MSI experiment. Since the first published article on MALDI-MSI by Caprioli and co-workers in 1997, a number of matrix deposition methods have been reported, some of which will be discussed in more detail in chapter 2, section 2.1.

1.3.2 Microscope and Microprobe MALDI-MSI

There are two modes of operation for MALDI-MSI; microscope and microprobe. In microscope MALDI, the area to be imaged is irradiated by a laser with a large diameter beam (typically 200 µm) and the spatial resolution obtained depends on the quality of the ion optics and the detector employed, rather than the laser spot size (Luxembourg *et al.*, 2004; Klerk *et al.*, 2009). Upon irradiation, the resulting ions are subsequently transferred to a TOF mass spectrometer, creating a two dimensional (2D) ion-optical image on a position sensitive detector, therefore maintaining the spatial integrity of the sample.

Microprobe mode is more commonly employed in typical MALDI-MSI experiments. In spot to spot analysis, the UV laser fires automatically, at a series of predetermined positions for a preselected length of time, causing desorption of the analyte and matrix ions. At each x, y coordinate, a mass spectrum is acquired, containing all the mass signals of the species desorbed. Eventually, a collection of mass spectra, each of them being the representation of the local molecular composition of the sample at each x, y coordinate is obtained. The intensities of individual *m/z* values in each spectrum can be extracted to visualise the presence and distribution of that specific ion over the sample (Luxembourg *et al.,* 2004). A recent development involves the use of

continuous raster imaging, which involves the laser firing at the sample continuously for an entire row, before stopping and restarting on the following row. During each row, the software "bins" the acquired data at specified intervals, depending on the spatial resolution and sampling speed selected (Prideaux *et al.*, 2007; Anderson *et al.*, 2009). In microprobe MALDI, the spatial resolution obtained is limited primarily by the diameter of the laser beam, although images have recently been obtained at a lateral spatial resolution of 2 μm using Scanning microprobe MALDI-MS (SMALDI) (Bouschen *et al.*, 2010).

Microprobe MALDI-MSI was employed in the work described in chapter 2 of the current study to image the distribution of species within latent fingermarks.

1.4 Vibrational Spectroscopy

Both Raman and Infrared (IR) spectroscopy enable the vibrational and rotational frequencies of molecules to be investigated, with each peak in a spectrum corresponding to a specific vibrational mode of the chemical bonds present (Smith and Dent, 2005). Selection rules enable us to predict whether a molecular vibration will be IR or Raman active. Raman spectroscopy involves a change in polarizability of the electron cloud surrounding the molecule, with non-polar bonds generating the most intense peaks. Conversely, IR absorption occurs due to a change in the bond dipole moment, with polar bonds producing the most intense peaks (Smith and Dent, 2005; Chalmers *et al.*, 2012). The mutual exclusion rule states that a vibration with a centre of symmetry is Raman active and IR inactive, whereas vibrations which are asymmetric to the centre of symmetry are IR active and Raman inactive. Molecules with different elements of symmetry may be active in IR, Raman, neither or both (Smith and Dent, 2005). For this reason, IR spectroscopy and Raman spectroscopy are considered complementary techniques.

The theory of molecular symmetry enables us to predict the number of IR and Raman bands that result from different modes of vibration. The energy of molecules can be divided into different "degrees of freedom". Three of these describe the translation of the molecule in space, and three describe the rotational movement of the molecule, with the exception of linear molecules, where there are only two possible rotations. If N equates to the number of atoms in a molecule, the number of possible vibrations is 3N – 6 for all molecules, apart from linear molecules where it is 3N-5 (Smith and Dent, 2005).

1.4.1 Raman Spectroscopy and Surface Enhanced Raman Spectroscopy (SERS)

The underlying principle in Raman spectroscopy is that monochromatic radiation interacts with the molecules in a sample, resulting in polarization of the cloud of electrons around the nuclei. Raman spectroscopy involves the inelastic scattering of light. Light from a laser irradiates the sample undergoing analysis, and a proportion of the light incident on the sample is scattered. Most of the scattered light will have the same energy as the incidence beam and is called Rayleigh scattering for molecules. Raman scattering occurs when energy is transferred from the incident photon to the molecules in the sample (Stokes scattering), or from the sample to the scattered photon (ant-Stokes scattering), leading to a slight shift in energy, known as the Raman shift. In Stokes scattering, the molecules in a sample return to a higher vibrational level, and the emitted photon has less energy and therefore a lower frequency (longer wavelength) than the initial photon. In anti-Stokes scattering, the molecules in a sample return to a lower vibrational level, and the emitted photon has more energy and therefore a higher frequency (shorter wavelength) than the initial photon (Pelletier, 1999). Figure 1.22 shows a simplified diagram depicting the changes in energy state for each of the three scattering processes.

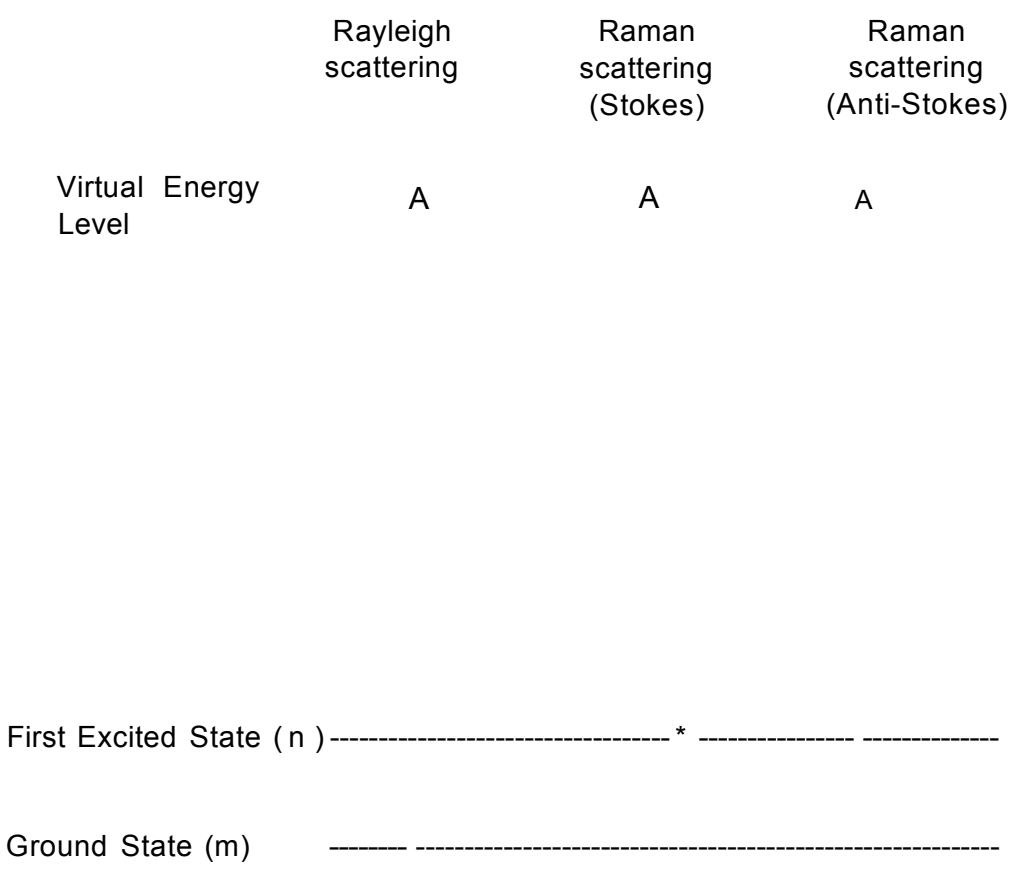

Figure 1-22: A simplified diagram depicting the changes in energy levels in Rayleigh**, **Stokes and anti-Stokes scattering.

1.4.1.1 Surface Enhanced Raman Scattering

Because approximately only one photon out of a million undergoes Raman scattering, the Raman signal is inherently weak for analytes present at low concentrations, such as within fingermarks. Therefore, techniques such as surface enhanced Raman spectroscopy (SERS) may be required to enhance the Raman signal (Popp and Mayerhofer, 2009).

SERS was initially observed by Fleischman and co-workers in 1974, after they observed an increase in Raman scattering from pyridine adsorbed on a roughened electrode (Fleischman *et al.,* 1974). SERS produces a 103-107 amplification of the Raman signal of an analyte when it is adsorbed on the

surface of noble metals incorporating distinct nanoscale properties, (Baena and Lendl, 2004).

Two theories exist as to how the SERS effect occurs. One is termed electromagnetic enhancement, and this involves the analyte of interest being adsorbed onto, or being held in close proximity to the roughened metal surface, resulting in an interaction between analyte and surface plasmons. The other is named charge transfer enhancement or chemical enhancement and involves the analyte chemically bonding to the metal surface, resulting in a transfer of electrons from the metal to the adsorbate and back to the metal surface again (McNay *et al.*, 2011; Cialla *et al.*, 2012). SERS has previously been employed in a number of forensic applications including: the analysis of drugs of abuse, (Ryder, 2005; Bell *et al.,* 2007; Yang *et al.*, 2012), the analysis of dyes found in ball-point pens (Jones and Wolstenholme, 2003; Geiman *et al.,* 2010), the non-destructive identification of synthetic and natural organic colorants in works of art (Leona *et al.*, 2011) and the detection of chemical warfare agents (Stuart *et al.*, 2006; Golightly *et al.*, 2009).

1.4.2 Raman/SERS Instrumentation

Raman instruments typically consist of a high intensity monochromatic light source (generally a laser), a collection of optics and filters, a spectrograph and a detector (Pelletier, 1999). The laser employed as an excitation source can be UV (approximately 10 - 400nm), visible (approximately 400 - 700 nm) or near IR (NIR) (approximately 700 – 950 nm). Visible lasers are predominantly used in Raman instruments, although fluorescence is a major issue. UV lasers offer improved sensitivity, although sample degradation is a potential problem due to the UV absorbing nature of many compounds. The use of NIR lasers eliminates strong fluorescence interferences, and sample degradation is minimised as NIR

lasers operate at a lower frequency than either UV or visible lasers (Smith and Dent, 2005).

The collection of optics and filters which are present within Raman instruments isolate the Raman scattered photons from the intense Rayleigh scattered light and light from other sources which can "flood" the detector and reduce the intensity of the Raman signal. The use of notch filters is popular in many Raman instruments, as these are designed to absorb all light of the frequency of the excitation source, although the quality of the filter dictates the range of frequencies absorbed (Smith and Dent, 2005).

Spectrographs separate the Raman signal into its constituent wavelengths for subsequent detection and processing in order to produce a sample's characteristic Raman spectrum (Pelletier, 1999). Spectrometers can be either Fourier Transform (FT) based or more commonly, dispersive instruments. Fourier transform based spectrometers are usually coupled to an indium gallium arsenide (InGaAs), or a germanium detector, and the excitation source is typically a NIR laser operating at 1064 nm. FT spectrometers are discussed in more detail in section 1.4.3. Dispersive instruments are typically coupled to a charge coupled device (CCD) detector, operating at low temperatures. In dispersive instruments, the Raman scattered light is separated into its composite wavelengths by focussing it onto diffraction gratings, which have closely spaced lines to promote dispersion (Harris, 2010). The spectral resolution achieved with dispersive instruments depends on the number of gratings per unit length and the optical arrangement within the spectrograph.

There are two types of dispersive based spectrometers; monochromators and Echelle. The SERS work presented in this thesis was performed using a

RamanStation 400 benchtop instrument, equipped with a two-dimensional Echelle spectrograph, a NIR laser at an excitation wavelength of 785 nm and a CCD detector. Figure 1.23 shows the principal components of a schematic of the RamanStation 400 series.

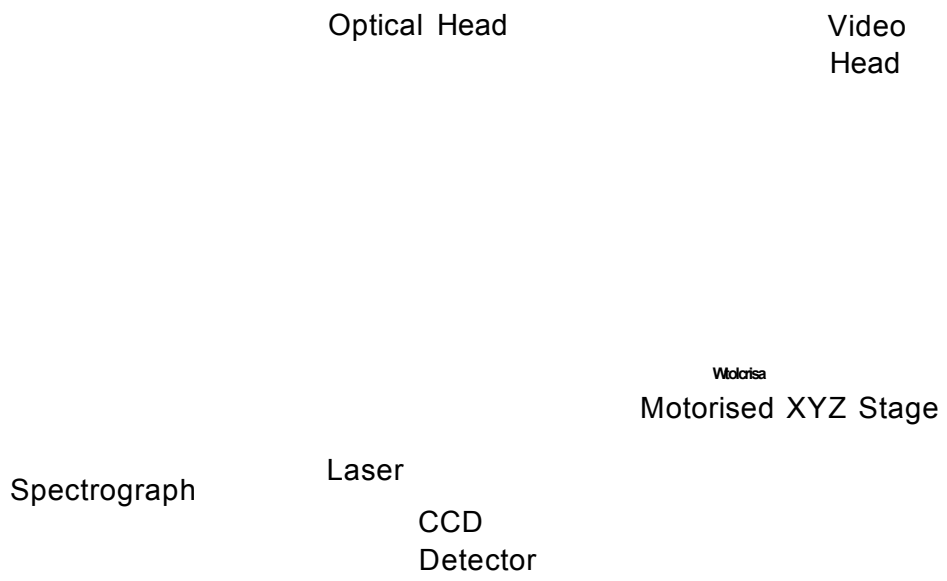

Figure 1-23: A schematic of the principal components of a RamanStation 400 Series spectrometer.

Image obtained from Perkin Elmer (2007).

The RamanStation 400 works by the laser irradiating the sample under investigation through an objective lens. The Raman scattered light from the sample is subsequently collected using the same objective lens and transmitted to the Echelle spectrograph. The spectrograph contains two gratings which disperse light in different directions. The first grating disperses light horizontally onto the second grating, whose etched lines are perpendicular to those of the first grating. The twice diffracted light is then focussed onto the CCD detector,

where it is dispersed over numerous strips that are collated simultaneously, enabling a full spectral range at high resolution to be obtained in a single acquisition (Perkin Elmer, 2007). Figure 1.24 shows a schematic of the Echelle spectrograph used in the RamanStation 400 instrument.

Figure 1-24: Schematic of an Echelle spectrograph.

The two gratings disperse light in two dimensions. The first grating initially scatters light horizontally onto the second grating, where it is further dispersed vertically onto the CCD detector. Image obtained from Perkin Elmer (2007).

1.4.3 Attenuated Total Reflectance - Fourier Transform Infrared Spectroscopy (ATR-FTIR)

The underlying principle of IR spectroscopy is the absorption of IR radiation at different frequencies by a molecule, which is typical of the vibrational energy levels of various functional groups present. For this to occur, the molecular

vibration should have the same frequency as the incident radiation, resulting in a change in the net dipole moment of the molecule.

As with Raman spectrometers, IR instruments can be either dispersive or Fourier transform (FT) based (Chalmers *et al.*, 2011). FT based spectrometers primarily employ an interferometer to collect a spectrum. The three main components of an interferometer are; a moving mirror, a fixed mirror and a beam splitter. The beam splitter splits the incoming infrared beam into two optical beams; one is transmitted to the moving mirror and the other reflected to the fixed mirror. The moving mirror travels back and forth a short distance from the beam splitter at a constant velocity. The two optical beams are subsequently reflected back from both mirrors and recombine at the beam splitter resulting in an interference pattern, which can be either destructive or constructive (Harris, 2010). The two beams then follow the same optical path, passing through the sample to the detector, resulting in an interferogram. The interferogram signal is subsequently converted to a single beam spectrum by the Fourier transform algorithm (Rouessac and Rouessac, 2007). There are several advantages of FT spectrometers over dispersive instruments. For one, the detectors used in FT-based instruments enable all the frequencies to be observed simultaneously, thereby reducing the time required to collect a complete spectrum, thus improving the overall sensitivity of the instrument. This is known as the Felgett advantage. Another advantage is known as Connes advantage, which improves the accuracy of the instrument due to the use of an internal reference laser for timing of sampling intervals leading to an absolute wavelength scale. Furthermore, FTIR employs a circular optical aperture rather than dispersion or filtering slits, which improves the optical throughput of the instrument as more light energy is available, resulting in a high signal to noise

ratio. This is known as the Jaquinot advantage (Griffiths and de Haseth, 1986). A schematic of an Interferometer is depicted in figure 1.25. Traditional FTIR measures the transmission of IR radiation through a sample; however, transmission is usually only beneficial when the sample is less than 10 μM thick. Furthermore, in the majority of situations, sample preparation is required prior to analysis in order to obtain a good quality spectrum. For solid samples, this traditionally involves grinding the solid into a fine powder and either dispersing it in a liquid such as mineral oil (Nujol™), or mixing it with an excess of potassium bromide (KBr) to form a disc. Liquid samples are traditionally analysed as thin films in cells, which typically consist of two IR transparent windows, containing a Teflon® spacer to provide the required pathlength, or alternatively a small quantity can be compressed between two sodium chloride (NaCl) or KBr discs (Rouessac and Rouessac, 2007). The complexity of the sample preparation protocols for both liquid and solid samples often results in poor reproducibility, as problems may arise from inconsistent sample to matrix ratios and inhomogeneous distribution of the sample throughout the matrix.

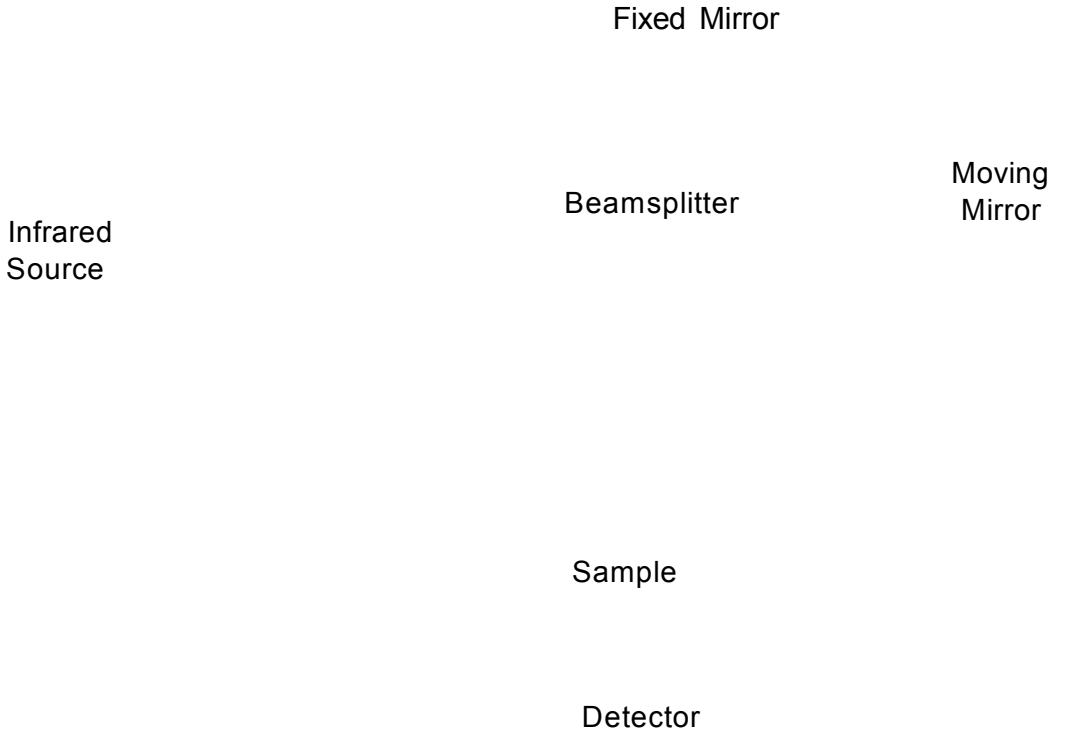

Figure 1-25: Schematic of an interferometer.

The beam splitter divides the incoming infrared beam into two optical beams; one is transmitted to the moving mirror and the other reflected to the fixed mirror. The two optical beams are reflected back from both mirrors and recombine at the beam splitter, where they pass through the sample, where some energy is transmitted to the detector, creating an interferogram. Image adapted from Rouessac and Rouessac (2007).

Besides transmission, FTIR spectra can also be obtained in reflectance mode. In recent years, attenuated total reflectance - Fourier transform infrared spectroscopy (ATR-FTIR) has revolutionised typical mid-infrared spectroscopy. ATR-FTIR enables small quantities of solid and liquid samples to be analysed directly, without sample preparation (Elkins, 2011). The technique involves placing the sample directly into contact with an ATR-FTIR accessory. The ATR accessory measures the changes that occur in a totally reflected IR beam, when the beam interacts with a sample (Perkin Elmer - Life and Analytical

Sciences, 2007). In ATR-FTIR, the IR beam is propagated onto an optically dense crystal with a high refractive index (RI). The angle of incidence must be greater than the critical angle in order for the IR beam to be totally internally reflected at the crystal-sample interface. This internal reflectance creates an evanescent wave, which exits the surface of the crystal and enters the sample. The evanescent wave extends a few microns from the crystal surface into the sample, where it interacts with the electronic dipoles of the molecules. The evanescent wave is attenuated in regions of the IR spectrum where the sample absorbs the energy of the IR beam. The attenuated wave, then returns back to the IR beam and is detected once it exits the ATR crystal, generating an IR spectrum. ATR crystals are typically composed of zinc selenide (ZnSe), germanium or diamond (Perkin Elmer - Life and Analytical Sciences, 2007). The penetration depth (d_p) of the evanescent wave at the interface of the sample can be calculated using equation 1.3. Where θ_{inc} is the angle of incidence, $n_{21} = n_2/n_1$, λ is wavelength of radiation in high RI medium ($\lambda 1 = \lambda/n_1$), n_1 is the RI of the ATR crystal, n_2 is the RI of the sample. Figure 1.26 shows a schematic of the evanescent wave extending from the ATR crystal into the sample.

$$dp = \frac{\lambda_1}{2\pi\left(\sin^2\theta_{inc} - n_{21}^2\right)^{\frac{1}{2}}}$$

Equation 1-3: Calculation of penetration depth (d_p) of the evanescent wave at the interface of the sample.

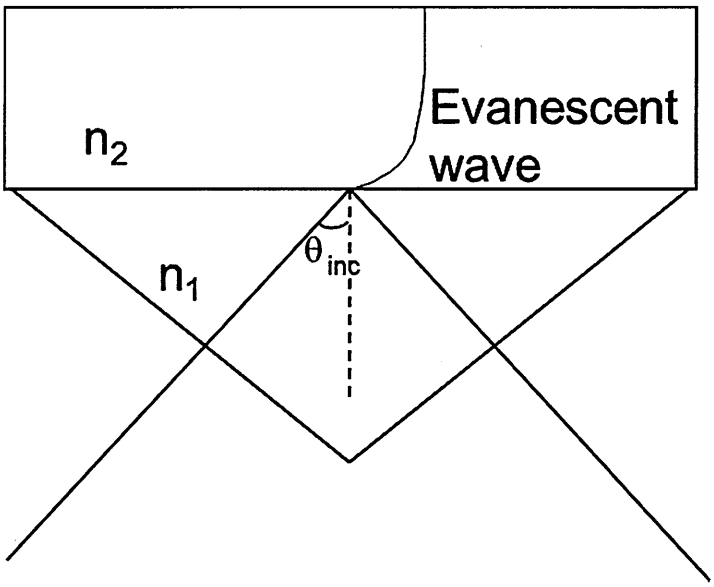

Figure 1-26: Schematic of the evanescent wave extending from the ATR crystal into the sample.

In regions of the infrared spectrum where the sample absorbs energy, the evanescent wave is attenuated and returned back to the IR beam, which then exits the opposite end of the crystal and is passed to the detector generating an IR spectrum. Figure courtesy of Dr C. Sammon.

ATR-FTIR has previously been employed in a forensic context for the analysis of drugs of abuse (Shultz *et al.*, 2004), counterfeit pharmaceuticals (Lanzarotta *et al.,* 2011), adhesives (Kumooka 2009), documents (Dirwono *et al.*, 2010) body fluids (Elkins 2011) and fingermarks (Ricci *et al.*, 2007a; Ricci *et al.*, 2007b). The forensic applications of ATR-FTIR will be discussed in more detail in section 4.1.

1.5 Fingermarks Lipidomics

The lipids present within fingermark residue originate primarily from the secretions of the sebaceous glands within the dermis of the skin. There are a variety of organic lipids present in sebum, and the composition of an individual's sebum profile can be affected by factors such as genetics and diet. The main lipid classes present and their relative abundances are; glycerides (33%), fatty

acids (30%), wax esters (22%), squalene (10%), cholesterol esters (2%), cholesterol (2%) (Goode and Morris, 1983).

Many of the latent fingermark studies conducted to date have focussed on the lipid components present namely fatty acids, long chain fatty acid esters, glycerides, squalene, cholesterol and wax esters (Archer *et al.*, 2005; Croxton *et al.*, 2010; Ricci *et al.*, 2007; Wolstenholme *et al.*, 2009; Weyermann *et al.*, 2011; Emerson *et al.*, 2011).

The fatty acid content of both "real" fingermarks and sebum enriched fingermarks were recently investigated by Croxton and collaborators. Fingermarks from 18 donors were deposited onto a non-porous surface and analysed by GC-MS after solvent extraction and derivatisation (Croxton *et al.*, 2010). Free fatty acids result from the hydrolysis of triglycerides and wax esters. From their results, the most abundant fatty acids present were hexadecanoic acid (16:0), octadecanoic acid (18:0) and cis-9-octadecenoic acid (18:1), which is in agreement with previously published data (Mong *et a*l., 1999). Other fatty acids detected included; dodecanoic acid (12:0), tridecanoic acid (13:0), tetradecanoic acid (14:0), pentadecanoic acid (15:0), cis -9-hexadecenoic acid (16:1), heptadecanoic acid (17:0), eicosanoic acid (20:0), and tetracosanoic acid (23:0). Squalene was also present in all the samples tested.

The presence of triglycerides (TG) within groomed fingermarks deposited directly onto MALDI stainless steel target plates has also recently been investigated using MALDI-TOF-MS and LDI-TOF-MS (Emerson *et al.*, 2011). The study found that no TG were detected with MALDI-TOF-MS, although TG could be detected by LDI-TOF-MS. The results of the study indicated that the majority of TG identified were consistent with sodium or potassium adducts, as

previously demonstrated by similar studies of TG in edible oils (Calvano *et al.*, 2005).

Absorption bands originating from lipids have also been reported by various research groups using vibrational spectroscopy techniques such as ATR-FTIR (Ricci *et al.*, 2007a) and FTIR microscopy (Antoine *et al.*, 2010). In their work, Ricci and collaborators investigated the changes in the ATR-FTIR spectra of lipids originating from groomed fingermarks obtained from five individuals. The donated fingermarks were subjected to changes in temperature over a duration of 16 hours, enabling changes in both the chemical and spatial distribution of the lipids present to be observed (Ricci *et al.*, 2007a)

In the work conducted by Antoine and co-workers, the changes in the lipid composition of adults and children's groomed fingermarks were compared over a 4 week ageing study. The study found that differences were apparent in the initial chemical composition of the fingermarks. Furthermore, the chemical changes that occurred over the time course enabled discrimination between the two groups of fingermark donors, based on differences in the degradation patterns observed (Antoine *et al.*, 2010).

1.6 Fingermarks Proteomics

The peptides and proteins present in fingermark residues originate from both the epidermis and dermis of the skin. The total protein concentration in sweat is between 15 and 25 mg/dL (Ramotowski, 2001). The epidermis is responsible for the presence of some proteins in fingermark residue such as keratins 1 and 10, resulting from the desquamation process required for skin renewal (Drapel *et al.*, 2009; Girod *et al.*, 2012) and antimicrobial species originating from keratinocytes of the epidermis such as psoriasin, cathelicidins, β-defensins and

lysozyme (Schroder and Harder 2006). Numerous peptides have also been identified in sweat originating from the eccrine glands within the dermis of the skin (Rieg *et al.*, 2005). These include innate antimicrobial peptides such as dermcidin and its proteolytically processed derivatives (Rieg *et al.*, 2006). In comparison to the lipid species present within latent fingermarks, limited research has been performed on higher molecular weight species such as peptides and proteins.

In the study by Drapel and co-workers in 2009, eccrine and groomed fingermarks were visualised after deposition on polyvinylidene fluoride (PVDF) membrane and white or non-whitened paper using antibodies directed against keratins 1 and 10, Cathepsin D and dermcidin. On the PVDF membrane, all three antibodies gave well defined images, although the groomed fingermarks were more developed than the eccrine ones. This is because the grooming procedure employed loads the fingertips with proteins, as well as sebum. Similar results were obtained for fingermarks deposited on white or non-whitened paper, although the images obtained were of a poorer quality (Drapel *et al.*, 2009).

Vibrational spectroscopy techniques such as FTIR (Ricci *et al.*, 2007a; Williams *et al.*, 2011) and SERS (Connatser *et al.*, 2010) have also shown the presence of proteins within latent fingermarks, although due to the poor chemical specificity of the techniques, the identity of the proteins couldn't be ascertained from the absorption bands detected.

The presence of antimicrobial peptides within fingermark residue has also been found in work performed by Belgorodsky and Gozin, (2010). Here MALDI-MS, Reverse Phase – High Performance Liquid Chromatography (RP-HPLC) and

Polyacrylamide Gel Electrophoresis (PAGE) were used to investigate the constituents of eccrine fingermarks.

1.7 Aims of Study

Although there are numerous conventional FET available, in recent years there has been an increase in the use of analytical methodologies to investigate the chemical constituents present within latent fingermarks, in order to gain additional intelligence regarding the fingermark donor. Of these analytical techniques MALDI-MSI has proven to be instrumental in obtaining chemical information that could potentially narrow down the pool of potential suspects, whilst simultaneously providing an image of the fingermark ridge detail (Francese *et al.*, 2013).

One of the aims of this PhD project was to optimise MALDI-MS and MALDI-MSI sample preparation protocols to extend the applicability of the method to detect a wider range of endogenous fingermark constituents, as well as exogenous contaminants.

Another aim was to develop a novel method of matrix application that enabled MALDI-MSI to be more forensically applicable.

Due to the large number of endogenous species present in sweat, an additional objective was to perform an inter-donor comparison studies on fingermarks collected from a variety of donors in order to verify whether the endogenous species detected could be utilised as biomarkers to enable discrimination between donors. As the majority of work previously carried out in this area was unsuccessfully undertaken on the lipid constituents present, the current work focussed on the peptidic and proteic content of fingermarks.

The final aim of this study was to investigate the feasibility of other spectroscopic techniques such as ATR-FTIR and SERS to support and provide complementary information to that obtained using MALDI-MS and MALDI-MSI in the study of latent fingermarks.

1.8 References

Almog, J., Sears, V.G., Springer, E., Hewlett, D.F., Walker, S., Wiesner, S., Lidor, R. and Bahar, E. (2000). Reagents for the chemical development of latent fingerprints: Scope and limitations of benzo-ninhydrin in comparison to ninhydrin. *Journal of Forensic Sciences,* **45** (3), 538-544

Amstalden van Hove, E.R., Smith, D.F. and Heeren, R.M.A. (2010). A concise review of mass spectrometry imaging. Journal of Chromatography A, **1217** (25), 3946-3954

Anderson, D.M.G., Carolan, V.A., Crosland, S., Sharples, K.R. and Clench, M.R. (2009). Examination of the distribution of nicosulfuron in sunflower plants by matrix-assisted laser desorption/ionisation mass spectrometry imaging. *Rapid Communications in Mass Spectrometry,* **23** (9), 1321-1327

Angel, P.M., Spraggins, J.M., Baldwin, H.S. and Caprioli, R. (2012). Enhanced sensitivity for high spatial resolution lipid analysis by negative ion mode matrix assisted laser desorption ionization imaging mass spectrometry. *Analytical Chemistry,* **84** (3), 1557-1564

Antoine, K.M., Mortazavi, S., Miller, A.D. and Miller, L.M. (2010). Chemical differences are observed in children's versus adults' latent fingerprints as a function of time. *Journal of Forensic Sciences,* **55** (2), 513-518

Archer, N.E., Charles, Y., Elliott, J.A. and Jickells, S. (2005). Changes in the lipid composition of latent fingerprint residue with time after deposition on a surface. *Forensic Science International,* **154** (2-3), 224-239

Baena, J. and Lendl, B. (2004). Raman spectroscopy in chemical bioanalysis. *Current Opinion in Chemical Biology,* **8** (5), 534-539

Bahr, U., Stahl-Zeng, J., Gleitsmann, E. and Karas, M. (1997). Delayed extraction time-of-flight MALDI mass spectrometry of proteins above 25,000 Da. *Journal of Mass Spectrometry,* **32** (10), 1111-1116

Baldwin, M.A., Medzihradszky, K.F., Lock, C.M., Fisher, B., Settineri, T.A. and Burlingame, A.L. (2001). Matrix-assisted laser desorption/ionization coupled with quadrupole/orthogonal acceleration time-of-flight mass spectrometry for protein discovery, identification, and structural analysis. *Analytical Chemistry,* **73** (8), 1707-1720

Bechara, C., Bolbach, G., Bazzaco, P., Sharma, K.S., Durand, G., Popot, J., Zito, F. and Sagan, S. (2012). MALDI-TOF mass spectrometry analysis of amphipol-trapped membrane proteins. *Analytical Chemistry,* **84** (14), 6128-6135

Becue, A., Moret, S., Champod, C. and Margot, P. (2010). Use of stains to detect fingermarks. *Biotechnic & Histochemistry: Official Publication of the Biological Stain Commission,* **86** (3), 140-160.

Belgorodsky, B., Fadeev, L. and Gozin, M., (2010. MALDI TOF Imaging of Latent Fingerprints a Novel Biosignature Tool. First Year Annual Report, Tel Aviv University, Tel Aviv, Israel. Available at: http://www.safesearch.net/search?q=Belgorodsky+fingerprints+annual+report. Last accessed on 3rd January 2012

Bell, S.E.J., Fido, L.A., Sirimuthu, N.M.S., Speers, S.J., Peters, K.L. and Cosbey, S.H. (2007). Screening tablets for DOB using surface-enhanced Raman spectroscopy. *Journal of Forensic Sciences,* **52** (5), 1063-1067

Benton, M., Rowell, F., Sundar, L. and Jan, M. (2010). Direct detection of nicotine and cotinine in dusted latent fingermarks of smokers by using hydrophobic silica particles and MS. *Surface and Interface Analysis,* **42** (5), 378-385

Bleay, S. M., Sears, V. G., Bandey, H. L., Gibson, A. P., Bowman, V. J., Downham, R., Fitzgerald, L., Ciuksza, T., Ramadani, J. and Selway, C. (2012). Fingerprint Source Handbook. CAST (Centre for Applied Technology, Home Office, UK)

Boddis, A.M. and Russell, D.A. (2011). Simultaneous development and detection of drug metabolites in latent fingermarks using antibody-magnetic particle conjugates. *Analytical Methods,* **3** (3), 519-523

Boddis, A.M. and Russell, D.A. (2012). Development of aged fingermarks using antibody-magnetic particle conjugates. *Analytical Methods,* **4** (3), 637-641

Bouschen, W., Schulz, O., Eikel, D. and Spengler, B. (2010). Matrix vapor deposition/recrystallization and dedicated spray preparation for high-resolution scanning microprobe matrix-assisted laser desorption/ionization imaging mass spectrometry (SMALDI-MS) of tissue and single cells. *Rapid Communications in Mass Spectrometry,* **24** (3), 355-364

Bowman, V. (ed.) (2005). *Home office fingerprint development handbook.* 2nd ed., Derbyshire, UK, Home Office, London, UK

Bradshaw, R., Wolstenholme, R., Blackledge, R.D., Clench, M.R., Ferguson, L.S. and Francese, S. (2011). A novel matrix-assisted laser desorption/ionisation mass spectrometry imaging based methodology for the identification of sexual assault suspects. *Rapid Communications in Mass Spectrometry,* **25** (3), 415-422

Bright, N.J., Webb, R.P., Bleay, S., Hinder, S., Ward, N.I., Watts, J.F., Kirkby, K.J. and Bailey, M.J. (2012). Determination of the deposition order of overlapping latent fingerprints and inks using secondary ion mass spectrometry. *Analytical Chemistry,* **84** (9), 4083-4087

Bunch, J., Clench, M.R. and Richards, D.S. (2004). Determination of pharmaceutical compounds in skin by imaging matrix-assisted laser desorption/ionisation mass spectrometry. *Rapid Communications in Mass Spectrometry,* **18** (24), 3051-3060.

Burrell, M., Earnshaw, C. and Clench, M. (2007). Imaging matrix assisted laser desorption ionization mass spectrometry: A technique to map plant metabolites within tissues at high spatial resolution. *Journal of Experimental Botany,* **58** (4), 757-763

Buryako, I., Krylov, E., Nazarov, E. and Rasulev, U. (1993). A new method of separation of multi-atomic ions by mobility at atmospheric-pressure using a high-frequency amplitude-asymmetric strong electric-field. *International Journal of Mass Spectrometry and Ion Processes,* **128** (3), 143-148

Calvano, C., Palmisano, F. and Zambonin, C. (2005). Laser desorption/ionization time-of-flight mass spectrometry of triacylglycerols in oils. *Rapid Communications in Mass Spectrometry,* **19** (10), 1315-1320

Caprioli, R.M., Farmer, T.B. and Gile, J. (1997). Molecular imaging of biological samples: Localization of peptides and proteins using MALDI-TOF-MS. *Analytical Chemistry,* **69** (23), 4751-4760

Chalmers, J. M., Edwards, H. G. M. and Hargreaves, M. D. (2012). *Infrared and Raman spectroscopy in forensic science.* Oxford, Wiley-Blackwell

Chaurand, P., Norris, J.L., Cornett, D.S., Mobley, J.A. and Caprioli, R.M. (2006). New developments in profiling and imaging of proteins from tissue sections by MALDI mass spectrometry. *Journal of Proteome Research,* **5** (11), 2889-2900

Chernushevich, I.V., Loboda, A.V. and Thomson, B.A. (2001). An introduction to quadrupole-time-of-flight mass spectrometry. *Journal of Mass Spectrometry,***36** (8), 849-865

Choi, M.J., Smoother, T., Martin, A.A., McDonagh, A.M., Maynard, P.J., Lennard, C. and Roux, C. (2007). Fluorescent TiO2 powders prepared using a new perylene diimide dye: Applications in latent fingermark detection. *Forensic Science International,* **173** (2-3), 154-160

Choi, M.J., McDonagh, A.M., Maynard, P. and Roux, C. (2008). Metal-containing nanoparticles and nano-structured particles in fingermark detection. *Forensic Science International,* **179** (2-3), 87-97

Cialla, D., Maerz, A., Boehme, R., Theil, F., Weber, K., Schmitt, M. and Popp, J. (2012). Surface-enhanced Raman spectroscopy (SERS): Progress and trends. *Analytical and Bioanalytical Chemistry,* **403** (1), 27-54

Cohen, M.J. and Karasek, F.W. (1970). Plasma chromatography TM-new dimension for gas chromatography and mass spectrometry. *Journal of Chromatographic Science*, **8**, 330

Cole, L.M., Djidja, M.C., Bluff, J., Claude, E., Carolan, V.A., Paley, M., Tozer, G.M. and Clench, M.R. (2011). Investigation of protein induction in tumour vascular targeted strategies by MALDI-MSI. *Methods,* **54** (4), 442-453

Connatser, R.M., Prokes, S.M., Glembocki, O.J., Schuler, R.L., Gardner, C.W., Lewis, S.A., Sr. and Lewis, L.A. (2010). Toward surface-enhanced Raman imaging of latent fingerprints. *Journal of Forensic Sciences,* **55** (6), 1462-1470

Cook, G.W., LaPuma, P.T., Hook, G.L. and Eckenrode, B.A. (2010). Using gas chromatography with ion mobility spectrometry to resolve explosive compounds in the presence of interferents. *Journal of Forensic Sciences,* **55** (6), 1582-1591

Cotter, R.J., Gardner, B.D., Iltchenko, S. and English, R.D. (2004). Tandem time-of-flight mass spectrometry with a curved field reflectron. *Analytical Chemistry,* **76** (7), 1976-1981

Croxton, R.S., Baron, M.G., Butler, D., Kent, T. and Sears, V.G. (2006). Development of a GC-MS method for the simultaneous analysis of latent fingerprint components. *Journal of Forensic Sciences,* **51** (6), 1329-1333

Croxton, R.S., Baron, M.G., Butler, D., Kent, T. and Sears, V.G. (2010). Variation in amino acid and lipid composition of latent fingerprints. *Forensic Science International,* **199** (1-3), 93-102

Cuce, P., Polimeni, G., Lazzaro, A.P. and De Fulvio, G. (2004). Small particle reagents technique can help to point out wet latent fingerprints. *Forensic Science International,* **146,** S7-8

Darie, C.C., Biniossek, M.L., Gawinowicz, M.A., Milgrom, Y., Thumfart, J.O., Jovine, L., Litscher, E.S. and Wassarman, P.M. (2005). Mass spectrometric evidence that proteolytic processing of rainbow trout egg vitelline envelope proteins takes place on the egg. *The Journal of Biological Chemistry,* **280** (45), 37585-37598

Day, J.S., Edwards, H.G., Dobrowski, S.A. and Voice, A.M. (2004a). The detection of drugs of abuse in fingerprints using Raman spectroscopy I: Latent fingerprints. *Spectrochimica Acta.Part A, Molecular and Biomolecular Spectroscopy,* **60** (3), 563-568

Day, J.S., Edwards, H.G., Dobrowski, S.A. and Voice, A.M. (2004b). The detection of drugs of abuse in fingerprints using Raman spectroscopy II: Cyanoacrylate-fumed fingerprints. *Spectrochimica Acta.Part A, Molecular and Biomolecular Spectroscopy,* **60** (8-9), 1725-1730

Dikshitulu, Y.S., Prasad, L., Pal, J.N. and Rao, C.V. (1986). Ageing studies on fingerprint residues using thin-layer and high performance liquid chromatography. *Forensic Science International,* **31** (4), 261-266

Dirwono, W., Park, J.S., Agustin-Camacho, M.R., Kim, J., Park, H., Lee, Y. and Lee, K. (2010). Application of micro-attenuated total reflectance FTIR spectroscopy in the forensic study of questioned documents involving red seal inks. *Forensic Science International,* **199** (1–3), 6-8

Djidja, M.C., Francese, S., Loadman, P.M., Sutton, C.W., Scriven, P., Claude, E., Snel, M.F., Franck, J., Salzet, M. and Clench, M.R. (2009). Detergent addition to tryptic digests and ion mobility separation prior to MS/MS improves peptide yield and protein identification for in situ proteomic investigation of frozen and formalin-fixed paraffin-embedded adenocarcinoma tissue sections. *Proteomics,* **9** (10), 2750-2763

Drapel, V., Becue, A., Champod, C. and Margot, P. (2009). Identification of promising antigenic components in latent fingermark residues. *Forensic Science International,* **184** (1-3), 47-53

Dreisewerd, K. (2003). The desorption process in MALDI. *Chemical Reviews,* **103** (2), 395-426

Eiceman, G.A., Krylov, E.V., Krylova, N.S., Nazarov, E.G. and Miller, R.A. (2004). Separation of ions from explosives in differential mobility spectrometry by vapor-modified drift gas. *Analytical Chemistry,* **76** (17), 4937-4944

Elkins, K.M. (2011). Rapid presumptive "fingerprinting" of body fluids and materials by ATR FTIR spectroscopy. *Journal of Forensic Sciences,* **56** (6), 1580-1587

Emerson, B., Gidden, J., Lay, J.O.,Jr and Durham, B. (2011). Laser desorption/ionization time-of-flight mass spectrometry of triacylglycerols and

other components in fingermark samples. *Journal of Forensic Sciences,* **56** (2), 381-389

Ewing, R. and Miller, C. (2001). Detection of volatile vapours emitted from explosives with a handheld ion mobility spectrometer. *Field Analytical Chemistry and Technology,* **5** (5), 215-221

Federal Bureau of Investigation. (1957). The Science of Fingerprints: Classifications and Uses. Available at: http://www.gutenberg.org/files/19022/19022-h/19022-h.htm. Last accessed on 24th October 2012

Ferguson, L., Bradshaw, R., Wolstenholme, R., Clench, M. and Francese, S. (2011). Two-step matrix application for the enhancement and imaging of latent fingermarks. *Analytical Chemistry,* **83** (14), 5585-5591

Ferguson, L.S., Wulfert, F., Wolstenholme, R., Fonville, J.M., Clench, M.R., Carolan, V.A. and Francese, S. (2012). Direct detection of peptides and small proteins in fingermarks and determination of sex by MALDI mass spectrometry profiling. *Analyst,* **137** (20), 4686-4692

Fleischmann, M.,Hendra, P.J. and McQuillan, A.J. (1974). Raman Spectra of Pyridine Adsorbed at a Silver Electrode. *Chemical Physics Letters*, **26** (2), 163–166

Francese, S., Bradshaw, R., Ferguson, L.S., Wolstenholme, R., Clench, M.R. and Bleay, S. (2013). Beyond the ridge pattern: Multi-informative analysis of latent fingermarks by MALDI mass spectrometry. *Analyst,* **138** (15), 4215-4228

Francese, S. and Clench, M.R. (2010). MALDI mass spectrometry imaging, a new frontier in biostructural techniques: Applications in biomedicine. In: SHAH, H.N. and GHARBIA, S.E. (eds.). *Mass spectrometry for microbial proteomics.* 1st ed., Chichester, UK, John Wiley & Sons

Francese, S., Dani, F.R., Traldi, P., Mastrobuoni, G., Pieraccini, G. and Moneti, G. (2009). MALDI mass spectrometry imaging, from its origins up to today: The state of the art. *Combinatorial Chemistry & High Throughput Screening,* **12** (2), 156-174

Franck, J., Arafah, K., Barnes, A., Wisztorski, M., Salzet, M. and Fournier, I. (2009). Improving tissue preparation for matrix-assisted laser desorption ionization mass spectrometry imaging. part 1: Using microspotting. *Analytical Chemistry,* **81** (19), 8193-8202.

Fraser, J., Sturrock, K., Deacon, P., Bleay, S. and Bremner, D.H. (2011). Visualisation of fingermarks and grab impressions on fabrics.part 1: Gold/zinc vacuum metal deposition. *Forensic Science International,* **208** (1-3), 74-78.

Fraser, J. and Williams, R. (2009). *Handbook of forensic science.* Cullompton, Willan.

Gasilova, N., Gassner, A. and Girault, H.H. (2012). Analysis of major milk whey proteins by immunoaffinity capillary electrophoresis coupled with MALDI-MS. *Electrophoresis,* **33** (15), 2390-2398

Gassner, C., Meyer, S., Frey, B.M. and Vollmert, C. (2013). Matrix-assisted laser Desorption/Ionisation, time-of-flight mass spectrometry-based blood group

genotyping - the alternative approach. *Transfusion Medicine Reviews,* **27** (1), 2-9

Geiman, I., Leona, M. and Lombardi, J.R. (2009). Application of Raman spectroscopy and surface-enhanced Raman scattering to the analysis of synthetic dyes found in ballpoint pen inks. *Journal of Forensic Sciences,* **54** (4), 947-952

Giles, K., Pringle, S.D., Worthington, K.R., Little, D., Wildgoose, J.L. and Bateman, R.H. (2004). Applications of a travelling wave-based radio-frequency-only stacked ring ion guide. *Rapid Communications in Mass Spectrometry,* **18** (20), 2401-2414

Gillig, K.J., Ruotolo, B., Stone, E.G., Russell, D.H., Fuhrer, K., Gonin, M. and Schultz, A.J. (2000). Coupling high-pressure MALDI with ion mobility/orthogonal time-of-flight mass spectrometry. *Analytical Chemistry,* **72** (17), 3965-3971

Girod, A., Ramotowski, R. and Weyermann, C. Composition of fingermark residue: A qualitative and quantitative review. *Forensic Science International,* **223** (1-3), 10-24

Golightly, R.S., Doering, W.E. and Natan, M.J. (2009). Surface-enhanced Raman spectroscopy and homeland security: A perfect match? *Acs Nano,* **3** (10), 2859-2869

Goode, G. C. and Morris, J. R. (1983). Latent Fingerprints: A Review of Their Origin, Composition, and Methods for Detection; AWRE Report No. 022/83; United Kingdom Atomic Weapons Research Establishment: Aldermaston, UK

Goodwin, R.J.A. (2012). Sample preparation for mass spectrometry imaging: Small mistakes can lead to big consequences. *Journal of Proteomics,* **75** (16), 4893-4911

Griffiths, P.R. and de Haseth, J.A. (1986). Fourier Transform Infrared Spectroscopy. John Wiley & Sons Inc. USA

Grigg, R. and Mongkolaussavaratana, T. (1990). 1, 8-diazafluorenone and related compounds. A novel reagent for the detection of amino acids and latent fingerprints. *Tetrahedron Letters,* **31** (49), 7215-7218

Gupta, A., Buckley, K. and Sutton, R. (2008). Latent fingermark pore area reproducibility. *Forensic Science International,* **179** (2–3), 172-175

Hall, A.B., Coy, S.L., Nazarov, E.G. and Vouros, P. (2012). Rapid separation and characterization of cocaine and cocaine cutting agents by differential mobility spectrometry-mass spectrometry. *Journal of Forensic Sciences,* **57** (3), 750-756

Harris, D. C. (2010). *Quantitative chemical analysis.* Basingstoke, W. H. Freeman

Hart, P.J., Francese, S., Claude, E., Woodroofe, M.N. and Clench, M.R. (2011). MALDI-MS imaging of lipids in ex vivo human skin. *Analytical and Bioanalytical Chemistry,* **401** (1), 115-125

Hazarika, P., Jickells, S.M. and Russell, D.A. (2009). Rapid detection of drug metabolites in latent fingermarks. *Analyst,* **134** (1), 93-96

Hoffmann, E. de and Stroobant, V. (2009). *Mass spectrometry: Principles and applications.* Chichester, Wiley

Ifa, D.R., Manicke, N.E., Dill, A.L. and Cooks, R.G. (2008). Latent fingerprint chemical imaging by mass spectrometry. *Science,* **321** (5890), 805

Jackson, A. R. W. and Jackson, J.M. (2011). Forensic Science. 3rd Ed, Harlow, Essex, Pearson Prentice Hall

Jagtap, R. and Ambre, A. (2005). Overview literature on matrix assisted laser desorption ionization mass spectroscopy (MALDI-MS): Basics and its applications in characterizing polymeric materials. *Bulletin of Materials Science,* **28** (6), 515-528

James, S.H. and Nordby, J.J. (2009). Forensic Science: An Introduction to Scientific and Investigative Techniques, 3rd Edition, CRC Press

Jasuja, O.P. and Singh, G. (2009). Development of latent fingermarks on thermal paper: Preliminary investigation into use of iodine fuming. *Forensic Science International,* **192** (1-3), e11-6

Jasuja, O.P., Singh, G.D. and Sodhi, G.S. (2008). Small particle reagents: Development of fluorescent variants. *Science & Justice: Journal of the Forensic Science Society,* **48** (3), 141-145

Jelly, R., Patton, E.L.T., Lennard, C., Lewis, S.W. and Lim, K.F. (2009). The detection of latent fingermarks on porous surfaces using amino acid sensitive reagents: A review. *Analytica Chimica Acta,* **652** (1-2), 128-142

Jones, A. and Wolstenholme, R. (2003). Non-destructive spectroscopic analysis of ballpoint and gel pen inks. *Forensic Science International,* **136**, 69-70

Jones, B.J., Downham, R. and Sears, V.G. (2012). Nanoscale analysis of the interaction between cyanoacrylate and vacuum metal deposition in the development of latent fingermarks on low-density polyethylene. *Journal of Forensic Sciences,* **57** (1), 196-200

Jones, N., Stoilovic, M., Lennard, C. and Roux, C. (2001). Vacuum metal deposition: Factors affecting normal and reverse development of latent fingerprints on polyethylene substrates. *Forensic Science International,* **115** (1-2), 73-88

Kafka, A.P., Kleffmann, T., Rades, T. and McDowell, A. (2011). The application of MALDI TOF MS in biopharmaceutical research. *International Journal of Pharmaceutics,* **417** (1-2), 70-82

Kaletas, B.K., van der Wiel, I.M., Stauber, J., Lennard J. Dekker, Guzel, C., Kros, J.M., Luider, T.M. and Heeren, R.M. (2009). Sample preparation issues for tissue imaging by imaging MS. *Proteomics,* **9** (10), 2622-2633

Kanu, A.B., Dwivedi, P., Tam, M., Matz, L. and Hill, H.H.,Jr. (2008b). Ion mobility-mass spectrometry. *Journal of Mass Spectrometry,* **43** (1), 1-22

Kanu, A.B. and Hill, H.H., Jr. (2008a). Ion mobility spectrometry detection for gas chromatography. *Journal of Chromatography A,* **1177** (1), 12-27

Karas, M., Bachmann, D., Hillenkamp, F. (1985). Influence of the wavelength in high-irradiance ultraviolet laser desorption mass spectrometry of organic molecules. *Analytical Chemistry*, **57** 2935-2939

Karas, M., Gluckmann, M. and Schafer, J. (2000). Ionization in matrix-assisted laser desorption/ionization: Singly charged molecular ions are the lucky survivors. *Journal of Mass Spectrometry,* **35** (1), 1-12

Karas, M. and Hillenkamp F. (1988). Laser desorption ionisation of proteins with molecular masses exceeding 10,000 daltons. *Analytical Chemistry*, **60**, 2299-2301

Karas, M. and Kruger, R. (2003). Ion formation in MALDI: The cluster ionization mechanism. *Chemical Reviews,* **103** (2), 427-440

Kaur-Atwal, G., Reynolds, J.C., Mussell, C., Champarnaud, E., Knapman, T.W., Ashcroft, A.E., O'Connor, G., Christie, S.D. and Creaser, C.S. (2011). Determination of testosterone and epitestosterone glucuronides in urine by ultra-performance liquid chromatography-ion mobility-mass spectrometry. *Analyst,* **136** (19), 3911-3916

Kent, T. (1990). Recent research on superglue, vacuum metal deposition and fluorescence examination, in: AI Conference, Nashville

Kent, T., Thomas, G.L., Reynoldson, T.E. and East, H.W. (1976). A vacuum coating technique for the development of latent fingerprints on polythene. *Journal of Forensic Science Society,* **16** (2), 93-101

Klerk, L.A., Altelaar, A.F.M., Froesch, M., McDonnell, L.A. and Heeren, R.M.A. (2009). Fast and automated large-area imaging MALDI mass spectrometry in microprobe and microscope mode. *International Journal of Mass Spectrometry,* **285** (1-2), 19-25

Knochenmuss, R. (2006). Ion formation mechanisms in UV-MALDI. *Analyst,* **131** (9), 966-986

Knochenmuss, R. and Zenobi, R. (2003). MALDI ionization: The role of in-plume processes. *Chemical Reviews,* **103** (2), 441-452

Knowles, A. (1978). Aspects of physicochemical methods for detection of latent fingerprints. *Journal of Physics E-Scientific Instruments,* **11** (8), 713-721

Kolakowski, B.M., D'Agostino, P.A., Chenier, C. and Mester, Z. (2007). Analysis of chemical warfare agents in food products by atmospheric pressure ionization-high field asymmetric waveform ion mobility spectrometry-mass spectrometry. *Analytical Chemistry,* **79** (21), 8257-8265

Kumooka, Y. (2009). Hierarchical cluster analysis as a tool for preliminary discrimination of ATR-FTIR spectra of OPP acrylic and rubber-based adhesives. *Forensic Science International,* **189** (1-3), 104-110

Lambourne, G.T. (1978). A brief history of fingerprints. *Journal - Forensic Science Society,* **17** (2-3), 95-98

Lanzarotta, A., Lakes, K., Marcott, C.A., Witkowski, M.R. and Sommer, A.J. (2011). Analysis of counterfeit pharmaceutical tablet cores utilizing macroscopic infrared spectroscopy and infrared spectroscopic imaging. *Analytical Chemistry,* **83** (15), 5972-5978

Lee, H. C. and Gaensslen, R. E. (2001). *Advances in fingerprint technology.* 2nd ed., Boca Raton, Fla.; London, CRC Press. CRC series in forensic and police science

Lennon, J.J. (1997). Matrix Assisted Laser Desorption Ionization Time-of-flight Mass Spectrometry [online]. Available at: 15/http://www.abrf.org/ABRFNews/1997/June1997/jun97lennon.html. Last accessed on 15/07/13.

Leona, M., Decuzzi, P., Kubic, T.A., Gates, G. and Lombardi, J.R. (2011). Nondestructive identification of natural and synthetic organic colorants in works of art by surface enhanced Raman scattering. *Analytical Chemistry,* **83** (11), 3990-3993

Lewis, L.A., Smithwick, R.W.,3rd, Devault, G.L., Bolinger, B. and Lewis SA, S. (2001). Processes involved in the development of latent fingerprints using the cyanoacrylate fuming method. *Journal of Forensic Sciences,* **46** (2), 241-246

Liu, L., Zhang, Z., Zhang, L. and Zhai, Y. (2009). The effectiveness of strong afterglow phosphor powder in the detection of fingermarks. *Forensic Science International,* **183** (1-3), 45-49

Lovejoy, K.S., Lou, A.J., Davis, L.E., Sanchez, T.C., Iyer, S., Corley, C.A., Wilkes, J.S., Feller, R.K., Fox, D.T., Koppisch, A.T. and Del Sesto, R.E. (2012). Single-pot extraction-analysis of dyed wool fibers with ionic liquids. *Analytical Chemistry,* **84** (21), 9169-9175

Lu, Y. and Harrington, P.B. (2007). Forensic application of gas chromatography-differential mobility spectrometry with two-way classification of ignitable liquids from fire debris. *Analytical Chemistry,* **79** (17), 6752-6759

Luxembourg, S.L., Mize, T.H., McDonnell, L.A. and Heeren, R.M. (2004). High-spatial resolution mass spectrometric imaging of peptide and protein distributions on a surface. *Analytical Chemistry,* **76** (18), 5339-5344

Makinen, M.A., Anttalainen, O.A. and Sillanpaa, M.E. (2010). Ion mobility spectrometry and its applications in detection of chemical warfare agents. *Analytical Chemistry,* **82** (23), 9594-9600

McDonnell, L.A. and Heeren, R.M.A. (2007). Imaging mass spectrometry. *Mass Spectrometry Reviews,* **26** (4), 606-643

McNay, G., Eustace, D., Smith, W.E., Faulds, K. and Graham, D. (2011). Surface-enhanced Raman scattering (SERS) and surface-enhanced resonance Raman scattering (SERRS): A review of applications. *Applied Spectroscopy,* **65** (8), 825-837

Menzel, E.R. and Duff, J.M. (1979). Laser detection of latent fingerprints-treatment with fluorescers. *Journal of Forensic Sciences,* **24** (1), 96-100

Miki, A., Katagi, M., Shima, N., Kamata, H., Tatsuno, M., Nakanishi, T., Tsuchihashi, H., Takubo, T. and Suzuki, K. (2011). Imaging of methamphetamine incorporated into hair by MALDI-TOF mass spectrometry. *Forensic Toxicology,* **29** (2), 111-116

Mong, G.M., Petersen C.E. and Claus, T.R.W. (1999). Advanced fingerprint analysis project final report – fingerprint constituents. Richland, WA: Pacific Northwest National Laboratory, 99352, Report PNNL-13019

Oden, S. and Von Hofsten, B (1954). Detection of fingerprints by the ninhydrin reaction. *Nature,* **173** , 449-450

Oppenheimer, S.R., Claude, E.and Bahrainwala, T. (2009). Tissue Imaging of Pharmaceuticals by Ion Mobility Mass Spectrometry. Waters Application Note, 720003216en

Oxley, J.C., Smith, J.L., Kirschenbaum, L.J., Marimganti, S. and Vadlamannati, S. (2008). Detection of explosives in hair using ion mobility spectrometry. *Journal of Forensic Sciences,* **53** (3), 690-693

Paine, M., Bandey, H.L., Bleay, S.M. and Willson, H. (2011). The effect of relative humidity on the effectiveness of the cyanoacrylate fuming process for fingermark development and on the microstructure of the developed marks. *Forensic Science International,* **212** (1-3), 130-142

Pannkuk, E.L., Gilmore, D.F., Savary, B.J. and Risch, T.S. (2012). Triacylglyceride (TAG) profiles of integumentary lipids isolated from three bat species determined by matrix-assisted laser desorption-ionization time-of-flight mass spectrometry (MALDI-TOF MS). *Canadian Journal of Zoology,* **90** (9), 1117-1127

Park, E., Yang, H., Kim, Y. and Kim, J. (2012). Analysis of oligosaccharides in beer using MALDI-TOF-MS. *Food Chemistry,* **134** (3), 1658-1664.

Paul, W. And Steinwedel, H.S. (1960) US Patent, 29939952. Apparatus for separating charged particles of different specific charges.

Pelletier, M.J. (1999). *Analytical Applications of Raman Spectroscopy*. Wiley-Blackwell

Perkin Elmer - Life and Analytical Sciences, (2007). "ATR-FTIR Spectroscopy" Available at:

http://las.perkinelmer.com/content/TechnicalInfo/TCH_FTIRATR.pdf. Last accessed 14/10/2012

Perkin Elmer (2007). *RamanStation 400 Series – Getting Stared Guide.*

Pol, J., Strohalm, M., Havlicek, V. and Volny, M. (2010).Molecular mass spectrometry imaging in biomedical and life science research. *Histochemistry and Cell Biology,* **134** (5), 423-443

Polimeni, G., Feudale Foti, B., Saravo, L. and De Fulvio, G. (2004). A novel approach to identify the presence of fingerprints on wet surfaces. *Forensic Science International,* **146,** S45-6

Popp, J. and Mayerhoefer, T. (2009). Surface-enhanced Raman spectroscopy. *Analytical and Bioanalytical Chemistry,* **394** (7), 1717-1718

Porta, T., Grivet, C., Kraemer, T., Varesio, E. and Hopfgartner, G. (2011). Single hair cocaine consumption monitoring by mass spectrometric imaging. *Analytical Chemistry,* **83** (11), 4266-4272

Prideaux, B., Atkinson, S.J., Carolan, V.A., Morton, J. and Clench, M.R. (2007). Sample preparation and data interpretation procedures for the examination of xenobiotic compounds in skin by indirect imaging MALDI-MS. *International Journal of Mass Spectrometry,* **260** (2-3), 243-251

Pringle, S.D., Giles, K., Wildgoose, J.L., Williams, J.P., Slade, S.E., Thalassinos, K., Bateman, R.H., Bowers, M.T. and Scrivens, J.H. (2007). An investigation of the mobility separation of some peptide and protein ions using a new hybrid quadrupole/travelling wave IMS/oa-ToF instrument. *International Journal of Mass Spectrometry,* **261** (1), 1-12

Ramotowski, R.S. (2001). Composition of latent print residue. In: Lee, H.C. and Gaensslen, R.E. (ed.). *Advances in fingerprint technology.* Boca Raton, Florida, CRC Press, 63-104

Reed, F.A. (1981). The fingermark. The prime piece of scientific evidence. *Journal of Forensic Science Society,* **21** (1), 9-13

Ricci, C., Bleay, S. and Kazarian, S.G. (2007b). Spectroscopic imaging of latent fingermarks collected with the aid of a gelatine tape. *Analytical Chemistry,* **79** (15), 5771-5776

Ricci, C., Phiriyavityopas, P., Curum, N., Chan, K.L.A., Jickells, S. and Kazarian, S.G. (2007a). Chemical imaging of latent fingerprint residues. *Applied Spectroscopy,* **61** (5), 514-522

Rieg, S., Seeber, S., Steffen, H., Humeny, A., Kalbacher, H., Stevanovic, S., Kimura, A., Garbe, C. and Shittek, B. (2006). Generation of multiple stable dermcidin-derived antimicrobial peptides in sweat of different body sites. *Journal of Investigative Dermatology,* **126** , 354-365

Rieg, S., Steffen, H., Seeber, S., Humeny, A., Kalbacher, H., Dietz, K., Garbe, C. and Schittek, B. (2005). Deficiency of dermcidin-derived antimicrobial peptides in sweat of patients with atopic dermatitis correlates with an impaired innate defence of human skin in vivo. *Journal of Immunology,* **174** (12), 8003-8010

Rouessac, F. and Rouessac, A.R. (2007). Chemical Analysis: Modern instrumentation methods and techniques. Chichester, Wiley

Rowell, F., Hudson, K. and Seviour, J. (2009). Detection of drugs and their metabolites in dusted latent fingermarks by mass spectrometry. *Analyst,* **134** (4), 701-707

Ryder, A.G. (2005). Surface enhanced Raman scattering for narcotic detection and applications to chemical biology. *Current Opinion in Chemical Biology,* **9** (5), 489-493

Sacristan, E. and Solis, A. (1998). A swept-field aspiration condenser as an ion-mobility spectrometer. *Transactions on Instrumentation and Measurement,* **47** (3), 769-775.

Saferstein, R. (2011). *Forensic science: An introduction.* Upper Saddle River, N.J, Pearson Prentice Hall

Schroder, J. and Harder, J. (2006). Antimicrobial skin peptides and proteins. *Cellular and Molecular Life Sciences,* **63** (4), 469-486

Schulz, H., Baranska, M., Quilitzsch, R. and Schutze, W. (2004). Determination of alkaloids in capsules, milk and ethanolic extracts of poppy (papaver somniferum L.) by ATR-FTIR and FT-Raman spectroscopy. *Analyst,* **129** (10), 917-920

Schwartz, S.A., Reyzer, M.L. and Caprioli, R.M. (2003). Direct tissue analysis using matrix-assisted laser desorption/ionization mass spectrometry: Practical aspects of sample preparation. *Journal of Mass Spectrometry,* **38** (7), 699-708

Shanta, S.R., Zhou, L.H., Park, Y.S., Kim, Y.H., Kim, Y. and Kim, K.P. (2011). Binary matrix for MALDI imaging mass spectrometry of phospholipids in both ion modes. *Analytical Chemistry,* **83** (4), 1252-1259

Shumate, C.B. and Hill, H.H. Jr., (1989). Coronaspray nebulization and ionization of liquid samples for ion mobility spectrometry. *Analytical Chemistry,* **61** (6), 601-606

Smith, E. and Dent, G. (2005). *Modern Raman spectroscopy: A practical approach.* Chichester, UK, John Wiley & Sons.

Smith, D.P., Knapman, T.W., Campuzano, I., Malham, R.W., Berryman, J.T., Radford, S.E. and Ashcroft, A.E. (2009). Deciphering drift time measurements from travelling wave ion mobility spectrometry-mass spectrometry studies *European Journal of Mass Spectrometry,* **15** (2), 113-130

Sodhi, G.S. and Kaur, J. (2001). Powder method for detecting latent fingerprints: A review. *Forensic Science International,* **120** (3), 172-176

Stuart, D.A., Biggs, K.B. and Van Duyne, R.P. (2006). Surface-enhanced Raman spectroscopy of half-mustard agent. *Analyst,* **131** (4), 568-572

Tanaka, K., Waki, H., Ido, Y., Akita, S., Yoshida, Y., Yoshida, T., Matsuo, T. (1988). Protein and polymer analyses up to *m/z* 100 000 by laser ionization time-of-flight mass spectrometry. *Rapid Communications in Mass Spectrometry,* **2** (8) 151-153

Theaker, B.J., Hudson, K.E. and Rowell, F.J. (2008). Doped hydrophobic silica nano- and micro-particles as novel agents for developing latent fingerprints. *Forensic Science International,* **174** (1), 26-34

Theys, P., Turgis, A., Lepareux, G., Chevet, P. And Ceccaldi, F. (1968). New technique for bringing out latent fingerprints on paper: vacuum metallization. *International Criminal Police Review*, **217**, 106-108

Trim, P.J., Atkinson, S.J., Princivalle, A.P., Marshall, P.S., West, A. and Clench, M.R. (2008). Matrix-assisted laser desorption/ionisation mass spectrometry imaging of lipids in rat brain tissue with integrated unsupervised and supervised multivariant statistical analysis. *Rapid Communications in Mass Spectrometry,* **22** (10), 1503-1509

Trim, P.J., Henson, C.M., Avery, J.L., McEwen, A., Snel, M.F., Claude, E., Marshall, P.S., West, A., Princivalle, A.P. and Clench, M.R. (2008). Matrix-assisted laser desorption/ionization-ion mobility separation-mass spectrometry imaging of vinblastine in whole body tissue sections. *Analytical Chemistry,* **80** (22), 8628-8634

Verkouteren, J.R. and Staymates, J.L. (2011). Reliability of ion mobility spectrometry for qualitative analysis of complex, multicomponent illicit drug samples. *Forensic Science International,* **206** (1-3), 190-196

Vickerman, J.C. (2011). Molecular imaging and depth profiling by mass spectrometry--SIMS, MALDI or DESI? *Analyst,* **136** (11), 2199-2217

Wallace-Kunkel, C., Lennard, C., Stoilovic, M. and Roux, C. (2007). Optimisation and evaluation of 1,2-indanedione for use as a fingermark reagent and its application to real samples. *Forensic Science International,* **168** (1), 14-26

Wargacki, S.P., Lewis, L.A. and Dadmun, M.D. (2007). Understanding the chemistry of the development of latent fingerprints by superglue fuming. *Journal of Forensic Sciences,* **52** (5), 1057-1062

West, M.J. and Went, M.J. (2008). The spectroscopic detection of exogenous material in fingerprints after development with powders and recovery with adhesive lifters. *Forensic Science International,* **174** (1), 1-5

West, M.J. and Went, M.J. (2009). The spectroscopic detection of drugs of abuse in fingerprints after development with powders and recovery with adhesive lifters. *Spectrochimica Acta.Part A, Molecular and Biomolecular Spectroscopy,* **71** (5), 1984-1988

Weyermann, C., Roux, C. and Champod, C. (2011). Initial results on the composition of fingerprints and its evolution as a function of time by GC/MS analysis. *Journal of Forensic Sciences,* **56** (1), 102-108

Wilkinson, D. (2000). Spectroscopic study of 1, 2-indandione. *Forensic Science International,* **114** (3), 123-132

Williams, D.K., Brown, C.J. and Bruker, J. (2011). Characterisation of children's latent fingerprint residue by Infrared microspectroscopy: Forensic Implications. Forensic Science International, 206 (1-3).161-165

Wolstenholme, R., Bradshaw, R., Clench, M.R. and Francese, S. (2009). Study of latent fingermarks by matrix-assisted laser desorption/ionisation mass spectrometry imaging of endogenous lipids. *Rapid Communications in Mass Spectrometry,* **23** (19), 3031-3039

Xiao, D., Zhao, F., Lv, M., Zhang, H., Zhang, Y., Huang, H., Su, P., Zhang, Z. and Zhang, J. (2012). Rapid identification of microorganisms isolated from throat swab specimens of community-acquired pneumonia patients by two

MALDI-TOF MS systems. *Diagnostic Microbiology and Infectious Disease,* **73** (4), 301-307

Yamada, M., Yao, I., Hayasaka, T., Ushijima, M., Matsuura, M., Takada, H., Shikata, N., Setou, M., Kwon, A.H. and Ito, S. (2012). Identification of oligosaccharides from histopathological sections by MALDI imaging mass spectrometry. *Analytical and Bioanalytical Chemistry,* **402** (5), 1921-193

Yang, Y., Li, Z.Y., Yamaguchi, K., Tanemura, M., Huang, Z., Jiang, D., Chen, Y., Zhou, F. and Nogami, M. (2012). Controlled fabrication of silver nanoneedles array for SERS and their application in rapid detection of narcotics. *Nanoscale,* **4** (8), 2663-2669

Zhang, M., Becue, A., Prudent, M., Champod, C. and Girault, H.H. (2007). SECM imaging of MMD-enhanced latent fingermarks. *Chemical Communications,* (38), 3948-3950

2 The "Dry-Wet" Method of MALDI Matrix Application

2.1 Introduction

MALDI Mass Spectrometry (MALDI-MS) has evolved to include imaging capabilities, which have been utilised in numerous applications since the first paper published by Caprioli *et al.*, (1997). The applications include: proteomics (van Remoortere *et al.*, 2010; Cole *et al.*, 2011), lipidomics (Jackson *et al.*, 2007; Hart *et al.,* 2011) and metabolomics (Stoeckli *et al.*, 2007; Lee *et al.*, 2012). Matrix application is a critical aspect in determining the success of the imaging experiment and extensive research has been undertaken over the years to enhance this vital sample preparative step, with the objective of optimising analyte extraction and image resolution, whilst minimising analyte delocalisation. The most prevalent mode of matrix application involves the use of "wet" matrix, where the selected matrix is dissolved in appropriate solvent combinations, prior to deposition by either microspotting or spraying. Microspotting provides a higher extraction efficiency leading to enhanced sensitivity, but the spatial resolution is limited to the diameter of the spot. It is suitable for imaging analysis although the fine features of the specimen under investigation are lost; however, analyte delocalisation is limited to the diameter of the spot. Contactless microspotting can currently be accomplished by piezo-dispensing the matrix solution using a chemical inkjet printer, as first reported by Sloan *et al.*, (2002), or through the use of acoustic droplet ejection technology, as first demonstrated by Aerni *et al.*, (2006). Matrix application using a chemical inkjet matrix printer (ChIP-1000) was recently advocated by Patel and co-workers. The research group applied sinapinic acid to human oral squamous cell carcinoma biopsy specimens, in order to evaluate the potential of MALDI–MSI to detect and image peptides and proteins within diseased and normal tissue sections, with reproducible results between adjacent sections and

different samples (Patel *et al.*, 2009). Figure 2.1 shows a Shimadzu chemical inkjet matrix printer (ChIP-1000).

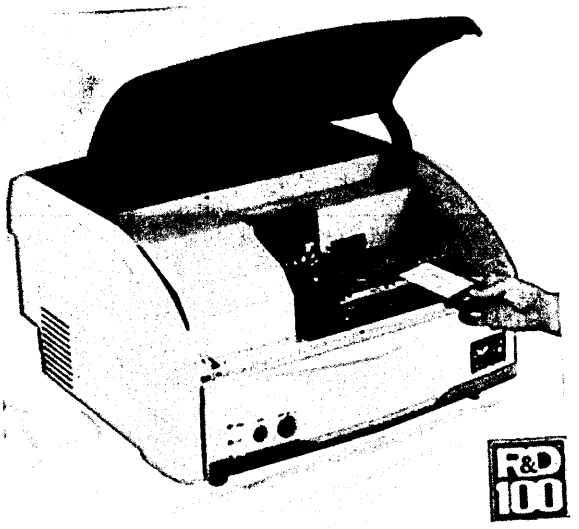

Figure 2-1: A Chemical Inkjet Printer (ChIP) which enables contactless microspotting of matrix onto samples.

Image obtained from http://www.shimadzu-biotech.net/pages/products/2/chip/php

The use of acoustic droplet ejection technology has previously been reported by Aerni and co-workers to be more reproducible than spraying, whilst also avoiding the potential problem of "clogging" capillaries or nozzles. Furthermore, the matrix composition and droplet size can be varied depending on the sample being investigated, with small, closely spaced droplets providing the highest resolution images (Aerni *et al.*, 2006). The Portrait 630 multi-reagent spotter (Labcyte Inc. CA, USA) uses acoustic droplet ejection technology to deposit matrix onto samples and is depicted in figure 2.2.

Figure 2-2: A Portrait 630 multi-reagent spotter, which uses acoustic droplet ejection technology to dispense matrix onto samples.

Image obtained from http.V/www.labcyte.com.portrait®_630_spotter/default.92.html)

Spraying as a method of matrix deposition can be achieved either manually or robotically. Spraying enables higher spatial resolution to be obtained than microspotting, although the sensitivity is lower due to reduced extraction of the analytes present. With spraying the matrix, analyte delocalisation can be minimised by preventing the sample becoming too wet, by ensuring sufficient drying time between successive matrix layers With manual spraying, parameters such as the distance between the spray nozzle and the sample, the number of passes and the time elapsed between consecutive passes, all require optimising to ensure a uniform deposition of matrix and good analyte extraction. Automated pneumatic sprayers such as the SunCollect auto-spraying system (figure 2.3) ensure more reproducible matrix deposition over manual spraying, although the restricted drying times available between consecutive layers may be insufficient for co-crystallization to occur for some analytes.

j

Figure 2-3: SunCollect auto-spraying system, which deposits matrix as a fine mist onto samples.

Image obtained from

http://www.sunchrom.de/pdf/SunChrom%20SunCollect_english_pdf

Parameters such as the deposition speed, the volume sprayed, the distance between the spray nozzle and the sample and the number of layers deposited, all have an impact on analyte-matrix co-crystallization and analyte extraction.

A recent development in automated spraying is the use of an automated spray chamber equipped with a modified commercial air atomising spray nozzle, which enables multiple samples to be homogenously coated with matrix simultaneously, due to the large spray coating area and spray volume capabilities of the system, thereby reducing the time required to spray samples for subsequent analysis by MALDI-MSI (Mounfield and Garrett, 2012).

Homogeneity of deposition, efficient analyte extraction and good image resolution are also achieved through alternative methodological strategies.

Sugiura and collaborators reported a combined matrix deposition technique, named the spray-droplet method. The protocol consisted of initially spraying

samples with a low concentration matrix solution in humid conditions, followed by microspotting matrix at a higher concentration via a chemical ink-jet printer. The initial spraying step is believed to act as a seeding step for enhanced crystal formation, resulting in a denser and more homogenous distribution of co-crystals. The corresponding mass spectra and images displayed enhanced signal intensity and an improved signal to noise ratio in comparison to matrix deposited by the direct droplet method (Sugiura *et al.*, 2006).

Dry matrices have also been applied to samples, which in most case act as seeding agents. Aerni and collaborators were the first to report the application of ground matrix powder directly to a tissue section. Sinapinic acid was applied in a thin layer using a painter's brush, followed by the application of wet matrix via an acoustic ejector. Microscope images showed that application of a seeding agent prior to depositing matrix solution resulted in the formation of smaller crystals with a more uniform coverage, which gave a more homogenous ion signal (Aerni *et al.*, 2006).

Vapour-phase sublimation was implemented as a means of applying dry matrix to samples by Hankin and co-workers in 2007. The apparatus employed for sublimation is depicted in figure 2.4 and in comparison to samples prepared by electrospray deposition, the sublimated matrix was more homogenous in appearance and the phospholipid ion signal intensity was higher (Hankin *et al.*, 2007).

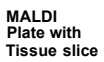

Figure 2-4: The apparatus required for matrix sublimation.

Image obtained from Hankin et al. (2007).

Recently, high resolution images of the distribution of proteins up to 30,000 Da have been obtained using a combined sublimation/re-crystallisation protocol (Yang & Caprioli, 2011). The authors investigated various parameters including tissue washing, tissue thickness, the amount of matrix applied and re-cystallisation conditions. The recommended protocol for imaging proteins with corresponding high quality spectra included a 6-step washing procedure, followed by sublimation and re-crystallisation using 1ml_ of a 5% acetic acid solution at 85° C for 3.5 minutes. Sublimation has also recently been applied to image various higher molecular weight lipids in brain, kidney and ocular tissue, with enhanced sensitivity, due to the uniformity in matrix application (Murphy ***et al.,*** 2011). Sublimation using a new matrix 1, 5-Diaminonapthalene (DAN) has also recently been reported for the analysis of lipids in mouse brain sections and whole body fish sections in both positive and negative ionisation modes. Application of DAN by sublimation enabled an abundance of lipid signals in both polarities to be detected and imaged from the same tissue section, with low background interferences (Thomas ***et al.,*** 2012).

A solvent-free matrix deposition method was utilised in 2008 by Puolitaival and collaborators, which enabled the detection and imaging of phospholipids within mouse brain sections, with a 30 – 100 µm lateral resolution. The paper reports the application of finely ground dihydroxybenzanoic acid (DHB) matrix, which had been applied through a 20 µm sieve. The dry-coated tissue sections were compared to sections prepared by spray coating. The results of the study concluded that the dry-coating method produced high quality phospholipid distribution images, with good signal intensity that were comparable to the images obtained from the spray-coated samples, but with the benefit of a shorter sample preparation time, whilst averting the issue of analyte delocalisation (Puolitaival *et al.*, 2008). The method has recently been successfully replicated by Goodwin and co-workers to image and quantify the presence of pharmaceutical agents within tissue sections (Goodwin *et al.*, 2010a & 2010b).

During this PhD programme, a new matrix deposition methodology has been invented which was specifically developed for the analysis of latent fingermarks. The two-step matrix deposition protocol was termed the "dry-wet method" (Ferguson *et al.,* 2011; Patent Number GB2489215). The dry-wet method incorporates the benefits of previous matrix application techniques (seeding through application of a dry-matrix and the use of solvents for efficient analyte extraction and co-crystallisation). Previous to this, the authors reported the use of MALDI-MSI for the analysis of latent fingermarks using the conventional spray-coating method (Wolstenholme *et al.*, 2009; Bradshaw *et al.*, 2011). However, given the invisible nature of latent fingermarks, a major constraint in the applicability of the technology was the inability to use MALDI-MSI if the fingermark was not previously located (enhanced). The dry-wet method

therefore bridged the gap; the MALDI matrix essentially acts as an enhancing agent and it is applied to the surface using a brush, enabling the fingermark to be visualised, before being recovered by lifting tape, sprayed with solvent and analysed by MALDI-MSI.

2.2 Materials

Trifluoroacetic acid (TFA), α-cyano-hydroxycinnamic acid (α-CHCA) and ALUGRAM SIL G/UV_{254} pre-coated aluminium sheets were purchased from Sigma Aldrich (Poole, UK). Acetone, ethanol and acetonitrile (ACN) were obtained from Fisher Scientific (Loughborough, UK). MALDI target OPTI spotless inserts were purchased from Applied Biosystems (CA, USA). SYNAPT MALDI spotless target plates were obtained from Waters (Manchester, UK). Double sided conductive carbon tape was obtained from TAAB (Aldermaston, UK). Zephyr brushes were purchased from CSI Equipment (http://www.csiequipment.com). Klenair air spray was obtained from Kenco Ltd (Swindon, UK). Dettol alcohol wipes were purchased from Sheffield branches of Wilkinson's (Worksop, UK). Forensic lifting tape was acquired from TETRA Scene of Crime (http://www.tetrasoc.com/).

2.3 Methods

2.3.1 Instrumentation

All mass spectrometric analyses were conducted using either a modified API Q-Star Pulsar-*i* hybrid quadrupole time-of-flight (QTOF) instrument (Applied Biosystems, CA, USA), or a SYNAPT G2 High Definition Mass Spectrometry (HDMS) system incorporating ion mobility (Waters Corporation, Manchester, UK).

An Applied Biosystems API Q-Star Pulsar-*i* MALDI qTOF mass spectrometer was employed to detect and image fingerprint constituents. The orthogonal

MALDI source has been modified to incorporate a 5 kHz solid-state laser having a wavelength of 355 nm (Trim *et al.*, 2010). All MALDI-MS spectra were obtained in positive ion mode in the mass range between *m/z* 100 and 1000. Declustering potential 2 was set at 15 arbitrary units and the focus potential at 10 arbitrary units, with an accumulation time of 0.117 min. MALDI-MSI analyses were performed at a resolution of 150 µm x 150 µm using 'continuous raster imaging' at a laser repetition rate of 5 kHz.

High mass accuracy mass spectra and high resolution images were obtained using a MALDI SYNAPT G2 HDMS system equipped with an Nd:YAG laser operated at 1 kHz, which equates to a laser energy of 10.5 µJ. Mass spectra and images were acquired in positive ion mode, in the *m/z* range 100 to 1000.

Data processing of mass spectra was performed using mMass, an open source MS tool (Strohalm *et al.*, 2008; Strohalm *et al.*, 2010) and MassLynx (Waters Corporation, Manchester, UK). Data processing of all images was performed using BioMap 3.7.5 software (Novartis, Basel, Switzerland).

Tandem mass spectrometry experiments were performed on a modified API Q-Star Pulsar-*i* hybrid quadrupole time-of-flight (QTOF) instrument.

Fingermarks were sprayed using either of two 'Suncollect' auto-spraying systems (Sunchrom GmbH, Friedrichsdorf, Germany). One system sprayed at a slow setting at a rate of 2 µL/min, and the other system sprayed at a faster rate of 5 µL/min.

Digital images were obtained using a Fujifilm IS Pro, 3488 x 2616 pixel CCD camera, with a Fujinon 50 mm UV lens (Fujifilm UK, Bedford, UK). The size of the image obtained was 4256 x 2848 pixels.

UV-Vis and fluorescent images of fingermarks were obtained using: (i) a video spectral comparator (VSC4CX, Foster & Freeman, Evesham, UK) at an excitation wavelength of 365 nm, (ii) using an Olympus BX51 fluorescent microscope (Olympus UK Ltd, Southend-on-Sea, UK) equipped with Cell-D software (Olympus), using U-MNU2 filter (excitation 360-370 nm, 400 nm dichromatic, emission 420 nm) and (x4) objective .

All Scanning Electron Microscopy (SEM) images were obtained using a FEI NOVA nanoSEM 200 (FEI, The Netherlands) fitted with a HELIX bullet/ detector system to enable electron imaging in Variable Pressure (VP) mode. Images were acquired using an accelerating voltage (HV) of 5 kV, a spot size between 3 and 4 mm and at a working distance of 4-5 mm. Samples were viewed at a magnification of x700 and x3000.

2.3.2 Fingermark Preparation

Groomed fingermarks were prepared by cleaning the hands with alcohol wipe or a 50% ethanol wash and rubbing the fingers on the forehead, nose and chin five times to obtain a sebum-rich mark before deposition onto ALUGRAM ® SIL G/UV $_{254}$ pre-coated aluminum sheets after removing the silica with acetone.

Ungroomed fingermarks were prepared by first cleaning hands with either alcohol wipes or a 50% ethanol wash and carrying on normal work activities for a period of 15 minutes before deposition onto ALUGRAM ® SILG/UV $_{254}$ pre-coated aluminum sheets after removing the silica with acetone.

Aluminium sheets were attached to either MALDI spotless inserts or SYNAPT G2 spotless target plates using double sided carbon conductive tape for analysis by MALDI-MS, MALDI-MS/MS and MALDI-MSI.

2.3.3 The Dry-Wet Matrix Application Method

Fingermarks were deposited onto ALUGRAM ® SIL G/UV $_{254}$ pre-coated aluminum sheets, prepared as described in section 2.3.2. The matrix (α-CHCA) was applied to fingermarks using a zephyr brush and excess matrix removed using a Klenair air sprayer. Fingermarks were then sprayed with either 3 layers of a 70:30 ACN/0.5% TFA solvent combination at a rate of 2 µL/min (slow spraying system) or 5 layers, at a rate of 5 µL/min (fast spraying system) using a "SunCollect" auto-spraying system[1]. The matrix employed in the experiments was either unground (as supplied by manufacturers), manually ground (ground using a pestle and mortar) or mechanically ground (ground using a Herzog vibrating disk mill) and passed through a 38 µm sieve.

2.3.4 Comparison of Groomed and Ungroomed Fingermarks Prepared by the Dry-Wet Method

Groomed and ungroomed fingermarks were obtained as described in section 2.3.2 and prepared by the dry-wet method as described in section 2.3.3, using manually ground α-CHCA and the slow matrix/solvent spraying system.

MALDI-MSI images were acquired using a modified API Q-Star Pulsar-*i* hybrid QTOF instrument, as stated in section 2.3.1. Data processing of all images was performed using BioMap 3.7.5 software.

2.3.5 Comparison of Ungroomed Fingermarks Prepared by the Dry-Wet and Solvent-Free Matrix Application Methods

Four ungroomed fingermarks were obtained as described in section 2.3.2. Two fingermarks were divided in half, and two were left whole. One half of each fingermark and one whole fingermark were prepared by the dry-wet method as described in section 2.3.3, using mechanically ground α-CHCA and the slow

[1] Two spraying systems were employed as initially experiments were performed using the slow spraying system. The SunCollect auto-spraying system was subsequently modified to enable spraying at a faster rate in order to reduce sample preparation time, without affecting the quality of the images obtained.

spraying system. The other half of each fingermark and the remaining whole fingermark were dusted with mechanically ground α-CHCA and the excess removed using a blast of air. These fingermarks were left unsprayed.

MALDI-MSI images were acquired using a modified API Q-Star Pulsar-*i* hybrid QTOF instrument, as stated in section 2.3.1. Data processing of all images was performed using BioMap 3.7.5 software.

2.3.6 Reproducibility Study

Four ungroomed fingermarks were obtained from the same donor as described in section 2.3.2 and prepared by the dry-wet method as described in section 2.3.3, using manually ground α-CHCA and the slow spraying system. After analysis by MALDI-MSI using a modified API Q-Star Pulsar-*i* hybrid QTOF instrument, data processing of all images was performed using BioMap 3.7.5 software. Average spectra obtained from the images were exported as text files from Biomap to mMass, which is an open source multifunctional mass spectrometry software package.

2.3.7 Investigations into Matrix Distribution and Crystal Size in Relation to Ridge Pattern Quality

Ungroomed fingermarks were obtained from one donor as described in section 2.3.2. Fingermarks were prepared by the dry-wet method as described in section 2.3.3, using either unground α-CHCA, manually ground α-CHCA or mechanically ground α-CHCA. Fingermarks were sprayed using the fast spraying system.

Scanning Electron Microscope images were obtained using a FEI NOVA nanoSEM 200.

MALDI-MSI images were acquired using a modified API Q-Star Pulsar-*i* hybrid QTOF instrument, as stated in section 2.3.1. Data processing of all images was performed using BioMap 3.7.5 software.

2.3.8 Comparison of the Dry-Wet Method with the Conventional Spray-Coating Matrix Application Method

Ungroomed fingermarks were obtained from three donors (a good, intermediate and poor secretor) on aluminium plates, which had been prepared as described in section 2.3.2. For each donor, fingermarks were divided in half. One half of each fingermark was prepared by the dry-wet method as described in section 2.3.3 using mechanically ground α-CHCA and the fast spraying system. The other half of each fingermark from each donor was prepared by spraying with 4 layers of a 5 mg/ml α-CHCA solution in 70:30 ACN/0.1% TFA at a rate of 1 µL/min, 2 µL/min, 2 µL/min, 2 µL/min, using the slow spraying SunCollect auto-sprayer system. Both matrix deposition methods had been previously optimised to provide the best quality image of the fingermark.

Scanning Electron Microscope images were obtained using a FEI NOVA nanoSEM 200.

MALDI-MS images were obtained using a modified API Q-Star Pulsar-*i* hybrid QTOF instrument, as stated in section 2.3.1. Data processing of all images was performed using BioMap 3.7.5 software.

2.3.9 High Mass Accuracy Measurements

Ungroomed fingermarks were obtained as described in section 2.3.2 and prepared by the dry-wet method as described in section 2.3.3 using mechanically ground α-CHCA and the fast spraying system. High mass accuracy spectra were recorded in positive mode directly from fingermarks using a MALDI SYNAPT G2 HDMS system. Spectra were acquired in resolution

mode (V), over the mass range 100 to 1000 Da. Spectra were initially calibrated using a standard solution of polyethylene glycol (PEG), using the PEG signal at *m/z* 525.2887 as a lock mass and centroided prior to generation of an accurate peak list. The centroided *m/z* values were then submitted to the Lipidmap database (http://www.lipidmaps.org) using a mass tolerance of 0.001 in order to generate a list of probable structures.

2.3.10 High Resolution MALDI-MSI

Ungroomed fingermarks were obtained as described in section 2.3.2 and prepared by the dry-wet method as described in section 2.3.3, using mechanically ground α-CHCA and the fast spraying system. Fingermarks were imaged in positive mode using a MALDI HDMS SYNAPT G2 System. Fingermarks were obtained in sensitivity mode, using a laser energy of 220 arbitrary units and a spatial resolution of 50 µm x 50 µm and 20 µm x 20 µm. The dimensions of the 50 micron image were 22.9 mm x 14.7 mm, which equated to 105992 laser shots and the dimensions of the 20 micron image were 9.1 mm x 4.6 mm, which equated to 103667 laser shots. The time taken to acquire each image was approximately 58 hours and 59 hours for the 50 µm and 20 µm images respectively. Data processing of all images was performed using BioMap 3.7.5 software.

2.3.11 Tandem Mass Spectrometry

Groomed fingermarks were obtained as stated in section 2.3.2 and prepared by the dry-wet method as stated in section 2.3.3 using mechanically ground and sieved α-CHCA and the fast spray setting. Tandem mass spectra (MS/MS) were acquired on a modified API Q-Star Pulsar-*i* hybrid QTOF instrument in positive ion mode. Declustering potential 2 was set at 20 arbitrary units and the focus potential at 5 arbitrary units, with an accumulation time of 1 minute.

MS/MS spectra of the precursor ions of two protonated fatty acids (oleic acid at *m/z* 283.3 and eicosenoic acid at *m/z* 311.3) were obtained directly from fingermarks. The MS/MS spectra of the precursor ions of both lipid standards (2 µg/mL in ACN mixed with an equal volume of a 10mg/mL α-CHCA in 70:30 ACN/0.5% TFA) were initially acquired in order to compare the spectra of the standards with those generated from the same species within fingermarks. MS/MS images of the precursor ion of protonated oleic acid (*m/z* 283.3) and various protonated product ions were also obtained, alongside two different concentrations of oleic acid standard (2 µg/mL and 1 µg/mL mixed with α-CHCA as stated above).

2.3.12 Application of the Dry-Wet Method to Ungroomed Fingermarks Deposited on Various Substrates

Ungroomed fingermarks from two donors were deposited on various non-porous and semi-porous surfaces including: a metal knife, a glass laboratory beaker, a semi-varnished wood tray, a leather belt, a plastic container (Ferguson *et al.*, 2011), an aluminium can, a reflective mirrored surface, an A4 plastic wallet and a cardboard tissue box.

After deposition, fingermarks were dusted with manually ground α-CHCA using a zephyr brush, and excess powder removed using a blast of air. Digital images of the fingermarks after dusting on the different deposition surfaces were obtained using a Fujifilm IS Propixel CCD camera.

The dusted fingermarks were then lifted off each surface using CSI lifting tape and sprayed with 3 layers of a 70:30 ACN/0.5% solvent combination at a rate of 2 µL/min using the slow auto-spraying system. Fingermarks were analysed by MALDI-MSI using a modified API Q-Star Pulsar-*i* hybrid QTOF instrument, as

stated in section 2.3.1. Data processing of all images was performed using BioMap 3.7.5 software.

2.4 Results and Discussion

2.4.1 Application of the Dry-Wet Method to Groomed and Ungroomed Fingermarks

A novel two-step matrix deposition method (the dry-wet method) has been developed and applied to the analysis of latent fingermarks. The method incorporates initial matrix deposition using a zephyr brush of ground matrix as a fine powder, followed by spraying with a 70:30 ACN/0.5% TFA solvent composition. The solvent composition was previously optimised (Wolstenholme et al., 2009) to ensure the best results with respect to ion signal intensity and signal to noise were achieved (data not shown). The initial application of finely ground matrix via brushing is analogous to the application of conventional powders by scene of crime officers (SOCOs) to visualise latent fingermarks on a variety of deposition surfaces. The dry-wet method combines the visualisation and acquisition of the evidence in the conventional forensic fashion (photographing and/or by acquiring UV/ fluorescent images) with the added possibility to apply MALDI-MSI. A benefit of utilising analytical techniques such as MALDI-MSI over conventional Fingermark Enhancing Techniques (FETs) is that additional information could potentially be gained from the chemical constituents detected within latent fingermarks. This could be helpful in cases where the fingermarks are too smudged and distorted to aid identification, as information could be gained that may provide some indication of the donors' lifestyle (Hazarika *et al.*, 2008; Benton *et al.*, 2010; Boddis and Russell, 2011).

Initial experiments involved investigating whether the novel method was suitable for detecting the chemical constituents in both groomed fingermarks (artificially

loaded with sebum) and ungroomed fingermarks, and whether adequate distribution images of the compounds could be obtained. Figure 2.5(a) shows a histogram depicting the relative intensity of ions at certain *m/z* values obtained from the MALDI-MS images of both groomed and ungroomed fingermarks, along with the corresponding mass spectra (figure 2.5(b)).

The *m/z* values chosen correspond to fatty acids that have previously been identified in fingermark residue including dehydrated palmitoleic acid at *m/z* 237.2, pentadecanoic acid at *m/z* 243.2, cis-9-octadecenoic acid (oleic acid) at *m/z* 283.3 and octadecanoic acid (stearic acid) at *m/z* 285.3 (Archer *et al.*, 2005; Croxton *et al.*, 2010). From figure 2.5, the relative abundance of each of the tentatively identified fatty acids shown was, as expected, greater in the groomed fingermarks than the ungroomed fingermarks. Groomed fingermarks are, in fact, artificially loaded with sebum from the sebaceous glands by wiping the fingertips across the "oily" parts of the face, which is known to contain an abundance of lipid species including fatty acids, glycerides, wax esters, sterols, cholesterol esters and squalene (Ramotowski, 2001). The distribution images obtained from both groomed and ungroomed fingermarks prepared by the dry-wet method provided images with excellent ridge detail and the *minutiae* were clearly evident, demonstrating the applicability of the method for both fingermark types. The ability to detect and image the distribution of the chemical constituents of ungroomed fingermarks clearly demonstrates the sensitivity of MALDI-MSI over other analytical techniques that have recently been used to image latent fingermark residue such as ATR-FTIR, DESI-MS, SALDI-TOF-MS and SERS, since these techniques all utilised groomed fingermarks or fingermarks artificially spiked with exogenous compounds (Ricci *et al.*, 2007; Ifa *et al.*, 2008; Rowell *et al.*, 2009; Connatser *et al.*, 2010).

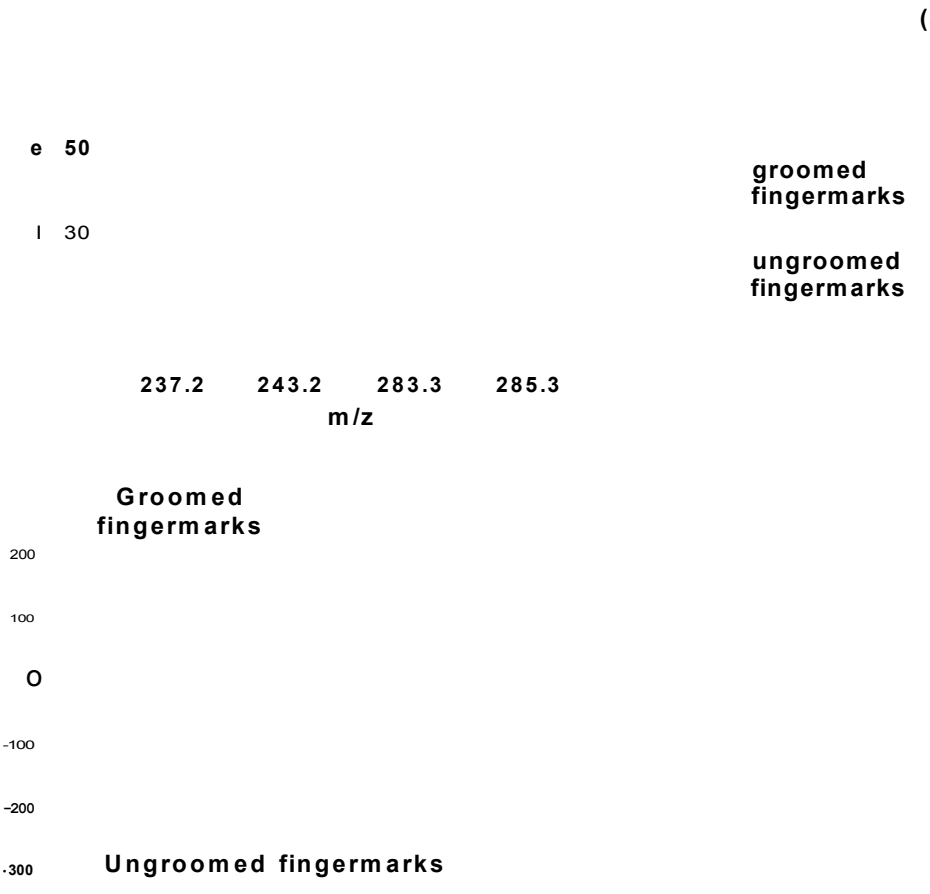

Figure 2-5: A histogram (a) and the corresponding mass spectra (b) showing the relative intensity of ions at specific m/z values obtained from groomed (in blue in panel a) and ungroomed fingermarks (in red in panel a) prepared by the dry-wet method.

The m/z values correspond to the tentatively identified fatty acids; dehydrated palmitoleic acid at m/z 237.2, pentadecanoic acid at m/z 243.2, cis-9-octadecenoic acid (oleic acid) at m/z 283.3 and octadecanoic acid (stearic acid) at m/z 285.3.

As groomed fingermarks are the least likely type to be found at "real" crime scenes, subsequent work concentrated on ungroomed fingermarks. The distribution images of a range of the endogenous species and an exogenous compound present within an ungroomed fingermark can be seen in figure 2.6. The putatively identified lipids include: dodecanoic acid (*m/z* 201.2), tetradecanoic acid (*m/z* 229.2), dehydrated palmitoleic acid (*m/z* 237.2), pentadecanoic acid (*m/z* 243.2), oleic acid (*m/z* 283.3), stearic acid (*m/z* 285.3), nonadecanoic acid (*m/z* 299.3), eicosenoic acid (*m/z* 311.3), dehydrated cholesterol (*m/z* 369.4), vitamin E (*m/z* 431.2) a diacylglycerol (DG) (*m/z* 583.6) and an exogenous ion previously identified as dimethyldioctadecylammonium (*m/z* 550.6) (Mannier *et al.*, 2008; Wolstenholme *et al.*, 2009).

2.4.2 Comparison of Ungroomed Fingermarks Prepared by the Dry-Wet and Solvent-Free Matrix Application Methods

To investigate the relevance of spraying fingermarks with solvents after initial application of ground matrix, ungroomed fingermarks were prepared by either the dry-wet method or the solvent free matrix application method, recently advocated by Puolitaival and co-workers (Puolitaival *et al.*, 2008). The intensity of the ions at specific *m/z* values corresponding to tentatively identified lipids were compared together with the corresponding distribution images. The intensity of the ions present in the fingermarks prepared by the dry-wet method was a lot higher than that of ions that remained unsprayed, demonstrating that spraying of the solvents after application of the matrix is a crucial step with respect to ionisation efficiency and the quality of the ridge detail in the imaged fingermarks. These results are in agreement with previously published results by Aerni and collaborators, who stated that no measurable ion signal was

observed after application of the powdered matrix, without subsequent application of "wet" matrix (Aerni ***et al.,*** 2006).

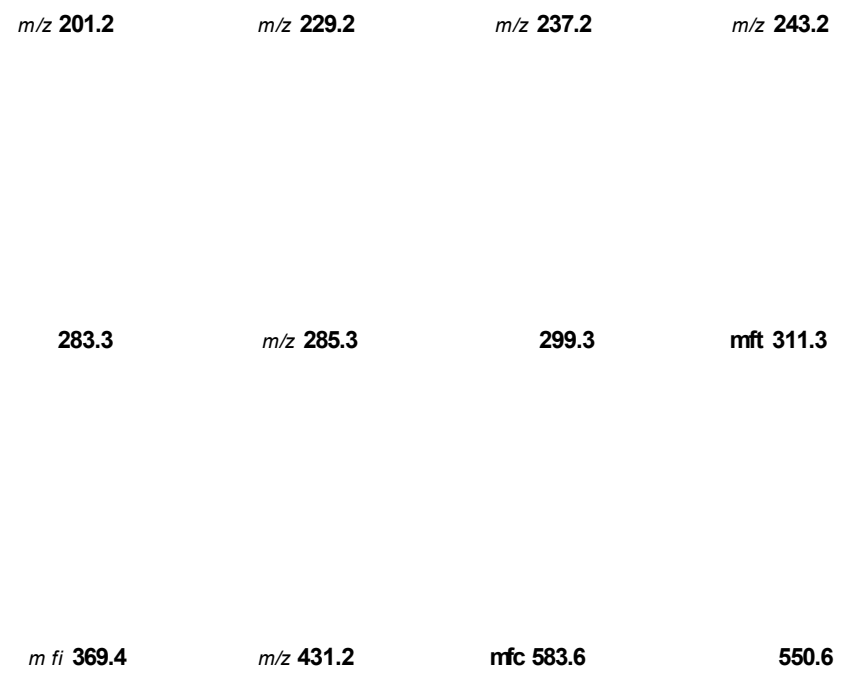

Figure 2-6: Distribution images of various lipid species within an ungroomed fingermark prepared by the dry-wet method.

Species tentatively identified include dodecanoic acid (m/z 201.2), tetradecanoic acid (m/z 229.2), dehydrated palmitoleic acid (m/z 237.2), pentadecanoic acid (m/z 243.2), oleic acid (m/z 283.3), stearic acid (m/z 285.3), nonadecanoic acid (m/z 299.3), eicosenoic acid (m/z 311.3), dehydrated cholesterol (m/z 369.4), vitamin E (m/z 431.2) a diacylglycerol (m/z 583.6) and an exogenous compound previously identified as dimethyldioctadecylammonium ion (m/z 550.6).

Figure 2.7(a) depicts a histogram of the average relative intensity of specific ions obtained from two ungroomed fingermarks that had been divided in half and prepared by the two matrix deposition methods, together with the corresponding spectra (figure 2.7(b)).

From the histogram and spectra, the ions at *m/z* 255.2, 283.3 and 311.3 which correspond to the tentatively identified fatty acids palmitoleic acid, oleic acid and eicosenoic acid respectively, are of a far higher intensity in the ungroomed fingermarks prepared by the dry-wet method, than the fingermarks prepared by the solvent-free matrix application method. This is also evident in the resulting distribution images of the three species within whole fingermarks prepared by the two matrix application methods as shown in figure 2.8. This shows that application of solvent is critical as it aids analyte solubility and extraction. However, even without the application of solvent, some crystallisation between the analyte and matrix occurs, which is hypothesised to be due to residual moisture in the fresh fingermarks (Puolitaival *et al.*, 2008; Goodwin *et al.*, 2010a). All the images depicted in figure 2.8 have been normalised to the total ion count (TIC). Normalisation is a process that modifies the individual mass spectra by multiplication of each spectrum in an image with an intensity scaling factor, with the objective of making each pixel comparable. Normalisation ensures that variation in the ion signals observed for specific ions of interest are not due to factors such as instrumental variation, inhomogeneous matrix application and different ionisation efficiencies of the analytes present. Besides normalising to the TIC, data can also be normalised to a single matrix peak (Trim *et al.*, 2008), or normalising to an internal standard (Bartsch *et al.*, 1996).

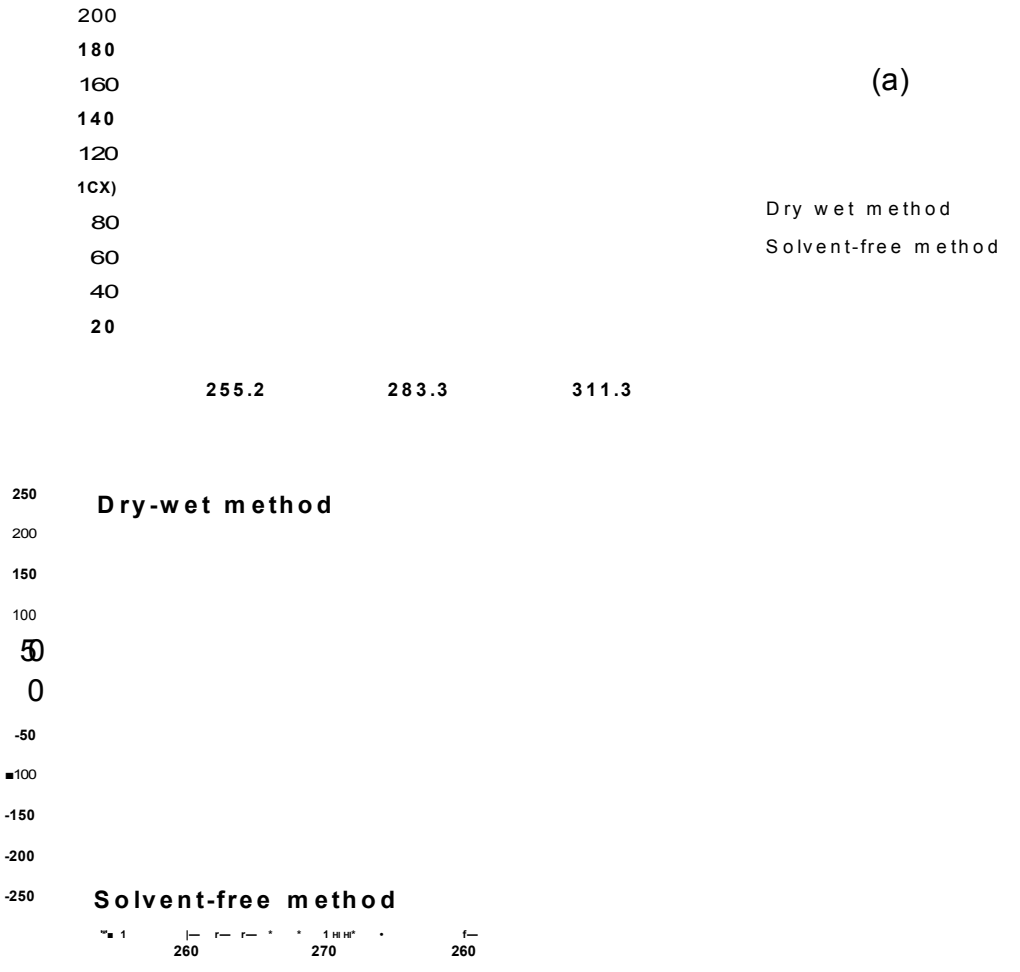

Figure 2-7: A histogram (a) and corresponding mass spectra (b) showing the average intensity at three m/z values obtained from two ungroomed fingermarks. *Fingermarks were divided in half and prepared by either the dry-wet method (in blue in panel (a)) or the solvent free matrix application method (in red in panel (a)). The m/z values correspond to three tentatively identified fatty acids; palmitoleic acid at m/z 255.2, oleic acid at m/z 283.3 and eicosenoic acid at m/z 311.3.*

Dry-wet method Solvent- free method

m/z 255.2

m/z 283.2

m/z 311.2

Figure 2-8: MALDI-MS Images showing the distribution of three tentatively identified fatty acids (palmitoleic acid at m/z 255.2, oleic acid at m/z 283.3 and eicosenoic acid at m/z 311.3) within ungroomed fingermarks prepared by the dry-wet method (left), or the solvent free matrix application method (right).

2.4.3 Reproducibility Study

The reproducibility of the dry-wet method was investigated by imaging four ungroomed fingermarks obtained from the same donor and prepared as stated in section 2.3.6. For each fingermark, a region of interest was defined, and an average spectrum of the selected area was obtained and exported from Biomap to mMass. The four mass spectra generated for the protonated α-CHCA peak, at *m/z* 190 were superimposed as shown in figure 2.9(a) (spectra were not normalised).

All four spectra demonstrated good reproducibility in terms of the ion signal intensity, which indicates the reproducibility of the matrix application method. The fact that all four spectra were not perfectly superimposed is likely to be the result of differences in the fingermark deposition process. Factors such as the amount of the pressure applied, the angle at which the fingermark is deposited on the surface and the duration of contact are all known to contribute to variations in fingermark deposition that may affect the quality of the resulting fingermark (Fieldhouse, 2011). Figure 2.9(b) shows four spectra at *m/z* 304.2, which correspond to an exogenous ion dimethylbenzylammonium (DBA), which is an antiseptic known to be present in the alcohol wipes used to clean hands prior to deposition (Ferrer and Furlong, 2001; Bradshaw *et al.*, 2011). The peaks obtained from the four replicates again showed good reproducibility of the ion signal intensity. Distribution images of the average peak intensities for this ion are also shown in figure 2.9(b), demonstrating the ability of the dry-wet method to generate images of reproducible quality, with the delta pattern clearly visible in each replicate (Ferguson *et al.*, 2011).

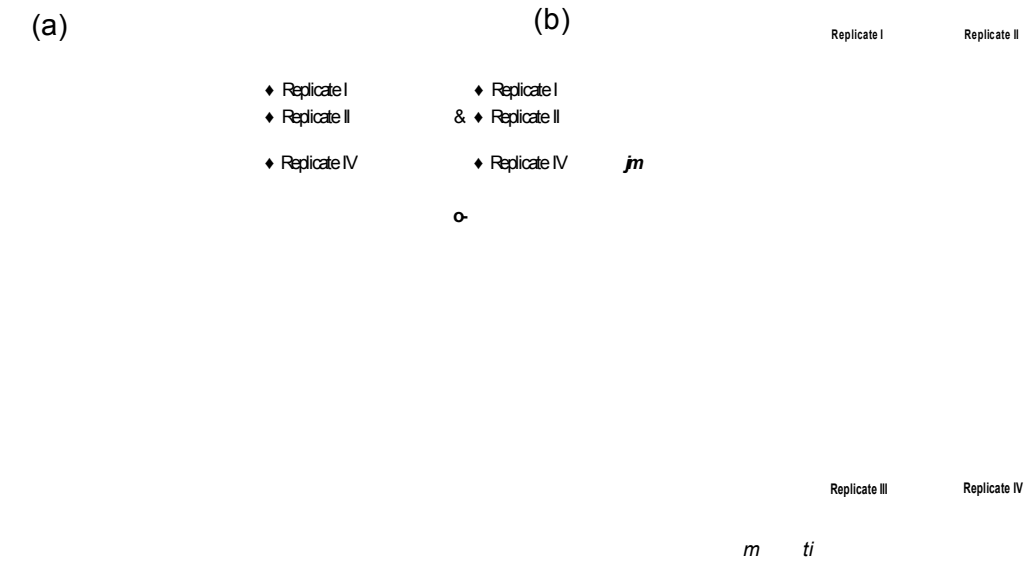

Figure 2-9: MALDI-MSI reproducibility study.

Panel (a) shows the superimposition of the a-CHCA ion signal at m/z 190.0 extracted from the four fingermark replicates prepared by the dry-wet method. The ordinate scale is the arbitrary scale directly provided by the spectrometer without further processing. Panel (b) shows the superimposition of the ion signal at m/z of 304.2 extracted from all 4 replicates, which corresponds to dimethylbenzylammonium ion (DBA). The distribution images of DBA are also shown with the delta pattern clearly visible in each replicate (Ferguson et al., 2011).

The issue of reproducibility in fingermark deposition was recently investigated using a device referred to as a fingermark sampler, which was believed to control the fingermark deposition process to ensure reproducibility in the quality of the fingermarks obtained (Fieldhouse, 2011). Fingermarks were obtained from ten donors with and without the aid of the fingermark sampler. The results of the study showed that the fingermark sampler produced marks of a statistically higher quality than those fingermarks deposited without it, with improved reproducibility both within and between donors. Such a device could potentially improve the results of the reproducibility study shown here, as variations in average peak signal intensity due to inconsistency in fingermark

deposition could be minimised. Figure 2.10 shows a photograph of the fingermark sampler used in the study by Fieldhouse (2011).

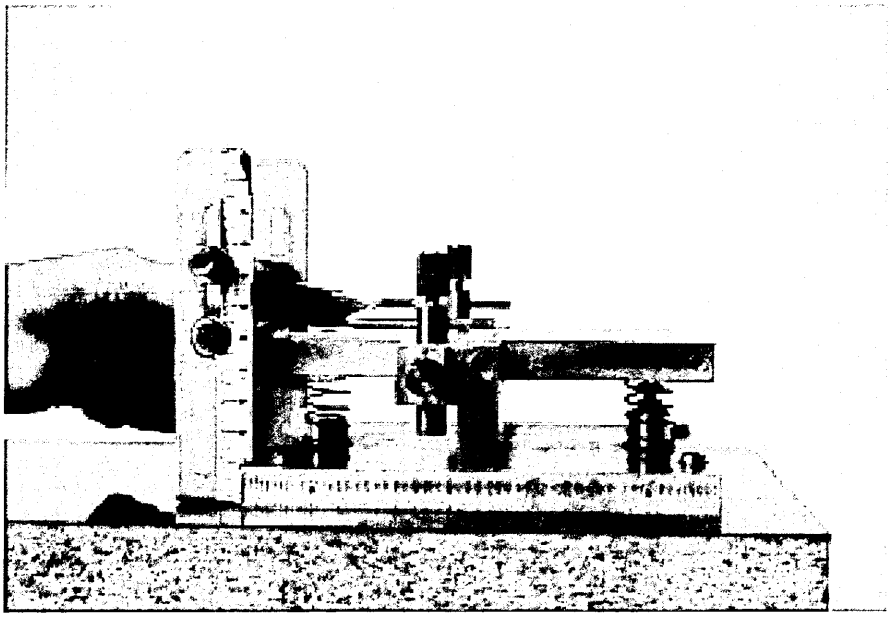

Figure 2-10: The Fingerprint sampler, which has been shown to improve reproducibility in fingermark deposition.

Image obtained from Fieldhouse (2011).

2.4.4 The Effect of Matrix Crystal Size and Distribution on the Quality of the Ridge Pattern Observed

Ungroomed fingermarks were obtained from the same donor and prepared by the dry-wet method using three different size matrix particles. Fingermarks were then submitted for analysis by scanning electron microscopy (SEM) and MALDI-MSI, in order to evaluate the impact of matrix particle size on the quality of the ridge pattern observed in the resulting MALDI-MS images (Ferguson *et al.*, 2013). Prior to solvent spraying, fingermarks were dusted with either unground matrix (as obtained from the manufacturer), manually ground matrix (ground using a pestle and mortar) or, mechanically ground matrix (ground using a Herzog vibrating disk mill and passed through a 38 µm sieve). Figure 2.11 shows the SEM micrographs of fingermarks prepared using the three particle sizes, as well as a fingermark prepared by the spray-coating method, together

with the corresponding MALDI-MS images at *m/z* 283.3. From the SEM images, it can be observed that, for fingermarks prepared by the dry-wet method, after excess matrix is removed, the powdered matrix adheres to only the friction ridges of the fingermarks, as occurs upon application of conventional dusting agents (Sodhi and Kaur, 2001). The average diameter of the co-crystals was approximately 54 µm for the unground, 16 µm for the manually ground and 7 µm for the mechanically ground and sieved. From the micrographs it can be observed that there is a general increase in both the homogeneity and the density of distribution of matrix co-crystals present on the fingermark ridges, as the diameter of the co-crystals decreases. Correspondingly, the quality of the ridge pattern observed improves as the matrix co-crystal average size decreases (figure 2.11, panels' (b)-(b1), (c)-(c1) and (d)-(d1). As the spatial resolution of MALDI-MS images is dictated by the diameter of the laser beam, this suggests that co-crystals smaller than the laser spot size will have no bearing on the image resolution obtained. However, as the homogeneity in matrix coverage improves as matrix co-crystal size decreases, this has been previously proven to improve the resulting image resolution (Crossman *et al.*, 2006). This is evident in the MALDI-MS images of the fingermarks prepared by the dry-wet method shown in figure 2.11. Conversely, the spray-coated fingermark appears amorphous, with less matrix deposited on the fingermark ridges (figure 2.11, panels (a)-(a1)), which offers some explanation for the lower intensity ion signal observed, with the exception of the fingermark prepared using unground matrix. However, as bench top ball mills are now readily available, the use of unground matrix can be easily avoided.

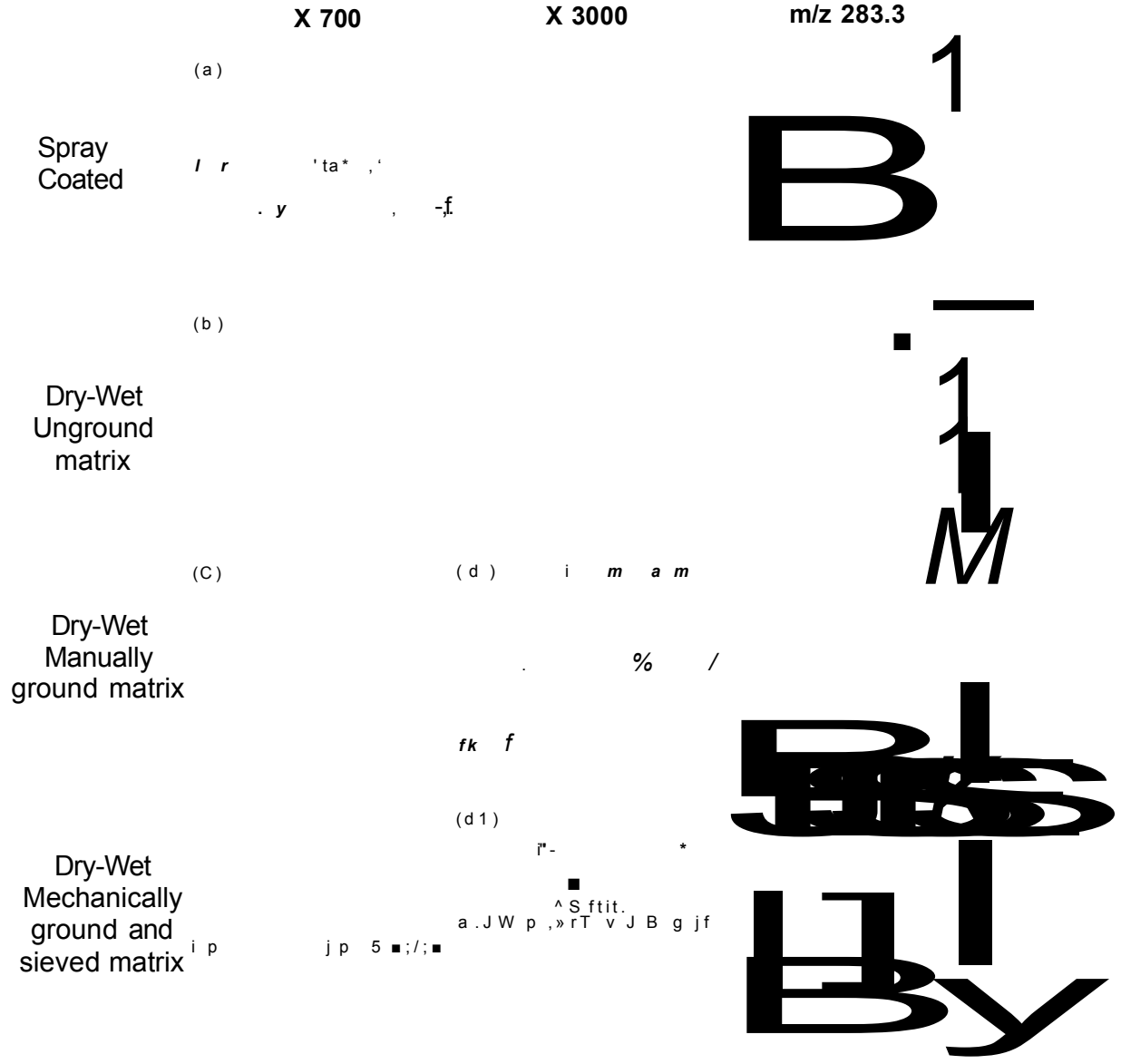

Figure 2-11: SEM and MALDI-MS images of fingermarks prepared by the spray coating matrix application method (a-a2), and the dry-wet method (b-b2), (c-c2) and (d-d2).

Panels (a-d) show SEM images at x700 magnification and panels (a1-d1) at x3000 magnification. Three different size matrix particles were used to prepare fingermarks by the dry-wet method; unground matrix (b-b1), manually ground matrix (c-c1) and mechanically ground and sieved matrix (d-d1). The corresponding MALDI-MSI images are also shown of the ion at m/z 283.3 (a2-d2) (Ferguson et al., 2013).

2.4.5 Comparison of the Dry-Wet and Spray-Coating Matrix Application Methods for the Analysis of the Latent Fingermarks Obtained from Three Donors

The robustness of the dry-wet (D-W) method was evaluated in terms of its ability to generate high intensity ion signals and high quality MALDI-MS images, in a comparison with the conventional spray-coating (S-C) method for the analysis of ungroomed fingermarks (Ferguson *et al.*, 2013). The comparison was made for three donors, previously classified as good, intermediate and poor secretors, which corresponds to an individual's ability to secrete sweat and has a direct impact on the amount of fingermark residue deposited (Bowman, 2005). Each donor's fingermarks were divided in half, in order to ensure a direct comparison of the methods. One half of each fingermark was prepared by the dry-wet method and the other half by the spray-coating method as described in sections 2.3.3 and 2.3.8 respectively. As a representative sample, the ion species at *m/z* 283.3, 311.3 and 668.6 were imaged. Figure 2.12 shows the images obtained for all three donors after normalising to the TIC. As the fingertips were rubbed together prior to deposition, a homogenous distribution of the fingermark secretions was expected. As can be observed, the fingermark halves prepared by the dry-wet method generally produce more continuous images with more defined ridge detail in terms of the *minutiae* obtained. Furthermore, the ion signal is more uniform in the fingermark halves prepared by the dry-wet method, demonstrating the improved homogeneity of the matrix application method over the spray-coating method for fingermark analysis. The ion signal was also generally more intense for fingermarks prepared by the dry-wet method, with the exception of the poor donor. One explanation for the latter circumstance is that the initial application of the ground matrix requires sufficient fingermark residue for the particles to adhere to; therefore with the poor donor the quantity of residue secreted may have been insufficient.

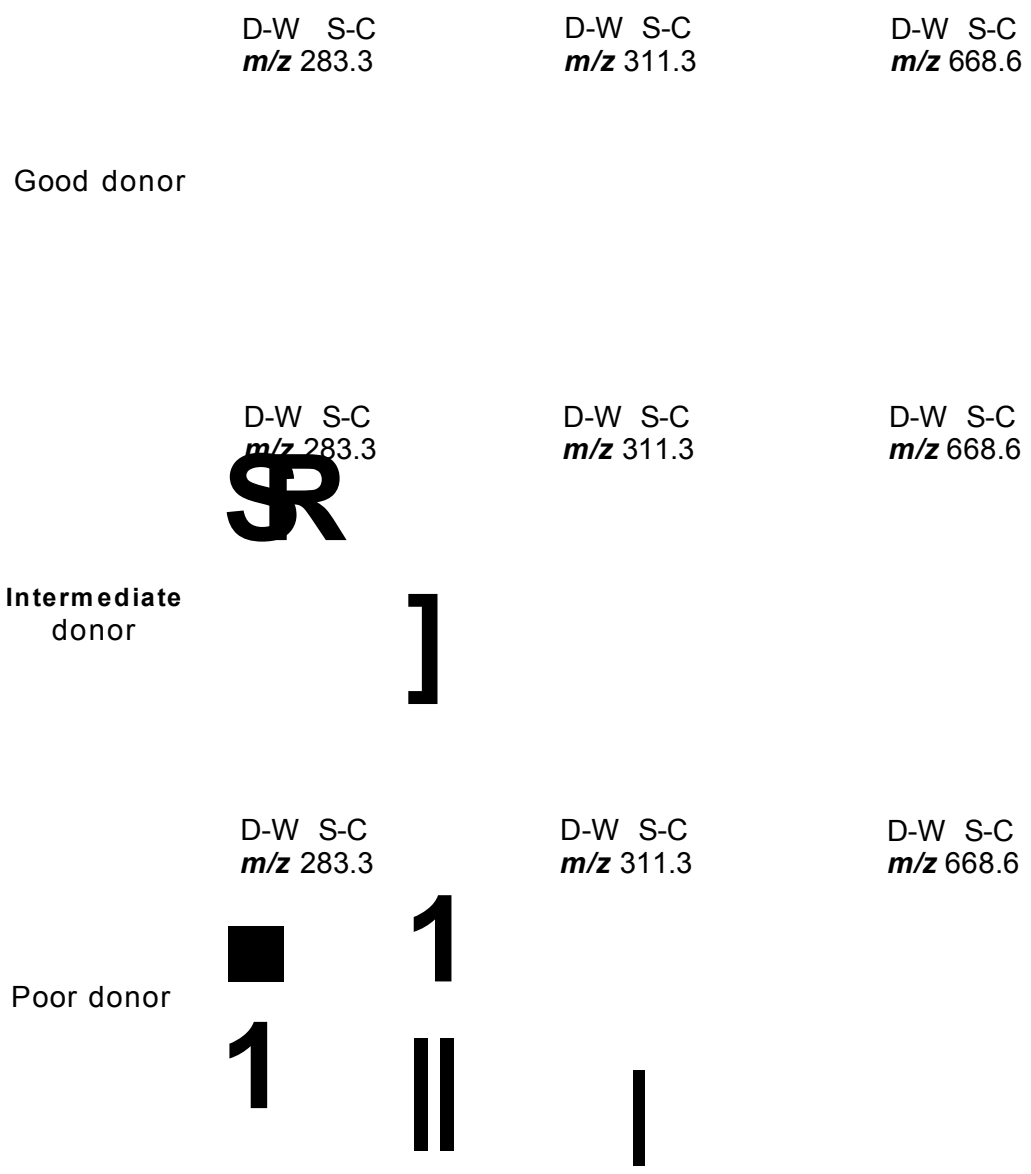

Figure 2-12: MALDI-MSI analysis of fingermarks prepared with either the dry-wet (D-W) or the spray coating (S-C) matrix application method.

Three fingermark donors were selected (previously classified as good, intermediate and poor secretors). For each donor, three ions were imaged at m/z 283.3, 311.3 and 668.6 for both fingermark halves (Ferguson et ai, 2013).

Overall, these results are in agreement with previously published work regarding the initial application of matrix as a fine powder (Aerni *et al.*, 2006). In this work, the authors initially applied sinapinic acid as a fine powder to biological tissues, which acted as a seeding step for the application of matrix by either micro-spotting or spraying. Initial incorporation of a seeding step, resulted in improved homogeneity of matrix deposition over the samples, with higher ion signal intensity, with less shot to shot variance. Furthermore, the authors experimented with other seeding strategies, such as initially immersing samples in saturated sinapinic acid solutions and spraying matrix dissolved in highly volatile solvents, although application of ground matrix provided the best results in terms of reproducibility (Aerni *et al.*, 2006).

2.4.6 High Mass Accuracy Measurements

Mass spectra were acquired directly from ungroomed fingermarks prepared by the dry-wet method as stated in section 2.3.3. Spectra were obtained in the mass range 100-1000 using the SYNAPT G2 HDMS system in resolution mode (V). The centroided *m/z* values obtained were submitted into the Lipidmap database (http://www.lipidmaps.org) using a mass tolerance of 0.001 and an intensity threshold of 5000 arbitrary units in order to generate a list of probable structures. Due to the high number of isobaric lipids, high mass accuracy measurements only enable a tentative identification to be obtained (Ferguson *et al.*, 2013). The lipid species tentatively identified include fatty acids, cholesterol esters (CE), diacylglycerols (DG) and triacylglycerols (TG). Table 2.1 shows a list of the possible lipid species identified, together with the experimental mass taken from the mass spectra and the calculated theoretical mass. All lipid species are identified within a mass error between 0 and 1.69 parts per million (ppm). The fatty acids putatively identified include palmitoleic acid (*m/z*

255.2319), oleic acid (*m/z* 283.2632) and stearic acid (*m/z* 285.2791), which are abundant fatty acids known to be present in latent fingermarks (Archer *et al.*, 2005, Croxton *et al.*, 2010). The other fatty acids putatively identified include nonadecadienoic acid (*m/z* 295.2637), nonadecenoic acid (*m/z* 297.2788), eicosatrienoic acid (*m/z* 307.2636), eicosadienoic acid (*m/z* 309.2790) and eicosenoic acid (*m/z* 311.3943). The higher molecular weight lipid species tentatively identified by high mass accuracy measurements include the cholesterol esters (CE) amino-hexadecanoic acid (*m/z* 640.6032) and amino-octadecanoic acid (*m/z* 668.6343), diacylglycerides (DG) such as the species at *m/z* 523.4723, *m/z* 535.4705, *m/z* 549.4853 and triacylglycerides (TG) such as the species at *m/z* 757.6317, *m/z* 759.6470, *m/z* 771.6473, *m/z* 773.6632, *m/z* 785.6630, *m/z* 797.6628, *m/z* 815.7093. The DG and TG detected in the present study cannot be unequivocally identified, as each one has many possible structural isomers, although a recent study by Emerson and co-workers identified various TG in fingermark residues by Laser Desorption/Ionisation (LDI) MS/MS. The study reported that the *m/z* values observed corresponded primarily to sodium adducts, which are the species tentatively identified in this study, and indeed some of the TG identified by high mass accuracy measurements correspond to TG confirmed by LDI-MS/MS such as the species at *m/z* 771.6 (C14:0, C14:0, C16:1), *m/z* 773.6 (C14:0, C14:0, C16:0), *m/z* 785.6 (C14:0, C15:0, C16:1), and *m/z* 815.6 (C15:0, C16:0, C16:0) (Emerson *et al.*, 2011). Conversely, in their study, Emerson *et al.*, (2011) reported that TG couldn't be detected by MALDI-MS, although TG have subsequently been detected in fingermarks using MALDI-MS by other research groups, which supports the work presented here (Yagnik *et al.*, 2013).

Calculated monoisotopic *m/z*	Experimental *m/z*	*m/z* error ppm (2dp)	Possible lipid species	Ion species
255.2315	255.2319	1.57	FA (16:1)	$[M+H]^+$
283.2632	283.2632	0	FA (18:1)	$[M+H]^+$
285.2788	285.2791	1.05	FA (18:0)	$[M+H]^+$
295.2632	295.2637	1.69	FA (19:2)	$[M+H]^+$
297.2792	297.2788	1.35	FA (19:1)	$[M+H]^+$
307.2632	307.2636	1.3	FA (20:3)	$[M+H]^+$
309.2788	309.2790	0.65	FA (20:2)	$[M+H]^+$
311.3945	311.3943	0.64	FA (20:1)	$[M+H]^+$
523.4722	523.4723	0.19	DG(O-16:0/0:0/12:0)	$[M+H]^+$
535.4697	535.4705	1.49	DG(O-16:0/0:0/13:0)	$[M+Na]^+$
549.4860	549.4853	1.27	DG(O-18:0/0:0/12:0)	$[M+Na]^+$
640.6026	640.6032	0.94	CE(16:0(NH2))	$[M+H]^+$
668.6339	668.6343	0.60	CE(16:0(NH2))	$[M+H]^+$
757.6316	757.6317	0.13	TG(43:1)21:0/2:0/20:1	$[M+Na]^+$
759.6473	759.6470	0.39	TG(43:0)21:0/2:0/20:0	$[M+Na]^+$
771.6467	771.6473	0.78	TG(44:1)14:0/14:0/16:0	$[M+Na]^+$
773.6629	773.6632	0.39	TG(44:0)14:0/14:0/16:0	$[M+Na]^+$
785.6629	785.6630	0.13	TG(45:1)14:0/15:0/16:1	$[M+Na]^+$
797.6629	797.6628	0.13	TG(46:2)22:0/22:2/2:0	$[M+Na]^+$
815.7099	815.7093	0.74	TG(47:0)15:0/16:0/2:0	$[M+Na]^+$

Table 2-1: A list of possible lipid species identified within ungroomed fingermarks by high mass accuracy measurements using a SYNAPT G2 HDMS System incorporating ion mobility.

All species are identified with a mass error less than 1.69 ppm. The lipid species putatively identified include fatty acids and higher molecular weight lipids such as cholesterol esters (CE), diacylglycerides (DG) and triacylglycerides (TG) (Ferguson et al., 2013).

2.4.7 High Resolution MALDI-MS Imaging

High resolution images were obtained of ungroomed fingermarks prepared by the dry-wet method and analysed by MALDI-MSI using a SYNAPT G2 HDMS system, incorporating ion mobility (Ferguson *et al.*, 2013). Ion mobility separates ions not only according to their *m/z*, but also their collisional cross sectional areas, which enables isobaric species to be separated. One of the major issues of imaging species such as lipids is interference from other endogenous species or matrix related ions in the lower mass region, especially in cases where α-CHCA has been used as the matrix. In a typical MALDI-MSI experiment, the resolution of the instrument employed may be insufficient to enable two overlapping peaks to be separated. The mass resolution required to separate two adjacent ions can be calculated using equation 2.1, where *M* is the *m/z* of the lowest ion and *ΔM* is the mass difference between the two adjacent ions.

$$Mass\ Resolution\ = \frac{M}{\Delta M}$$

Equation 2-1: Mass resolution required to separate two adjacent ions

The distribution images of some of the putatively identified endogenous lipids can be seen in figure 2.13. The images were obtained at a spatial resolution of 50 µm x 50 µm, and all images were normalised to the TIC. The MALDI-IMS-MS images show overall excellent ridge details and the *minutiae* are clearly evident.

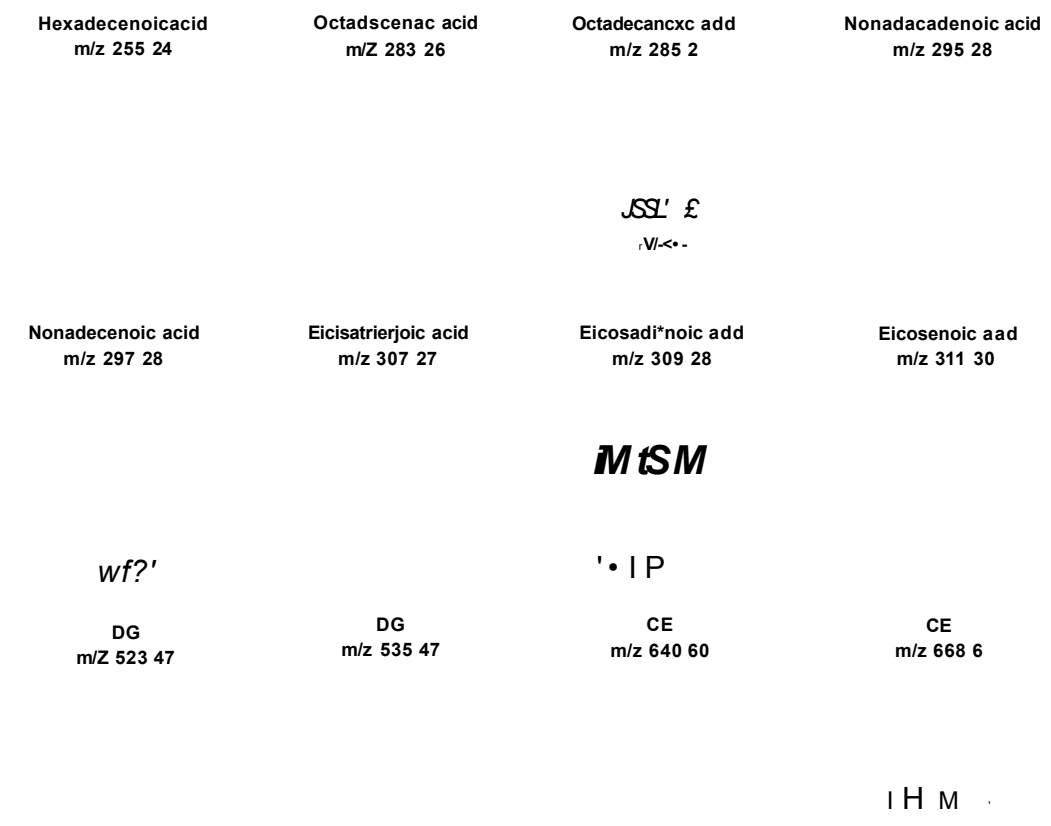

Figure 2-13: High resolution images of ungroomed fingermarks prepared by the dry-wet matrix application method.

Images were acquired on a SYNAPT G2 HDMS system at a spatial resolution of 50 pM x 50 pM. The distribution images of various lipid species are shown including fatty acids, cholesterol esters (CE) and diacylglycerides (DG), which have previously been tentatively identified by high mass accuracy measurements (Ferguson et al., 2013).

Distribution images are also shown at a spatial resolution of 20pm x 20pm for two tentatively identified lipid species, oleic acid at *m/z* 283.3 and eicosenoic acid at *m/z* 311.3, alongside dimethyldodecylammonium ion at *m/z* 550.6 (figure 2.14). At this resolution, Galton level 3 features can be observed, such as pores, which can potentially add another dimension, when trying to ascertain that a fingermark recovered at a crime scene unequivocally belongs to a suspect believed to be involved in a crime.

oleic acid m/z283.3 | eicosenoic acid *m/z* 311.3 | Dimethyldodecylammonium ion *m/z* 550.6

Figure 2-14: High resolution images of ungroomed fingermarks prepared by the dry-wet matrix application method.

Images were obtained at a spatial resolution of 20 pm x 20 pm on a SYNAPT G2 HDMS System. The distribution images of two endogenous lipids are shown; oleic acid at m/z 283.3 and eicosenoic acid at m/z 311.3, as well as dimethyldodecylammonium ion at m/z 550.6 (Ferguson et al., 2013).

2.4.8 Tandem Mass Spectrometry

Tandem mass spectrometry (MS/MS) was performed on two endogenous fatty acids tentatively identified by high mass accuracy measurements; oleic acid at ***m/z*** 283.3 and eicosenoic acid at ***m/z*** 311.3, (Ferguson ***et al.,*** 2013). Groomed fingermarks prepared by the dry-wet method were used for each MS/MS analysis.

For eicosenoic acid, a MS/MS spectrum of a standard was initially acquired and compared to the MS/MS spectra of the fatty acid obtained directly from fingermarks (Fig 2.15). The precursor ion MS/MS spectra of both the lipid standard and the endogenous lipid contained peaks at: ***m/z*** 311.3 corresponding to protonated eicosenoic acid $[CH_3(CH_2)_9CH=CH(CH_2)_7COOH+H]^+$, at ***m/z*** 293, deriving from the loss of water from the protonated molecular ion $[M - H_2O+H]^+$, at ***m/z*** 265 corresponding to the loss of -COOH from the protonated molecular ion to give

$[CH_3(CH_2)_9CH=CH(CH_2)_5CH=CH_2+H]^+$ and at *m/z* 171 corresponding to the loss of $CH_3(CH_2)_9$- from the protonated molecular ion to leave $[CH_2=CH(CH_2)_7COOH+H]^+$.

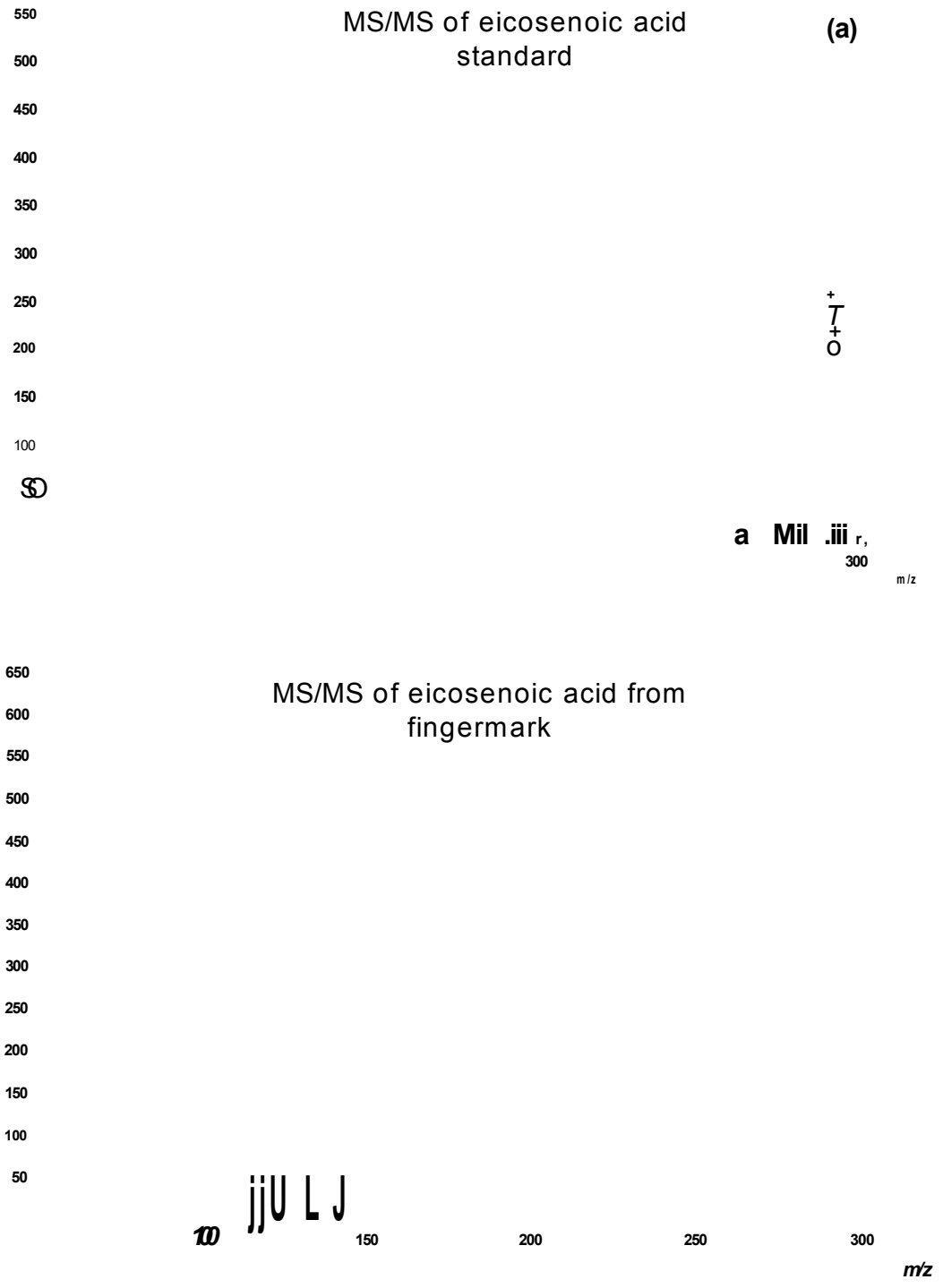

Figure 2-15: MS/MS spectra of the precursor ion of eicosenoic acid (m/z 311.3) obtained from (a) eicosenoic acid standard and (b) directly from a fingermark prepared by the dry-wet method.

(Ferguson et al., 2013).

For oleic acid, a MS/MS spectrum of a standard was initially acquired and compared to the MS/MS spectra of the fatty acid obtained directly from fingermarks. The precursor ion MS/MS spectra of both the standard and the endogenous lipid contained peaks at: *m/z* 283.3 corresponding to protonated oleic acid $[CH_3(CH_2)_7CH=CH(CH_2)_7COOH+H]^+$, at *m/z* 265 corresponding to the loss of water from the protonated molecular ion $[M - H_20+H]^+$, at *m/z* 237 corresponding to the loss of –COOH from the protonated molecular ion to give $[CH_3(CH_2)_7CH=CH(CH_2)_5CH=CH_2+H]^+$, at *m/z* 209 corresponding to the loss of $-(CH_2)_2COOH$ from the protonated molecular ion to give $[CH_3(CH_2)_7CH=CH(CH_2)_7CH=CH_2+H]^+$ and at *m/z* 171 corresponding to the loss of $CH_3(CH_2)_7-$ from the protonated molecular ion to leave $[CH_2=CH(CH_2)_7COOH+H]^+$. Figure 2.16 shows the MS/MS spectra of the oleic acid standard and oleic acid obtained from fingermark residue. For each fatty acid, the MS/MS spectra obtained from the fingermarks did not match those obtained from the lipid standard perfectly. This is due to the limited resolving power of the quadrupole in a qTOF instrument, to select the precursor ion, resulting in a "mixed MS/MS spectrum" as the instrument cannot unequivocally select and fragment only the desired precursor ion. Therefore, with samples such as fingermarks, which contain an abundance of endogenous and exogenous species, many ions are potentially being selected for CID in the collision cell. As high mass accuracy is unable to differentiate between structural isomers and if ion mobility MS/MS is not employed, one alternative possibility is to use MALDI-MS/MS to confirm identification of a species. The corresponding distribution images of the fragment ions after MALDI-MS/MS of the species at *m/z* 283.3 obtained from a fingermark and two spots of an oleic acid standard are shown in figure 2.17. This provides further confirmation

together with the high mass accuracy measurement that the species being fragmented is oleic acid, as the protonated precursor ion at *m/z* 283.3 and its protonated fragments at *m/z* 265.3, 237.1, 209.1 and 171.2 are highlighted in both the standards and the fingermark when subsequently analysed using Biomap software.

MS/MS of oleic acid

MS/MS of oleic acid from fingermark

Figure 2-16: MS/MS spectra of the precursor ion of oleic acid (m/z 283.3) obtained from (a) an oleic acid standard and (b) directly from a fingermark prepared by the dry-wet method. (Ferguson et al., 2013).

Figure 2-17: The distribution images of the MS/MS protonated fragment ions after CID of the species at m/z 283.3 corresponding to protonated oleic acid.

The spots on each image correspond to two concentrations of an oleic acid standard 2pg/mL (top spot) and 1pg/mL (bottom spot) (Ferguson et al., 2013).

2.4.9 Forensic Applicability of the Dry-Wet Method

In the first step of the dry-wet matrix deposition method, the application of finely ground matrix effectively acts as a visual enhancer analogous to the powdering techniques commonly used by SOCOs to develop latent fingermarks on various non-porous deposition surfaces. The powdered matrix essentially adheres to the aqueous and lipid constituents present in the fingermark residue, and after excess matrix is removed, the developed fingermark can be photographed and compared to fingerprints held in the police database. Figure 2.18 shows a photograph of a fingermark deposited on an aluminium plate (a) prior to and (b) after dusting with matrix. After dusting, the ridge features of the fingermark are evident and the ***minutiae*** clearly visible. A further advantage of utilising the MALDI matrix as an enhancing medium is due to its ability to absorb UV radiation, resulting in fluorescence. The fluorescent images shown in figure 2.18 were obtained using both a video spectra comparator (VSC), which enabled the whole fingermark to be visualised (c), and a fluorescent microscope, which enables the fingermark to be examined in more detail (d). From figure 2.18d, the higher magnification employed enables further distinguishing features such

as the presence of pores to be visualised. The same fingermark can subsequently be analysed by MALDI-MSI (figure 2.18e), which allows a further image of the ridge detail and *minutiae* present to be visualised, whilst simultaneously providing chemical information regarding the endogenous and exogenous species present. This may provide additional intelligence regarding the lifestyle choices of a donor, even in situations where inadequate optical images are obtained preventing a conclusive identification. The MALDI-MSI image shown in panel *e* shows the distribution of DBA at *m/z* 304.2. The concept of a multipurpose dusting agent has previously been reported by Rowell *et al.*, 2009. The authors used a hydrophobic silica dusting agent containing carbon black to enhance latent fingermarks prior to analysis by SALDI-TOF-MS. The dusting agent enabled a range of drugs to be detected, although the resolution observed in the SALDI-TOF–MS image was insufficient to allow any clear ridge pattern to be visualised. Subsequent work by the research group has involved utilising the silica dusting agent in the analysis of smokers' fingermarks, in order to establish whether nicotine and its metabolite cotinine could be detected. Intensity maps (0.9 cm x 0.9 cm) showing the distribution and intensity of nicotine and cotinine were obtained, although the resolution was again inadequate for clear ridge features to be visualised (Benton *et al.*, 2010). In comparison, analysis of fingermarks by MALDI-MSI following matrix application by the dry-wet method enables fingermark images to be obtained with sufficient clarity and detail to allow the fingermark to be classified as grade 4 (full development, clear ridge pattern observed), according to the HOSDB grading system (Ferguson et al., 2011).

(a) (b) (c) (d) (e)

Figure 2-18: Potential latent fingermark examination workflow.

A fingermark present at a simulated crime scene shown under visible light (a) can be enhanced by dusting with the a-CHCA matrix and photographed (b). Due to the fluorescent properties of the MALDI matrix, exposing the fingermark to UV light provides a more accurate database comparison when visualised under a VSC (c) and fluorescent microscope (d). Finally, the fingermark can be analysed by MALDI-MSI, providing images and chemical information; in particular panel e shows the distribution image of DBA at m/z 304.2 (Ferguson et al., 2011).

2.4.10 Fingermarks Lifted from Different Deposition Surfaces

The major feature of the dry-wet method which makes it superior to the conventional spray-coating method previously utilised as a proof-of-concept study by our research group for the analysis of ungroomed fingermarks is that the spray-coating method can only be applied to: (a) previously enhanced fingermarks (providing the development method is compatible with MALDI-MSI) and, (b) fingermarks laid flat on a suitable MALDI-MSI substrate. In the study by Wolstenholme and collaborators, the fingermarks were deposited onto aluminium sheets prior to MALDI-MSI analysis and therefore the technology at the time was deemed inapplicable in “real” crime situations. In comparison, the dry-wet method initially enhances latent fingermarks by application of the MALDI matrix, which enables fingermarks to be visualised on a range of potential crime scene surfaces, prior to lifting and analysis by MALDI-MSI. To

test the feasibility of the method, a range of deposition surfaces have been tested including non-porous surfaces such as metal, plastic and glass, and semi-porous surfaces such as leather, glazed cardboard and varnished wood. Two different donors each deposited fingermarks onto different substrates. Figure 2.19 shows the deposition surfaces employed prior to (a)-(h) and after dusting with α-CHCA (a1)-(h1). The distribution images of two species, an endogenous compound, oleic acid, at *m/z* 283.3 and DBA ion at *m/z* 304.2, are shown for each deposition surface. For each recovered fingermark, both non-normalised and normalised images are shown for the two species. All images are reported with differing contrast and brightness, in order to enhance the ridge details present, and maximise the number of *minutiae* retrievable. Images that have not been normalised generally are of the highest quality in terms of the observable ridge features. The normalisation process can therefore be omitted when the requirements are to obtain a clear fingermark image, with as many *minutiae* as possible. Normalisation is necessary when the distribution of a particular species is required on an absolute scale, or relative to other substances, or when a comparison of the distribution of the same substance within different fingermarks is made, for example, when comparing a the distribution of a compound in a fresh and aged fingermark. However, even after normalisation, it was possible to retrieve a distribution image of both the endogenous and exogenous compounds, with DBA exhibiting the highest quality images for both fingermark donors. With the conventional powders currently employed to visualise fingermarks at crime scenes, the results obtained are often inadequate as fingermarks are often overlaid and distorted. In situations like these, the combination of MALDI-MSI and the dry-wet method could potentially allow a fingermark image to be obtained, as images can

potentially be overlaid using appropriate software in order to improve the clarity of the fingermark images observed. Furthermore, the dry-wet method has recently been applied to overlapping fingermarks, prior to analysis by MALDI-MSI. The methodology enabled the separation of fingermarks from two donors based on differences in the chemical constituents present. Additionally, the technology was able to successfully image the presence of caffeine in the fingermark of one donor, which demonstrates that even in situations where inadequate images are obtained, chemical information pertaining to the donors' lifestyle such as dietary habits or drug use could potentially be obtained that may shorten the list of probable suspects (Bradshaw *et al.*, 2012).

Figure 2-19: Recovery and MALDI-MSI analysis of ungroomed fingermarks deposited by two donors on a range of surfaces.

The surfaces included: metal, glass, varnished wood, leather, an aluminium can, a cardboard box, a reflective surface and an A4 plastic wallet (panels a – h).The dry-wet method was tested by dusting the fingermarks with α-CHCA (panels a1 – h1), lifting the fingermarks, spraying them with the appropriate solvents and submitting them for analysis by MALDI-MSI. Representative MALDI-MS images of an endogenous fatty acid (oleic acid at m/z 283.3), and dimethylbenzylammonium ion at m/z 304.2) are shown for each deposition surface. For each species, both normalised and non-normalised MS images are displayed, demonstrating that even after normalisation, sufficient ridge detail is observed, to ascertain identification. (Figure 2.20 (a-d), taken from Ferguson et al., 2011).

Prior to dusting	After dusting	m/z283.2 (not normalised)	*m/z* 283.2 (normalised)	m/z304.2 (not normalised)	m/z 304.2 (normalised)

2.5 Conclusions

Since the first published paper by Wolstenholme *et al.*, (2009) on the use of MALDI-MSI to investigate the endogenous and exogenous species in latent fingermarks, the technology has progressed significantly. The development of the dry-wet method has been fundamental in the advances made, as it enables MALDI-MSI to be more forensically applicable. The initial application of ground matrix is analogous to the enhancement of fingermarks at a crime scene using any one of the myriad of powders currently available to Scene of Crime Officers (SOCOs). In the present study, the dry-wet method has been used to enhance ungroomed fingermarks on a range of nonporous and semi-porous surfaces, which enables the optical image of the fingermark to be obtained, prior to lifting, spraying and analysis by MALDI-MSI. The methodology has enabled the distribution of numerous lipids and exogenous compounds to be imaged and many of the lipids detected have been tentatively identified using high mass accuracy with a ppm error of less than 1.69. Furthermore, the identities of two of the lipids (eicosenoic acid and oleic acid) have been confirmed by MS/MS. The ability to obtain chemical information, as well as an optical image demonstrates the benefits of MALDI-MSI in combination with the dry-wet method for providing additional information that may reduce the pool of potential suspects. Indeed, work is currently on going to establish how MALDI-MSI can be integrated with the conventional fingermark development techniques currently employed, with the aim of the technology being implemented at real crime scenes in the future.

2.6 References

Aerni, H., Cornett, D. and Caprioli, R. (2006). Automated acoustic matrix deposition for MALDI sample preparation. *Analytical Chemistry,* **78** (3), 827-834

Archer, N.E., Charles, Y., Elliott, J.A. and Jickells, S. (2005). Changes in the lipid composition of latent fingerprint residue with time after deposition on a surface. *Forensic Science International,* **154** (2-3), 224-239

Bartsch, H.,Konig, W., Strassner, M. and Hintze, U. (1996). Quantitative determination of native and methylated cyclodextrins by matrix-assisted laser desorption/ionization time-of-flight mass spectrometry. *Carbohydrate Research,* **286,** 41-53

Benton, M., Rowell, F., Sundar, L. and Jan, M. (2010). Direct detection of nicotine and cotinine in dusted latent fingermarks of smokers by using hydrophobic silica particles and MS. *Surface and Interface Analysis,* **42** (5), 378-385

Boddis, A.M. and Russell, D.A. (2011). Simultaneous development and detection of drug metabolites in latent fingermarks using antibody-magnetic particle conjugates. *Analytical Methods,* **3** (3), 519-523

Bowman, V. (ed.) (2005). *Home office fingerprint development handbook.* 2nd ed., Derbyshire, UK, Home Office, London, UK

Bradshaw, R., Rao, W., Wolstenholme, R., Clench, M.R., Bleay, S. and Francese, S. (2012). Separation of overlapping fingermarks by matrix assisted laser desorption ionisation mass spectrometry imaging. *Forensic Science International,* **222** (1-3), 318-326

Bradshaw, R., Wolstenholme, R., Blackledge, R.D., Clench, M.R., Ferguson, L.S. and Francese, S. (2011). A novel matrix assisted laser desorption/ionisation mass spectrometry imaging based methodology for the identification of sexual assault suspects. *Rapid Communications in Mass Spectrometry,* **25** (3), 415-422

Caprioli, R.M., Farmer, T.B. and Gile, J. (1997). Molecular imaging of biological samples: Localization of peptides and proteins using MALDI-TOF-MS. *Analytical Chemistry,* **69** (23), 4751-4760

Cole, L.M., Djidja, M., Bluff, J., Claude, E., Carolan, V.A., Paley, M., Tozer, G.M. and Clench, M.R. (2011). Investigation of protein induction in tumour vascular targeted strategies by MALDI-MSI. *Methods,* **54** (4), 442-453

Connatser, R.M., Prokes, S.M., Glembocki, O.J., Schuler, R.L., Gardner, C.W., Lewis, S.A., Sr. and Lewis, L.A. (2010). Toward surface-enhanced Raman imaging of latent fingerprints. *Journal of Forensic Sciences,* **55** (6), 1462-1470

Crossman, L., McHugh, N., Hsieh, Y., Korfmacher, W. and Chen, J. (2006). Investigation of the profiling depth in matrix-assisted laser desorption/ionization imaging mass spectrometry. *Rapid Communications in Mass Spectrometry,* **20** (2), 284-290

Croxton, R.S., Baron, M.G., Butler, D., Kent, T. and Sears, V.G. (2010). Variation in amino acid and lipid composition of latent fingerprints. *Forensic Science International,* **199** (1-3), 93-102

Emerson, B., Gidden, J., Lay, J.O.Jr and Durham, B. (2011). Laser desorption/ionization time-of-flight mass spectrometry of triacylglycerols and

other components in fingermark samples. *Journal of Forensic Sciences,* **56** (2), 381-389

Ferguson, L., Bradshaw, R., Wolstenholme, R., Clench, M. and Francese, S. (2011). Two-step matrix application for the enhancement and imaging of latent fingermarks. *Analytical Chemistry,* **83** (14), 5585-5591

Ferguson, L.S, Creasey, S., Wolstenholme, R., Clench, M.R. and Francese, S. (2013). Efficiency of the dry-wet method for the MALDI-MSI analysis of latent fingermarks. *Journal of Mass Spectrometry,* **48,** 677-684

Ferrer, I. and Furlong, E. (2001). Identification of alkyl dimethylbenzylammonium surfactants in water samples by solid-phase extraction followed by ion trap LC/MS and LC/MS/MS. *Environmental Science & Technology,* **35** (12), 2583-2588

Fieldhouse, S. (2011). Consistency and reproducibility in fingermark deposition. *Forensic Science International,* **207** (1-3), 96-100

Goodwin, R.J., MacIntyre, L., Watson, D.G., Scullion, S.P. and Pitt, A.R. (2010). A solvent-free matrix application method for matrix-assisted laser desorption/ionization imaging of small molecules. *Rapid Communications in Mass Spectrometry,* **24** (11), 1682-1686

Goodwin, R.J.A., Scullion, P., MacIntyre, L., Watson, D.G. and Pitt, A.R. (2010). Use of a solvent-free dry matrix coating for quantitative matrix-assisted laser desorption ionization imaging of 4-bromophenyl-1,4-diazabicyclo(3.2.2)nonane-4-carboxylate in rat brain and quantitative analysis of the drug from laser microdissected tissue regions. *Analytical Chemistry,* **82** (9), 3868-3873

Hankin, J.A., Barkley, R.M. and Murphy, R.C. (2007). Sublimation as a method of matrix application for mass spectrometric imaging. *Journal of the American Society for Mass Spectrometry,* **18** (9), 1646-1652

Hart, P.J., Francese, S., Claude, E., Woodroofe, M.N. and Clench, M.R. (2011). MALDI-MS imaging of lipids in ex vivo human skin. *Analytical and Bioanalytical Chemistry,* **401** (1), 115-125

Ifa, D.R., Manicke, N.E., Dill, A.L. and Cooks, R.G. (2008). Latent fingerprint chemical imaging by mass spectrometry. *Science,* **321** (5890), 805

Lee, Y.J., Perdian, D.C., Song, Z., Yeung, E.S. and Nikolau, B.J. (2012). Use of mass spectrometry for imaging metabolites in plants. *Plant Journal,* **70** (1), 81-95

Manier, M.L., Cornett, D.S., Hachey, D.L. and Caprioli, R.M. (2008). Identification of dimethyidioctadecylammonium ion (m/z 550.6) and related species (m/z 522.6, 494.6) as a source of contamination in mass spectrometry. *Journal of the American Society for Mass Spectrometry,* **19** (5), 666-670

Mounfield, W. P.III and Garrett, T.J. (2012). Automated MALDI matrix coating system for multiple tissue samples for imaging mass spectrometry. *Journal of the American Society for Mass Spectrometry,* **23** (3), 563-569

Murphy, R.C., Hankin, J.A., Barkley, R.M. and Berry, K.A.Z. (2011). MALDI imaging of lipids after matrix sublimation/deposition. *Biochimica and Biophysica Acta-Molecular and Cell Biology of Lipids,* **1811** (11), 970-975

Patel, S.A., Barnes, A., Loftus, N., Martin, R., Sloan, P., Thakker, N. and Goodacre, R. (2009). Imaging mass spectrometry using chemical inkjet printing

reveals differential protein expression in human oral squamous cell carcinoma. *Analyst,* **134** (2), 301-307

Puolitaival, S.M., Burnum, K.E., Cornett, D.S. and Caprioli, R.M. (2008). Solvent-free matrix dry-coating for MALDI imaging of phospholipids. *Journal of the American Society for Mass Spectrometry,* **19** (6), 882-886

Ramotowski, R.S. (2001). Composition of latent print residue. In: Lee, H.C. and Gaensslen, R.E. (Ed.). *Advances in fingerprint technology.* Boca Raton, Florida, CRC Press, 63-104

Ricci, C., Phiriyavityopas, P., Curum, N., Chan, K.L.A., Jickells, S. and Kazarian, S.G. (2007). Chemical imaging of latent fingerprint residues. *Applied Spectroscopy,* **61** (5), 514-522

Rowell, F., Hudson, K. and Seviour, J. (2009). Detection of drugs and their metabolites in dusted latent fingermarks by mass spectrometry. *Analyst,* **134** (4), 701-707

Sloane, A., Duff, J., Wilson, N., Gandhi, P., Hill, C., Hopwood, F., Smith, P., Thomas, M., Cole, R., Packer, N., Breen, E., Cooley, P., Wallace, D., Williams, K. and Gooley, A. (2002). High throughput peptide mass fingerprinting and protein macroarray analysis using chemical printing strategies. *Molecular & Cellular Proteomics,* **1** (7), 490-499

Sodhi, G.S. and Kaur, J. (2001). Powder method for detecting latent fingerprints: A review. *Forensic Science International,* **120** (3), 172-176

Stoeckli, M., Staab, D. and Schweitzer, A. (2007). Compound and metabolite distribution measured by MALDI mass spectrometric imaging in whole-body tissue sections. *International Journal of Mass Spectrometry,* **260** (2-3), 195-202

Strohalm, M., Hassman, M., Bedrich, K., Kodicek, M. (2008). mMass data miner:an open source alternative for mass spectrometric data analysis. *Rapid Communications in Mass Spectrometry*, **22**, 905-908

Strohalm, M., Kavan, D., Novak, P., Volny, M. and Havlicek, V. (2010). A cross-platform software environment for precise analysis of mass spectrometric data. *Analytical Chemistry*, **82**, 4648-4651

Sugiura, Y., Shimma, S. and Setou, M. (2006). Two-step matrix application technique to improve ionization efficiency for matrix-assisted laser desorption/ionization in imaging mass spectrometry. *Analytical Chemistry,* **78** (24), 8227-8235

Thomas, A., Charbonneau, J.L., Fournaise, E. and Chaurand, P. (2012). Sublimation of new matrix candidates for high spatial resolution imaging mass spectrometry of lipids: Enhanced information in both positive and negative polarities after 1, 5-diaminonapthalene deposition. *Analytical Chemistry,* **84** (4), 2048-2054

Trim, P.J., Atkinson, S.J., Princivalle, A.P., Marshall, P.S., West, A. and Clench, M.R. (2008). Matrix-assisted laser desorption/ionisation mass spectrometry imaging of lipids in rat brain tissue with integrated unsupervised and supervised multivariant statistical analysis. *Rapid Communications in Mass Spectrometry,* **22** (10), 1503-1509

Trim, P.J., Djidja, M.C., Atkinson, S., Oakes, K., Cole, L.M., Anderson, D.M.G., Hart, P.J., Francese, S.and Clench, M.R. (2010). Introduction of a 20kHz Nd:YVO4 laser into a hybrid quadrupole time-of-flight mass spectrometer for MALDI-MS imaging. *Analytical and Bioanalytical Chemistry*, **397**, 3409-3419

van Remoortere, A., van Zeijl, R.J.M., van den Oever, N., Franck, J., Longuespee, R., Wisztorski, M., Salzet, M., Deelder, A.M., Fournier, I. and McDonnell, L.A. (2010). MALDI imaging and profiling MS of higher mass proteins from tissue. *Journal of the American Society for Mass Spectrometry,* **21** (11), 1922-1929

Wolstenholme, R., Bradshaw, R., Clench, M.R. and Francese, S. (2009). Study of latent fingermarks by matrix-assisted laser desorption/ionisation mass spectrometry imaging of endogenous lipids. *Rapid Communications in Mass Spectrometry,* **23** (19), 3031-3039

Yang, J. and Caprioli, R.M. (2011). Matrix Sublimation/Recrystallization for imaging proteins by mass spectrometry at high spatial resolution. *Analytical Chemistry,* **83** (14), 5728-5734

3 Peptide Chapter

3.1 Introduction

3.1.1 Detection of Peptides and Proteins in Latent Fingermarks

A variety of endogenous lipids and small molecular weight exogenous contaminants have recently been tentatively identified and imaged in ungroomed fingermarks by MALDI-MSI (Wolstenholme *et al.*, 2009; Bradshaw *et al.*, 2011; Ferguson *et al.*, 2011; Bradshaw *et al.*, 2012). In comparison to the lipid content of latent fingermarks, limited research has been undertaken on the peptides and proteins present within fingermark residue. In 2009, Drapel and co-workers used fluorescently tagged antibodies to detect and image the proteins keratins 1 and 10, cathepsin D and the antimicrobial peptide dermcidin within eccrine and groomed fingermarks. Fingermarks were deposited on polyvinylidene fluoride (PVDF), whitened and non-whitened paper. The groomed fingermarks were more developed than the eccrine ones, due to the higher abundance of proteins present, which results from the fingertips becoming artificially loaded with proteins alongside lipids during the grooming procedure. Indeed, the authors reported that the concentration of proteins was at least three times higher in mixed fingermarks than eccrine ones (Drapel *et al.*, 2009).

Recently, Song and co-workers employed Surface Enhanced Raman Spectroscopy (SERS) in imaging mode to indirectly detect proteins within latent fingermarks. Fingermarks were artificially loaded with human immunoglobulin G (IgG) and antibodies directed towards the protein were bound to modified silver nanoparticles. The antibody modified nanoparticles deposited predominantly on the fingermark ridges due to more IgG residing there, resulting in high resolution SERS images of the fingermark ridge pattern and chemical information regarding the protein present. However, no SERS images were obtained in the

absence of the modified nanoparticles, or without artificially loading the fingermarks with IgG first, which clearly demonstrates the limitations of the methodology at present (Song *et al.*, 2012).

3.1.2 Discrimination Studies

As previously stated, the fingermarks recovered at crime scenes are often too smudged and distorted to allow a positive identification to be achieved; in these cases, additional chemical intelligence would be highly desirable. The ability to detect the chemical constituents of fingermarks has led to various research groups attempting to discriminate between the fingermarks of individuals based on the endogenous content present. In one biomarker discovery study, gas chromatography – mass spectrometry (GC-MS) was employed to differentiate between adults and children's fingermarks. The study found that the fingermark residues of children differed to those obtained from adults in the quantity of sebaceous species present such as fatty acids, cholesterol, squalene and wax esters (Buchanan *et al.,* 1997). More recently Fourier transform infrared microscopy (FTIRM) enabled adult groomed fingermarks to be distinguished from children's for up to 4 weeks after deposition on an infrared reflective (MirrIR) glass microscope slide, based on variations in the sebaceous material present in both fresh and aged fingermarks (Antoine *et al.,* 2010).

Differences in the sebaceous content of fingermarks obtained from individuals of a similar age have also been investigated. In a recent study, Weyermann and collaborators used GC-MS to investigate the initial composition of fingermarks in both inter-donor and intra-donor variability studies. In the inter-donor variability study, six donors (three female and three male) deposited groomed fingermarks onto five different substrates. Squalene and cholesterol were identified in all donors' fingermarks, as well as other sebaceous compounds

such as wax esters and fatty acids. The composition of the donated fingermarks varied substantially between different donors, as well as those obtained from the same donor (intra-donor study) (Weyermann *et al.,* 2011). The results of this investigation support the findings of previous studies, which also reported variations in the sebaceous composition of fingermarks collected from different donors and within the same donor (Dikshitula *et al.,* 1986; Archer *et al.,* 2005).

The influence of sex on the chemical composition of fingermark residues has also been investigated by various research groups. Asano and collaborators attempted to determine the sex of the donors based on the peak area ratios between ten lipid components and squalene using GC-MS. Although differences were apparent between the fingermarks collected, no statistically significant variability was established between the sexes (Asano *et al.,* 2002). More recently, Laser Desorption/Ionisation (LDI) Time-of-Flight Mass Spectrometry (TOF MS) was employed in the same kind of study. Groomed fingermarks were collected from 16 donors (8 female and 8 male) in order to establish whether any discrimination could be ascertained from triacylglycerols and other sebaceous constituents of the donated marks. Although several triacylglycerols were found to be significant at the 95% and 97.5% confidence levels, the differences were found to be close to the standard deviation of the measurements and the study concluded that sex specificity could not be determined by the methodology employed (Emerson *et al.,* 2011).

In a completely different approach, it was reported by Zelson that the ridge width measurement, (independent from body size) can be correlated to the sex of the fingermark donor, with a high degree of confidence. However, a major limitation of the methodology is that it depends on retrieving and measuring the

width of ten parallel ridges, which may not be possible if the fingermark is heavily smudged or distorted (Zelson, 2000).

In contrast to previous studies which have focussed on lipid biomarkers as potential indicators of the donor's sex, here MALDI mass spectrometry profiling (MSP) has been employed to detect endogenous peptides and small proteins within latent fingermarks, with the aim of discriminating the sex of individuals based on these species using multivariate statistical analysis (UK. Patent number 1120533.3. International Patent Application no. PCT/GB2012/051775). Further work is presented regarding imaging the distribution of these higher molecular weight species within fingermarks.

3.1.3 Partial Least Squares Discriminate Analysis (PLSDA)

Partial Least Squares Discriminate Analysis (PLSDA) is a multivariate inverse least squares discrimination method used to classify samples. This multivariate approach is ideally suited for prediction of binary classification problems and analyses the whole spectra to obtain characteristic "biomarker profiles". Several papers have highlighted the problems associated with validation of PLSDA models when analysing multivariate data such as mass spectral data. For example, too small sample size results in improper validation of the classification models, although this can be avoided by initially performing a multivariate power calculation (Westerhuis *et al.*, 2008). In order to validate the results obtained, cross-validation is necessary. However, cross-validation only provides an infallible error rate when the complete modelling procedure is cross-validated, and the variable that is predicted has not been used to build the initial model (Anderssen *et al.*, 2006). For a given data set, cross-validation involves a number of sub-validation experiments, each of which involves the removal of a subset of items from the dataset (the test set). The remaining

items in the dataset are used to build the model (the training set). The test set is then used to test the performance of the model. There are a number of cross-validation methods available and each of these varies with regards to how the different sample subsets are chosen for the sub-validation experiments. With the Eigenvector PLS Toolbox used for this study, five different cross validation methods are available (Venetian Blinds, Contiguous Blocks, Random Subsets, Leave-One-out and Custom) and each has different properties and parameters (Eigenvector Research Inc., 2009). For the work presented here, the Custom cross-validation method was implemented, which enables the test set to be defined such that all spectra from a donor will either be in the model building or the prediction set.

The analysis of complex data sets by PLSDA produces regression vector plots, which allow visualisation of which ions (variables) are important for a particular classification. The Variable Importance in Projection (VIP) scores can also be ascertained from the regression model, which evaluates the importance of each variable in the projection. In any given PLS model, a variable with a VIP score close to or higher than 1 is considered important in the model.

3.2 Materials

Trifluoroacetic acid (TFA), ALUGRAM ® SIL G/UV_{254} Pre-Coated Aluminium Sheets, α-cyano-4-hydroxycinnamic acid (α-CHCA), sinapinic acid (SA) and aniline were obtained from Sigma-Aldrich, (Poole, UK). Acetone, acetonitrile (ACN), chloroform, ethanol and denatured ethanol were purchased from Fisher Scientific (Loughborough, UK). MALDI target OPTI TOF spotless inserts were obtained from Applied Biosytems (Foster City, Ca, USA). Double sided conductive carbon tape was purchased from TAAB (Berks, UK). Dermcidin standard was purchased from Anaspec (http://www.anaspec.com/contact/)

3.3 Methods

3.3.1 Instrumentation and Instrumental Settings

Mass spectrometric profiling and imaging were conducted using an Applied Biosystems MALDI TOF Voyager De-STR mass spectrometer (Foster City, Ca, USA) equipped with a 355 nm Nd-YAG solid state laser operating at a repetition rate of 20 Hz. Full scan mass spectra were recorded in positive linear mode. The accelerating voltage was set at 25,000 Volts, the grid voltage was set at 93% and the delay time was 150 ns. Profiling data were pre-processed using Data Explorer (Applied Biosystems, Foster City, CA, USA), mMass (Strohalm *et al.*, 2008; Strohalm *et al.*, 2010) or SpecAlign (Wong *et al.*, 2005). Images were acquired using MALDI Imaging Tool (Applied Biosystems, Foster City, CA, USA) and processed using Biomap Software 3.7.5.5 (Novartis, Basel, Switzerland). Images were acquired in positive linear mode at a spatial resolution of 150 µm x 150 µm.

3.3.2 Fingermark Preparation

Eccrine fingermarks were prepared by cleansing hands with a 50% aqueous ethanol solution and placing one hand in a plastic freezer bag, secured in place with an elastic band for a period of 15 minutes. Three fingermarks were then deposited onto pre-coated aluminium sheets after removing the silica with acetone.

Ungroomed fingermarks were prepared by cleaning hands with a 50% aqueous ethanol solution and carrying on normal work activities for a period of 15 minutes before rubbing the fingertips against each other and depositing 3 fingermarks onto aluminium sheets as described above.

Groomed fingermarks were prepared by cleaning hands with a 50% ethanol wash and rubbing the fingers on the forehead, nose and chin five times to obtain a sebum-rich mark before deposition in triplicate on aluminium sheets (as described above).

Aluminium sheets were attached to MALDI spotless inserts using double sided carbon conductive tape for analysis by MALDI-MS.

3.3.3 Optimisation of MALDI Matrix and Composition

Matrix solutions of 5 mg/ml α-CHCA were prepared using different ratios of ACN to TFA (50:50, 60:40, 70:30, 80:20 and 90:10). The optimal concentration of TFA was also probed (0.1%, 0.2%, 0.3%, 0.4% and 0.5%). Ungroomed fingermarks were then subjected to MALDI-MS profiling and the spectral intensity evaluated.

3.3.4 Optimisation of the Ion Abundance and Intensity from Groomed Fingermarks

Three groomed fingermarks were cut in half and one half of each was washed in 750 µL of either acetone, chloroform or denatured ethanol. After washing, five droplets (of 0.5 µL each) of a 5 mg/ml α-CHCA solution in 70:30 ACN/0.5% TFA were spotted on both the washed and the unwashed fingermark halves in five different areas and profiling mass spectra were acquired.

3.3.5 Sex Discrimination Studies

In the pilot study (32 donors) and the larger study (80 donors), recruited participants were older than 20 and younger than 45 years old. Volunteers having made use of medications or drugs within the two weeks preceding the collection were excluded from the studies. Both of the studies were conducted under full ethical approval of the Biosciences Research Ethics Review Group

(Faculty of Health and Wellbeing, Research Ethics Committee Sheffield Hallam University).

3.3.5.1 Pilot Sex Discrimination Study

Ungroomed fingermarks were collected as described in section 3.3.2 from 32 donors (15 females and 17 males) in triplicate. Five 0.5 µL spots of a 5 mg/mL α-CHCA solution in 70:30 ACN/0.5% TFA were deposited on different regions of each fingermark and five corresponding MALDI mass spectra profiles were acquired, resulting in fifteen spectra per donor.

3.3.5.2 Large Sex Discrimination Study

Ungroomed fingermarks were collected as described in section 3.3.2 from 80 donors (40 females and 40 males) in triplicate. Three 0.5 µL spots of a 5 mg/mL α-CHCA solution in 25:25:50 ACN/ethanol/ 0.5% TFA were deposited close to the centre of each mark; three corresponding MALDI mass spectra profiles were acquired, resulting in 9 spectra per donor.

3.3.6 Statistical Analysis

3.3.6.1 Pilot Sex Discrimination Study

Mass spectral profiles were acquired from three replicate fingermarks obtained from each donor; five spectra were acquired for each replicate, resulting in fifteen spectra per donor. Data quality control was performed by identifying outliers, for which the signal-to-noise threshold was substantially lower than for the other replicates for that donor. The remaining mass spectra were converted into text files and imported into SpecAlign software for pre-processing (Wong *et al.*, 2005). The pre-processing stage consisted of baseline correction to a factor of 20 and spectral alignment using PAFFT (Peak alignment by Fast Fourier Transform). Spectra for all donors were then converted into CSV files and

imported and analysed in MATLAB (The Mathworks Inc, Natick, MA, USA). In MATLAB, the data was analysed using PLSDA (PLS Toolbox v6.2.1, Eigenvector Research Inc, Wenatchee, WA, USA). The data was pre-processed by spectral normalisation to unit power (square sum of all data points per spectrum equals to one) and subsequent mean centring (subtraction of the average spectrum of each individual spectrum). These two pre-processing steps ensure that the spectrum to spectrum variance due to different sensitivities and ionisation efficiencies are corrected for through normalisation and that the PLSDA algorithm is based purely on spectral differences. The data were randomly divided into a training set (spectra from 24 donors; 13 males and 11 females), resulting in an initial data set with 340 spectra and 12260 *m/z* values, and a test set (spectra from 8 donors, 4 male and 4 female), resulting in a data set with 115 spectra and 12,260 *m/z* values. The training set data were used to build the PLSDA model; internal cross validation leaving out iteratively all spectra from each donor once (24 cross validation rounds) indicated a minimum classification error when employing a model with 6 latent variables. The data from the test set was subsequently predicted using the previously built PLSDA model and the predictive accuracy assessed by assigning each donor to the sex that the majority of its spectra were classified to by the model and comparing that with the donor's actual sex.

3.3.6.2 Large Sex Discrimination Study

Mass spectral profiles were acquired from three replicate fingermarks that were obtained for each donor; three spectra were acquired for each replicate fingermark, resulting in nine spectra per donor. The mass spectra were pre-processed in Spec Align as for the pilot study described in section 3.3.6.1 and imported into MATLAB (The Mathsworks Inc, Natick, MA, USA) and analysed

using PLSDA (PLS Toolbox, v6.2.1, Eigenvector Research Inc, Wenatchee, WA, USA).

In MATLAB, the 100 data spectral variables on each end of the spectrum were deleted, as these regions contain mainly artifacts resulting from the baseline correction and spectral alignment performed through SpecAlign. The data was normalised and mean centred as for the pilot study and divided into two halves by randomly selecting 20 males and 20 females as a training set and leaving the other 40 donors (20 males, 20 females) as a test set for validation. This resulted in two data matrices containing 360 spectra by 12,047 *m/z* values. The training set data were used to build the PLSDA model and internal cross validation, leaving out iteratively all spectra from each donor once (40 cross validation rounds) was used to assess the number of latent variables necessary for an accurate and stable prediction model. Subsequently the data from the test set were used with the previously built PLSDA model and the predictive accuracy assessed by assigning each donor to the sex that the majority of its spectra were classified as by the model and comparing that with the donor's actual sex. From the cross validation result it was clear that the MS data contains a large amount of variation unrelated to the sex classification, hence a selection of variables based on the VIP score was performed to provide a more concise model (Chong *et al.*, 2005).

3.3.7 MALDI-MS Imaging of Peptides and Small Proteins

For all imaging experiments, groomed fingermarks were obtained as stated in section 3.3.2 and were deposited onto pre-coated aluminium sheets, prepared as stated in section 3.3.2. All fingermarks were washed with denatured ethanol and prepared using one of the matrix application methods stated in sections 3.3.7.1 to 3.3.7.4.

For each matrix deposition method tested, mass spectral profiles were taken in order to determine whether any ion signal could be detected, prior to imaging. In all cases, mass spectral profiles were also obtained of fingermarks after application of the same matrix via the direct droplet method as a means of verifying that the peptides could indeed be detected in the fingermark samples tested and any failure to detect them was a consequence of their insufficient extraction by the matrix application system under test.

3.3.7.1 Application of Matrix via Automated Spraying

Groomed, washed fingermarks were sprayed using the SunCollect auto-spraying system (SunChrom, Frankfurt, Germany), with either: (i) 5 mg/mL α-CHCA in either 70:30 ACN/0.5% TFA or 50:50 ACN/0.5% TFA, (ii) 5 mg/mL α-CHCA with an equimolar volume of aniline added in either 70:30 ACN/0.5% TFA or 50:50 ACN/0.5% TFA, (iii) 5 mg/mL α-CHCA/SA mix in either 70:30 ACN/0.5% TFA or 50:50 ACN/0.5% TFA, or (iv) 5 mg/mL α-CHCA in 25:25:50 ACN/ethanol/0.5% TFA. For each experiment, instrumental parameters such as the number of layers sprayed; the velocity at which the sample was sprayed or the distance between the spraying capillary and the sample were optimised.

3.3.7.2 Application of Matrix via Manual Spraying

Groomed, washed fingermarks were sprayed with approximately 15 mL of α-CHCA using an Iwata Eclipse gravity feed manual sprayer (Iwata – Media Inc, Portland, OR, USA) set to 40 psi, at concentrations of 10 mg/mL and 20 mg/mL in both 70:30 and 50:50 ACN/0.5% TFA solvent combinations. The drying time between each consecutive pass was approximately 45 seconds and the distance between the sample and the end of the spray nozzle was approximately 45 cm.

3.3.7.3 Application of Matrix via Acoustic Ejection Technology

Various matrices were applied to groomed; washed fingermarks using the Portrait 630 acoustic spotter (Labcyte Inc. CA, USA). The matrices utilised were 10 mg/mL α-CHCA in 50:50 ACN/0.5% TFA, 10 mg/mL α-CHCA with an equimolar quantity of aniline added in 50:50 ACN/0.5% TFA and 10 mg/mL of α-CHCA/SA in 50:50 ACN/0.5% TFA. All matrices were applied using 50 cycles at a spatial resolution of 150 µm. After matrix application, mass spectral profiles were obtained in order to determine whether any ion signal could be detected, prior to imaging.

3.3.7.4 Application of Matrix via Dry-Wet Method

Finely ground α-CHCA was applied to groomed, washed fingermarks using a zephyr brush. Fingermarks were sprayed with either a 70:30 ACN/0.5% or a 50:50 ACN/0.5% TFA solvent combination using the SunCollect auto-spraying system (SunChrom, Frankfurt, Germany). For each experiment, instrumental parameters such as the number of layers sprayed; the velocity at which the sample was sprayed and the height of the capillary were optimised.

Mass spectra of fingermarks were also acquired after application of a 5 mg/mL α-CHCA solution in 70:30 ACN/0.5% TFA by the direct droplet method as a means of determining that the peptides could indeed be detected in the fingermark samples tested.

3.4 Results and Discussion

Latent fingermarks are composed of the secretions of the eccrine and sebaceous glands. Eccrine secretions consist of 98% water, as well as water soluble organic species and inorganic constituents such as amino acids, urea, lactate, peptides and proteins (Ramotowski, 2001). The chemical composition

of eccrine sweat has been investigated by various research groups and many innate antimicrobial peptides and small proteins have been identified. These include: human cathelicidin LL-37, psoriasin, lysozyme, dermcidin (DCD) and various DCD-derived derivatives including DCD-1L, DCD-1 and LEK-45 (Baechle *et al.*, 2006; Rieg *et al.*, 2005; Rieg *et al.*, 2006). Sebaceous secretions consist predominantly of fat soluble organic compounds such as fatty acids, wax esters and glycerides, although the sebaceous gland is also believed to contribute to epithelial defence by releasing antimicrobial species to the skin surface (Harder and Schroder 2006; Lee *et al.*, 2008). As these higher molecular weight species are known to be present in the secretions that make up the fingermark residue, it was hypothesised that it should be possible to detect these species directly from latent fingermarks using MALDI-MSP. Matrix optimisation was initially performed on ungroomed fingermarks as these consist primarily of eccrine secretions, but may also contain some sebaceous content and are the fingermark type most likely to be encountered at real crime scenes. Various peptides and small proteins were putatively identified based on their *m/z* ratios and their previous identification in sweat by other research groups (Schittek *et al.*, 2001; Flad *et al.*, 2002; Rieg *et al.*, 2005; Rieg *et al.*, 2006; Baechle *et al.*, 2006; Harder and Schroder 2006).

The tentatively identified species include the antimicrobial protein psoriasin at *m/z* 11,377.2, positions 2-120, serine acylated, 1 disulphide bridge, as well as various antimicrobial peptides that originate from a recently discovered 110 amino acid long antimicrobial protein named dermcidin (DCD). DCD is constitutively expressed in eccrine sweat glands (Schittek *et al.*, 2001). In eccrine sweat, DCD undergoes post-secretory processing by various proteases including the aspartate protease Cathepsin D, a 1, 10-phenanthroline sensitive

carboxypeptidase and an endopeptidase, generating many C-terminal derived and N-terminal derived peptides as shown in table 3.1 (Rieg *et al.*, 2006).

DCD- Derived Peptide	*Average Mass*	Amino Acid Positions
DCD-1L	4818.5	63-110
DCD-1	4705.3	63-109
SSL-46	4606.2	63-108
SSL-45	4519.1	63-107
SSL-29	2869.3	63-91
SSL-25	2412.8	63-87
LEK-45	4531.2	66-110
YDP-42 and YPD-42 (dimer)	4302.6/8605.2	20-61

Table 3-1 Dermcidin (DCD) derived peptides, together with their average mass and amino acid positions.

Table adapted from Rieg et al., (2006).

Figure 3.1 displays MALDI-MS spectra obtained from an ungroomed fingermark showing the presence of various DCD-derived antimicrobial peptides and the antimicrobial protein psoriasin.

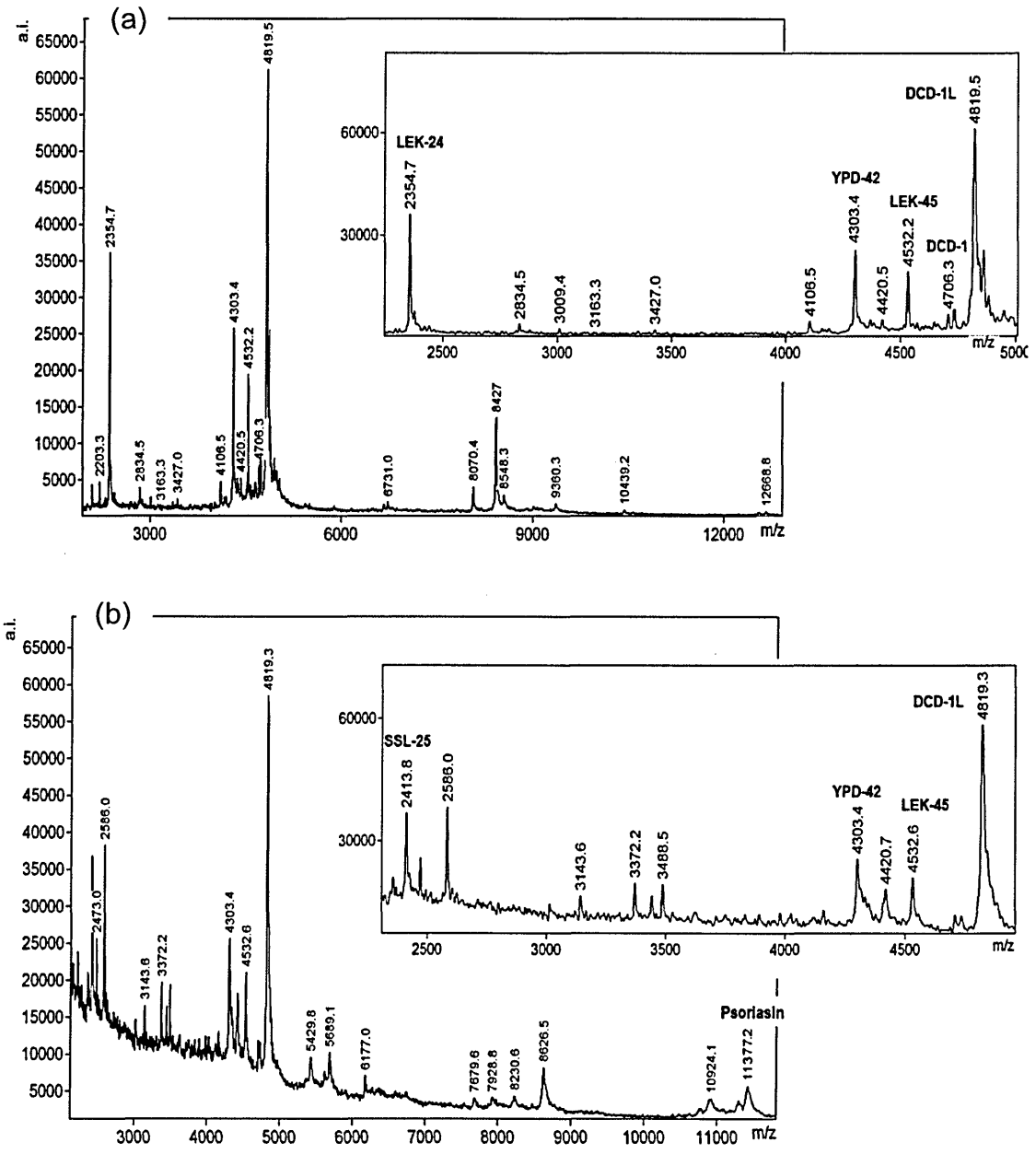

Figure 3-1: MALDI-TOF-MS spectra of an ungroomed fingermark showing the presence of various tentatively identified DCD-derived antimicrobial peptides and the antimicrobial peptide psoriasin.

The DCD-derived antimicrobial peptides include: DCD-1L at m/z 4819, DCD-1 at m/z 4706, LEK-45 at m/z 4532, YDP-42 at m/z 4303, SSL-25 at m/z 2413, LEK-24 at m/z 2354. Psoriasin is shown at m/z 11,377 (Ferguson et al., 2012).

In contrast to previously published data by Rieg *et al.*, (2006) and Baechle *et al.*, (2006), who both used saturated solutions of sinapinic acid (SA) to analyse sweat by Surface Enhanced Laser Desorption Ionisation Mass Spectrometry

(SELDI-MS) and MALDI-MS respectively, the best results in terms of ion abundance and signal intensity were obtained, for ungroomed marks, when α-CHCA was employed at a concentration of 5 mg/mL. The optimum solvent composition was determined by preparing 5 mg/mL α-CHCA solutions in 70:30 ACN/TFA and changing the percentage of TFA added from 0.1% to 0.5% (figure 3.2). It was found that the best signal ion intensity was obtained when a 0.5% TFA concentration was used.

Further experiments were subsequently performed to determine the optimum ratio of ACN to 0.5% TFA. The ratios investigated were 50:50, 60:40, 70:30, 80:20 and 90:10, with 70:30/0.5% TFA providing the best results with respect to ion signal intensity, with good signal to noise (figure 3.3) (Ferguson *et al.*, 2012).

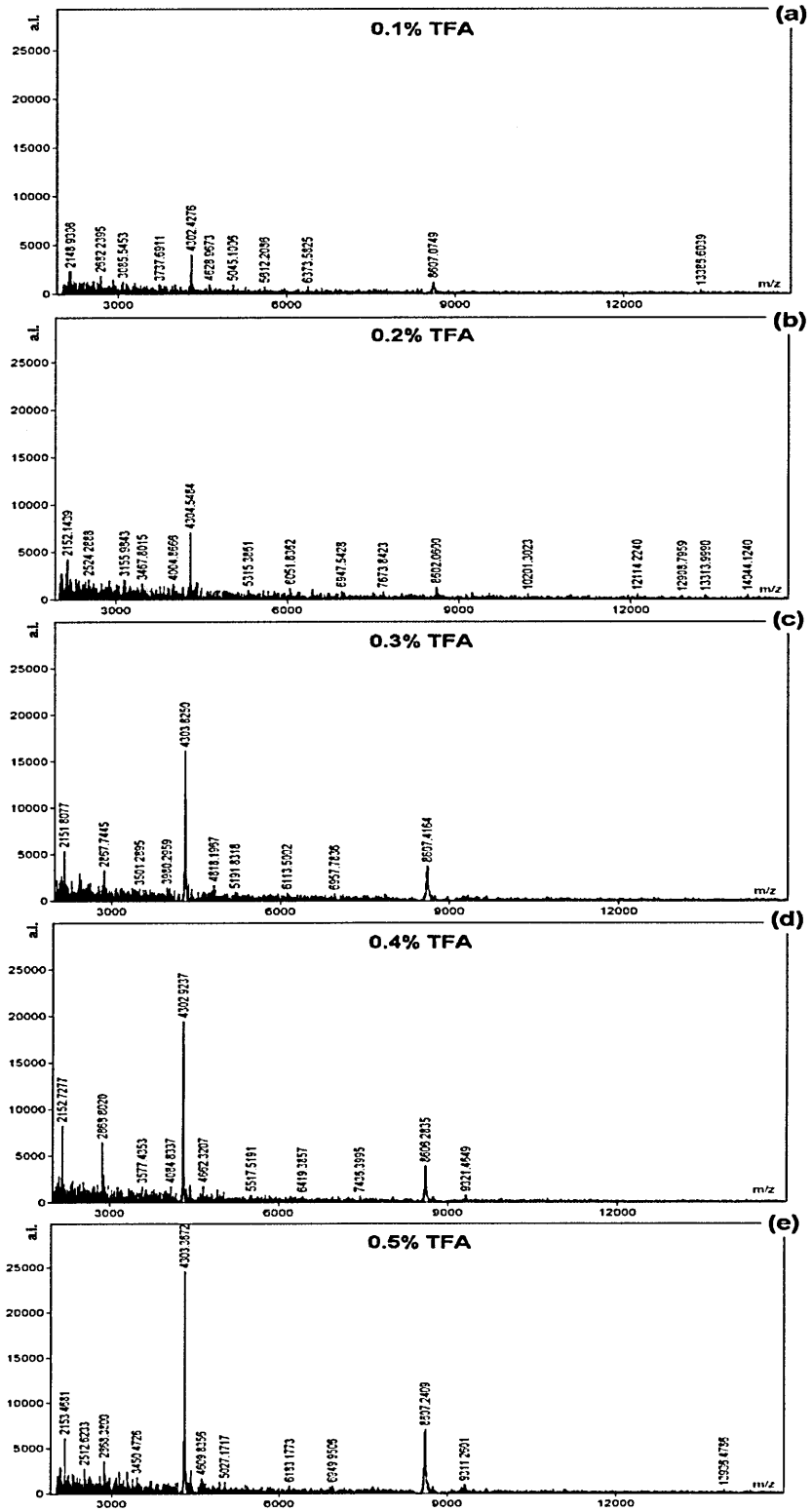

Figure 3-2: MALDI-MS spectra of an ungroomed fingermark spotted with 5 mg/ml α-CHCA in a 70:30 ACN/TFA solution, with varying concentrations of TFA added.

Figures (a) to (e) show the spectra obtained using 0.1, 0.2, 0.3, 0.4 and 0.5% TFA respectively (Ferguson et al., 2012).

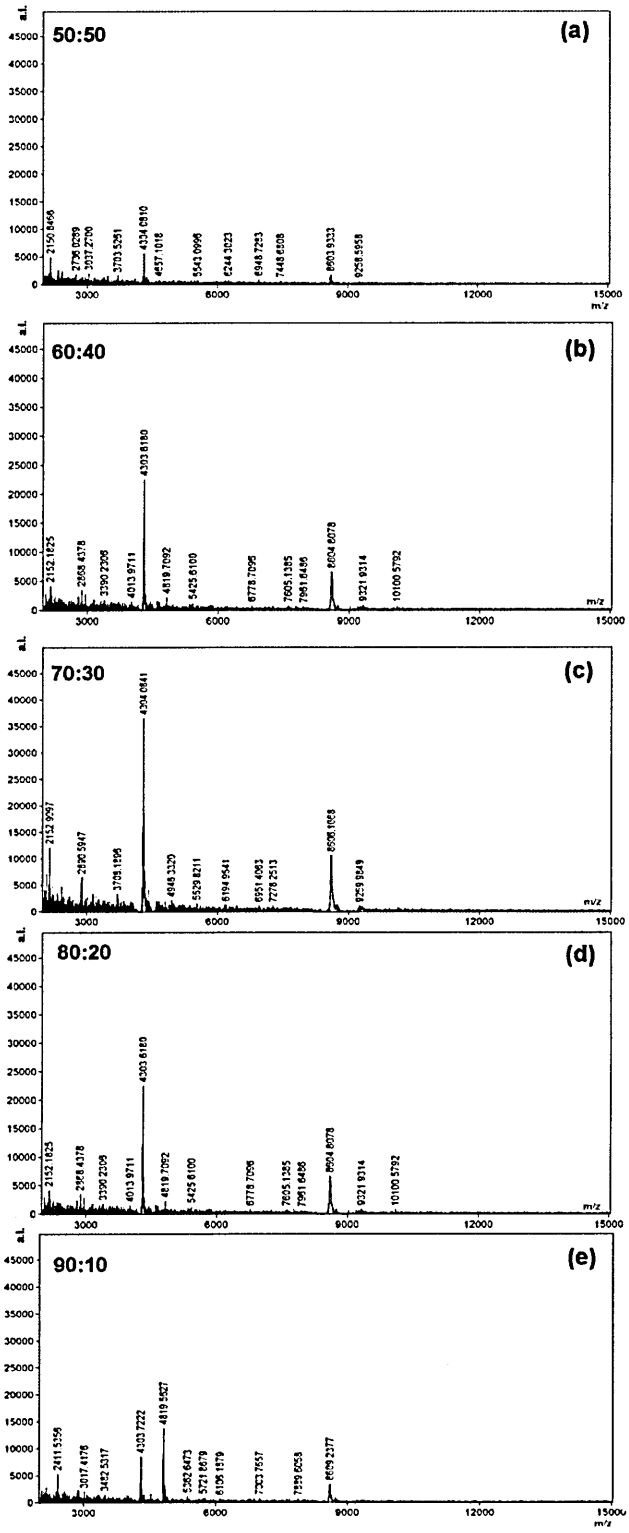

Figure 3-3: MALDI-MS spectra of an ungroomed fingermark spotted with 5 mg/mL α-CHCA matrix prepared with different ratios of ACN to 0.5% TFA.

Figures (a) to (e) show the spectra obtained using ACN/0.5% TFA ratios of 50:50, 60:40, 70:30, 80:20 and 90:10 respectively (Ferguson et al., 2012).

As initial studies were successfully conducted on ungroomed fingermarks, eccrine and groomed fingermarks were also evaluated in terms of their suitability for enabling detection of peptides and proteins by MALDI-MSP. Eccrine fingermarks are obtained by inducing excess sweating of the hand as described in section 3.3.2 and consist of secretions from the eccrine glands only. There were no peaks evident in the corresponding mass spectra obtained from unwashed eccrine fingermarks (figure 3.4a), probably as a result of the naturally occurring salts present in sweat exerting an ion suppression effect, as previously reported by Flad *et al.*, (2002). This absence of ion signals and the fact that eccrine fingermarks are the least likely fingermark type to be encountered at crime scenes, led to them being rejected as feasible test samples for the sex discrimination study.

Groomed fingermarks are obtained by wiping the fingertips across the areas of the face that contain an abundance of sebaceous glands such as the nose, chin and forehead; therefore artificially loading the fingertips with peptides and proteins, as well as sebaceous material. Due to the high ionisation efficiency of the lipids present in sebum, ion suppression of other biomolecules such as peptides and proteins is often evident (Schwartz *et al.*, 2003). The removal of lipids from tissues by washing with organic solvents is widely reported for improved proteomic analysis (Lemaire *et al.*, 2006, Seeley *et al.*, 2008). In this study, three organic solvents (acetone, chloroform and denatured ethanol) were used to wash groomed fingermarks prior to analysis by MALDI-MSP, and the impact on the abundance and intensity of the peptides and proteins present evaluated.

Of the three solvents tested, groomed fingermarks that were washed with acetone showed the lowest ion signal intensities, with chloroform giving slightly

better results. Denatured ethanol provided the best mass spectrum profile in terms of ion population and abundance. Figure 3.4(b) shows the mass spectra obtained after washing groomed fingermarks with (b1) acetone, (b2) chloroform and (b3) denatured ethanol. As expected, given the higher concentration of peptides and proteins associated with sebaceous material, groomed fingermarks exhibited improved ion population and abundance in comparison to ungroomed fingermarks, especially after washing with denatured ethanol (figure 3.4c). However, the mass resolution and signal to noise in the mass spectra were poorer. This observation, together with the extra washing step required for the improved detection of the peptide and protein species present in groomed fingermarks, and the fact that ungroomed fingermarks are the fingermark type most likely to be encountered at real crime scenes led to ungroomed fingermarks being selected as the most appropriate fingermark type on which to perform the sex discrimination study (Ferguson *et al.*, 2012).

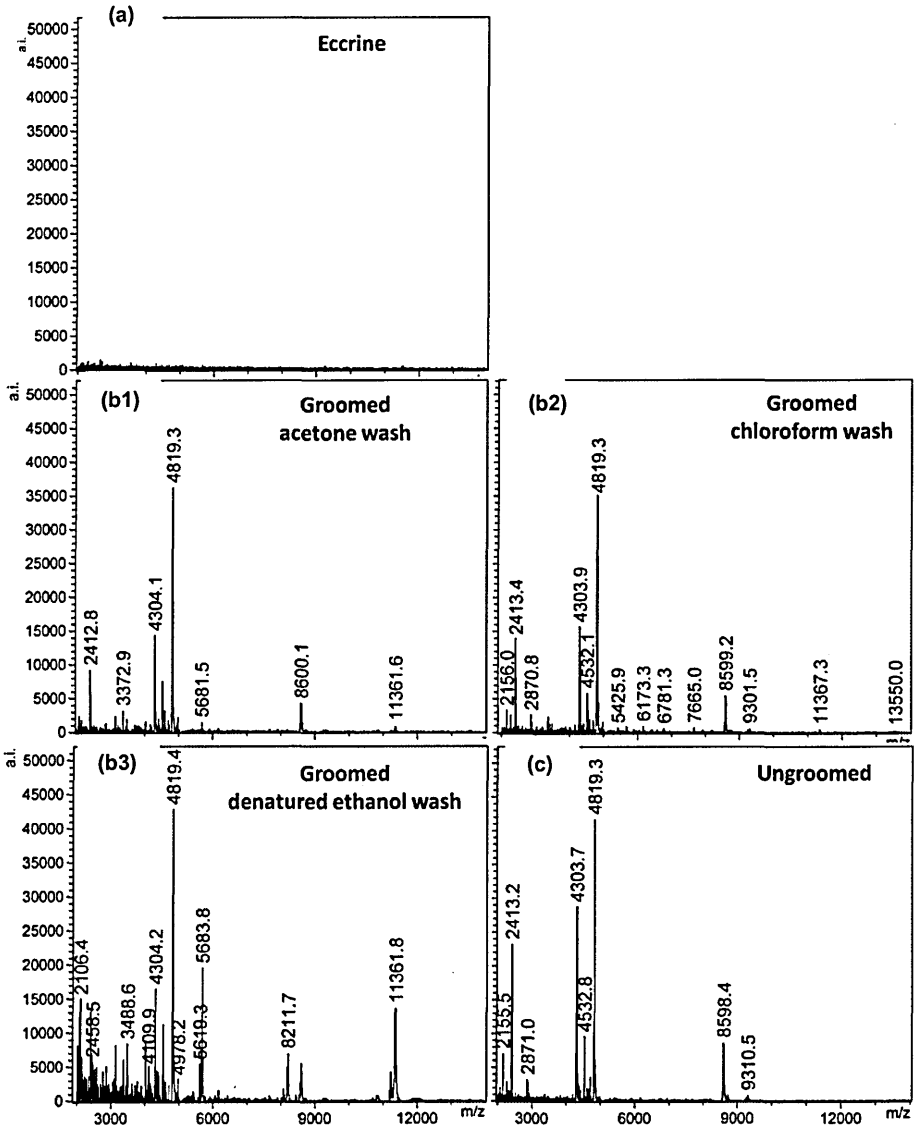

Figure 3-4: MALDI TOF MS spectra of eccrine, groomed and ungroomed fingermarks.

Panel (a) shows an unwashed eccrine fingermark where no ion signals were detected in the m/z 3000 – 15000 range. Panels (b1) – (b3) show examples of mass spectra obtained from groomed fingermarks that have been anaysed after washing with acetone (b1), chloroform (b2) and denatured ethanol (b3), with the latter proving to be the best solvent in terms of ion abundance and intensity. Panel c shows an unwashed ungroomed fingermark where fewer, but higher mass resolution at improved signal-to-noise could be detected (Ferguson et al., 2012).

3.4.1 Pilot Sex Discrimination Study

For the pilot study, ungroomed fingermarks were collected from a cohort of 32 donors (17 males and 15 females). Spectral data from this study were classified with supervised multivariate analysis using PLSDA. This multivariate approach is ideal for prediction of binary classification problems and analyses the whole spectra to provide characteristic "biomarker profiles". Given a large enough and representative training data set, the PLSDA methodology can correct for background signal or variations in the data unrelated to the classification problem, i.e. the method is insensitive to changes in peaks that do not relate to sex discrimination.

The classification based on the first PLSDA model (all 12,260 spectral variables, 6 latent variables, training set of 11 female and 13 male donors) of the left out donors during the cross validation resulted in an accurate sex prediction of 68.2% and 77.4% for females and males respectively, resulting in an overall cross validation predictive accuracy of 72.8%. The prediction for the independent test set gave an accuracy of 51.7% and 81.8% for females and males respectively, resulting in an overall validated predictive accuracy of 66.8%.

These results indicated that there was, in principle, a potential to discriminate between males and females with the available data, suggesting that information on sex could be extracted from MALDI-MSP detection of peptides in fingermarks followed by multivariate statistical analysis. The prediction for each spectrum of the test set is depicted in figure 3. 5.

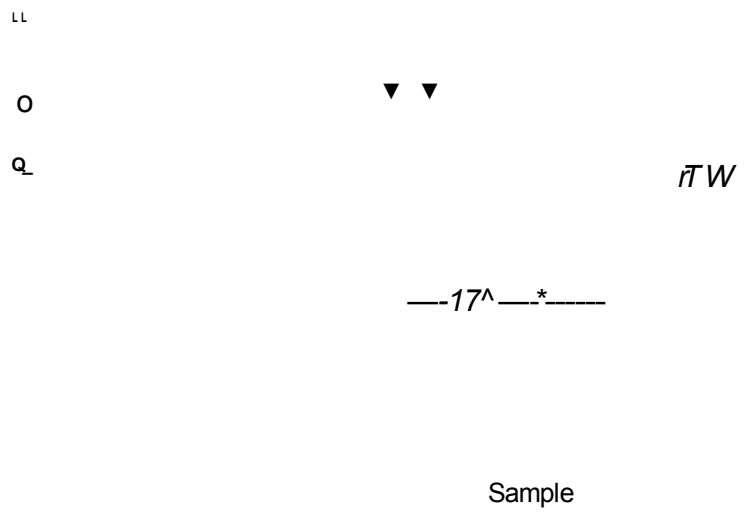

Figure 3-5: Classification results and validation using an independent test set.

Spectra from each of the 8 donors in the test set (4 female and 4 male) have the same plotted symbol (red for female, green for male). Prediction above the red threshold line results in female sex assignment and below the threshold in a male sex assignment. The model correctly predicted 2 (out of 4) females and 3 (out of 4) males, resulting in an overall accuracy of prediction of 66.8%.

PLSDA calculates a regression coefficient for each variable that represents the respective variables' contributions to the prediction of sex. Additionally, for each *m/z* variable, the VIP score can be calculated, these estimate the importance of each *m/z* value, in the projection used by the algorithm. The regression coefficients vector is given in figure 3.6. Peaks that appear on the top half of the regression vector plot are important for prediction of females and peaks appearing on the bottom half of the plot are important for male sex assignment.

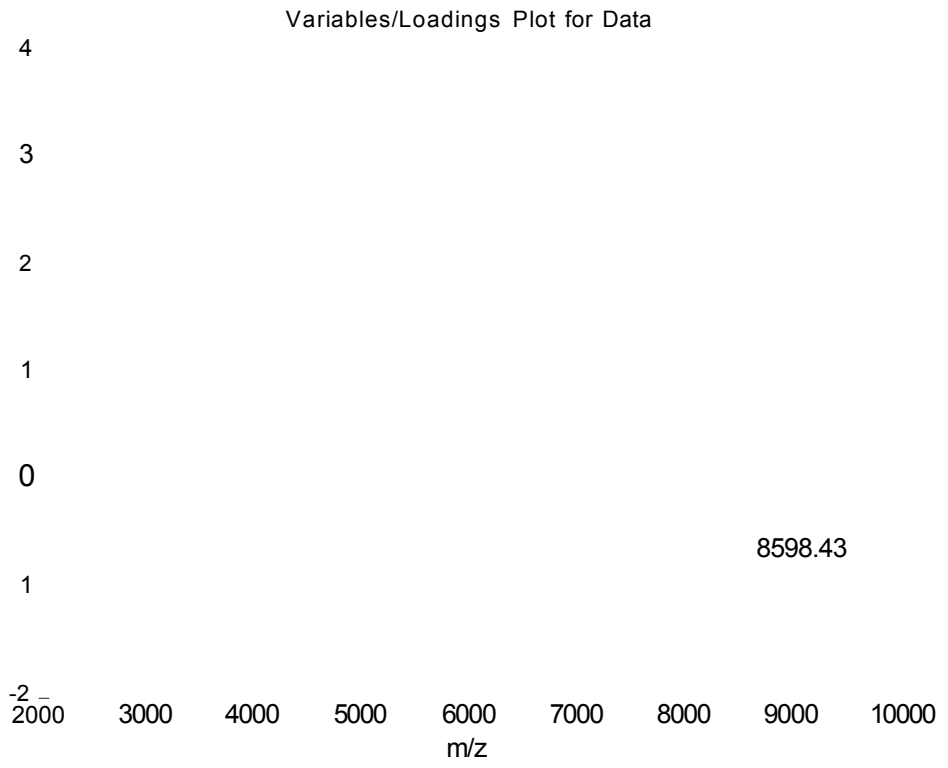

Figure 3-6: Regression vector for the PLSDA model using 6 ***latent variables.***

A positive regression coefficient indicates that the ion signal for that spectral variable is higher in females, whilst a negative coefficient indicates m/z values that have a higher ion signal for male donor fingermarks.

The aim of the pilot study was to investigate the feasibility of the methodology to discriminate donors' sex from MALDI-MS profiles of fingermarks. Even though the cohort was relatively small, it showed, for its size, promising predictive performance by accurately predicting the sex for 5 out of 8 donors in the independent test set. In order to validate the results of the pilot study, a subsequent investigation including a bigger cohort size was performed. Prior to undertaking this study, it was noted that although the matrix system selected produced the best results with respect to ion signal abundance and intensity, "sweet spots" were often observed. This phenomenon, which is a regular occurrence in MALDI-MS, causes substantial variations in ion signal resolution and intensity at different positions of a sample (Garden and Sweedler, 2000).

Subsequent method development determined that the addition of ethanol to the matrix solvent composition, together with an increase in the aqueous content resulted in an improvement in the shot-to-shot reproducibility of the methodology, presumably due to better matrix-analyte co-crystal homogeneity. Therefore, ungroomed fingermarks collected from the cohort of 80 donors participating in the larger sex discrimination study were spotted with 5 mg/mL α-CHCA in 25:25:50 ACN/ethanol/0.5% TFA. Figure 3.7 shows SEM images at x700 and x3000 magnification of an ungroomed fingermark spotted with 5mg/mL α-CHCA in 70:30 ACN/0.5% TFA and 5 mg/mL α-CHCA in 25:25:50 ACN/ethanol/0.5% TFA applied by the direct droplet method. From the SEM images, it can be observed that the co-crystals formed by the 25:25:50 matrix composition are slightly larger, although they look more particulate and homogenously distributed than the co-crystals formed by the 70:30 matrix composition, which look more dendritic. Even though the matrix crystals are slightly bigger with the 25:25:50 matrix, the higher percentage of water potentially results in slower crystal formation, which it can be speculated results in less sweet spots forming and therefore more reproducible spectra.

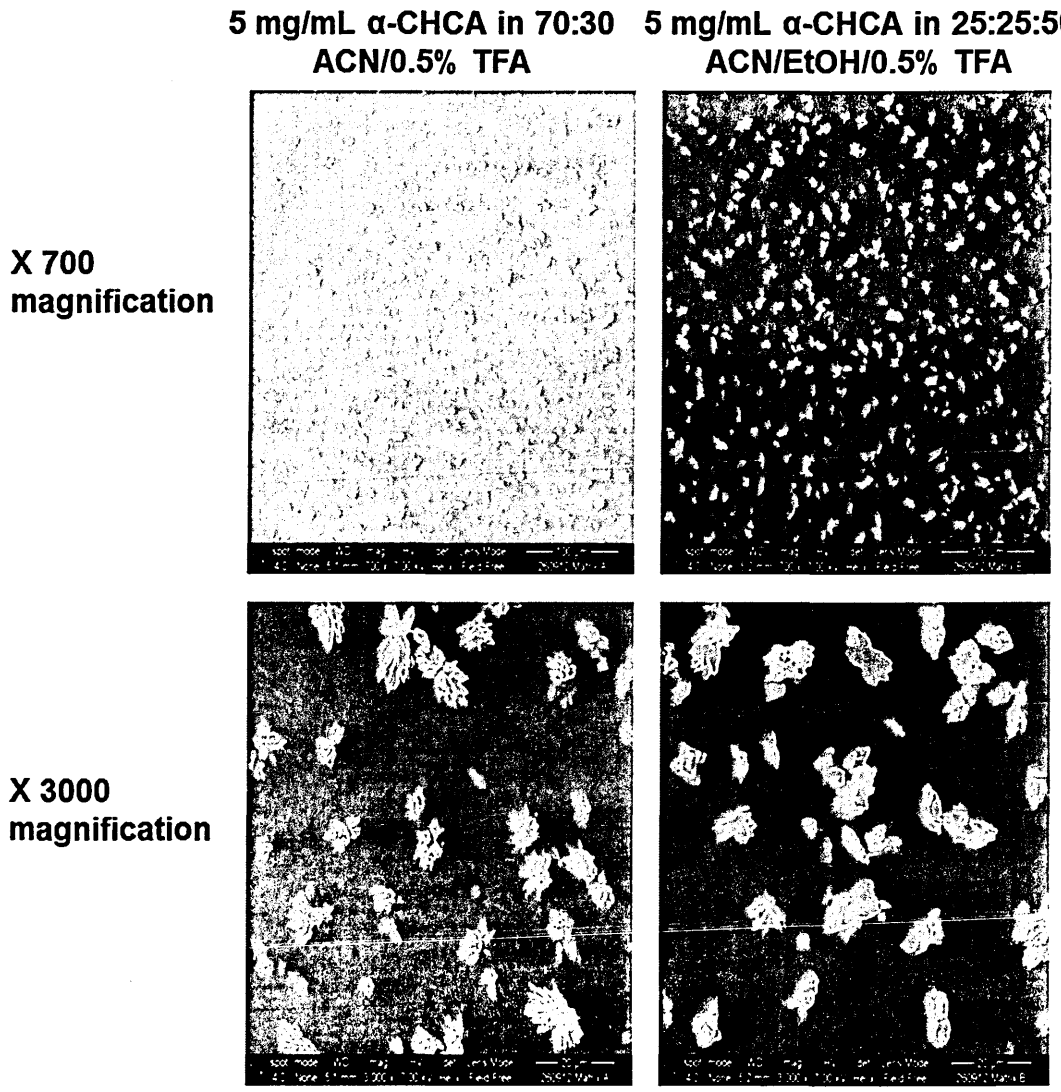

Figure 3-7: SEM images at x700 and x3000 magnification showing the co-crystal formation of two different matrices: 5 mg/mL α-CHCA in 70:30 ACN/0.5% TFA and 5 mg/mL α-CHCA in 25:25:50 ACN/ethanol/0.5% TFA deposited onto an ungroomed fingermark by the direct droplet method.

3.4.2 Large Sex Discrimination Study

For the larger sex discrimination study, fingermarks were collected from a cohort of 80 donors (40 females and 40 males) for analysis by MALDI-MSP. Spectral data from this study were again classified with supervised multivariate analysis using PLSDA.

The classification based on the first PLSDA model (all 12,047 spectral variables, 4 latent variables, training set of 20 female and 20 male donors) of the left out donors during cross validation resulted in a correct sex prediction for 18 (out of 20) females and all 20 males (90% and 100% accuracy respectively). The prediction for the independent test set gave an accuracy of 18 and 13 correct predictions for the 20 female and 20 male donors, resulting in an accuracy of 90% and 65% respectively.

When only spectral variables with a VIP score greater than 10 were used in the model, 199 spectral variables were selected. The resulting model utilised 5 latent variables and correctly predicted the sex of 19 (out of 20) donors, for both sexes, during cross validation and the sex of 17 donors for both sexes for the validation test set. This resulted in an accuracy of prediction of 95% and 85% for the training set and test set respectively. The prediction for each spectrum of the test set is depicted in figure 3.8 (Ferguson *et al.*, 2012). These results provide further confirmation that there is the potential to discriminate between males and females with the available data, indicating that information on sex could be extracted from MALDI-MSP detection of peptides and small proteins in fingermarks followed by multivariate statistical analysis.

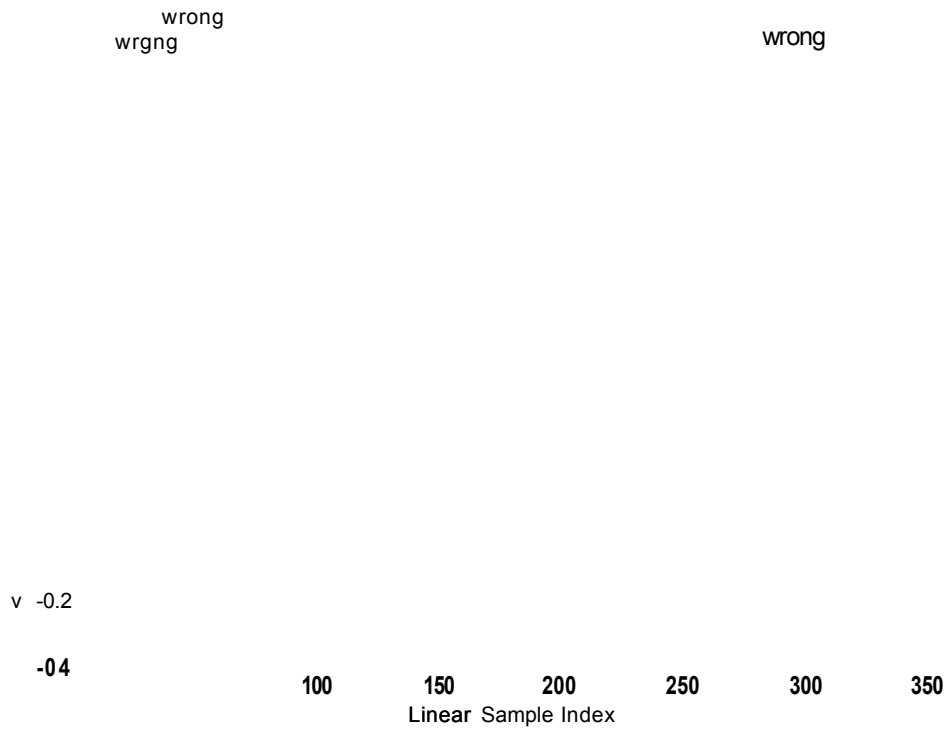

Figure 3-8: Classification results and validation using an independent test set.

Spectra from each of the 40 donors in the test set (20 males and 20 females) have the same plotted symbol and are grouped together with an outline. Prediction above the blue threshold line results in female sex assignment and below the threshold in a male sex assignment. Donors plotted in red are correctly predicted as female, green represents correct male sex prediction and donors plotted in black and labelled as "wrong" have more than half of their spectra assigned to the opposite sex (Ferguson et al., 2012).

It has to be noted though, that, for the majority of donors, some of their 9 spectra were predicted to be from the "opposite" sex (figure 3.8). If a stricter criterion for sex prediction is adopted, the accuracy would be reduced. For example, if at least 2/3 instead of more than half of the spectra have to be classified as one sex for definite assignment, then for the test set, this would result in 27 (67.5%) correct, 5 (12.5%) wrong and 8 (20%) undecided sex predictions. This results in accuracy for each individual spectrum of the test set of 68.9% for female and 74.4% for male associated spectra.

PLSDA calculates, for each variable, a regression coefficient that represents the respective variable's contributions to the prediction of the sex. The regression coefficients vector for the final model (based on 199 VIP selected *m/z* values) is given in figure 3.9. Peaks that appear on the top half of the regression vector plot are relatively higher in females and peaks pointing downwards are relatively higher in males.

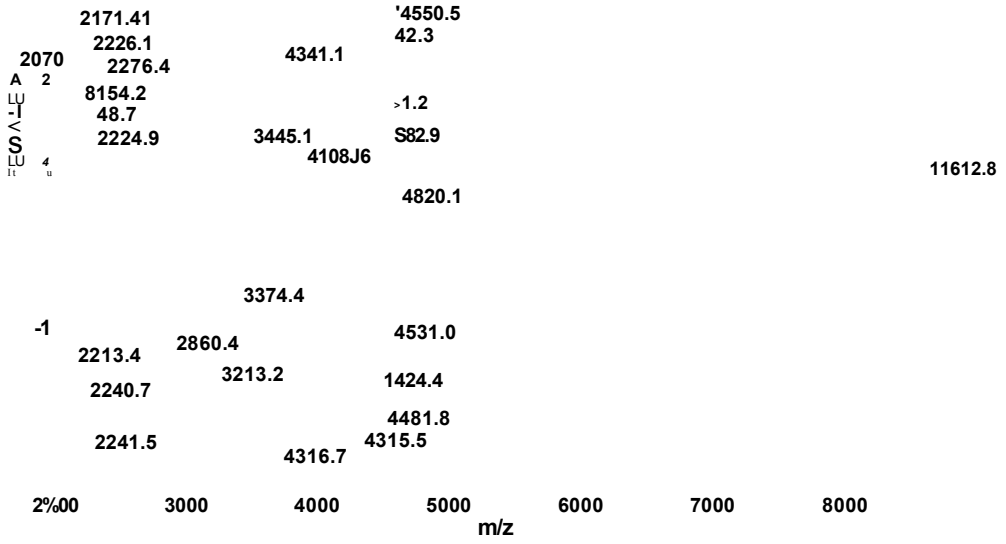

Figure 3-9: Regression vector for the PLSDA model using only spectral variables with a VIP score (Variable Importance in Projection) greater than 10 in the initial model and 5 latent variables.

A positive regression coefficient indicates that the ion signal for that spectral variable is higher in females, whilst a negative coefficient indicates m/z values that have a higher ion signal for male donor fingermarks (Ferguson et al., 2012).

According to our PLSDA classification model, amongst these species, the putatively identified peptides SSL-29 at *m/z* 2869.4 (theoretical *m/z* 2870.3) and LEK-45 at *m/z* 4531.2 (theoretical *m/z* 4532.2), appear to be important in the molecular profile for determining males. While the putatively identified peptides YDP-42 at *m/z* 4301.2 (theoretical *m/z* 4303.6) and DCD-1L at *m/z* 4820.1 (theoretical *m/z* 4819.5) appear to be important in the molecular profile for

determining females (Ferguson *et al.*, 2012). These results contradict the findings of the pilot sex discrimination study as both YDP-42 and DCD-1L appear as important biomarkers for predicting males in the earlier study, whereas in the larger study, they are important in predicting females. A possible explanation is the smaller cohort of donors resulted in a lower predictive accuracy, indeed, only 51.7% of females in the test set were predicted correctly, which means that 48.3% were predicted as male. As YDP-42 and DCD-1L were subsequently found in the larger cohort to be important biomarkers for the prediction of females, this may offer one possible explanation for the inconclusive results obtained in the smaller study for female sex prediction. Furthermore, in the larger study, only peaks with a VIP score greater than 10 were involved in the prediction of sex, resulting in a more concise model and a more stable prediction.

Besides potentially having important implications from a forensic viewpoint, the ability to detect the DCD-derived peptides and small proteins such as psoriasin within fingermarks may also be beneficial from a clinical perspective, as many of the tentatively identified species are known to be potential biomarkers for some disease states. In a study by Rieg *et al.,* (2005), the DCD-derived peptides, DCD-1L, DCD-1, SSL-46, LEK-45, LEK-43, YDP-42 and its dimer were found to be significantly reduced in the sweat of patients suffering with atopic dermatitis (AD), resulting in an impaired innate defence of the epidermal barrier. AD is an inflammatory skin disease, commonly complicated by recurrent skin infections primarily due to the bacterium *S. aureus.* Furthermore, DCD-1L has recently been found to induce the production of cytokines and chemokines including tumour necrosis factor-α, interferon-inducible protein 10, interleukin and macrophage inflammatory protein-3α by human keratinocytes *in vitro*, thus

suggesting the wider implication of DCD-1L in regulating skin immunity (Niyonsaba *et al.*, 2009).

In contrast, the tentatively identified S-100 protein psoriasin (S100A7) has recently been shown to be up-regulated in patients with AD in comparison to healthy controls (Harder *et al.*, 2010), and its antimicrobial activity is well documented. Indeed, psoriasin has been identified as the primary *E.coli*-cidal antimicrobial protein in healthy human skin *stratum corneum* extracts (Schroder and Harder, 2006).

The ability to detect these antimicrobial species in fingermarks by MALDI-MSP enables a rapid and effortless method for analysis of these potential biomarkers, eliminating many of the limitations of previous studies in terms of time and sample preparation (Flad *et al.*, 2002; Rieg *et al.*, 2005; Rieg *et al.*, 2006). In the future, detection of these biomarkers in fingermarks may not only be used to provide additional intelligence in forensic investigations, but also prove to be an important diagnostic tool in clinical applications, or a potential therapeutic target for a) prognosis of patients with chronic and acute skin disorders and b) early and non-invasive diagnosis of cancer.

3.4.3 Imaging Peptides and Proteins within Fingermarks

MALDI-MSI has recently been employed to image a variety of endogenous lipids and exogenous contaminants in ungroomed fingermarks residue (Wolstenholme *et al.*, 2009; Bradshaw *et al.*, 2011; Ferguson *et al.*, 2011; Bradshaw *et al.*, 2013). Subsequent work has involved investigating the possibility of imaging the distribution of higher molecular weight species such as peptides and small proteins within ungroomed fingermarks. The ability to detect and image a range of endogenous species in a single analysis potentially

eliminates issues regarding which class of compounds should be targeted to enable visualisation of the fingermark ridge detail. Various different matrix compositions and matrix application methods were tested in an attempt to image the distribution of the previously detected peptides and small proteins present within groomed fingermarks. Groomed fingermarks were chosen as the best fingermark type on which to optimise the imaging method due to the higher concentration of peptides and proteins associated with sebaceous material. Prior to imaging, mass spectral profiles were taken of the samples after matrix application in order to determine whether any species could be detected using each of the deposition methods employed. Mass spectral profiles were also taken of fingermarks after application of the given matrix via the direct droplet method in order to verify whether any of the relevant species could in fact be detected in the fingermarks tested, as proof that the lack of ion signal was a consequence of the species not being sufficiently extracted by the particular matrix application method employed, rather than it being absent in the deposited fingermarks.

Various matrix compositions and methods of deposition were employed in an attempt to image the distribution of the previously detected peptides and small proteins within latent fingermarks. Matrix deposition using an automatic sprayer was initially performed and the matrix compositions tested can be seen in table 3.2.

Matrix	Solvent Composition
5 mg/mL α-CHCA	70:30 ACN/0.5% TFA
5 mg/mL α-CHCA	50:50 ACN/0.5% TFA
5 mg/mLα-CHCA/aniline	70:30 ACN/0.5% TFA
5 mg/mLα-CHCA/aniline	50:50 ACN/0.5% TFA
5 mg/mL α-CHCA/SA mix	70:30 ACN/0.5% TFA
5 mg/mL α-CHCA/SA mix	50:50 ACN/0.5% TFA
5 mg/mL α-CHCA	25:25:50 ACN/EtOH/0.5% TFA

Table 3-2: The various matrix compositions applied to groomed fingermarks using the SunCollect auto-spraying system.

Instrumental spraying parameters were varied including the numbers of layers sprayed, the velocity at which the sample was sprayed and the distance between the spraying capillary and the sample. The matrix compositions tested enabled some ion peaks to be observed, although the ion signal intensity and signal to noise ratio were poor for all matrix systems tested and no adequate distribution images of peptides or proteins within groomed fingermarks were obtained after matrix application by the SunCollect auto-spraying system. This result suggested reduced sensitivity and extraction efficiency of this matrix application method compared to the direct droplet method. Figure 3.10(a) shows a mass spectrum obtained after spraying fingermarks with 5 layers of 5 mg/mL α-CHCA in 70:30 ACN/0.5% TFA using the SunCollect auto-spraying

system at a velocity of 2 µL/min. Figure 3.10(b),shows a mass spectrum after application of the same matrix via the direct droplet method. From the spectra, it is evident that the direct droplet method successfully extracts peptides from groomed fingermarks. The ion signals observed are of a high intensity with good signal-to-noise, whereas the species detected after application of the same matrix via the automated spraying method, are of a much lower intensity with poor signal-to-noise, resulting in no distribution images being obtained. A possible explanation for why inadequate results were obtained after application of the matrix via automated spraying is the restricted drying times between consecutive layers may be insufficient for co-crystallisation to occur for some analytes, thereby resulting in their limited extraction. Furthermore, when applying matrix via the auto spraying system, care has to be taken to ensure environmental conditions such as the humidity and temperature do not cause a the matrix to crystallise prior to reaching the sample, which would impede analyte/matrix co-crystallisation in the fingermark.

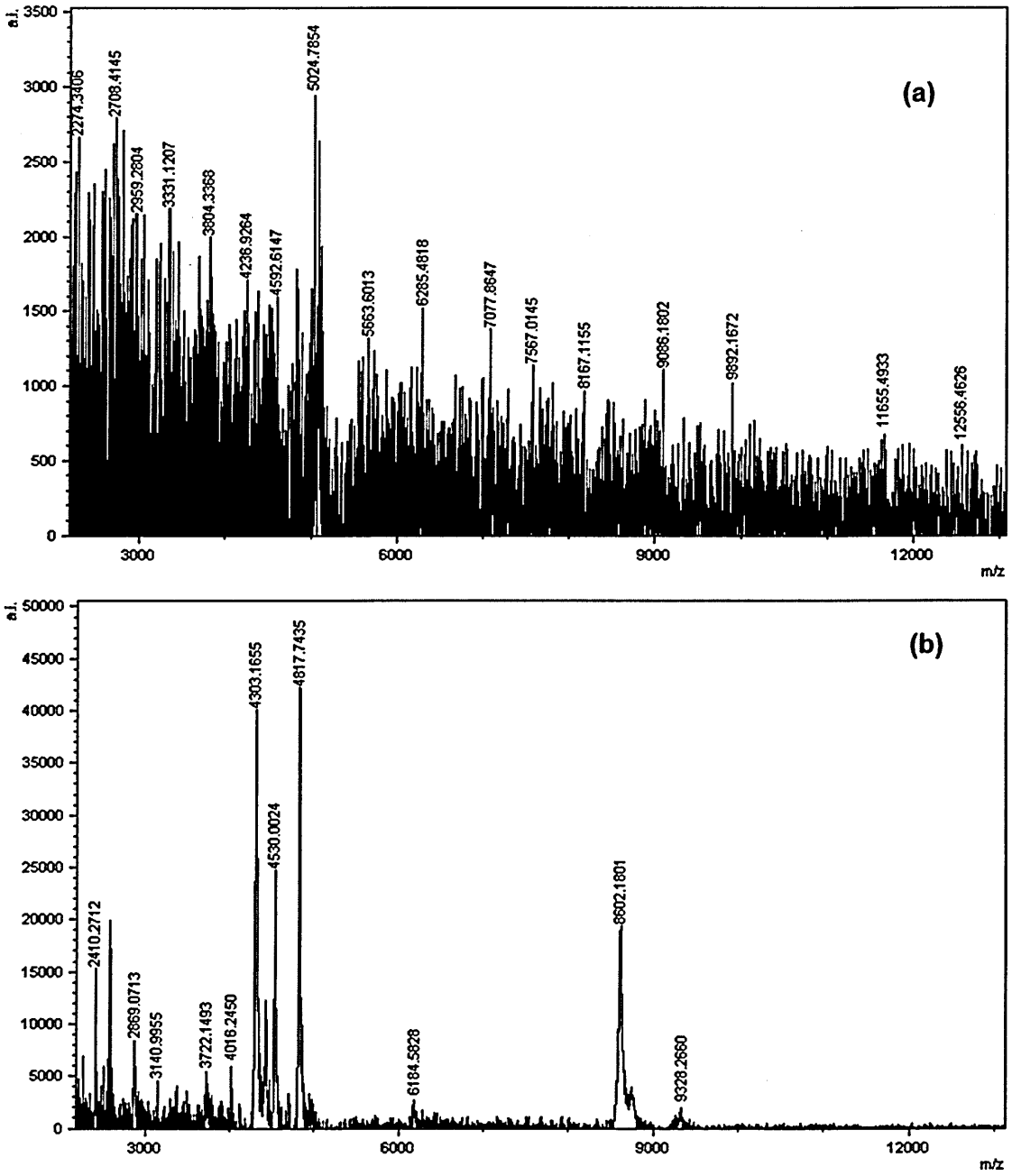

Figure 3-10: Mass spectra obtained of groomed fingermarks after application of 5 mg/mL α-CHCA in 70:30 ACN/0.5% TFA by (a) the SunCollect auto-spraying system, and (b) the direct droplet method.

The peaks present in spectrum (b) correspond to the tentatively identified DCD-derived peptides and are of a high intensity with good signal-to-noise. In comparison, spectrum (a) shows peaks that are of a lot lower intensity with poor signal-to noise.

Figure 3.11 displays the mass spectrum obtained after spraying fingermarks with 5 layers of a 5 mg/mL α-CHCA/aniline matrix solution in 70:30 ACN/0.5%

TFA at a rate of 2 µL/min. The addition of aniline to matrix solutions has previously been reported to produce mass spectra with similar or improved signal-to-noise ratio, compared to when α-CHCA was used alone (Calvano *et al.*, 2009). Aniline is reported to improve the solubilisation of the solid acidic matrix, facilitating the formation of the matrix/analyte co-crystals, thereby improving the results attained (Franck *et al.*, 2009). From figure 3.11(a), it is evident that the mass signals observed after spraying fingermarks with the matrix system are again of a low intensity with poor signal-to-noise, whereas peaks were evident in the spectrum obtained after application of the matrix via the direct droplet method (figure 3.11(b)). Consequently, no distribution images were obtained of peptides or small proteins within groomed fingermarks after spraying fingermarks with the α-CHCA/aniline matrix system. In the paper by Calvano and co-workers, the combined α-CHCA/aniline matrix was used to directly analyse three peptide standards (Calvano *et al.*, 2009). In comparison, fingermark residue consists of a mixture of both endogenous and exogenous compounds, some of which are more abundant and have higher ionisation efficiencies than peptides and proteins. This therefore suggests one plausible reason for why the addition of aniline to the matrix systems tested did not result in sufficient extraction of the peptides and proteins present within fingermarks to enable their detection and subsequent imaging.

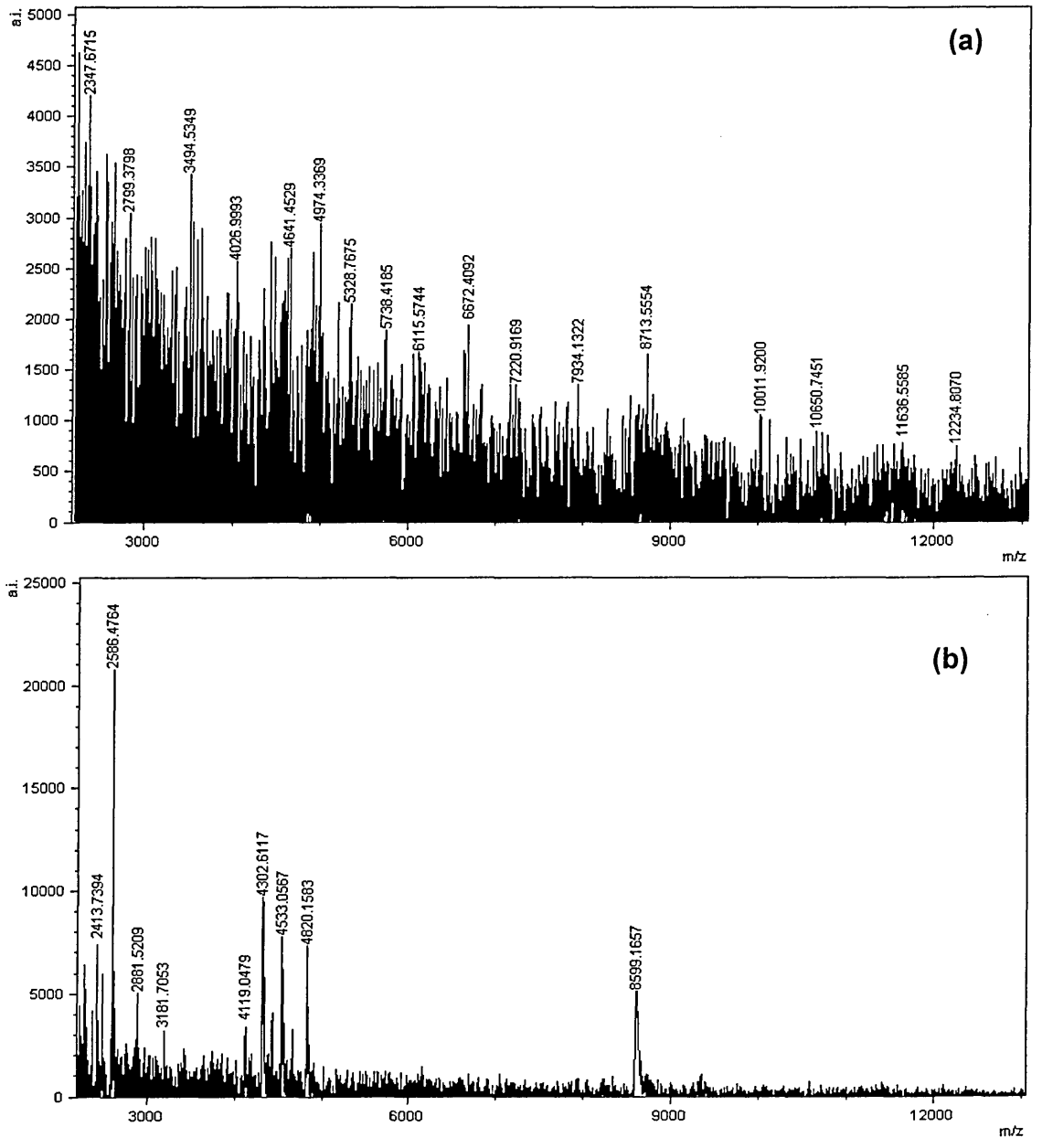

Figure 3-11: Mass spectra obtained from groomed fingermarks after application of 5 mg/mL α-CHCA/aniline in 70:30 ACN/0.5% TFA by (a) the SunCollect auto-spraying system and (b) the direct droplet method.

The peaks present in spectrum (b) correspond to the tentatively identified DCD-derived peptides and are of a high intensity with good signal-to-noise. In comparison, spectrum (a) shows peaks relating to unidentified ions that are of a low intensity with poor signal-to noise.

Although all previously tested matrix combinations applied with the SunCollect auto-spraying system proved to be unsuccessful at generating adequate peptide distribution images, the matrix system consisting of 5 mg/mL α-CHCA in 25:25:50 ACN/ethanol/0.5% TFA did provide some peaks of interest in the mass spectra obtained after application of 5 layers of the matrix via spray-coating at a velocity of 2 µL/min. This matrix generated the most reproducible shot-to-shot ion signals presumably due to improved homogeneity in the analyte/matrix co-crystals formed in previously conducted profiling experiments, which explains the improved results achieved. A mass spectrum obtained after spraying fingermarks with 5 layers of the matrix can be seen in figure 3.12a. Although the spectra contains significant background noise, two peaks at *m/z* 4534.6 and 4821.9 can be clearly seen, which correspond to the tentatively identified peptides LEK-45 (theoretical *m/z* 4532.2) and DCD-1L (theoretical *m/z* 4819.5) respectively; these peaks could also be found after application of the same matrix by the direct droplet method (figure 3.12b). However, the corresponding distribution images appear "dotted" and generally of poor quality, with no clear ridge detail evident. Figure 3.13 shows the distribution image obtained of an area of a fingermark at *m/z* 4821.9, which correlates to the putatively identified peptide DCD-1L.

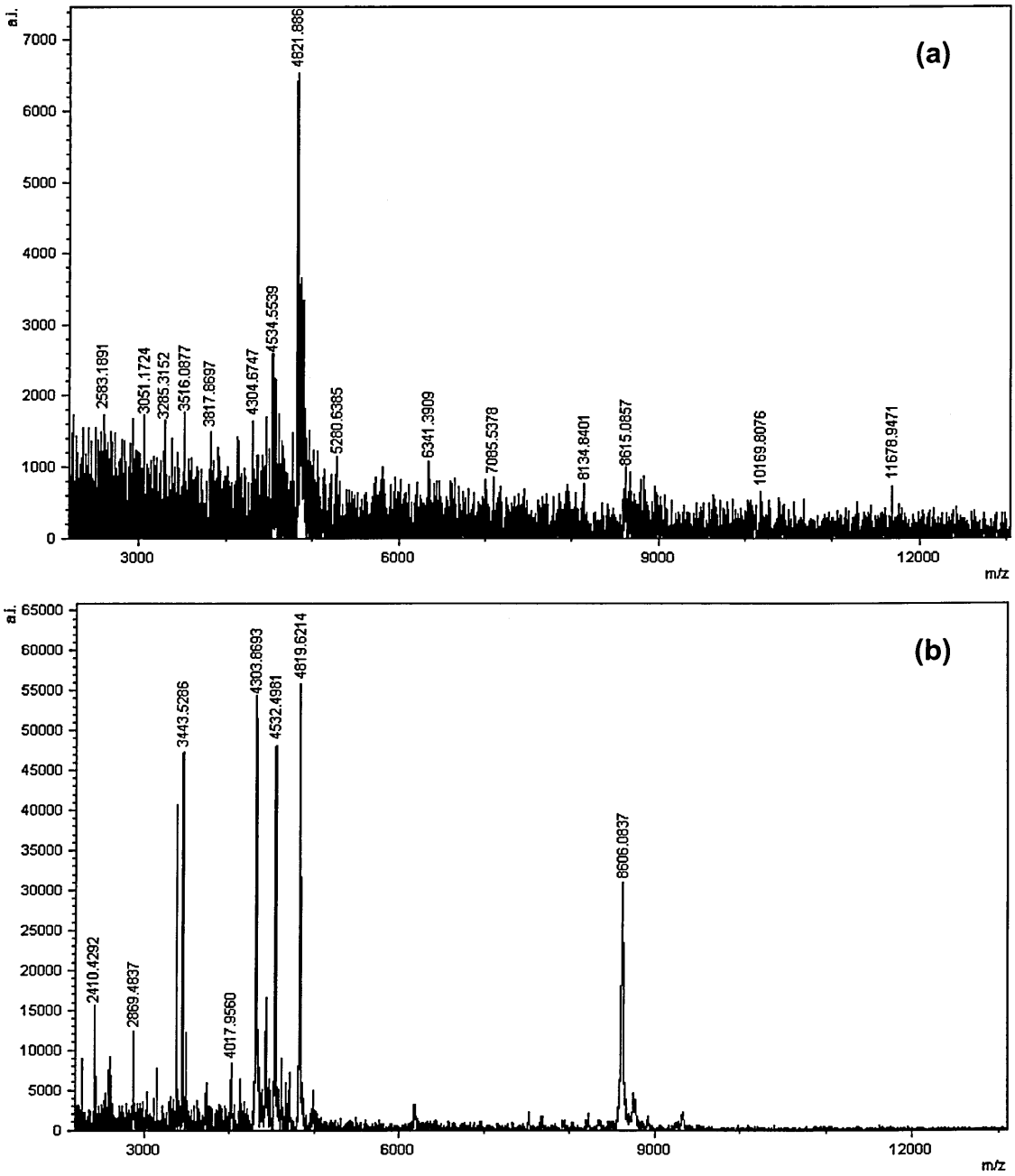

Figure 3-12: Spectra of 5 mg/mL α-CHCA in 25:25:50 ACN/ethanol/0.5% TFA by (a) the SunCollect auto-spraying system, and (b) the direct droplet method.

The peaks present in spectrum (b) correspond to the tentatively identified DCD-derived peptides and are of a high intensity with good signal-to-noise. Two peaks putatively identified as LEK-45 and DCD-1L at m/z 4534.6 (theoretical m/z 4532.2) and 4821.9 (theoretical m/z 4819.5) respectively are also present in spectrum (a) although the peaks are of a lower intensity.

Figure 3-13: Image obtained of a small area of a groomed fingermark at m/z 4821.9, which corresponds to the tentatively identified antimicrobial peptide, DCD-1L.

From the image no clear ridge detail of the fingermark can be seen.

One of the problems of imaging with the automatic sprayer employed here is its unsuitability to spray matrix concentrations greater than 5 mg/mL as higher concentrations cause the fine capillary and needle to become blocked, therefore other matrix application methods were exploited in an attempt to image the distribution of peptides and proteins within fingermarks.

The use of a manual sprayer enabled higher concentrations of matrix to be applied to fingermarks. Table 3.3 shows the matrix compositions applied to groomed fingermarks using the pneumatic manual sprayer.

Matrix	Solvent Composition
10 mg/mL α-CHCA	70:30 ACN/0.5% TFA
10 mg/mL α-CHCA	50:50 ACN/0.5% TFA
20 mg/mL α-CHCA	70:30 ACN/0.5% TFA
20 mg/mL α-CHCA	50:50 ACN/0.5% TFA

Table 3-3: The various matrix compositions applied to groomed fingermarks using the pneumatic manual sprayer.

None of the matrix compositions applied using the manual sprayer enabled peptides or small proteins to be imaged directly from fingermarks. Figure 3.14a shows a mass spectrum obtained after spraying fingermarks with 10 mg/mL α-CHCA in 70:30 ACN/0.5% TFA. The mass signals detected are all of a relatively low intensity, with almost no peaks characterised by a 3:1 signal-to-noise ratio. In contrast, when the same matrix composition was applied via the direct droplet method, some peaks of interest were present (figure 3.14b).

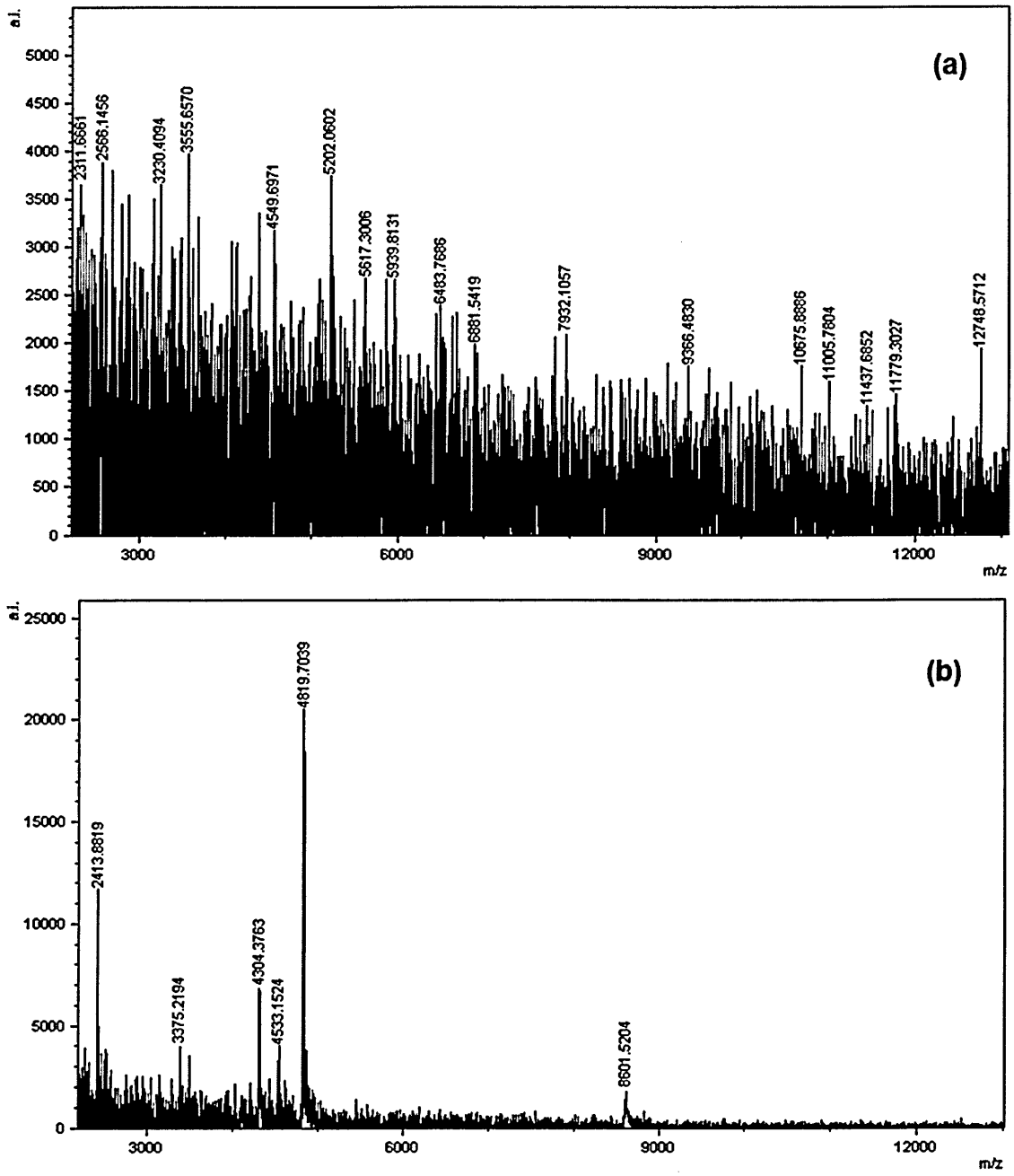

Figure 3-14: Mass spectra obtained from groomed fingermarks after application of a 10 mg/mL α-CHCA in 70:30 ACN/0.5% TFA by (a) manually spraying and (b) the direct droplet method.

The peaks present in spectrum (b) correspond to some of the tentatively identified DCD-derived peptides and are of a high intensity with good signal-to-noise. In comparison, spectrum (a) shows peaks that are of a lot lower intensity with poor signal-to noise.

Similarly, figure 3.15 shows the mass spectrum obtained after application of 20 mg/mL α-CHCA in 70:30 ACN/0.5% TFA using the manual sprayer (figure 3.15a) and after application of the same matrix by the direct droplet method (figure 3.15b). Again, the mass signals detected in spectrum (a) are mainly noise with very few peaks characterised by a 3:1 signal-to-noise ratio.

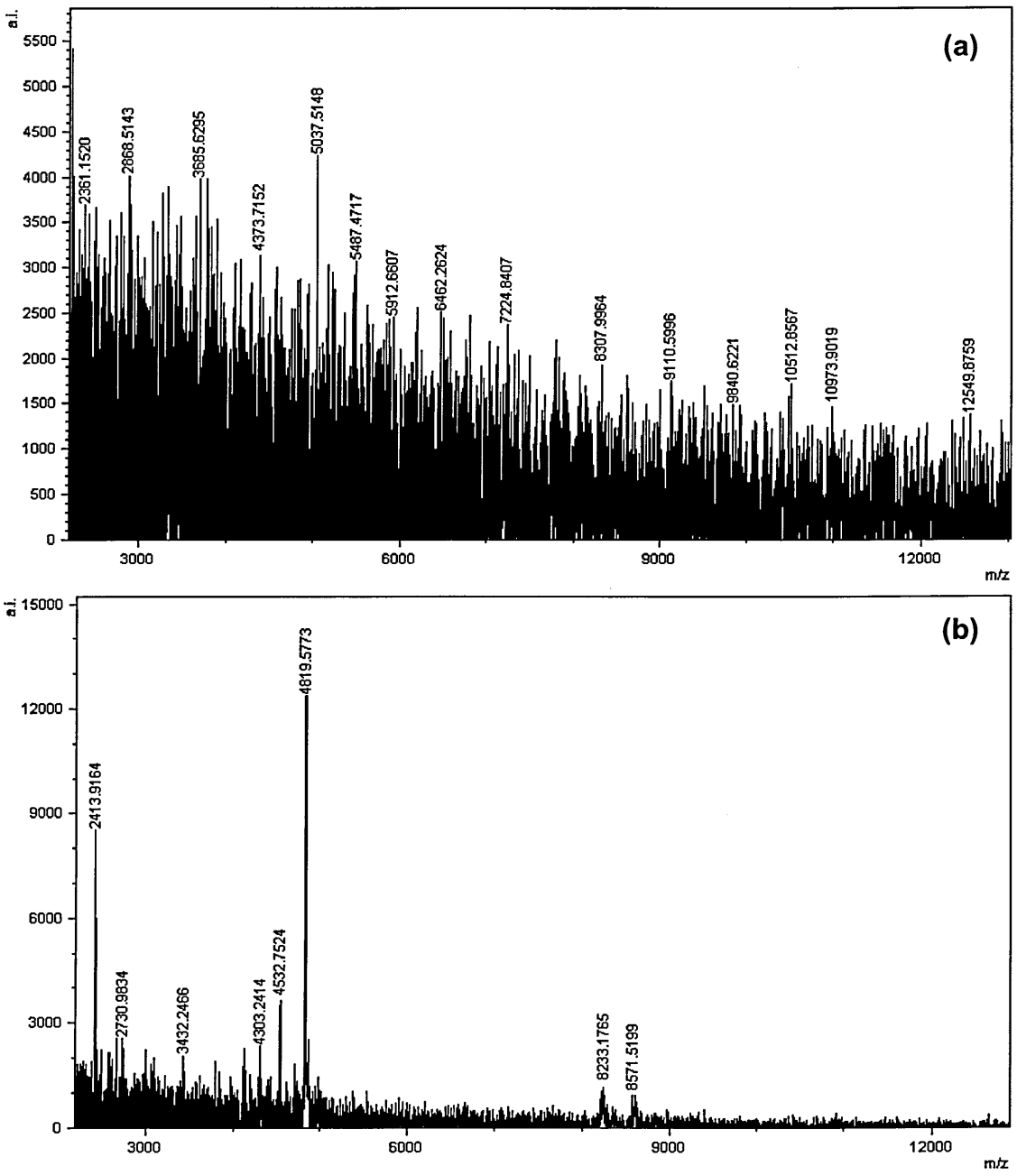

Figure 3-15*: *Mass spectra obtained from groomed fingermarks after application of a 20 mg/mL α-CHCA in 70:30 ACN/0.5% TFA by (a) manually spraying and (b) the direct droplet method.

The peaks present in spectrum (b) correspond to some of the tentatively identified DCD-derived peptides and are of a high intensity with good signal-to-noise. In comparison, spectrum (a) shows limited peaks above the 3:1 signal to noise ratio.

Matrix application using a pneumatic manual sprayer also requires optimisation of various instrumental parameters including: the number of passes, the time

lapse between application of consecutive layers and the distance between the spray nozzle and the sample. For each fingermark sample, sufficient matrix was deemed to have been applied by visually inspecting the samples after spraying to ensure the matrix had been uniformly deposited. One of the main issues of applying "wet" matrix to samples via spraying is the potential to cause delocalisation of the analytes present, although this problem is avoidable by ensuring samples do not become too wet and there is sufficient drying time before application of the next matrix layer. Although spraying is known to improve the spatial resolution observed, it is less sensitive in terms of analyte extraction than other matrix application methods such as microspotting and sublimation (Yang and Caprioli 2011). In order for analytes to be detected by MALDI-MS, they need to be incorporated into the matrix crystals upon solvent evaporation (Bouschen and Spengler, 2007). As spraying involves application of the matrix solutions as a fine mist, a possible explanation is that a proportion of the solvent evaporates prior to reaching the fingermark sample and so the limited peptides and proteins present in fingermark residue are not being sufficiently incorporated into the matrix crystals for their subsequent detection by MALDI-MS and MALDI-MSI. Matrix application via acoustic ejection technology was also tried in an attempt to image peptides and small proteins within groomed fingermarks. Acoustic ejection was first introduced as a prototype by Aerni *et al.*, (2006) and the technology was subsequently employed in the Portrait 630^{TM} instrument by Labcyte. Acoustic ejection enables contactless microspotting of the chosen matrix onto samples, thereby limiting delocalisation of any analytes present to within the spot diameter. Table 3.4 shows the various matrices applied to groomed fingermarks using the Portrait 630 acoustic ejection instrument.

Matrix	Solvent Composition
10 mg/mL α-CHCA	50:50 ACN/0.5% TFA
10 mg/mLα-CHCA/aniline	50:50 ACN/0.5% TFA
10 mg/mL α-CHCA/SA mix	50:50 ACN/0.5% TFA

Table 3-4: The various matrix compositions applied to groomed fingermarks using the Portrait 30 acoustic ejection instrument.

All the matrices tested were unsuccessful at enabling peptides and proteins to be imaged within groomed fingermarks after application by acoustic ejection technology, although some peptides and proteins could be detected by directly spotting the matrices onto the fingermark samples. Figure 3.16a shows a mass spectrum obtained after application of 10 mg/mL α-CHCA in 50:50 ACN/0.5% TFA by the Portrait 630 and figure 3.16b shows a mass spectrum obtained after application of the same matrix by the direct deposition method.

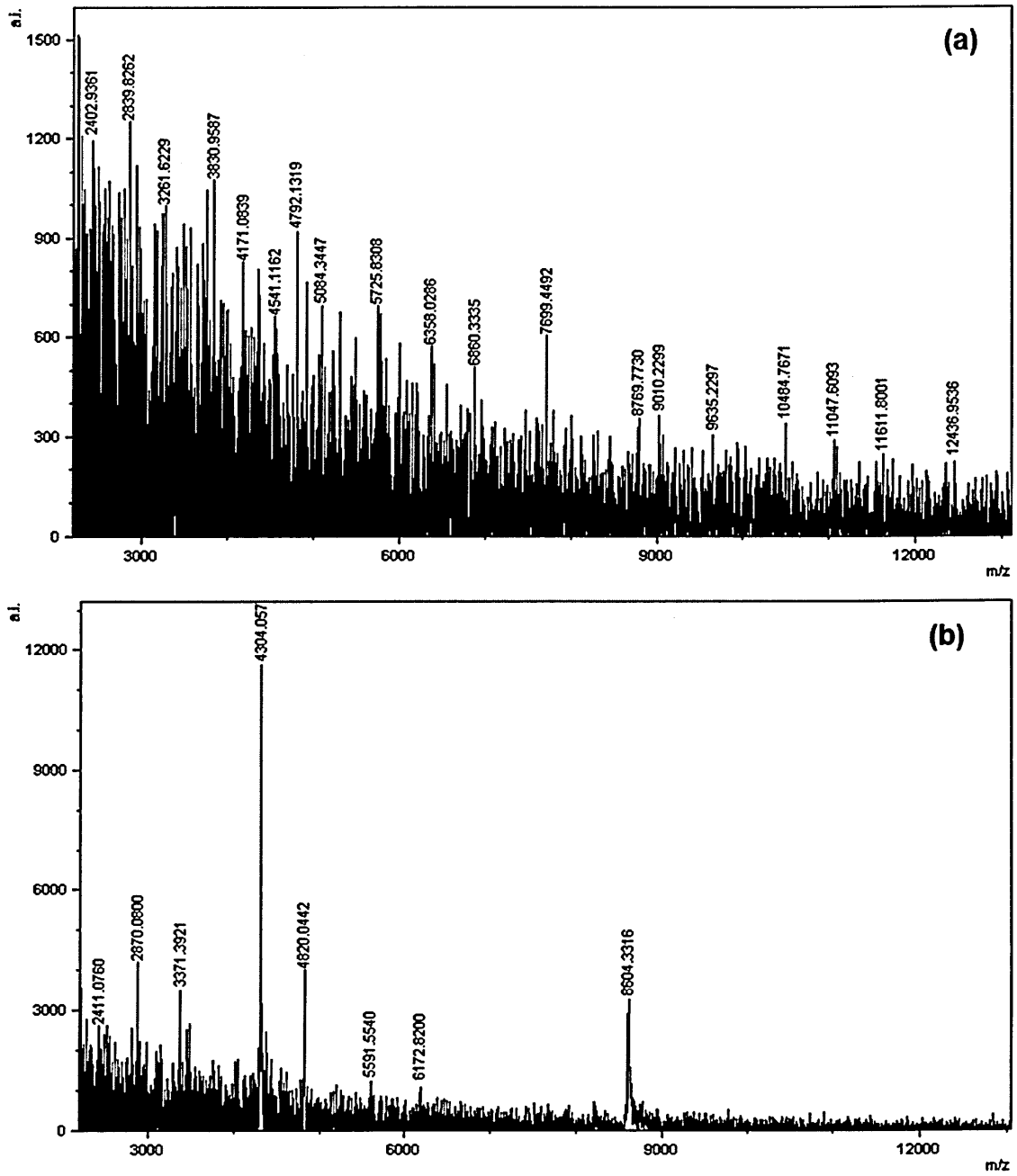

Figure 3-16: Mass spectra obtained from groomed fingermarks after application of a 10 mg/mL α-CHCA in 50:50 ACN/0.5% TFA by: acoustic ejection technology (a) and the direct droplet method (b).

The peaks present in spectrum (b) correspond to the tentatively identified DCD-derived peptides and are of a relatively high intensity with good signal-to-noise. In comparison, spectrum (a) shows peaks that are of a low intensity with poor signal-to noise for most peaks present.

Similarly, figure 3.17a shows a mass spectrum obtained after application of 10 mg/mL α-CHCA/aniline in 50:50 ACN/0.5% TFA by acoustic ejection and figure 3.17b shows a spectrum acquired after application of the same matrix by the direct deposition method. The ability to detect the peptide species by spotting the matrices directly onto the samples proves the endogenous species are indeed present in the fingermark samples tested, but are not being sufficiently extracted by the acoustic ejection technology employed to apply the matrices. In the study by Aerni and collaborators, SA was applied by acoustic ejection technology to mouse brain and liver sections after initial application of ground matrix, which acted as a seeding step (Aerni *et al.*, 2006). Brain and liver samples contain a far higher abundance of protein/peptide species than are reported to be present in fingermark residue, which may offer one explanation for why the applied matrix was not able to sufficiently extract the analytes present to allow their subsequent imaging by MALDI-MS. The application of ground matrix as a seeding step, prior to application of matrix was not tested in the present study, although matrix application via the dry-wet method was tried in an attempt to image the distribution of peptides and proteins in fingermark residue, the results of which are discussed below.

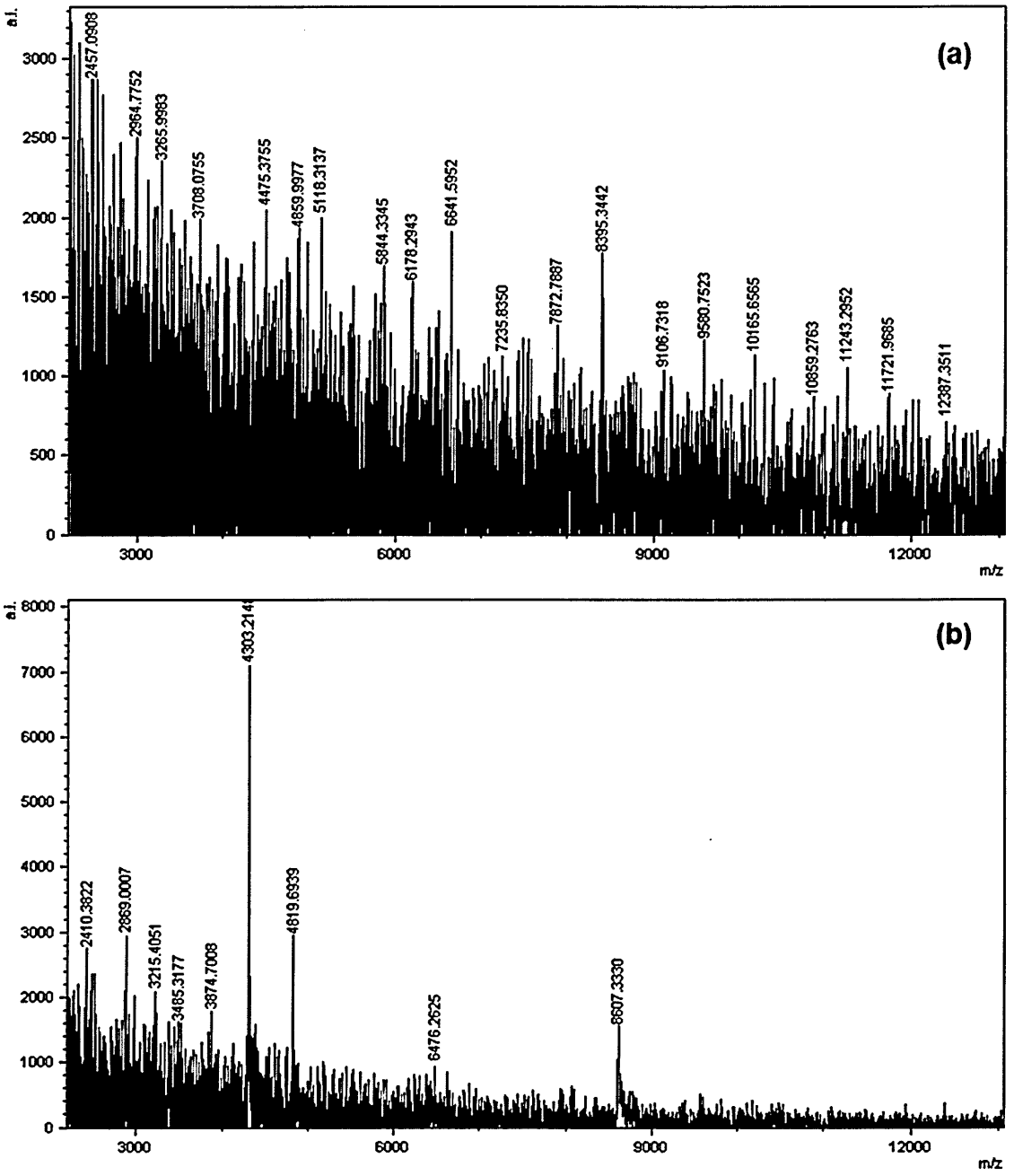

Figure 3-17: Mass spectra obtained from groomed fingermarks after application of 10 mg/mL α-CHCA/aniline in a 50:50 ACN/0.5% TFA by: acoustic ejection technology (a) and the direct droplet method (b).

The peaks present in spectrum (b) correspond to the tentatively identified DCD-derived peptides and are of a relatively high intensity with good signal-to-noise. In comparison, spectrum (a) shows peaks that are of a low intensity with poor signal-to noise for most peaks present.

The recently developed dry-wet method (Ferguson *et al.*, 2011) was also utilised in an attempt to detect and image intact peptides and proteins within groomed fingermarks. Finely ground matrix was initially dusted onto fingermarks using a zephyr brush and solvents were applied by the SunCollect auto-spraying system. The matrices employed and the solvent compositions are shown in table 3.5.

Dusted Matrix	**Solvent Composition**
α-CHCA	70:30 ACN/0.5% TFA
α-CHCA	50:50 ACN/0.5% TFA
α-CHCA/SA mix	70:30 ACN/0.5% TFA
α-CHCA/SA mix	50:50 ACN/0.5% TFA

Table 3-5: The ground matrices applied to groomed fingermarks using a zephyr brush and the applied solvent compositions.

Neither of the solvent compositions tested after dusting fingermarks with α-CHCA enabled peptides or proteins to be imaged within groomed fingermarks, demonstrating the reduced extraction efficiency of this matrix application method compared to the direct droplet method. Figure 3.18a shows the mass spectrum obtained after spraying fingermarks with 5 layers of a 70:30 ACN/0.5% TFA solvent combination using the SunCollect auto-spraying system at a velocity of 5 µL/min. The spectrum shows the presence of some peaks, although the signal-to-noise and ion signal intensity are inadequate. In comparison, when matrix (5 mg/mL α-CHCA 70:30 ACN/0.5% TFA) is applied

by the direct droplet method, the peaks of interest are of a high intensity, with good signal-to-noise

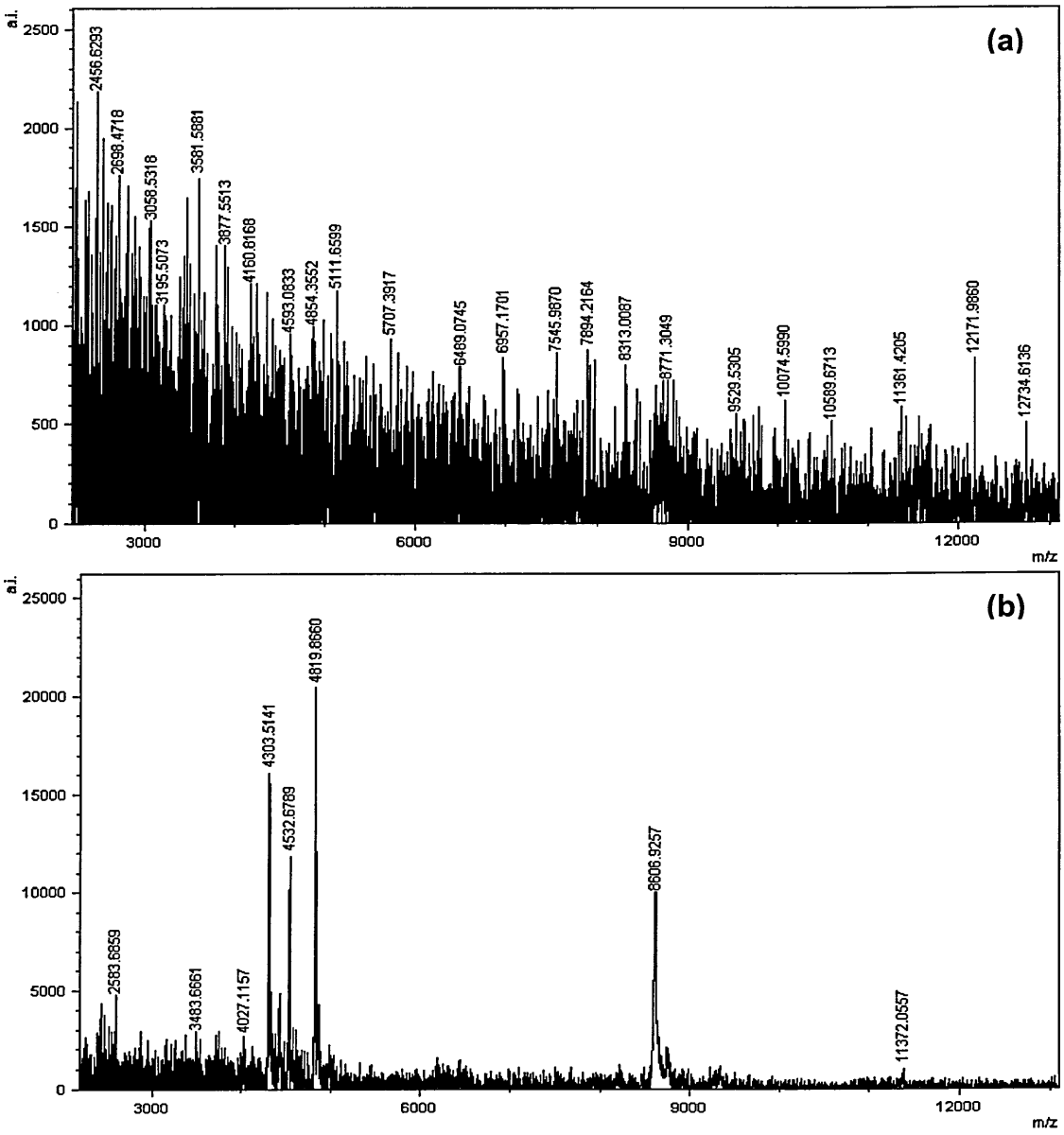

Figure 3-18: Mass spectra obtained from groomed fingermarks. Spectrum (a) shows a fingermark that was dusted with α-CHCA and sprayed with 70:30 ACN/0.5 TFA. Spectrum (b) shows a fingermark after application of 5 mg/mL α-CHCA 70:30 ACN/0.5% TFA by the direct droplet method.

The peaks present in spectrum (b) correspond to the tentatively identified DCD-derived peptides and are of a high intensity with good signal-to-noise. In comparison, spectrum (a) shows very few peaks above the 3:1 signal-to-noise threshold.

Similarly neither of the solvent combinations tested after dusting fingermarks with a mixture of manually ground α-CHCA/SA resulted in any distribution images of peptides and proteins being obtained. Figure 3.19a displays a mass spectrum obtained after spraying fingermarks that had been dusted with α-CHCA/SA with 5 layers of a 70:30 ACN/0.5% TFA solvent combination using the auto-sprayer. From figure 3.19a, it is evident that although mass signals are present, they are of a low intensity with inadequate signal-to-noise resulting in no distribution images being obtained for the peptides and proteins present in fingermark residue, whereas peaks were evident in the spectrum after application of matrix via the direct droplet method (figure 3.19b).

All of the work performed in the present study in an attempt to image the distribution of peptides and small proteins in fingermark residue used matrices above 5mg/ml as these matrices provided the best results in profiling experiments. A possible continuation of the work should investigate whether images can be obtained using lower concentrations of matrix (<5mg/ml), as although matrices <5mg/ml were inadequate to optimally extract peptides and small proteins in profiling mode, due to the limited amount of these species present in latent fingermarks, this may not be the case in imaging mode.

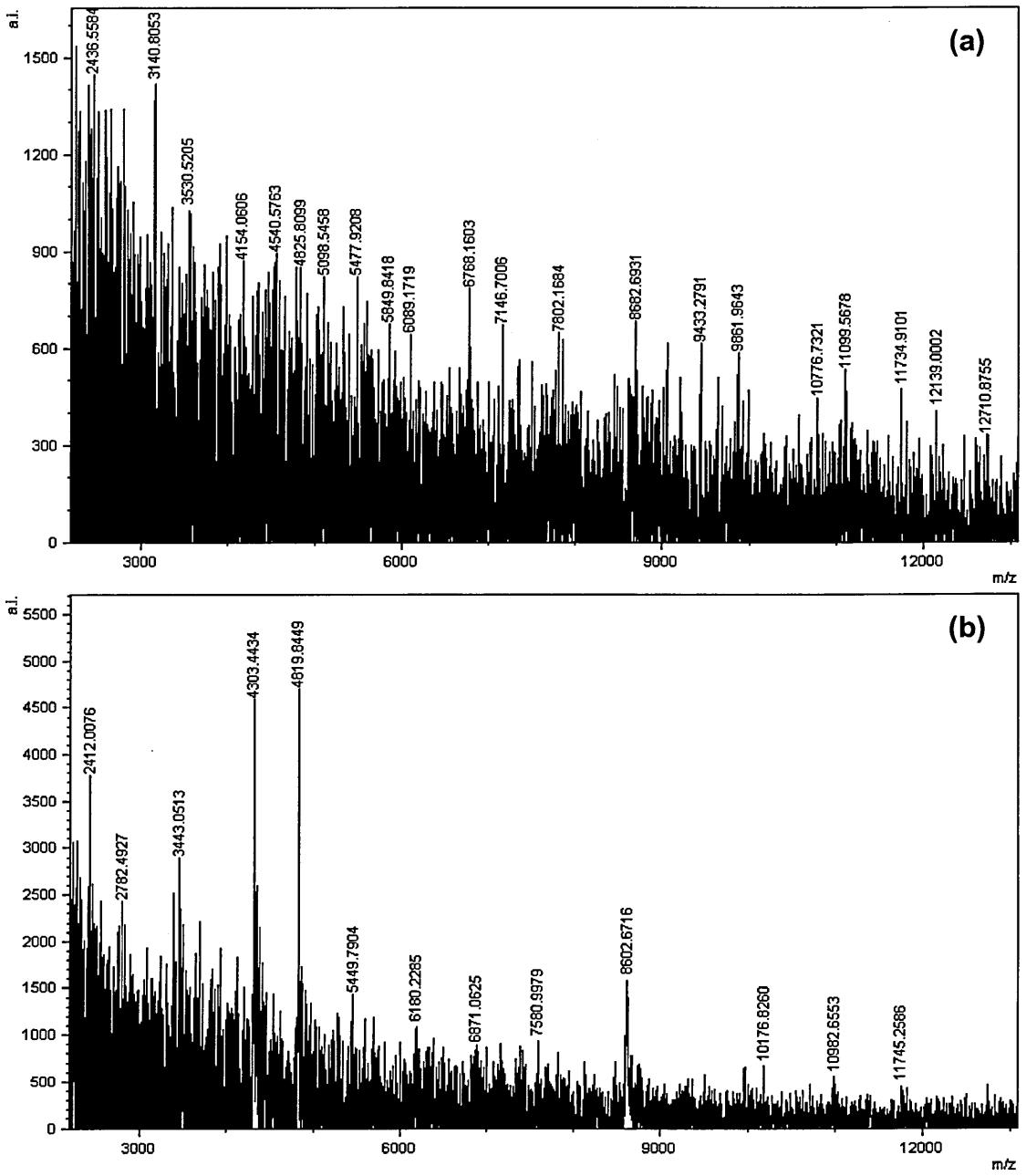

Figure 3-19: Mass spectra obtained from groomed fingermarks. Spectrum (a) shows a fingermark that was dusted with α-CHCA/SA and sprayed with 70:30 ACN/0.5 TFA. Spectrum (b) shows a fingermark after application of 5 mg/mL α-CHCA 70:30 ACN/0.5% TFA by the direct droplet method.

The peaks present in spectrum (b) correspond to the tentatively identified DCD-derived peptides and are of a relatively high intensity with adequate signal-to-noise. In comparison, spectrum (a) shows peaks that are of a lot lower intensity with poor signal-to noise.

3.5 Conclusion

A novel method to successfully detect various antimicrobial peptides and small proteins in fingermark residue by MALDI-MSP has been developed. Whereas, the majority of discrimination studies performed on latent fingermarks have involved classification based on the lipid constituents present, here peptides and proteins were detected and subjected to multivariate statistical analysis. The results enabled the sex of the donor to be determined with a validated prediction accuracy ranging from 67.5% to 85% (depending on the assignment criteria) in the larger sex study, demonstrating the potential of the methodology to discriminate between the sexes.

Even though various tentatively identified antimicrobial peptides and proteins were detected in latent fingermarks by MALSI-MSP, all attempts to image the distribution of these species were unsuccessful. In comparison to other biological tissues, the amount of peptides and proteins present in fingermark residue is minimal (Drapel *et al.*, 2009), which possibly offers one explanation for why these species could only be detected using the direct droplet matrix application method, as the matrix deposition methods employed for imaging purposes are too insensitive to efficiently extract the small quantities present to enable their distribution to be visualised. Salts, endogenous lipids and some exogenous contaminants are also known to supress ionization of peptides and proteins, which could provide another explanation for why the antimicrobial species present within fingermark residues were not sufficiently extracted by the matrix deposition methods employed to enable their distribution images to be visualised. Even though the groomed fingermarks were washed with denatured ethanol to remove the lipids that are present, some may have remained, which could have suppressed the intended ion signals.

3.6 References

Aerni, H., Cornett, D. and Caprioli, R. (2006). Automated acoustic matrix deposition for MALDI sample preparation. *Analytical Chemistry,* **78** (3), 827-834

Anderssen, E., Dyrstad, K.,Westad, F. and Martens, H. (2006). Reducing over-optimism in variable selection by cross-model validation. *Chemometrics and Intelligent Laboratory Systems*, **84** (1-2), 69-74

Antoine, K.M., Mortazavi, S., Miller, A.D. and Miller, L.M. (2010). Chemical differences are observed in children's versus adults' latent fingerprints as a function of time. *Journal of Forensic Sciences,* **55** (2), 513-518

Archer, N.E., Charles, Y., Elliott, J.A. and Jickells, S. (2005). Changes in the lipid composition of latent fingerprint residue with time after deposition on a surface. *Forensic Science International,* **154** (2-3), 224-239

Asano, K.G., Bayne, C.K., Horsman, K.M. and Buchanan, M.V. (2002). Chemical composition of fingerprints for gender determination. *Journal of Forensic Sciences,* **47** (4), 805-807

Baechle, D., Flad, T., Cansier, A., Steffen, H., Schittek, B., Tolson, J., Herrmann, T., Dihazi, H., Beck, A., Mueller, G., Mueller, M., Stevanovic, S., Garbe, C., Mueller, C. and Kalbacher, H. (2006). Cathepsin D is present in human eccrine sweat and involved in the post-secretory processing of the antimicrobial peptide DCD-1L. *Journal of Biological Chemistry,* **281** (9), 5406-5415

Bouschen, W. and Spengler, B. (2007). Artefacts of MALDI sample preparation investigated by high-resolution scanning microprobe matrix-assisted laser

desorption/ionization (SMALDI) imaging mass spectrometry. *International Journal of Mass Spectrometry,* **266** (1-3), 129-137

Bradshaw, R., Rao, W., Wolstenholme, R., Clench, M.R., Bleay, S. and Francese, S. (2012). Separation of overlapping fingermarks by matrix assisted laser desorption ionisation mass spectrometry imaging. *Forensic Science International,* **222** (1-3), 318-326

Bradshaw, R., Wolstenholme, R., Blackledge, R.D., Clench, M.R., Ferguson, L.S. and Francese, S. (2011). A novel matrix-assisted laser desorption/ionisation mass spectrometry imaging based methodology for the identification of sexual assault suspects. *Rapid Communications in Mass Spectrometry,* **25** (3), 415-422

Buchanan, M., Asano, K. and Bohanon, A. (1997). Chemical characterisation of fingerprints from adults and children. *Proc. SPIE-Int. Soc. Opt. Eng.*, **2941**, 89-95

Calvano, C.D., Carulli, S. and Palmisano, F. (2009). Aniline/α-cyano-4-hydroxycinnamic acid is a highly versatile ionic liquid for matrix assisted laser desorption/ionization mass spectrometry. *Rapid Communications in Mass Spectrometry*, **23**, 1659-1668

Chong, I. and Jun, C. (2005). Performance of some variable selection methods when multicollinearity is present. *Chemometrics and Intelligent Laboratory Systems,* **78** (1-2), 103-112

Dikshitulu, Y.S., Prasad, L., Pal, J.N. and Rao, C.V. (1986). Aging studies on fingerprint residues using thin-layer and high performance liquid chromatography. *Forensic Science International,* **31** (4), 261-266

Drapel, V., Becue, A., Champod, C. and Margot, P. (2009). Identification of promising antigenic components in latent fingermark residues. *Forensic Science International,* **184** (1-3), 47-53

Eigenvector Research Inc (2012) *About PLS Toolbox and Solo*. Available at URL: http://wiki.eigenvector.com, last accessed 13/04/13

Emerson, B., Gidden, J., Lay, J.O.,Jr and Durham, B. (2011). Laser desorption/ionization time-of-flight mass spectrometry of triacylglycerols and other components in fingermark samples. *Journal of Forensic Sciences,* **56** (2), 381-389

Ferguson, L., Bradshaw, R., Wolstenholme, R., Clench, M. and Francese, S. (2011). Two-step matrix application for the enhancement and imaging of latent fingermarks. *Analytical Chemistry,* **83** (14), 5585-5591

Ferguson, L.S, Creasey, S., Wolstenholme, R., Clench, M.R. and Francese, S. (2013). Efficiency of the dry-wet method for the MALDI-MSI analysis of latent fingermarks. *Journal of Mass Spectrometry,* **48,** 677-684

Flad, T., Bogumil, R., Tolson, J., Schittek, B., Garbe, C., Deeg, M., Mueller, C.A. and Kalbacher, H.:.(2002). Detection of dermcidin-derived peptides in sweat by ProteinChip technology. *Journal of Immunological Methods,* **270,** 53-62

Garden, R. and Sweedler, J. (2000). Heterogeneity within MALDI samples as revealed by mass spectrometric imaging. *Analytical Chemistry,* **72** (1), 30-36

Harder, J., Dressel, S., Wittersheim, M., Cordes, J. Meyer-Hoffert, U., Mrowietz, U., Follster-Holst, R., Proksch, E. Schroder, J.M., Schwarz, T. and Glaser, R. (2010). Ehnanced expression and secretion of antimicrobial peptides in atopic dermatitis and after superficial skin injury. *Journal of Investigative Dermatology*, **130**, 1355-1364

Lee, D., Yamasaki, K., Rudsil, J., Zouboulis, C.C., Park, G.T., Yang, J. and Gallo, R.L. (2008). Sebocytes express functional cathelicidin antimicrobial peptides and can act to kill propionibacterium acnes. *Journal of Investigative Dermatology,* **128** (7), 1863-1866

Lemaire, R., Wisztorski, M., Desmons, A., Tabet, J.C., Day, R., Salzet, M. and Fournier, I. (2006). MALDI-MS direct tissue analysis of proteins: Improving signal sensitivity using organic treatments. *Analytical Chemistry,* **78** (20), 7145-7153

Niyonsaba, F., Suzuki, A., Ushio, H., Nagaoka, I., Ogawa, H. and Okumura, K. (2009). The human antimicrobial peptide dermcidin activates normal human keratinocytes. *British Journal of Dermatology,* **160** (2), 243-249

Ramotowski, R.S. (2001). Composition of latent print residue; In: Lee, H.C. and Gaensslen, R.E. (ed.). *Advances in fingerprint technology.* Boca Raton, Florida, CRC Press, 63-104

Rieg, S., Seeber, S., Steffen, H., Humeny, A., Kalbacher, H., Stevanovic, S., Kimura, A., Garbe, C. and Shittek, B. (2006). Generation of multiple stable

dermcidin-derived antimicrobial peptides in sweat of different body sites. *Journal of Investigative Dermatology,* **126** , 354-365

Rieg, S., Steffen, H., Seeber, S., Humeny, A., Kalbacher, H., Dietz, K., Garbe, C. and Schittek, B. (2005). Deficiency of dermcidin-derived antimicrobial peptides in sweat of patients with atopic dermatitis correlates with an impaired innate defense of human skin in vivo. *Journal of Immunology,* **174** (12), 8003-8010

Schittek, B., Hipfel, R., Sauer, B., Bauer, J., Kalbacher, H., Stevanovic, S., Schirle, M., Schroeder, K., Blin, N., Meier, F., Rassner, G. and Garbe, C. (2001). Dermcidin: A novel human antibiotic peptide secreted by sweat glands. *Nature Immunology,* **2** (12), 1133-1137

Schroder, J. and Harder, J. (2006). Antimicrobial skin peptides and proteins. *Cellular and Molecular Life Sciences,* **63** (4), 469-486

Schwartz, S., Reyzer, M. and Caprioli, R. (2003). Direct tissue analysis using matrix-assisted laser desorption/ionization mass spectrometry: Practical aspects of sample preparation. *Journal of Mass Spectrometry,* **38** (7), 699-708

Seeley, E.H., Oppenheimer, S.R., Mi, D., Chaurand, P. and Caprioli, R.M. (2008). Enhancement of protein sensitivity for MALDI imaging mass spectrometry after chemical treatment of tissue sections. *Journal of the American Society for Mass Spectrometry,* **19** (8), 1069-1077

Song, W., Mao, Z., Liu, X., Lu, Y., Li, Z., Zhao, B. and Lu, L. (2012). Detection of protein deposition within latent fingerprints by surface-enhanced Raman spectroscopy imaging. *Nanoscale,* **4** (7), 2333-2338

Westerhuis, J.A., Hoefsloot, H.C.J., Smit, S., Vis, D.J., Smilde, A.K., van Velzen, E.J.J., van Duijnhoven, J.P.M. and van Dorsten, F.A. (2008). Assessment of PLSDA cross validation. *Metabolomics,* **4** (1), 81-89

Weyermann, C., Roux, C. and Champod, C. (2011). Initial results on the composition of fingerprints and its evolution as a function of time by GC/MS analysis. *Journal of Forensic Sciences,* **56** (1), 102-108

Wolstenholme, R., Bradshaw, R., Clench, M.R. and Francese, S. (2009). Study of latent fingermarks by matrix-assisted laser desorption/ionisation mass spectrometry imaging of endogenous lipids. *Rapid Communications in Mass Spectrometry,* **23** (19), 3031-3039

Wong, J., Cagney, G. and Cartwright, H. (2005). SpecAlign - processing and alignment of mass spectra datasets. *Bioinformatics,* **21** (9), 2088-2090

Yang, J. and Caprioli, R.M. (2011). Matrix Sublimation/Recrystallization for imaging proteins by mass spectrometry at high spatial resolution. *Analytical Chemistry,* **83** (14), 5728-5734

Zelson, A. S. (2000). Fingerprint analysis method. International Publication number WO 00/46739

4 Analysis of Fingermarks by SERS & ATR-FTIR

4.1 Introduction

Of all the vibrational spectroscopy techniques, Raman and Infrared (IR) spectroscopy are the most widely used. Both techniques provide information regarding the specific vibrational modes of the chemical bonds present in a molecule. Selection rules predict whether a molecular vibration will be Raman or IR active. Molecules can be either Raman or IR active depending on whether the vibration is symmetrical or asymmetrical according to the mutual exclusion rule. Furthermore, molecules with different elements of symmetry may be active in Raman, IR, neither or both. Raman spectroscopy and IR spectroscopy are therefore considered complementary techniques (Smith and Dent 2005; Chalmers *et al.*, 2012).

Surface Enhanced Raman spectroscopy (SERS) and Attenuated Total Reflectance (ATR) Fourier transform Infrared spectroscopy (FTIR) were used in the present study as a means of providing additional complementary chemical information to that obtained by MALDI-MSI. Both techniques have been employed in a wide range of forensic applications including the analysis of drugs of abuse (Bell *et al.*, 2007; Yang *et al.*, 2012), explosives (Mou and Rabalais, 2009), dyes (Jones and Wolstenholme, 2003; Geiman *et al.*, 2009), paints (Zieba Palus *et al.*, 2011; Leona *et al.*, 2011), body fluids (Virkler and Lednev, 2008; Boyd *et al.*, 2013; Elkins, 2011) and fingermarks (Day *et al.*, 2004a; Ricci *et al.*, 2007a; West and Went, 2009).

Raman spectroscopy has previously been used to identify body fluids that may be discovered at a crime scene. The body fluids analysed were blood, semen, saliva, vaginal fluid and sweat. The various body fluids could be differentiated from their specific Raman signatures, providing a non-destructive means of identification (Virgler and Lednev, 2008). More recently, Surface Enhanced

Raman Spectroscopy (SERS) has been used to overcome some of the problems with low sensitivity that are often evident with Raman spectroscopy. SERS enhances the inherently weak Raman signal by a factor of $10^3 - 10^7$ and has many forensic applications. In a study by Boyd and co-workers, blood could be identified to a dilution of 1:100,000 after direct application to a specific SERS substrate composed of nickel nanotips coated with silver nanoparticles. Furthermore, Raman spectra were also obtained after using the SERS substrate as a swab following wetting a dried blood sample deposited on fabric (Boyd *et al.*, 2013). The use of ATR-FTIR in the analysis of human biological samples (blood, saliva, tears, urine, nasal mucus, vaginal mucus, faeces, earwax, fingernails, fingermarks, hair and semen) has also been reported (Elkins, 2011). Samples were tested in their natural state and after application to a piece of white cotton or white paper, as a means of simulating possible crime scene contaminated samples. The study concluded that ATR-FTIR spectroscopy demonstrated potential in differentiating between the various biological materials tested due to the unique peaks exhibited in the spectra of the samples, particularly in the fingerprint region.

4.1.1 Raman Spectroscopy and ATR-FTIR Analysis of Latent Fingermarks

Raman spectroscopy has been used previously to investigate the presence of various drugs of abuse and over the counter drugs in groomed and ungroomed fingermarks, which were artificially loaded with the dopants prior to deposition. Raman spectroscopy enabled all the drugs to be identified in both fingermark types; although the spectra originating from the "spiked" groomed fingermarks contained many interfering bands originating from the sebaceous constituents present (Day *et al.*, 2004a). In a separate study, the same authors reported the possibility of using Raman spectroscopy to detect the same exogenous

compounds within groomed fingermarks after enhancement by cyanoacrylate fuming (Day *et al.,* 2004b). The presence of the cyanoacrylate polymer created background fluorescence, which interfered with the resulting spectra and the intensities of the Raman bands were lower. The presence of over the counter analgesics in fingermarks has also been investigated using Raman spectroscopy incorporating a confocal microscope. Fingermarks were initially dusted with powders and lifted with adhesive tape or hinge lifters. Subsequent work enabled the detection of the dopants in the lifted fingermarks, without removing them from their evidence bags (West and Went, 2008; West and Went, 2009).

Infrared spectroscopy has also been used to investigate the presence of exogenous compounds in fingermarks. In a study by Grant and co-workers, IR spectromicroscopy was employed to detect and identify a mixture of various materials in fingermark residue, including Vitamin C, ibuprofen, Sweet' N Low and a non-dairy creamer. The study also used an ATR accessory to analyse larger particles where analysis by conventional IR-spectromicroscopy had proven to be difficult due to saturated absorbances being evident in the resulting spectra (Grant *et al.*, 2005).

More recently, ATR-FTIR spectromicroscopy has been used to detect three explosive particles, trinitrotoluene, trinitrobenzene and ammonium nitrate in fingermarks deposited on a stainless steel substrate. ATR-FTIR spectromicroscopy enabled the detection and identification of the three explosive residues after matching the resulting spectra to an infrared spectral library (Mou and Rabalais 2009).

The presence of cosmetics within fingermarks has also been investigated using ATR-FTIR. Fingermarks were obtained after wiping fingers over a forehead which had previously been treated with various cosmetics. Fingermarks were either deposited directly onto the zinc selenide (ZnSe) ATR crystal or lifted from non porous surfaces using a BVDA gelatine lift. Spectra obtained from the resulting images showed that peaks originating from the various cosmetics tested could be differentiated from the intense peaks originating from the gelatine lifts. Subsequent work enabled the detection of cosmetics directly from a porous substrate. Fingermarks contaminated with body butter or lip gloss were deposited onto a cotton and polyester shirt. ATR-FTIR enabled the two cosmetics to be identified, although the fingermark ridge pattern could not be reconstructed (Ricci and Kazarian 2009).

Besides exogenous contaminants, both SERS and ATR-FTIR have also been used to investigate the endogenous constituents of fingermarks. SERS was employed in the analysis of the eccrine components of fingermarks after degradation by both heat and light in research performed by De Paoli *et al.*, (2010). The authors concluded that neither amino acids nor urea underwent degradation after exposure to UV light, although both constituents displayed the onset of degradation at temperatures of 100°C. In contrast, lactic acid showed both photo and thermal degradation. The research was subsequently expanded in another paper to include imaging capabilities (Connatser *et al.*, 2010). More recently, SERS was used to indirectly image proteins within latent fingermarks. High resolution SERS images of the fingermark ridge pattern were obtained after artificially loading the fingermarks with immunoglobulin G (IgG) due to the augmented presence of the modified nanoparticles of the ridges of the fingermark (Song *et al.*, 2012).

FTIR chemical imaging has previously been employed to detect and visualise latent fingermarks on various deposition surfaces. Images of both untreated and cyanoacrylate enhanced fingermarks were obtained after deposition on glass substrates (Tahtou *et al.*, 2005). More recently, FTIR spectroscopy was used to image untreated fingermarks on various porous and non-porous surfaces following various data processing methods which enabled the fingermarks to be differentiated from the background, whilst simultaneously preserving trace evidence associated with the fingermarks (Crane *et al.*, 2007).

Subsequent work utilised an ATR accessory to analyse the endogenous components of fingermarks. Ricci and collaborators obtained distribution maps of amino acid and lipid constituents of latent fingermarks under controlled conditions after deposition on a ZnSe crystal. Fingermarks were aged over 14 days in varying temperatures and humidities and the resulting dataset was subjected to statistical analysis. The results indicated that changes in the lipid constituents present were evident with changes in temperature and after ageing (Ricci *et al.*, 2007a).

In the present study, both SERS and ATR-FTIR have been used to investigate the feasibility of establishing a forensic workflow to support and provide complementary information to that obtained using MALDI-MS and MALDI-MSI in the study of latent fingermarks. SERS was used to investigate the feasibility of detecting and imaging the chemical constituents of fingermarks deposited on various deposition surfaces. ATR-FTR was used in a combined approach with MALDI-MSI in order to establish a potential sequential workflow to detect and image both endogenous and exogenous species in fingermarks deposited on non-porous surfaces.

4.2 Materials

Gold Colloids (50nm, 100nm and 150nm) were purchased from PerkinElmer (Shelton, Connecticut, USA) and BritishBiocell International (Cardiff, UK). Klarite was obtained from D3 Technologies Ltd (Glasgow, UK). ALUGRAM SIL G/UV_{254} pre-coated aluminium sheets, α-CHCA, TFA, vinyl-polydimethysiloxane (PDMS) and polyethylene glycol (PEG) 3000 were purchased from Sigma Aldrich (Poole, UK). MALDI target OPTI spotless inserts were purchased from Applied Biosystems (CA, USA). Anhydrous sodium sulphate (Na_2SO_4), acetonitrile, ethanol and acetone were obtained from Fisher Scientific (Loughborough, UK). Dettol alcohol wipes, freezer bags and elastic bands were purchased from Wilkinson's (Sheffield, UK). Condomi max-love condoms were obtained from www.britishcondoms.co.uk. Gelatine lifts were obtained courtesy of Dr Stephen Bleay from CAST (Centre for Applied Technology, Home Office, UK) and from Bureau Voor Dactyloscopische Attikelen (BVDA, Haarleem, The Netherlands). Forensic lifting tape was acquired from TETRA Scene of Crime (http://www.tetrasoc.com/).

4.3 Methods

4.3.1 Instruments and Instrumental Parameters

4.3.1.1 Raman Instrumentation

Raman spectra were acquired using a RamanStation 400 benchtop Raman spectrometer (PerkinElmer, Shelton, Connecticut, USA). The excitation source was a 350 mW near- infrared (NIR) 785 nm laser (100 mW at the surface), with a spot size of 100 micron. A spectral range of 400-3200 cm^{-1} was employed. The detector was a temperature controlled charged coupled device (CCD) detector (-50°C) incorporating a 1024 x 256 pixel sensor. Spectra were acquired

using Spectrum software and images were acquired using SpectrumIMAGE software, both supplied by PerkinElmer.

4.3.1.2 ATR-FTIR Instrumentation

ATR-FTIR spectra and images were acquired using a Varian 680-IRFTIR spectrometer (Lexington, KY, USA) fitted with a 64 x 64 mercury cadium telluride focal plane array detector. The FTIR spectrometer was coupled to a Specac Imaging Golden Gate diamond accessory (Orpington, UK). Images were obtained and processed using Resolutions Pro® software (Varian Ltd, Lexington, USA). Images were obtained over a wavelength range of 3600 – 950 cm^{-1} and at a spatial resolution of 4 cm^{-1}.

4.3.1.3 MALDI-MSI Instrumentation

MALDI-MS images were obtained using a modified API Q-Star Pulsar *i* Hybrid quadrupole time-of-flight (QTOF) instrument (Applied Biosystems, CA, USA). The orthogonal MALDI source has been modified to incorporate a 5 kHz solid-state laser having a wavelength of 355 nm. MALDI-MSI analyses were performed at a resolution of 150 µm x 150 µm using 'continuous raster imaging' at a laser repetition rate of 5 kHz and over a mass range of 100-1000.

4.3.2 Preparation of Fingermarks

4.3.2.1 Groomed Fingermarks

Groomed fingermarks were prepared by cleaning the hands with alcohol wipes and rubbing the fingers on the forehead, nose and chin five times to obtain a sebum-rich mark. For analysis by SERS, fingermarks were then deposited on either ALUGRAM ® SIL G/UV $_{254}$ pre-coated aluminum sheets after removing the silica with acetone, MALDI spotless inserts or Klarite™, a SERS specific substrate. For analysis by ATR-FTIR and MALDI-MSI, fingermarks were

deposited on a clean aluminium can and recovered using a BVDA gelatine lift and subjected to ATR-FTIR analysis.

4.3.2.2 Condom Lubricant Contaminated Fingermarks

Condom lubricant contaminated fingermarks were obtained by rubbing the fingertips on the outer surface of a freshly opened condom in order to simulate real usage, resulting in the fingermarks being artificially loaded with condom lubricant. The fingertips were subsequently rubbed together in order to obtain a homogenous distribution of the lubricant over the fingertip surface. Fingermarks were then deposited onto a clean ceramic tile and the deposited fingermarks were lifted using BVDA gelatine lifts and subjected to analysis by ATR-FTIR.

4.3.3 Analysis of Latent Fingermarks by Surface Enhanced Raman Spectroscopy (SERS)

4.3.3.1 Deposition of Gold Colloid of Different Concentrations and Particle Size

Groomed fingermarks were prepared as stated in section 4.3.2.1 and deposited on aluminum sheets, after removing the silica with acetone and MALDI spotless inserts. 1 μL of each gold colloid (50 nm, 100 nm and 150 nm) was spotted onto the fingermarks. For layered deposition, successive layers of the 100 nm colloid were applied to fingermarks either by spotting or spraying with an aerosol spray bottle. Each spot or layer was allowed to dry before application of the subsequent spot or layer.

4.3.3.2 Pre-Concentrating the 100 nm Colloid

The 100 nm aqueous colloid was pre-concentrated by taking 10 ml and centrifuging at 2750 rpm for 30 minutes, and then removing 9.5 ml of the supernatant, resulting in a 20-fold concentrated SERS suspension. The resulting solution was subsequently applied on top of groomed fingermarks.

4.3.3.3 Order of Deposition of 150 nm Colloid

A single layer of the 150 nm colloid was applied directly onto both the MALDI and aluminium substrates and allowed to dry. Groomed fingermarks were then deposited on top of the colloid and the spectra obtained were compared to those where the fingermark had been positioned below the colloid..

4.3.3.4 Use of Salt Aggregates with 100nm Colloid

Gold colloid (100 nm) was mixed with a 0.1M solution of sodium sulphate in a 1:1 ratio, to give final concentrations of 0.05 M. The resulting solutions were applied above and below groomed fingermarks and spectra were obtained in order to determine the effects of the salt aggregate on the SERS spectrum.

4.3.3.5 Raman Images

For images obtained on aluminium plates and MALDI stainless steel inserts, 1 µL of the 150 nm colloid was applied directly onto the deposition surface, before groomed fingermarks were laid on top. For images on Klarite™, groomed fingermarks were laid directly onto the 4mm x 4mm Klarite™ active area. Images were acquired over a wavelength range of 3200 – 400 cm^{-1} and at a resolution of 0.05 mm, with 2.00 s x 2 scans at each point.

4.3.4 Analysis of Fingermarks by Attenuated Total Reflectance Fourier Transform Infrared Spectroscopy (ATR-FTIR)

4.3.4.1 Analysis of Groomed Fingermarks

Groomed fingermarks were obtained as described in section 4.3.2.1 and deposited on a clean aluminium can. Fingermarks were lifted using BVDA gelatine lifts and placed directly onto the diamond ATR-FTIR crystal. Images were acquired over a wavelength range of 3200 – 950 cm^{-1} and at a spectral resolution of 4cm^{-1}, averaging 256 scans. Images were generated using the peak height at 1743.5 cm^{-1}.

4.3.4.2 Analysis of Condom Lubricant Contaminated Fingermarks

Condom lubricant contaminated fingermarks were obtained as described in section 4.3.2.2 and deposited onto a clean ceramic tile. After lifting the fingermarks from the deposition surface, the BVDA gelatine lift was placed directly onto the diamond ATR crystal for data collection. Background spectra of the gelatine lift alone were also obtained, as well as spectra of vinyl-PDMS and PEG-3000 standards. The distribution map of PDMS was obtained within fingermarks by integrating the area of a Si-O stretching band at approximately 1258 cm^{-1} using an integration range of 1248-1278 cm^{-1}. The distribution map of PEG was obtained by integrating the peak area of a C-H bending band at approximately 1365 cm-1, over an integration range of 1325 – 1470 cm^{-1}.

4.3.5 Analysis of Groomed and Condom Lubricant Contaminated Fingermarks by MALDI-MSI

After recovery of the groomed and condom lubricant contaminated fingermarks from the aluminium can and ceramic tile using the BVDA gelatine lifts, the remaining fingermark residue was dusted with mechanically ground α-CHCA prepared as stated in section 2.3.3. Fingermarks were then lifted with forensic lifting tape and sprayed with 5 layers of a 70:30 ACN/0.5% TFA solution at a speed of 5 µl/min. Fingermarks were analysed as stated in section 4.3.1.3.

4.4 Results and Discussion

4.4.1 Surface Enhance Raman Spectroscopy (SERS)

4.4.1.1 Effect of Gold Colloid Concentration and Particle size

Raman scattering is often very weak, for analytes present at low concentrations such as the endogenous species within fingermarks. SERS enhances the Raman signal by up to 10^6 when analytes are adsorbed onto a roughened metal

surface such as the colloidal gold nanoparticles employed in the present study to enhance the Raman signal.

Three colloidal gold solutions of different concentrations and particle size were tested. Both the 50 nm and 100 nm colloid were dilute solutions, whose primary use was for biological assay applications. The 150 nm colloid was specifically developed for SERS applications and was a more expensive alternative to the biological colloids, therefore initial work concentrated on investigating the plausibility of reducing costs by using the more economical colloids. Figure 4.1 shows the SERS spectra obtained after application of the three different colloidal gold solutions to groomed fingermarks deposited onto spotless MALDI inserts. From the spectra, it is evident that the 150 nm SERS specific colloid is the only one that provides sufficient enhancement of the Raman signal as more peaks are present, which are of a higher intensity (Ferguson *et al.*, 2010a and 2010b).

Two theories exist for the mechanisms for SERS enhancement. One is named electromagnetic enhancement and the other is termed charge transfer or chemical enhancement. According to Doering and Nie (2002), electromagnetic enhancement is the primary contributor to the SERS effect. There are a number of key factors that are believed to be fundamental in enabling the nanoparticle colloidal solutions that are frequently used in SERS applications to facilitate the enhancement of the weak Raman signal. These factors include: the diameter and shape of the particles, the inter-particle distance, the excitation wavelength and the presence of aggregating agents (Stamplecoskie *et al.*, 2011).

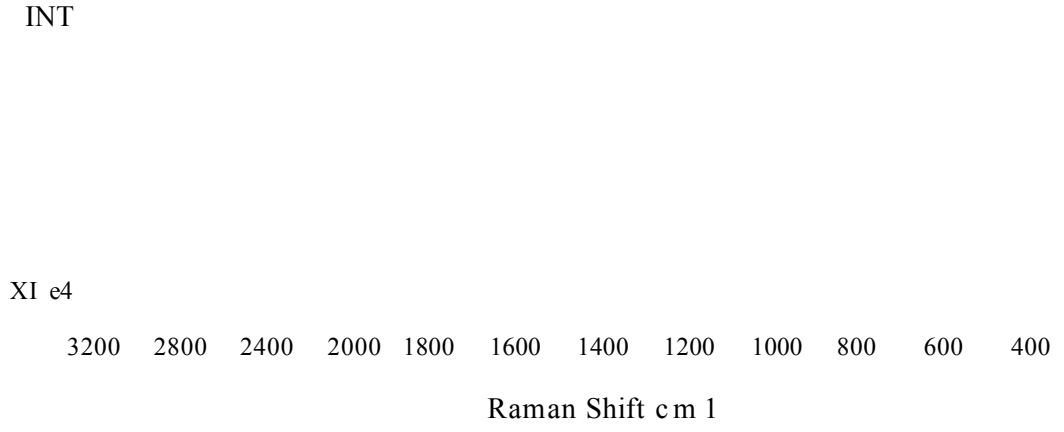

Figure 4-1: SERS spectra obtained after application of a single drop (1pL) of three gold colloids of different particle size and concentration (a) 50 nm dilute colloid, (b) 100 nm dilute colloid, and (c) 150 nm Raman specification colloid to a groomed fingermark deposited on a MALDI spotless insert (Ferguson et ai, 2010a and 2010b).

Various studies have been performed using unaggregated colloid solutions in order to correlate the Raman signal intensity of the analyte being investigated with the diameter of the nanoparticles employed. There is a strong correlation between the size of the nanoparticles employed and the colloids' plasmon absorptions, which consequently greatly affects the intensity of the SERS effect observed. However, despite the numerous studies conducted incorporating isolated particles in solution, there are wide disparities in the optimum particle size, even when the same excitation wavelength is used (Bell and McCourt 2009).

Even though the best results were obtained with application of a single drop of the 150 nm SERS specific substrate, subsequent work concentrated on depositing multiple layers of the 100 nm colloid by both spraying and spotting, in order to ascertain whether this would improve the chemical information obtained. From Figure 4.2, panel 1, it can be seen that the peaks become more pronounced and of a higher intensity as the number of layers of colloid sprayed increases. Similar results were obtained after application of 20 successive drops of the 100 nm gold colloid and after application of pre-concentrated colloid to the groomed fingermark as seen in figure 4.2, panel 2 (Ferguson *et al.*, 2010a and 2010b). However, the improvement in spectral quality was inadequate to justify the time involved. As the size of the nanoparticles used has a direct effect on the enhancement factor observed, the slight improvement in spectral quality observed after application of successive layers of 100 nm colloid and the pre-concentrated colloid could be due to the colloid becoming aggregated, thereby increasing the size of the nanoparticles and therefore the enhancement factor.

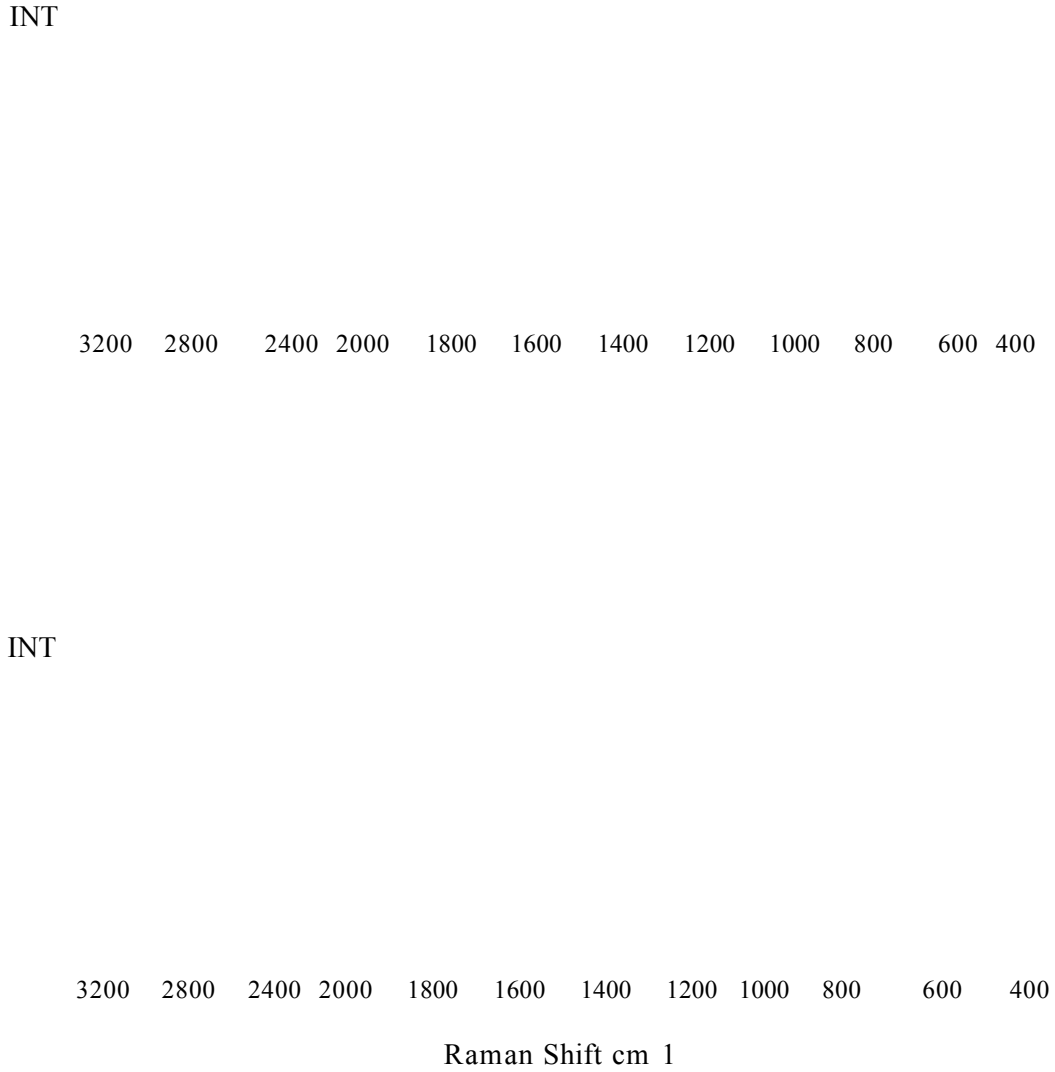

Figure 4-2: SERS spectra of a groomed fingermark deposited on a MALDI spotless insert after application of multiple layers of a 100 nm dilute gold colloid. *Panel 1 shows the resulting spectra after spraying (a) 1 layer, (b) 5 layers, and (c) 25 layers. Panel 2 shows the spectra obtained after application of (a) 20-fold pre-concentrated 100 nm dilute colloid and (b) 20 successive spotted layers of 100 nm dilute colloid (Ferguson et al., 2010a and 2010b).*

4.4.1.2 Use of Salt Aggregates with 100 nm Colloid

Salt aggregates have been used to improve the SERS effect by various research groups. In a study by Bell and Sirimuthu (2005), magnesium sulphate ($MgSO_4$) aggregated to citrate reduced gold colloids was used to enhance the SERS signal of anions. The authors concluded that aggregation was imperative for obtaining a strong SERS signal for analytes at parts per million (ppm) concentrations. More recently, various experimental parameters including type of nanoparticle, pH and the effect of various aggregation salts (NaCl, Na_2SO_4, KNO_3, and K_2SO_4) were tested in order to optimise the SERS signal for mephedrone (4-methylmethcathinone), a much publicised synthetic stimulant more commonly known by the street names MCAT and Meow Meow. The results of the study found that the most consistent limit of detection (LOD) results were obtained for a 10% mephedrone solution when a 70% silver colloid solution was used with a 6% NaCl solution (Mabbott *et al.*, (2013).

Electrolyte salts are recommended because they do not bind strongly to the colloidal metal surface and are believed to augment the formation of clusters, resulting in enhancement of the SERS signal. The 100 nm gold colloid was mixed in a 1:1 ratio with 0.1M Na_2SO_4 to ascertain whether the use of a salt aggregate would improve the results of the less expensive colloid, thereby limiting the costs involved. Figure 4.3 shows the spectra obtained for groomed fingermarks with the salt aggregate mixture. It is apparent from the spectra that some peaks look enhanced by the application of the salt aggregates; however, the majority of peaks observed in the spectra of the fingermark are also present in the spectra of the salt aggregates alone. Furthermore, many of the peaks originating from the fingermark are masked by the peaks in the salt aggregate spectra, which is problematic when trying to correctly assign peaks specifically

originating from the fingermarks (Ferguson ***et al.,*** 2010a and 2010b). It has also been reported that some aggregating salts prevent the adsorption and detection of analytes due to competitive binding of aggregates to the surface of the gold colloid particles, which may offer one explanation for the results presented here (Bell and Sirimuthu 2005).

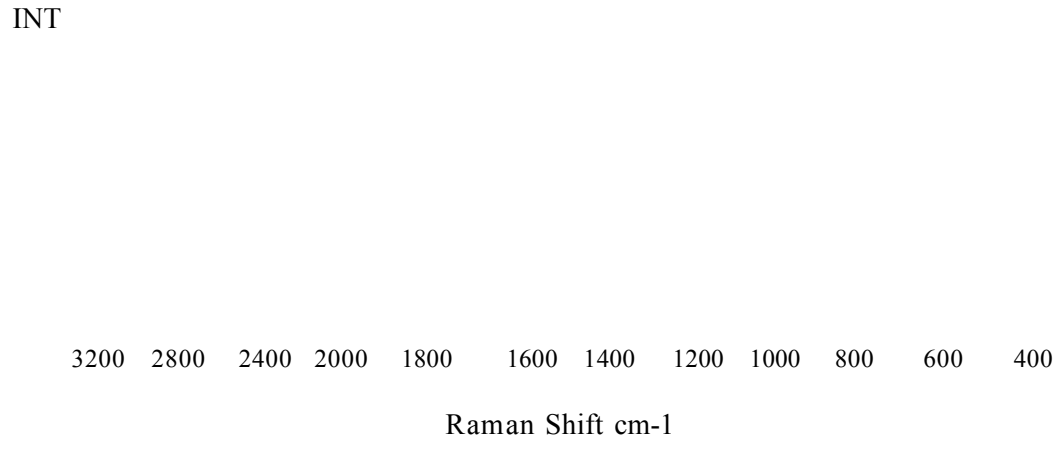

Figure 4-3: Spectra of (a) a groomed fingermark with a 1:1 mixture of 100 nm dilute colloid and 0.1M Na2S04, (b) 100 nm colloid and 0.1M Na2S04 only, and (c) 100 nm colloid and a fingermark only (Ferguson et al., 2010a and 2010b).

Another explanation for the poor results obtained could be due to the colloid and salt aggregate solutions being mixed together prior to deposition. Although some research groups advocate mixing the colloid and salt aggregate solutions (Mabbott ***et al.,*** 2013), other literature recommends applying them in separate steps. For example, in a study to analyse the synthetic dyes present in ballpoint pen inks, silver colloid was initially applied to dye spots previously separated by TLC, followed by application of 0.5M KN03 (Geiman ***et al.,*** 2009). In a subsequent study, trace amounts of controlled substances were identified by

SERS after being deposited on top of a 0.5M NaCl solution, followed by application of silver colloid solution (Rana ***et al.,*** 2011).

4.4.1.3 Order of Deposition of 150 nm Colloid

In light of the failure to acquire adequate SERS spectra of groomed fingermarks using the 100 nm colloid by any method, the 150 nm Raman specific gold colloid was employed for the remainder of the study. The spectra obtained of groomed fingermarks deposited both above and below the gold colloid employed in the study can be seen in figure 4.4. The spectra are shown on the same intensity scale and clearly demonstrate that greater enhancement of the Raman signal is achieved if the fingermark is deposited on top of the colloid (Ferguson ***et al.,*** 2010a and 2010b).

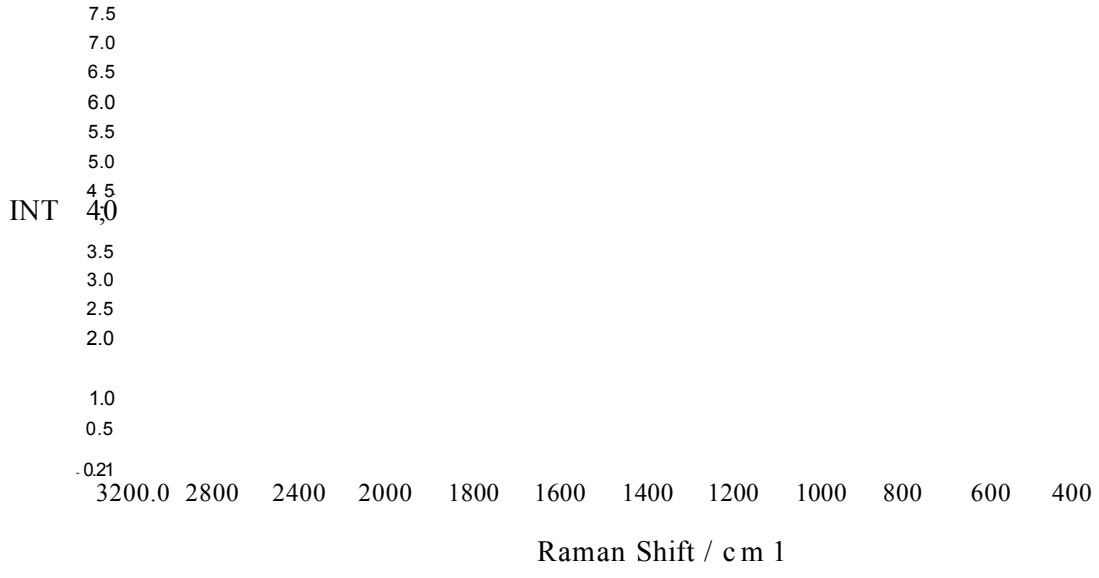

Figure 4-4: SERS spectra after deposition of (a) 150 nm gold colloid below a groomed fingermark and (b) above a groomed fingermark (Ferguson et al 2010a and 2010b).

The application of nanoparticle colloids below the analyte being investigated correlates with the use of pre-prepared SERS substrates such as Klarite™, which was used as a fingermark deposition surface in the work presented here. Specifically designed SERS substrates such as Klarite™ allow reproducible Raman signals to be generated in a broad range of applications from forensics to medical diagnostics. Reproducibility is often a problem with SERS when using gold colloids as the nanoparticles may not be homogenously dispersed, resulting in inconsistencies in the Raman signal observed. Klarite™ has a regular pattern of holes on the surface that generate photonic crystals that regulate the surface plasmons and ensure a more reproducible Raman signal (D3 Technologies Ltd). More recently, a gold nanoparticle coated sol-gel derived SiO_2 SERS substrate was used in the analysis of whole human blood, red blood cells and plasma in research performed by Premasiri *et al.*, (2012). As Klarite™ is not practical for analysing fingermarks at present, future advancements in pre-prepared SERS substrates may result in specific fingermark lifting media that are coated with a monolayer of nanoparticles for recovery of fingermarks from various deposition surfaces, which can be analysed *in situ* at a crime scene.

4.4.1.4 SERS Imaging

SERS images of fingermarks were acquired on three different deposition surfaces; MALDI stainless steel spotless inserts, pre-cleaned aluminium sheets and Klarite™. For the stainless steel and aluminium surfaces, a drop of colloid was applied to each surface resulting in a spot size diameter of approximately 1.5 mm, which restricts the size of the image obtained. For the Klarite™ substrate, a larger image was obtained as the active area is 4 mm x 4 mm, although this is still insufficient to allow imaging of a whole fingermark. All three

of the deposition surfaces tested contributed to the spectra obtained, although peaks specifically originating from the groomed fingermark could be seen. A peak at 1000 cm^{-1}, attributed to the C-N stretching vibration of urea in sweat by Virkler and Lednev (2008), was used to generate all the SERS images of the fingermark ridge pattern presented in figure 4.5, by integrating the peak area between 1010 and 990 cm^{-1} (Ferguson *et al.*, 2010a and 2010b). Subsequent research into the presence of urea in fingermarks using SERS is in agreement with the work presented here, as the dominant urea peak was assigned at 1004 cm^{-1} (Leordeon *et al.*, 2012). One plausible explanation for the slight difference in peak wavenumber is that their data was acquired using a 633 nm HeNe laser, whereas a 785 nm laser was used in the present study.

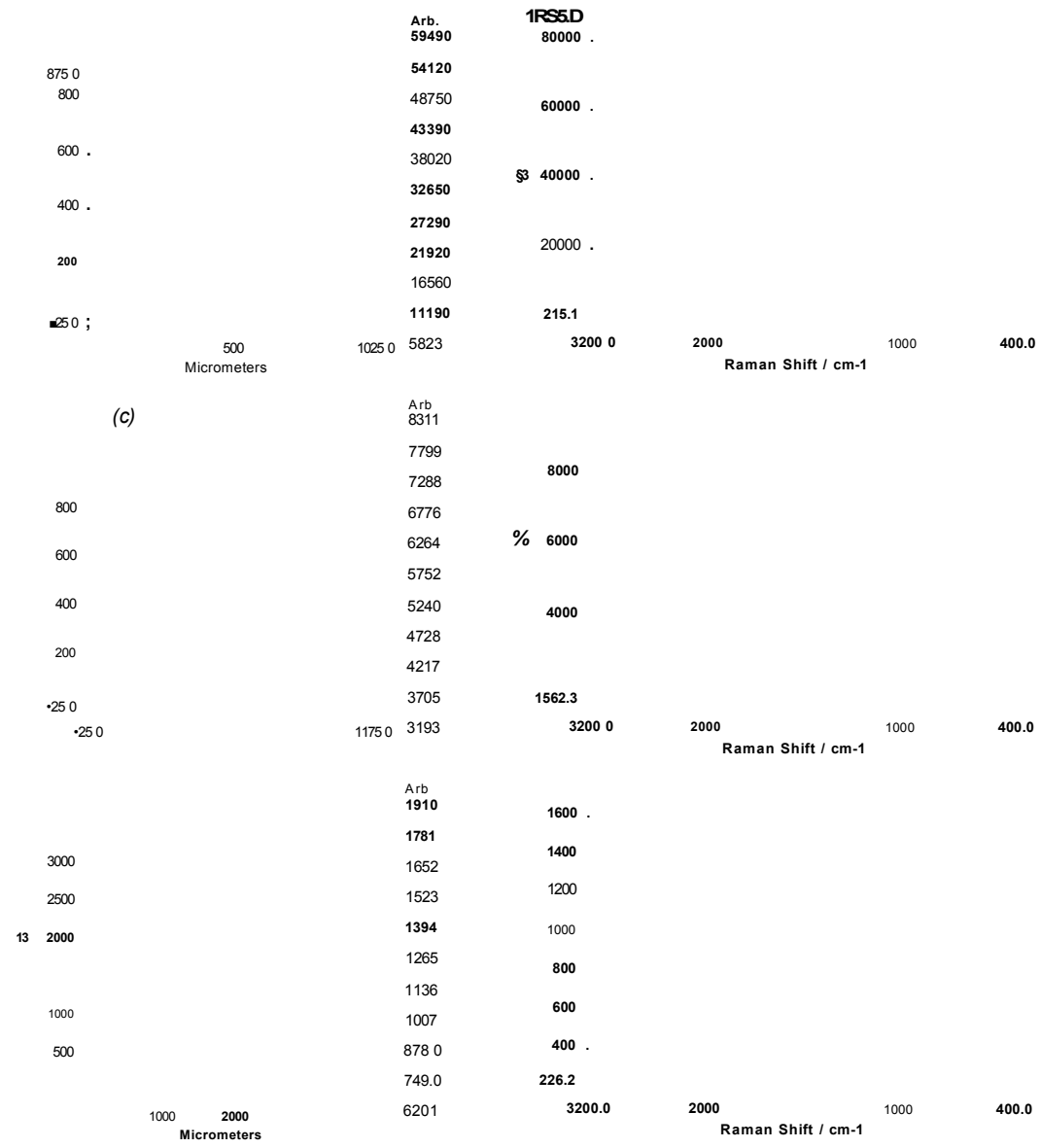

Figure 4-5: Fingermark images obtained by integrating the peak area between 1010 and 990 cm'1 and the corresponding SERS spectra on three different deposition surfaces: MALDI stainless steel insert, aluminium plate and Klarite™.

(a) Image of a fingermark deposited on top of 150 nm gold colloid on a MALDI stainless steel insert; (b) spectra obtained from positions 1 (black) and 2 (blue) on image A. (c) Image of a fingermark deposited on top of 150 nm gold colloid on an aluminium plate ; (d) spectra obtained from positions 1 (black) and 2 (blue) on image C. (e) Image of a fingermark deposited on Klarite™; (f) spectra obtained from positions 1 (black) and 2 (blue) on image (Ferguson et al., 2010a and 2010b).

4.4.2 Sequential Use of Attenuated Total Reflectance Fourier Transform Infrared Spectroscopy (ATR-FTIR) and MALDI-MSI

4.4.2.1 Analysis of Groomed Fingermarks by ATR-FTIR

Groomed fingermarks were initially deposited onto a pre-cleaned aluminium can. The deposited fingermarks were recovered using BVDA gelatine lifts and placed directly onto the ATR-FTIR crystal. Spectra were initially acquired of the BVDA lift alone in order to obtain background spectra and ensure that peaks specifically originating from the fingermark could be differentiated from those arising from the lifting media. Images were acquired between 3800 and 900 cm^{-1}. Fig 4.6(a) shows the ATR image obtained using the peak height at 1743.5 cm^{-1}. From the spectra in figure 4.6, it is evident that the peak correlates to a molecular vibration originating from the friction ridge of the fingermark (figure 4.6, panel b1) and is absent in the spectra orientating from the valley between the fingermark ridges (fig 4.6, panel b2). The peak at 1743.5 cm^{-1} is due to a C=O stretch most probably from an endogenous lipid present in the sebum enriched fingermark, as previously reported by Ricci *et al.* (2007a).

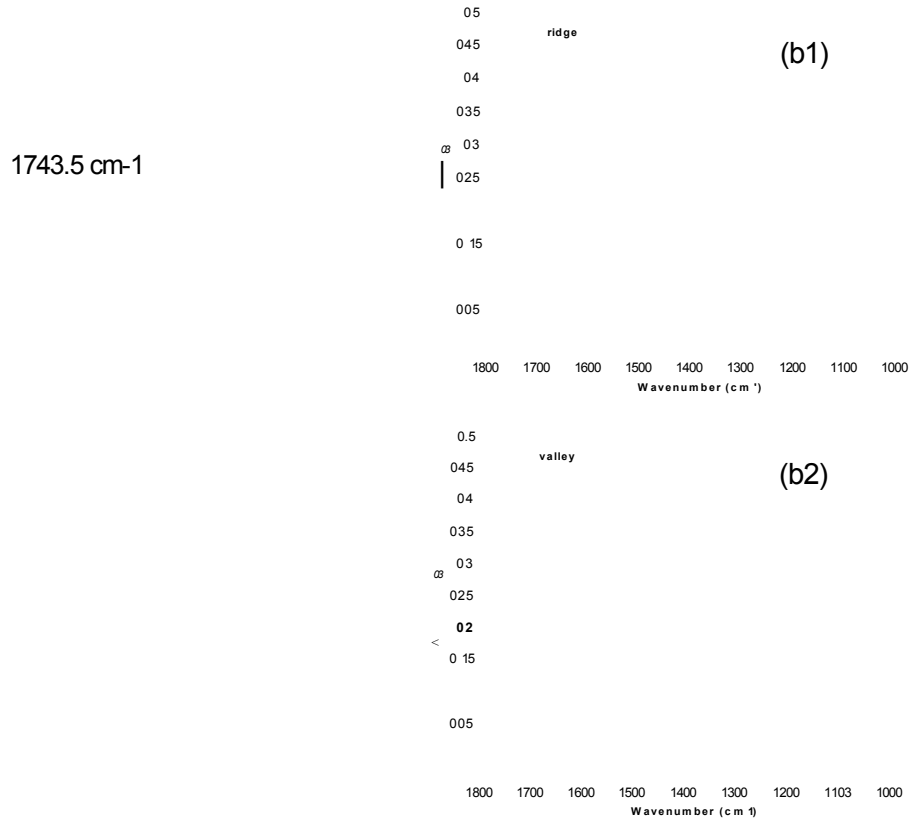

Figure 4-6: ATR-FTIR image and spectra showing the ATR-FTIR image of a groomed fingermark recovered from an aluminium can with a BVDA gelatine lift. The image obtained shows the distribution of the peak at 1743.5 cm'1, which has been attributed to a C=0 ***stretching vibration originating from a triglyceride present in the sebaceous material. Panel (b1) shows the presence of the peak in the spectra obtained from the fingermark ridge and panel (b2) shows the spectra obtained from the valley between the ridges, where the peak at 1743.5 cm'1 is clearly absent.***

In the study by Ricci and collaborators, a peak present at 1745 cm'1 was attributed to the presence of triglygerides and/or phospholipids in groomed fingermarks deposited directly onto a ZnSe crystal, which correlates to the work presented here (Ricci ***et al.,*** 2007a). Subsequent work by the same research group aimed to make the technique more forensically applicable by analysing fingermarks recovered from a metallic deposition surfaces using two different lifting media (Dycem Gel Print Lifter and BVDA Gelatine Lifter), thereby

simulating a possible real crime scene scenario. The authors reported that both lifting media contained absorption bands that dominated the spectra obtained and masked many of the absorption bands that are normally present when analysing groomed fingermarks deposited directly onto the ATR crystal. However, the BVDA gel lifter provided better differentiation as peaks corresponding to the C=O stretching vibration at 1745 cm-1 resulting from the sebaceous material present could be observed. In the study the authors used a variable angle accessory in order to change the angle of incidence and the penetration depth of the IR beam (Ricci *et al.*, 2007b).

A typical IR spectrum of latent fingermarks contains peaks at 1744 cm^{-1} and 1712 cm^{-1} corresponding to the C=O stretching vibrations from triglycerides and fatty acids respectively. In the work presented here, the peak at 1712 cm^{-1} is absent in the spectra, as the BVDA lifting media displays strong absorption in the 900 – 1700 cm^{-1}, which masks the peak at 1712 cm^{-1} (figure 4.7). This means that the carbonyl absorption of the higher molecular weight species is the only peak free from interferences from the BVDA lifting gel, as previously demonstrated by Ricci *et al.*, 2007b.

Figure 4-7: The ATR-FTIR spectrum of a groomed fingermark recovered from an aluminium substrate with a BVDA gelatine lift.

Panel (a) shows the ATR-FTIR spectrum of the recovered fingermark. Panel (b) shows the ATR-FTIR spectrum of the gelatine lift alone. From the spectrum in panel (a), the small peak at 1743.5 cm'1is the only discernable peak not originating from the gelatine lift. Panel c shows the two spectra overlaid over a wavelength range of 1800 - 1000 cm'1

4.4.2.2 Analysis of Groomed Fingermarks by MALDI-MSI

After lifting groomed fingermarks from the aluminium can using a BVDA gelatine lifter for analysis by ATR-FTIR, the remaining fingermark residue was dusted with mechanically ground a-CHCA in order to ascertain if enhancement of the fingermark was still possible. The dusted fingermark was then lifted using a conventional forensic lifting tape and attached to a MALDI spotless insert using double sided carbon tape and sprayed with 5 layers of a 70:30 ACN/0.5% TFA solution. The recovered fingermark was subsequently analysed by MALDI-MSI

in order to ascertain whether distribution images of the various lipid components present could still be obtained after lifting fingermarks a second time. From figure 4.8, the distribution images of various endogenous lipids were obtained following analysis by MALDI-MSI. The distribution images of four endogenous species, oleic acid at *m/z* 283.3, eicosadienoic acid at *m/z* 309.3, eicosenoic acid at *m/z* 311.3 and a cholesterol ester amino-octadecanoic acid at *m/z* 668.6 are shown, which have previously been tentatively identified by high mass accuracy measurements as previously shown in section 2.4.6.

For the recovered fingermark, both non-normalised and normalised images are shown for all four species. It can be observed from figure 4.5, that images that have not been normalised provide the highest quality images as expected in terms of the observable ridge features. However, even after normalisation, the distribution images of the endogenous compounds can still be obtained. The ability to recover fingermarks a second time and still obtain distribution maps of the endogenous compounds present demonstrates the sensitivity of MALDI-MSI for the forensic analysis of fingermarks. Furthermore, the ability to perform FTIR prior to MALDI-MSI theoretically enables additional chemical information to be obtained. The analysis of fingermarks using the combined approach of ATR-FTIR and MALDI-MSI demonstrates the potential application of the techniques in real crime scene scenarios.

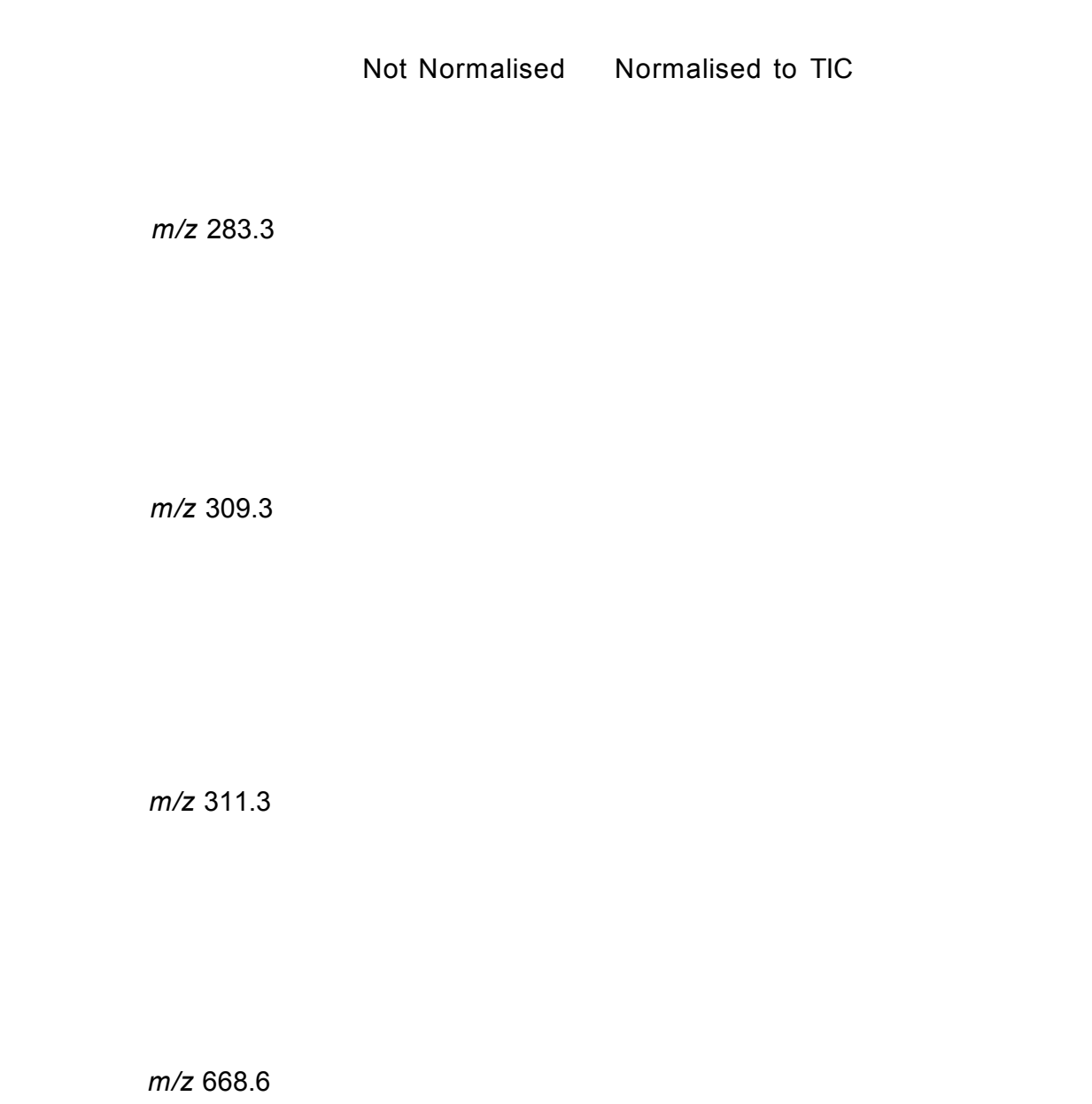

Figure 4-8: MALDI-MS images of oleic acid at m/z 283.3, eicosadienoic acid at m/z 309.3, eicosenoic acid at m/z 311.3 and amino-octadecanoic acid at m/z 668.6.

Groomed fingermarks were initially deposited on an aluminium can and lifted using a BVDA gelatine lift and subjected to ATR-FTIR analysis. The remaining fingermark residue was then lifted and prepared by the dry-wet method and analysed by MALDI-MSI.

4.4.2.3 Analysis of Condom Lubricant Contaminated Fingermarks by ATR-FTIR prior to MALDI-MSI Analysis

Condom lubricants can be grouped into four different types: silicone based, PEG based, water-based and oil-based. Most condom lubricants are silicone based, and therefore analytical methods which enable silicone based constituents such as PDMS to be detected, offer improved forensic applicability (Maynard *et al.*, 2001). The majority of condoms sold in the United Kingdom are silicone based, with the three major brands being Durex®, Mates® and Pasante (Coyle and Anwar, 2009). In the study by Coyle and Anwar (2009), FT-Raman spectroscopy was used to detect PDMS in condom lubricants obtained from directly swabbing a piece of cotton fabric, thereby omitting the extraction protocols that may be necessary when analysing condom lubricants by analytical techniques such as GC-MS (Campbell and Gordon 2007).

In the present study, prior to the analysis of the condom lubricant contaminated fingermarks, spectra were acquired of the BVDA lift alone in order to obtain background spectra and ensure that peaks specifically originating from the fingermark could be differentiated from those arising from the lifting media. Reference spectra were also obtained of vinyl-PDMS and PEG 3000 standards. Figure 4.9(a) shows the reference spectra of the gelatine lift, vinyl PDMS and PEG 3000 between 1800 and 900 cm^{-1}. From the spectra, an intense peak originating from the vinyl-PDMS standard is evident at 1258 cm^{-1} which is clearly absent in the spectra of the BVDA gelatine lift. It is also in evident in figure 4.9(a) that the peaks present in the spectra of PEG 3000 are masked by the peaks originating from the gelatine lift used in the recovery of the contaminated fingermarks, which is problematic in terms of visualising the distribution of this component in the recovered condom lubricant contaminated

fingermarks. In order to produce a distribution image of PEG 3000, the gelatine lift was used as a reference background by which to ratio the resulting fingermark spectra, thereby essentially subtracting the intense bands associated with the gelatine lift in the resulting distribution image (Bradshaw *et al.*, 2013).

A *Condomi Max love* contaminated fingermark was initially deposited onto a pre-cleaned ceramic tile. The deposited fingermark was recovered using a BVDA gelatine lift and placed directly onto the ATR-FTIR diamond crystal. Figure 4.9 (b) and (c) show the corresponding distribution images of the PDMS signal at 1258 cm^{-1} and PEG 3000 at 1365 cm^{-1} respectively. The size of the image shown is 640 x 640 µm, which enables two fingermark ridges to be clearly observed. Panel (d) shows two spectra extracted from the ridges (d1) and the valley (d2) of the resulting images, which corresponds to the high and low quantities of the two polymers present respectively (Bradshaw et al., 2013).

The work presented here demonstrates the potentially forensic applicability of ATR-FTIR. Lubricant contaminated fingermarks were recovered from non-porous surfaces and subjected to direct analysis by ATR-FTIR without the need for sample preparation. The detection of peaks corresponding to both PDMS and PEG 3000, supports previous work conducted by Maynard and co-workers in 2001. From their studies, the IR spectra of siloxane based lubricants showed a peak at 1263 cm^{-1}, resulting from a symmetric CH_3 deformation. In their IR spectra of the PEG based lubricants; a peak with a wavenumber of 1353 cm^{-1} was recorded. This could correlate to the PEG peak detected in the recovered fingermark shown here. Their study utilised diffuse reflectance infrared Fourier transform spectroscopy (DRIFTS), rather than ATR-FTIR, which may account for the slight differences in wave numbers observed (Maynard *et al.*, 2001).

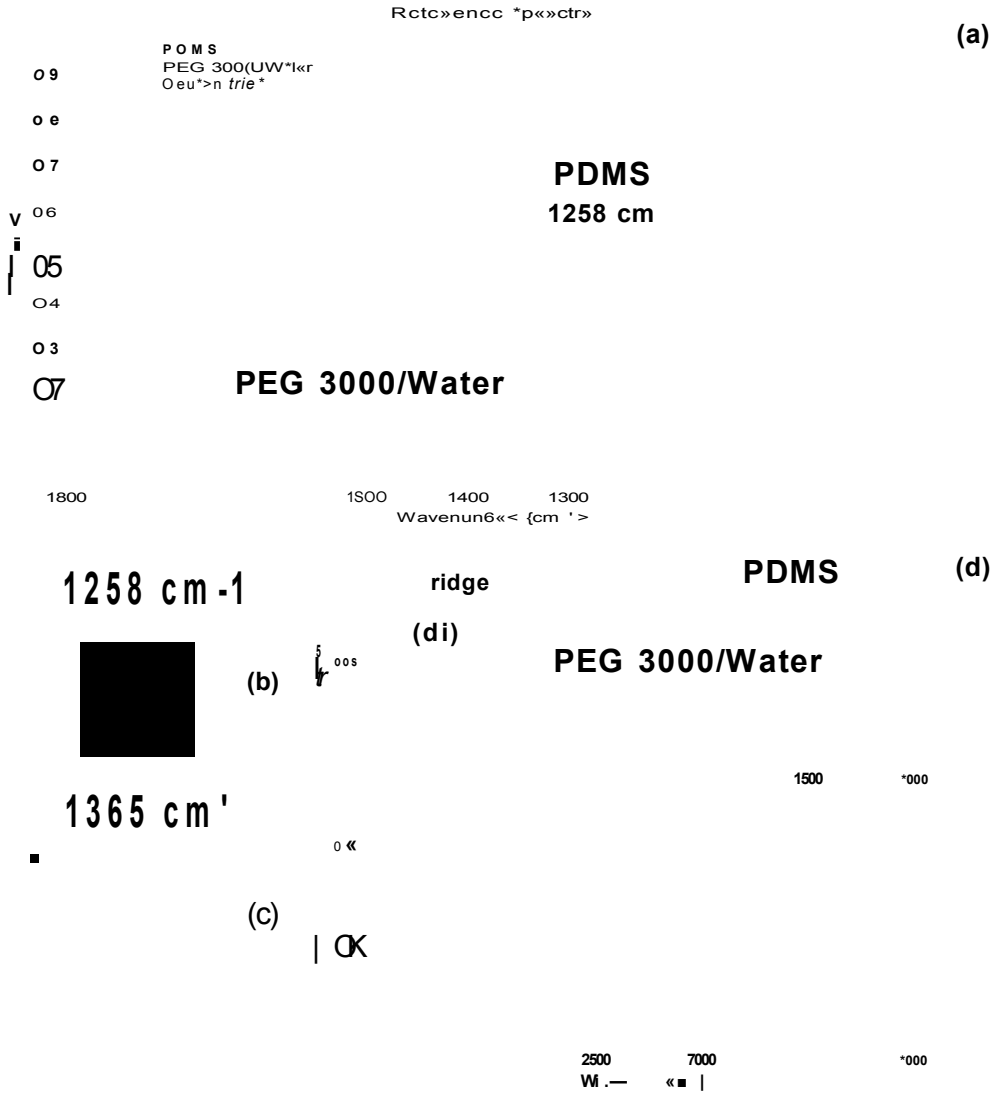

Figure 4-9: ATR-FTIR imaging analysis of a Condomi Max Love lubricant contaminated fingermark recovered from a ceramic tile with a BVDA gelatine lift.

Panel (a) shows the reference spectra for PDMS and PEG 3000, with the characteristic peaks present at 1258 cm-1 and 1365 cm-1 respectively, superimposed with the spectrum of a BVDA gelatine lift. The ATR-FTIR images of a lubricant contaminated fingermark are obtained showing the distribution of PDMS (panel b) and PEG 3000 (panel c). Panel (d) shows two ATR-FTIR spectra obtained from the ridge (d1) and the valley (d2) respectively, demonstrating the high and low concentrations of the two polymers present (Bradshaw et al., 2013).

4.4.2.4 Analysis of Condom Lubricant Contaminated Fingermarks by MALDI-MSI following ATR FTIR Analysis.

After recovering the condom lubricant contaminated fingermark using the BVDA gelatine lifts for subsequent analysis by ATR-FTIR, the application of the dry-wet method enabled the remaining fingermark residue to be enhanced and recovered a second time prior to solvent spaying and analysis by MALDI-MSI. The MALDI-MSI analysis shows that even after a second lift, images of the distribution of PEG at *m/z* 1449.8, 1493.9 and 1537.8, corresponding to the 32-mer, 33-mer and 34-mer respectively could still be obtained (figure 4.10). In addition to PEG, endogenous fatty acids could also be detected and images of their distribution obtained, alongside the total ion count (TIC) image, which enables all the ridge detail to be clearly visualised.

PDMS was not detected in the sample in the MALDI imaging experiment; however, it has been detected in condom lubricant contaminated fingermarks using MALDI-MS in profiling mode (Bradshaw *et al.*, 2013). Interestingly, the work showed the PDMS ion signal to be significantly suppressed in the presence of PEG, which may offer one explanation for its absence in the MALDI images reported here.

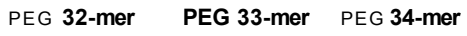

Figure 4-10: MALDI-MS images of 32-mer, 33-mer and 34-mer PEG ion signals and a selection of tentatively identified fatty acids at m/z 230.2, 255.2, 257.2 and oleic acid at 283.2.

The complete ridge pattern is also provided by the image of the complete total ion current (TIC). Lubricant contaminated fingermarks were initially deposited on a ceramic tile and lifted using a BVDA gelatine lift and subjected to ATR-FTIR analysis. The remaining fingermark residue **was** *then prepared by the dry-wet method and analysed by MALDI-MSI (Bradshaw et al., 2013).*

The work presented here serves as a proof of concept study for a combined workflow incorporating ATR-FTIR and MALDI-MSI. The fluorescent properties of some of the constituents present within condom lubricants potentially enable contaminated fingermarks left by an assailant at the scene of a sexual assault to be preliminary visualised using the various light sources and filters that are commonly used in crime scene searches (Bradshaw ***et al.,*** 2013). However, the integration of an initial compatible enhancement technique would further augment the forensic applicability of the combined workflow, provided the chemical information attainable by the analytical techniques employed was not significantly diminished.

4.5 Conclusion

Both SERS and ATR-FTIR provide non-destructive methods for fingermark analysis. SERS enables weak Raman signals to be amplified for analytes present at low concentrations such as within fingermarks. From the SERS spectra obtained here, the 150 nm colloid deposited below the fingermarks gave the best results. Images of the fingermark ridge pattern have also been successfully obtained on three non-porous deposition surfaces, MALDI stainless steel inserts, aluminium plates and Klarite™. However, the size of the images produced was restricted by the diameter of the deposited colloid for the MALDI and aluminium substrates and the size of the active area for Klarite™. As Raman spectroscopy is already a portable technique, advancements in pre-prepared SERS substrates may result in specific SERS fingermark lifting media for recovery of fingermarks from various deposition surfaces, which can be analysed *in situ* at the crime scene.

ATR-FTIR has been used in conjunction with MALDI-MSI in a combined analytical approach for the analysis of both groomed and condom lubricant contaminated fingermarks deposited on non-porous surfaces. Fingermarks were initially recovered using BVDA lifting media and analysed by ATR-FTIR. Ridge pattern images were obtained from peaks specifically originating from both fingermark types. The peak originating from a C=O stretching vibration at 1743.5 cm^{-1} was the only peak due to the groomed fingermark that was discernible from the gel lift. In the analysis of the condom lubricant contaminated fingermark, peaks arising from the presence of both PDMS at 1258 cm^{-1} and PEG 3000 at 1365 cm^{-1} could be differentiated from the peaks originating from the gelatine lift. Subsequent analysis of the remaining fingermark residue by MALDI-MSI enabled distribution maps of both

endogenous and exogenous compounds to be obtained demonstrating the potential of an integrated forensic workflow. The ability to analyse fingermarks in a non-destructive and timely manner by ATR-FTIR could potentially be used as a presumptive test to ascertain whether condom lubricants or other contaminants are present in the fingermark as a means of establishing prospective targets for subsequent analysis by MALDI-MS. Furthermore, analysis by ATR-FTIR followed by MALDI-MSI, offers a means of obtaining complementary information, which can only strengthen the applicability of the analytical techniques in a forensic context.

4.6 References

Bell, S. and Sirimuthu N. (2005). Surface-enhanced Raman spectroscopy as a probe of competitive binding by anions to citrate-reduced silver colloids. *Journal of Physical Chemistry a,* **109** (33), 7405-7410

Bell, S.E.J., Fido, L.A., Sirimuthu, N.M.S., Speers, S.J., Peters, K.L. and Cosbey, S.H. (2007). Screening tablets for DOB using surface-enhanced Raman spectroscopy. *Journal of Forensic Sciences,* **52** (5), 1063-1067

Bell, S.E.J. and McCourt, M.R. (2009). SERS enhancement by aggregated au colloids: Effect of particle size. *Physical Chemistry Chemical Physics,* **11** (34), 7455-7462

Boyd, S., Bertino, M.F., Ye, D., White, L.S. and Seashols, S.J. (2013). Highly sensitive detection of blood by surface enhanced Raman scattering. *Journal of Forensic Sciences,* **58** (3), 753-756

Bradshaw, R., Wolstenholme, R., Ferguson, L.S., Sammon, C., Mader, K., Claude, E., Blackledge, R.D., Clench, M.R. and Francese, S. (2013). Spectroscopic imaging based approach for condom identification in condom contaminated fingermarks. *Analyst,* **138** (9), 2546-2557

Campbell, G.P. and Gordon, A.L. (2007). "Analysis of condom lubricants for forensic casework". *Journal of Forensic Sciences,* **52** (3), 630-642

Chalmers, J.M., Edwards, H. G. M. and Hargreaves, M. D. (2012). *Infrared and Raman spectroscopy in forensic science.* Oxford, Wiley-Blackwell

Connatser, R.M., Prokes, S.M., Glembocki, O.J., Schuler, R.L., Gardner, C.W., Lewis, S.A., Sr. and Lewis, L.A. (2010). Toward surface-enhanced Raman imaging of latent fingerprints. *Journal of Forensic Sciences,* **55** (6), 1462-1470

Coyle, T. and Anwar, N. (2009). A novel approach to condom lubricant analysis: In-situ analysis of swabs by FT-Raman spectroscopy and its effects on DNA analysis. *Science & Justice,* **49** (1), 32-40

Crane, N.J., Bartick, E.G., Perlman, R.S. and Huffman, S. (2007). Infrared spectroscopic imaging for non-invasive detection of latent fingerprints. *Journal of Forensic Sciences,* **52** (1), 48-53

D3 Technologies Ltd (online). Available at: http//www.d3diagnostics.com/en/what-is raman-spectroscopy—10371. Last accessed on 03/01/2013

Day, J.S., Edwards, H.G., Dobrowski, S.A. and Voice, A.M. (2004). The detection of drugs of abuse in fingerprints using Raman spectroscopy I: Latent fingerprints. *Spectrochimica Acta. Part A, Molecular and Biomolecular Spectroscopy,* **60** (3), 563-568

Day, J.S., Edwards, H.G., Dobrowski, S.A. and Voice, A.M. (2004). The detection of drugs of abuse in fingerprints using Raman spectroscopy II: Cyanoacrylate-fumed fingerprints. *Spectrochimica Acta. Part A, Molecular and Biomolecular Spectroscopy,* **60** (8-9), 1725-1730

De Paoli, G., Lewis, S.A., Sr., Schuette, E.L., Lewis, L.A., Connatser, R.M. and Farkas, T. (2010). Photo- and thermal-degradation studies of select eccrine fingerprint constituents. *Journal of Forensic Sciences,* **55** (4), 962-969

Doering, W. and Nie, S. (2002). Single-molecule and single-nanoparticle SERS: Examining the roles of surface active sites and chemical enhancement. *Journal of Physical Chemistry B,* **106** (2), 311-317

Elkins, K.M. (2011). Rapid presumptive "fingerprinting" of body fluids and materials by ATR-FTIR spectroscopy. *Journal of Forensic Sciences,* 56 (6), 1580-1587

Ferguson L., Francese S., Wolstenholme R. and Lozano-Diz, E. (2010a): Gold nanoparticles for SERS in fingermark Identification- Perkin Elmer Application Note [online]: Available at: http://www.perkinelmer.com.cn/cmsresources/images/46-74273app sersinfingerprints.pdf

Ferguson L., Lozano-Diz E., Francese S., Wolstenholme R., (2010b): Gold nanoparticles for SERS in fingermark Identification[online], *Spectroscopy Wavelength.* Available at: http://spectroscopvonline.findanalvtichem.com/spectroscopy/Gold-Nanoparticles-for-SERS-in-Finqermark-Identifi/ArticleStandard/Article/detail/672789

Geiman, I., Leona, M. and Lombardi, J.R. (2009). Application of Raman spectroscopy and surface-enhanced Raman scattering to the analysis of synthetic dyes found in ballpoint pen inks. *Journal of Forensic Sciences,* **54** (4), 947-952

Grant, A., Wilkinson, T., Flolman, D. and Martin, M. (2005).Identification of recently handled materials by analysis of latent human fingerprints using infrared spectromicroscopy. *Applied Spectroscopy,* **59** (9), 1182-1187

Jones, A. and Wolstenholme, R. (2003).Non-destructive spectroscopic analysis of ballpoint and gel pen inks. *Forensic Science International,* **136,** 69-70

Leona, M., Decuzzi, P., Kubic, T.A., Gates, G. and Lombardi, J.R. (2011). Non-destructive identification of natural and synthetic organic colorants in works of art by surface enhanced Raman scattering. *Analytical Chemistry,* **83** (11), 3990-3993

Leordean, C., Canpean, V. and Astilean, S. (2012). Surface-enhanced Raman scattering (SERS) analysis of urea trace in urine, fingerprints, and tears samples. *Spectroscopy Letters,* **45** (8), 550-555

Mabbott, S., Correa, E., Cowcher, D.P., Allwood, J.W. and Goodacre, R. (2013).Optimization of parameters for the quantitative surface-enhanced Raman scattering detection of mephedrone using a fractional factorial design and a portable Raman spectrometer. *Analytical Chemistry,* **85** (2), 923-931

Maynard, P., Allwell, K., Roux, C., Dawson, M. and Royds, D. (2001).A protocol for the forensic analysis of condom and personal lubricants found in sexual assault cases.*Forensic Science International,* **124** (2-3), 140-156

Mou, Y. and Rabalais, J.W. (2009). Detection and identification of explosive particles in fingerprints using attenuated total reflection-fourier transform infrared spectromicroscopy. *Journal of Forensic Sciences,* **54** (4), 846-850

Premasiri, W.R., Lee, J.C. and Ziegler, L.D. (2012). Surface-enhanced Raman scattering of whole human blood, blood plasma, and red blood cells: Cellular processes and bioanalytical sensing. *Journal of Physical Chemistry B,* **116** (31), 9376-9386

Rana, V., Canamares, M.V., Kubic, T., Leona, M. and Lombardi, J.R. (2011). Surface-enhanced Raman spectroscopy for trace identification of controlled substances: Morphine, codeine, and hydrocodone. *Journal of Forensic Sciences,* **56** (1), 200-207

Ricci, C., Bleay, S. and Kazarian, S.G. (2007b). Spectroscopic imaging of latent fingermarks collected with the aid of a gelatine tape. *Analytical Chemistry,* **79** (15), 5771-5776

Ricci, C. and Kazarian, S.G. (2010). Collection and detection of latent fingermarks contaminated with cosmetics on nonporous and porous surfaces. *Surface and Interface Analysis,* **42** (5), 386-392

Ricci, C., Phiriyavityopas, P., Curum, N., Chan, K.L.A., Jickells, S. and Kazarian, S.G. (2007a). Chemical imaging of latent fingerprint residues. *Applied Spectroscopy,* **61** (5), 514-522

Smith, E. and Dent, G. (2005).*Modern Raman spectroscopy: A practical approach.* Chichester, UK, John Wiley & Sons

Song, W., Mao, Z., Liu, X., Lu, Y., Li, Z., Zhao, B. and Lu, L. (2012). Detection of protein deposition within latent fingerprints by surface-enhanced Raman spectroscopy imaging. *Nanoscale,* **4** (7), 2333-2338

Stamplecoskie, K.G., Scaiano, J.C., Tiwari, V.S. and Anis, H. (2011). Optimal size of silver nanoparticles for surface-enhanced Raman spectroscopy. *Journal of Physical Chemistry C,* **115** (5), 1403-1409

Tahtouh, M., Kalman, R.J., Roux, C., Lennard, C. and Reedy, B.J. (2005). The detection and enhancement of latent fingermarks using infrared chemical imaging. *Journal of Forensic Science*.**50** (1), 64-72

Virkler, K. and Lednev, I.K. (2008).Raman spectroscopy offers great potential for the nondestructive confirmatory identification of body fluids. *Forensic Science International,* **181** (1-3), E1-E5

West, M.J. and Went, M.J. (2008). The spectroscopic detection of exogenous material in fingerprints after development with powders and recovery with adhesive lifters. *Forensic Science International,* **174** (1), 1-5

West, M.J. and Went, M.J. (2009). The spectroscopic detection of drugs of abuse in fingerprints after development with powders and recovery with adhesive lifters. *Spectrochimica Acta .Part A, Molecular and Biomolecular Spectroscopy,* **71** (5), 1984-1988

Yang, Y., Li, Z.Y., Yamaguchi, K., Tanemura, M., Huang, Z., Jiang, D., Chen, Y., Zhou, F. and Nogami, M. (2012). Controlled fabrication of silver nanoneedles array for SERS and their application in rapid detection of narcotics. *Nanoscale,* **4** (8), 2663-2669

Zieba-Palus, J., Michalska, A. and Weselucha-Birczynska, A. (2011). Characterisation of paint samples by infrared and Raman spectroscopy for criminalistic purposes. *Journal of Molecular Structure,* **993** (1-3), 134-141

5 Final Conclusions

5.1 Conclusions

Despite the plethora of development techniques available for enhancing latent fingermarks at crime scenes, there still remains a need for further advances to be made. In recent years, advanced analytical techniques have become instrumental in providing additional information regarding the chemical constituents present within latent fingermarks. Of these analytical techniques, MALDI-MSI has proven to be pivotal in acquiring chemical information that could potentially reduce the pool of potential suspects, whilst simultaneously providing multiple images of the fingermark ridge detail. The use of MALDI-MSI to detect and image the chemical species present within fingermarks was first reported by Wolstenholme *et al.*, (2009). The study involved initial deposition of ungroomed fingermarks onto aluminium plates and subsequent spraying of the CHCA matrix. The study demonstrated the sensitivity of the technology in detecting and imaging minute amounts of material (given the type of marks employed). In particular, distribution images of various endogenous lipids and an exogenous contaminant were obtained. The methodology employed, however, had feasibility issues due to the fingermarks being deposited directly onto a MALDI compatible surface, an unrealistic scenario for "real" crime scenes. This limitation was addressed in the work presented in chapter 2 of this thesis. The development of the dry-wet method (Patent number GB2489215) enabled the analysis of ungroomed fingermarks by MALDI-MSI to be more forensically applicable. Unlike other analytical techniques that have been used to investigate the chemical composition of latent fingermarks, the dry–wet method involves initial application of ground matrix to fingermarks, which is analogous to dusting fingermarks with the conventional fingermark enhancing powders currently used by scene of crime personnel, thereby enabling an

optical image of the fingermark ridge detail to be obtained, prior to instrumental analysis (Ferguson *et al.*, 2011). As shown in the work presented within this thesis, the novel methodology can be applied to fingermarks deposited on a range of surfaces, which further demonstrates its potential applicability at "real" crime scenes. The optical image obtained can be photographed prior to lifting and spraying with appropriate solvents and subsequent imaging by MALDI-MSI. Furthermore, the fluorescent nature of the UV absorbing matrix extends the enhancement potential, as the ridge pattern and *minutiae* may be more clearly visible under UV light, which may aid identification of the suspect (Ferguson *et al.*, 2011). Recently, the dry-wet method has been applied in conjunction with MALDI-MSI to separate overlapping fingermarks deposited on two substrates. Separation was achieved by imaging both endogenous and exogenous species, including a metabolite of caffeine, further demonstrating the forensic potential of the methodology (Bradshaw *et al.*, 2012).

The use of Surface Enhanced Raman Spectroscopy (SERS) to obtain images of the fingermark ridges is presented in chapter 4 of this thesis. Groomed fingermarks were deposited on three deposition surfaces (MALDI stainless steel inserts, aluminium plates and Klarite™). The size of the images obtained was restricted by the diameter of the deposited gold colloid (approximately 1.5 mm) for the MALDI and aluminium substrates and to the active area (4 mm x 4 mm) for Klatite™. For the 150 nm gold colloid, the best enhancement was observed when the fingermarks were laid on top of the deposited colloid, which concurs with fingermarks deposited on top of Klarite™ (Ferguson *et al.*, 2010a and 2010b). The use of a gold nanoparticle coated sol-gel derived SiO_2 SERS substrate has recently been advocated by Premasiri *et al.*, (2012) to analyse whole human blood, red blood cells and plasma. Lifting media that are coated

with a layer of nanoparticles may in the future enable fingermarks to be lifted and analysed *in situ* using one of the recently developed portable Raman spectrometers (Virkler and Lednev, 2009). The recovery of fingermarks using an appropriate SERS substrate could potentially be analogous to the two-step workflow incorporating ATR-FTIR and MALDI-MSI presented in chapter 4 of this thesis, where fingermarks are initially recovered for SERS analysis and the remaining fingermark residue is prepared by the dry-wet method and analysed by MALDI-MSI. As both ATR-FTIR and Raman spectroscopy are considered non-destructive and complementary techniques, recovered fingermarks can initially be analysed by one of these techniques, followed by MALDI-MSI analysis of fingermarks prepared by the dry-wet method. This could ultimately lead to a three step multi-informative analytical approach for chemical characterisation of fingermark residue, thereby increasing the chemical information obtained from a single fingermark.

The development of the dry-wet method has been fundamental in the significant advances that have been made with respect to the forensic analysis of latent fingermarks by MALDI-MSI. Indeed, MALDI-MSI has now been listed as an analytical technology having high potential to be implemented within casework in the new Edition of the Home Office Fingerprint Development Handbook (due to be published at the end of 2013).

Initial work establishing the feasibility of MALDI-MSI for fingermark analysis, concentrated predominantly on the lipids species present, as lipids are more readily ionised than higher molecular weight species such as peptides and proteins (Wolstenholme *et al.*, 2009). In this study, MALDI mass spectrometry was also employed in profiling mode (MALDI-MSP) to detect various tentatively identified antimicrobial peptides and small proteins in both groomed and

ungroomed fingermarks (UK. Patent number 1120533.3, International Patent Application no. PCT/GB2012/051775). The species detected include dermcidin (DCD 1L), a 48 amino acid long constituent of eccrine sweat. In sweat, DCD-1L is cleaved by various proteases generating other peptides such as DCD-1, LEK-45, SSL-25 and YDP-42 (Flad *et al.*, 2002: Rieg *et al.*, 2006). The reproducibility of the methodology used to detect these species was tested by collecting ungroomed fingermarks from multiple donors in two inter-donor variability studies as shown in chapter 3 of this thesis. The resulting data were subjected to multivariate statistical analysis in order to determine whether discrimination based on sex could be ascertained. Remarkably, unlike previous discrimination studies, which have been performed on the lipid constituents of latent fingermarks (Weyermann et al., 2011; Emerson et al., 2011), in the work presented here, the sex of the donor was determined with a validated predicted accuracy of 85% when using ion peaks with a VIP score of 10 or more. This therefore demonstrates the potential of the methodology to provide chemical information that would reduce the pool of potential suspects even in cases where the ridge detail coverage is inadequate to permit identification (Ferguson *et al.*, 2012).

5.2 References

Bradshaw, R., Rao, W., Wolstenholme, R., Clench, M.R., Bleay, S. and Francese, S. (2012). Separation of overlapping fingermarks by matrix assisted laser desorption ionisation mass spectrometry imaging. Forensic Science International, 222 (1-3), 318-326

Emerson, B., Gidden, J., Lay, J.O.,Jr and Durham, B. (2011). Laser desorption/ionization time-of-flight mass spectrometry of triacylglycerols and other components in fingermark samples. *Journal of Forensic Sciences,* 56 (2), 381-389

Ferguson, L., Bradshaw, R., Wolstenholme, R., Clench, M. and Francese, S. (2011). Two-step matrix application for the enhancement and imaging of latent fingermarks. *Analytical Chemistry,* 83 (14), 5585-5591

Ferguson L., Francese S., Wolstenholme R. and Lozano-Diz, E. (2010a): Gold nanoparticles for SERS in fingermark Identification- Perkin Elmer Application Note [online]: Available at:
http://www.perkinelmer.com.cn/cmsresources/imaqes/46-74273app sersinfinqerprints.pdf

Ferguson L., Lozano-Diz E., Francese S., Wolstenholme R., (2010b): Gold nanoparticles for SERS in fingermark Identification[online], *Spectroscopy Wavelength.* Available at:
http://spectroscopvonline.findanalvtichem.com/spectroscopy/Gold-Nanoparticles-for-SERS-in-Finqermark-Identifi/ArticleStandard/Article/detail/672789

Ferguson, L.S., Wulfert, F., Wolstenholme, R., Fonville, J.M., Clench, M.R., Carolan, V.A. and Francese, S. (2012). Detection of peptides and small proteins in fingermarks and determination of sex by MALDI mass spectrometry profiling. Analyst, 137, 4686-4692

Flad, T., Bogumil, R., Tolson, J., Schittek, B., Garbe, C., Deeg, M., Mueller, C.A. and Kalbacher, H.:. (2002). Detection of dermcidin-derived peptides in sweat by ProteinChip technology. *Journal of Immunological Methods,* **270** , 53-62

Premasiri, W.R., Lee, J.C. and Ziegler, L.D. (2012). Surface-enhanced Raman scattering of whole human blood, blood plasma, and red blood cells: Cellular processes and bioanalytical sensing. *Journal of Physical Chemistry B,* **116** (31), 9376-9386

Rieg, S., Seeber, S., Steffen, H., Humeny, A., Kalbacher, H., Stevanovic, S., Kimura, A., Garbe, C. and Shittek, B. (2006). Generation of multiple stable dermcidin-derived antimicrobial peptides in sweat of different body sites. *Journal of Investigative Dermatology,* **126** , 354-365.

Virkler, K. and Lednev, I.K. (2009). Analysis of body fluids for forensic purposes: From laboratory testing to non-destructive rapid confirmatory identification at a crime scene. *Forensic Science International,* **188** (1-3), 1-17

Weyermann, C., Roux, C. and Champod, C. (2011). Initial results on the composition of fingerprints and its evolution as a function of time by GC/MS analysis. *Journal of Forensic Sciences,* **56** (1), 102-108

Wolstenholme, R., Bradshaw, R., Clench, M.R. and Francese, S. (2009). Study of latent fingermarks by matrix-assisted laser desorption/ionisation mass spectrometry imaging of endogenous lipids. *Rapid Communications in Mass Spectrometry,* **23** (19), 3031-3039

6 Publications, Poster Presentations and Oral Presentations

6.1 Publications

Ferguson L.S., Creasey S., Wolstenholme R., Clench M.R., Francese S. (2013): Efficiency of the dry-wet method for the MALDI-MSI analysis of latent fingermarks. *Journal of Mass Spectrometry*, **48**, 677-684

Bradshaw R., Wolstenholme R., Ferguson L.S., Sammon C., Mader K., Claude E., Blackledge R.D., Clench M.R., Francese S. (2013): Spectroscopic imaging based approach for condom identification in condom contaminated fingermarks. *Analyst*, **138** (9), 2546-2557

Francese, S., Bradshaw, R., Ferguson, L.S., Wolstenholme, R., Clench, M.R. and Bleay, S. (2013). Beyond the ridge pattern: multi-informative analysis by MALDI mass spectrometry. *Analyst*

Ferguson L.S., Wulfert F., Wolstenholme R., Fonville J.M., Clench M.R., Carolan V.A., Francese S., (2012): Direct detection of peptides and small proteins in fingermarks and determination of sex by MALDI mass spectrometry profiling. *Analyst*, **137** (20), 4686-4692

Bailey M.J., Bright N.J, Croxton R.S, Francese S., Ferguson L.S., Hinder S., Jickells S., Jones B.J., Jones B.N., Kazarian S.G., Ojeda J.J., Webb R.P., Wolstenholme R., Bleay S. (2012): Chemical characterisation of Latent fingermarks by matrix-assisted laser desorption ionization, time-of-flight secondary ion mass spectrometry, mega electron volt secondary mass spectrometry, gas chromatography/mass spectrometry, X-ray photoelectron spectroscopy, and attenuated total reflection Fourier transform infrared spectroscopic imaging: an inter-comparison. *Analytical Chemistry*, **84** (20), 5814-

Ferguson L.S., Bradshaw R., Wolstenholme R., Clench M.R., Francese S., (2011): Two-step matrix application for the enhancement and imaging of latent fingermarks. *Analytical Chemistry*, **83**, 5585 – 5591

Bradshaw R., Wolstenholme R., Blackledge R.D, Clench M.R., Ferguson L.S., Francese S., (2011): A novel matrix assisted laser desorption/ionisation mass spectrometry imaging based methodology for the identification of sexual assault suspects. *Rapid Communications in Mass Spectrometry*, **25**, 415-422

Ferguson L., Francese S., Wolstenholme R. and Lozano-Diz, E. (2010): Gold nanoparticles for SERS in fingermark Identification- Perkin Elmer Application Note [online]: Available at: http://www.perkinelmer.com.cn/cmsresources/imaqes/46-74273app sersinfinqerprints.pdf

Ferguson L., Lozano-Diz E., Francese S., Wolstenholme R., (2010): Gold nanoparticles for SERS in fingermark Identification[online], ***Spectroscopy Wavelength.*** Available at: http://spectroscopvonline.findanalvtichem.com/spectroscopy/Gold-Nanoparticles-for-SERS-in-Finqermark-Identifi/ArticleStandard/Article/detail/672789.

6.2 Poster Presentations

Ferguson, L., Bradshaw, R., Wolstenholme, R., Clench, M. and Francese, S.: Detection and Mapping of Peptides and Small Proteins in Latent Fingermarks by MALDI-MSI. British Mass Spectrometry Society, (Cardiff, UK, 2010)

Ferguson, L.S., Wolstenholme, R., Wulfert, F., Bradshaw, R., Flinders, B., Carolan, V.A., Clench, M.R. and Francese, S.: An Intra-Donor Variability Study of Peptides Present in Latent Fingermarks. American Society of Mass Spectrometry, (Denver, USA, 2011)

Ferguson, L., Bradshaw, R., Wolstenholme, R., Carolan, V., Clench, M. and Francese, S.: Matrix Assisted Laser Desorption Ionisation Mass Spectrometry Imaging (MALDI-MSI) of Fingermarks Recovered from Different Deposition Surfaces. International Association of Forensic Scientists, (Madeira, Portugal, 2011)

Ferguson, L.S., Wolstenholme, R., Carolan, V.A., Clench, M.R. and Francese, S.: High Resolution MALDI-MS Images of Fingermarks Prepared by the Dry-Wet Matrix Application Method. American Society of Mass Spectrometry, (Vancouver, Canada, June 2012)

6.3 Oral Presentations

Ferguson, L., Francese, S. and Wolstenholme R.: Analysis of the Composition and Ageing of Latent Fingermarks by Spectroscopic Imaging Techniques. Analytical Research Forum, (Loughborough, UK, 2010)

Ferguson, L.S., Bradshaw, R., Wolstenholme, R., Carolan, V.A., Clench, M.R. and Francese, S.: Analysis of Latent Fingermarks by Matrix Assisted Lader Desorption Ionisation – Mass Spectrometry Imaging. The Fingerprint Society, (Derby, UK, 2012)

Ferguson, L., Bradshaw, R., Wolstenholme, R., Sammon, C., Carolan, V., Clench, M. and Francese, S.: Analysis of Latent Fingermarks by Matrix Assisted Laser Desorrption Ionisation Mass Spectrometry Imaging. Ourcon, (Ourense, Spain, 2012)